6770

NAME OF AUTHOR. JACOBUS   HUBERTUS   WYNHOVEN

TITLE OF THESIS. ELASTIC - PLASTIC ANALYSIS
.OF THREE DIMENSIONAL
.STRUCTURES

UNIVERSITY. ALBERTA

DEGREE FOR WHICH THESIS WAS PRESENTED. Ph.D.

YEAR THIS DEGREE GRANTED. 1970

(Signed). J. H. Wynhoven

PERMANENT ADDRESS:
.6 CAROL COURT.
NEWCOMB, GEELONG
VICT. , AUSTRALIA

DATED. 29th September. 19 70

NL-91 (10-68)

THE UNIVERSITY OF ALBERTA

ELASTIC-PLASTIC ANALYSIS OF

THREE DIMENSIONAL STRUCTURES

by

© JACOBUS HUBERTUS WYNHOVEN

A THESIS

SUBMITTED TO THE FACULTY OF GRADUATE STUDIES

IN PARTIAL FULFILMENT OF THE REQUIREMENTS FOR THE DEGREE

OF DOCTOR OF PHILOSOPHY

DEPARTMENT OF CIVIL ENGINEERING

EDMONTON, ALBERTA

FALL, 1970

UNIVERSITY OF ALBERTA

FACULTY OF GRADUATE STUDIES

The undersigned certify that they have read, and recommend
to the Faculty of Graduate Studies for acceptance, a thesis entitled
"ELASTIC-PLASTIC ANALYSIS OF THREE DIMENSIONAL STRUCTURES" submitted
by JACOBUS HUBERTUS WYNHOVEN in partial fulfilment of the requirements
for the degree of Doctor of Philosophy.

P.F. Adams   Supervisor

J.R. Colbourne

D.W. Murray

S.H. Simmonds

J. Tartar

Jacob Gluck - External Examiner

Date 15 Sept 70

ABSTRACT

This dissertation presents a method of analysis to predict the complete load-displacement response for large multi-story structures. The structures are composed of sets of planar bents arranged in two perpendicular directions. The structure is assumed to deform in these two principal directions and twist about a vertical axis. The bents may contain both uncoupled frame and coupled frame-shear wall elements.

The actual structure is replaced by an analytical model in which the number of unknown displacements have been considerably reduced. Slope-deflection equations are used to relate the member displacements to the end moments. Equilibrium equations are written as linear functions of the unknown displacements. The slope-deflection equations are modified in the presence of plastic hinges. The secondary moments due to the column axial loads acting through the sway displacements are considered, however, the effects of axial shortening, changes in axial load, variations in stiffness and carry over factors, and shear deformations are not considered.

The equilibrium equations are symmetric and only one half band width of the stiffness matrix is generated. The equations are solved using a modified Gauss Elimination technique. A computer program has been developed to perform the analysis; its validity has been verified by analyzing several structures for which data is available in the literature.

An extensive behavioral study is performed using a ten and a twenty-four story structure as its basis. The influence of various structural parameters are considered. The results indicate the importance of considering the torsional displacements when predicting the ultimate load carrying capacity for asymmetric structures. The torsional loads increase the net sway displacements which increase the P-Δ moments and reduce the ultimate load carrying capacity.

ACKNOWLEDGEMENTS

TABLE OF CONTENTS

TABLE OF CONTENTS (continued)

LIST OF TABLES

LIST OF FIGURES

LIST OF FIGURES (continued)

LIST OF FIGURES (continued)

LIST OF SYMBOLS

Subscripts

0	subscript referring to the origin of the co-ordinate system
j	subscript referring to a particular bent
i	subscript referring to a particular story or floor
b	subscript referring to, column to wall, beams
m	subscript referring to individual members within a bent, before lumping
c	subscript referring to a column
w	subscript referring to a wall
1,2	subscripts referring to member ends
x,y	subscripts referring to directions X and Y

Variables

X,Y,Z	system of co-ordinate axes
u,v	displacements in the co-ordinate directions X and Y
ϕ	rotation about the Z axis
x,y	distance of bent from the reference point
L	beam length
n	number of spans in a bent, before lumping
k	member stiffness (I/L)
I	moment of inertia
M_p	plastic moment capacity

M_{pc}	plastic moment capacity reduced due to the presence of an axial load
P	axial load
P_y	yield load of a member
M_t	total torsional resistance of a section
K_T, I_ω	torsional and warping constants
E, G	modulus of elasticity and modulus of rigidity
C_T, C_ω	uniform and non-uniform torsional resistances
ϕ', ϕ'''	first and third derivative of the floor rotation, ϕ
Δ	story sway displacement
θ	member end rotation
M	member end moment
M_F	fixed end moment
C	coefficient (EI/L)
L_W	wall width
h	story height
k_c, k_w	stiffness of rotational spring at base of column and wall
V	shear force
F	resisting floor force
N_x, N_y	number of bents
H	applied lateral load
T	applied torque
X_H, Y_H	distance of applied lateral load from the reference point

LIST OF SYMBOLS (continued)

R	resisting torque
A	coefficient matrix
δ	displacement vector
b	load vector
K	conditioning number

Computer Program Notation

A complete listing of the notation used in the computer program is presented in SECTION A.3 of APPENDIX A.

CHAPTER I

INTRODUCTION

A typical arrangement used for contemporary multi-story
buildings is shown in FIGURE 1.1. The structure consists of a service
core, surrounded by, and coupled to, a three dimensional space frame.
The service core is commonly formed by several open or "semi-closed"
reinforced concrete shear walls.

Because of the complexity of such structures it has been
common practice to analyze the structure as a number of planar bents,
such as that shown in the elevation in FIGURE 1.1. The lateral load
to be resisted by a particular bent is based on its tributary area; or
alternatively; on the stiffness of the bent relative to that of the
complete structure. The selection of member sizes for a particular
bent would normally proceed on the basis of allowable stress criteria.

The introduction, and consequent adoption, (1,2), of plastic
strength methods provides a more rational approach to structural design.
Load factors are selected to ensure the attainment of a particular col-
lapse load. In addition, the deflections of the structure are checked
under the working load conditions. Because of the increase in economy
that results from a consideration of the inelastic action, plastic de-
sign methods are gaining increasing acceptance (13).

In tall slender structures the secondary effects of axial load

1

may become of primary concern (3). Simple plastic theory does not consider stability effects. However, many computer oriented analyses have been developed for predicting the collapse loads of tall planar frames (4,5,6,7). These analyses considered various axial load effects, such as; member shortening, changes of member stiffness and finally the additional overturning moments produced by the gravity loads acting on the displaced structure. Because the inelastic behavior of a structure depends on the loading history, incremental load procedures were employed to trace the behavior of the structure up to its ultimate load. These procedures detect, and modify the structure for, successive yield violations. The behavior of the structure is depicted by the load-displacement curves shown in FIGURE 1.2. In FIGURE 1.2 the load factor, λ, is plotted against a characteristic displacement, Δ. The dashed curve presents the response for a structure where the secondary moments have been ignored. This curve approaches the load corresponding to the formation of a mechanism in the structure. In the solid curve, the effect of the secondary overturning moments reduces the collapse load, as well as the stiffness of the structure. The mechanism condition is generally not reached until after the ultimate load has been attained and the structure is unloading.

The presence of shear walls, which have finite width and large stiffnesses, relative to those of the frame members, modifies the response of a real structure. The shear deformation of the frame must be compatible with the cantilever type of deformation of the shear

wall. Analyses for coupled frame-shear wall structures, which consider the resulting interaction, have been presented (8,9).

The above methods imply that all bents in the structure translate only in the plane of the applied loads. This condition is rarely met. Rotation of floor diaphragms due to asymmetry of structural layout and/or loading is unavoidable. The resulting complex interaction between stiffening elements cannot be predicted by a planar analysis.

First order elastic analyses, which consider the out-of-plane and twisting action of coupled frame-shear wall structures, are available (10,11,12). Results obtained by these methods indicate that increasing asymmetry will develop between the lateral load and center of stiffness as loading progresses. External bents undergo larger displacements, resulting in earlier formation of plastic hinges, thus reducing the bent stiffness and shifting the center of stiffness of the structure. The complete load-displacement relationship must therefore be predicted to rationally assess the ultimate load capacity of actual structures.

The large number of unknowns, together with the number of separate analyses necessary to trace the progression of inelastic behavior, has retarded the development of procedures to predict the complete response. This dissertation will present a second-order elastic-plastic analysis for three dimensional, coupled frame-shear wall, structures. The method is computer oriented, and is suitable for the analysis of large structures.

Extensive analytical and experimental work has been performed to investigate the behavior of multi-story structures. A review of that work, applicable to this dissertation, is presented in CHAPTER II. The main aspects considered are; the behavior of biaxially loaded beam columns, the behavior of shear walls, and the methods of predicting the load-displacement response for planar frames and complete structures.

By considering the floor diaphragms to be infinitely stiff (in their own planes) each floor of the structure has only three degrees of freedom. Further simplification is obtained by lumping the members within each bent, thus replacing the actual structure by a simplified analytical model. The simplifying steps, and the assumptions regarding member behavior are outlined in CHAPTER III.

The displacement method of analysis, developed in CHAPTER IV, is based on the slope-deflection equations. Equilibrium is formulated on the deformed structure, thus considering the overturning, due to the vertical loads. Shear deformations, axial shortening, and changes in axial load are neglected. The slope-deflection equations are modified in the presence of plastic hinges. An incremental loading procedure is used, which locates the plastic hinges individually in their order of formation.

The analysis has been programmed for the computer. Algorithms and flow diagrams are presented in CHAPTER V. Because of symmetry only one half band of the coefficient matrix is stored. The equations are

solved by a modified Gauss Elimination technique.

To verify the accuracy of the procedure, several structures have been analyzed and the results compared with those previously reported in the literature. This is discussed in CHAPTER VI.

The influence of various parameters on the response of three dimensional structures is considered in a behavioral study, which forms CHAPTER VII. Particular attention is paid to the effect of the assumptions made, their validity and the influence of asymmetry of load and structural layout.

In CHAPTER VIII the results from the behavioral study are presented and discussed. The influence of lumping within a bent is considered. A method is presented which will modify the analysis to consider non-uniform torsion for those shear walls where warping is restrained.

CHAPTER IX presents the limitations of the method of analysis and discusses the accuracy of the computer program. Consideration is given to utilizing the program in design. Recommendations are made regarding the conditions under which the torsional displacements may become of primary concern.

ELEVATION AA

PLAN
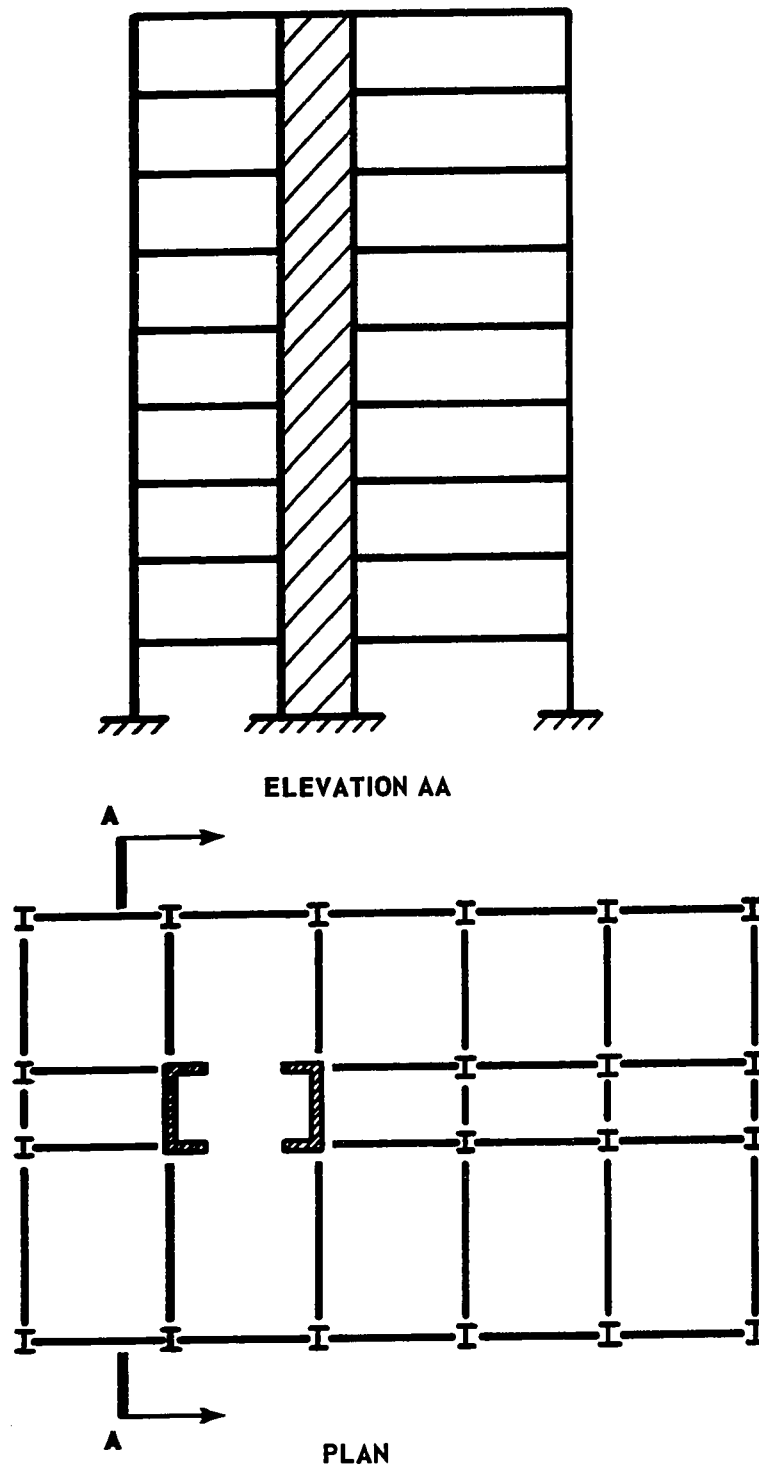
FIGURE 1.1 TYPICAL THREE DIMENSIONAL BUILDING
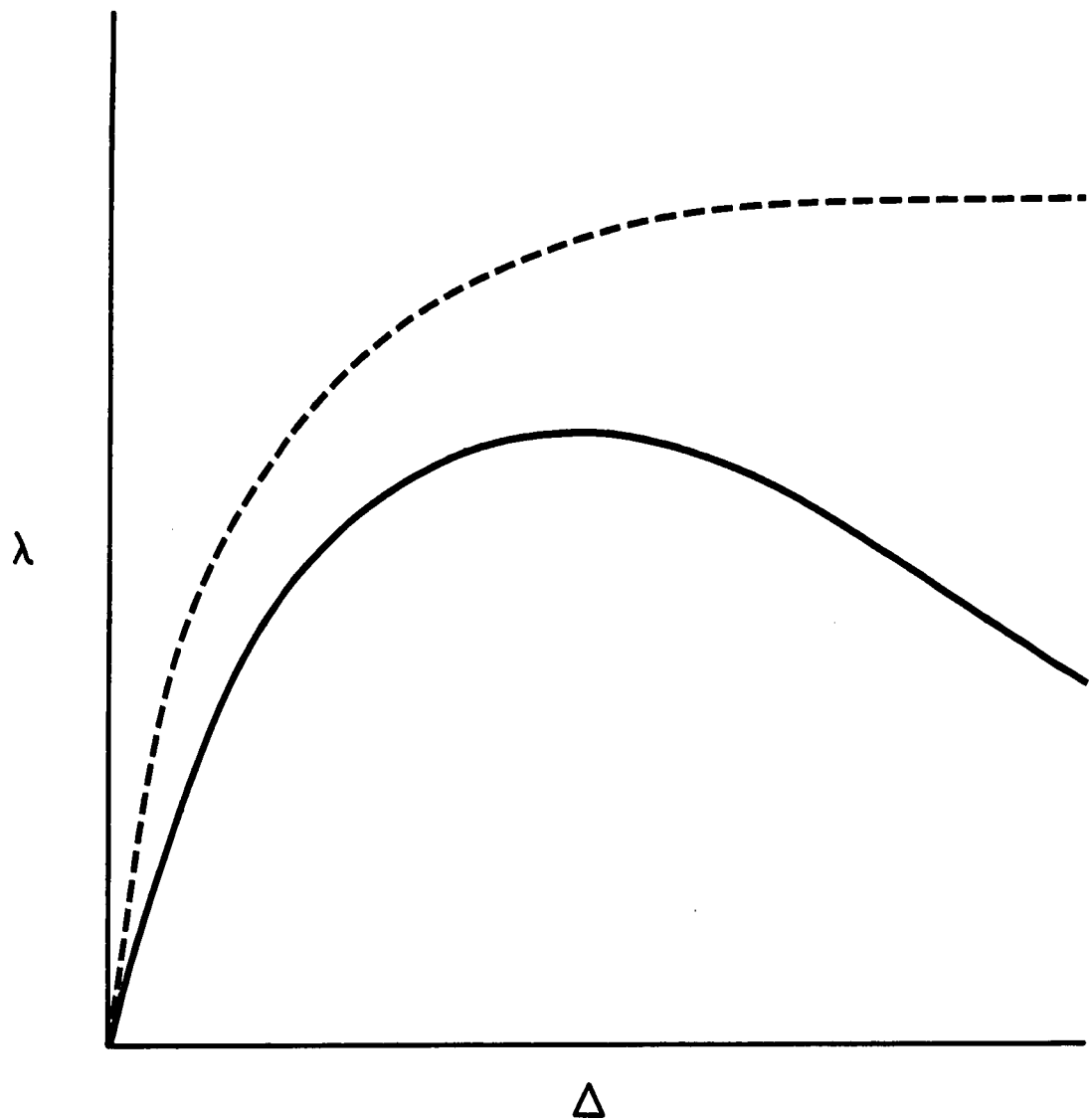
FIGURE 1.2 LOAD-DISPLACEMENT RESPONSE

CHAPTER II

REVIEW OF PREVIOUS INVESTIGATIONS

2.1 Introduction

The review is limited to investigations related to the behavior and analysis of, three dimensional structures and their component elements. The review of component behavior will include; biaxial bending of beam columns, bending and torsion of open and semiclosed shear walls, and the interaction of coupled frame-shear wall bents. The methods of determining the collapse loads of planar bents and three dimensional structures will also be briefly reviewed. Code requirements, as to loads, and methods of load distribution to the stiffening elements will also be considered.

2.2 Beam Columns

In a building frame a beam column may be subjected to an axial load, bending moments about both axes and twisting forces. The column ends may or may not be permitted to translate and twist. The forces on the individual members must be in equilibrium and the deformations of the member ends must be compatible with the surrounding structure. No solution exists to predict the behavior of wide flange beam columns deformed into the inelastic range under these conditions.

The behavior of wide flange beam columns subjected to uni-

axial bending (both strong and weak axis) has been well documented (47). The basic building block in beam-column analysis is the Moment-Thrust-Curvature (M-P-ϕ) relationship for the cross section. Moment-Thrust interaction relationships are established from analyses of individual members, with the end moment ratio and effective column length as parameters (14,15). These serve to define solutions for the limiting case of biaxial bending, where the moment about one of the principal axes is equal to zero.

A review of the past investigations (analytical and experimental) performed on the biaxial bending of beam columns is presented by Chen and Santathadaporn (16). Most of the work to date (September 1970) deals with isolated columns subjected to biaxially eccentric loads. Baker et al (15) reported the results, obtained in 1950 by Roderick (18), of a series of tests on elastically restrained columns bent in single curvature about both principal axes. For both rectangular and I shaped cross sections failure occurred by bending about the weak axis, without any noticeable twisting of the cross-section. However, the columns were connected to heavy end plates, which would restrict warping and contribute to the torsional stiffness of the column. Nine cases of column loading were considered, ranging from the pin ended column to the more general case of a biaxially loaded column with elastic restraints at both ends. Approximate design rules are presented for each case. Milner (46) performed an analytical and experimental study of restrained biaxially loaded H columns. A nu-

merical integration procedure was used for solving the equations of equilibrium. The order of load application had a significant effect on the failure load. The predicted maximum loads agreed closely with those obtained in the experimental program.

Harstead et al (17) presented a numerical procedure for predicting the ultimate strength of biaxially loaded isolated H columns. The analysis assumes that the material is elastic-perfectly plastic and that the load is applied with equal eccentricities at both ends. Various degrees of warping restraint at the column ends may be considered. The predicted results compared closely with experimental values. The warping restraint increased the ultimate carrying capacity of the members. It was also concluded that the residual strains had a considerable influence on the response of isolated columns.

Sharma and Gaylord (19) assumed a sinusoidal shape for the lateral displacement and twist of the cross section. The equilibrium conditions for the deformed member were enforced only at the ends and mid-height of the column. The results compared favorably with those obtained by the more exact method of Harstead et al (17).

Although the above methods provide a good indication of the ultimate strength of the column, they are not suitable for incorporation into an analysis of three dimensional structures. In the analysis of planar structures the use of an interaction equation, relating the axial load to the reduced plastic moment capacity, has proved satisfactory (5,6). Drucker (20) states that, interaction curves are not

unique and depend on the loading condition along the entire length of
the member. Despite this, Santathadaporn and Chen (21) point out that
the use of interaction curves is warranted since present design pro-
cedures (22), neglect completely the biaxial bending effect. The upper
and lower bound theories of limit analysis are applied to obtain in-
teraction curves for wide flange sections. The lower bound theory re-
sults in interaction curves similar to those obtained previously by
Pfrang and Toland (23).

Interaction curves are correct only for columns of zero
length and do not take into account the effect that change of geometry
may have on equilibrium. Despite this, interaction curves can easily
be used in the elastic-plastic analysis of three dimensional structures.
If desired, a more complete investigation may then be performed on
critical individual columns within the structure, using the results of
the overall analysis. This procedure will ensure that the predicted
load capacity is maintained throughout the range of deformation required
for the entire structure to reach its ultimate load.

2.3 Shear Walls

Two factors distinguish the behavior of shear walls from that
of columns. First, the high ratio of wall to beam stiffness causes the
displacements in a particular story to be highly dependent on the dis-
placements in the stories above and below. This results in a canti-
lever type of deformation for the free shear wall as opposed to a
shear (portal) type of deformation for a column. Secondly, the width

of the shear wall is generally of the same order as the story height;
consequently as the wall rotates the adjacent floor beams undergo a
sway displacement. This increases the rotational restraint of the
beam on the wall.

Methods have been proposed for the analysis of shear walls
with one or more rows of openings (24,25,26). In these methods the
beams, formed by the openings, are treated as an equivalent elastic
medium, distributed along the story height. The problem can then be
formulated as a second order differential equation. The assumptions
generally made in the solution require that the walls, link beams and
story height are uniform throughout the structure. Girijavallabhan (27),
however, has applied a finite element technique to the analysis of
shear walls with openings. This provides a better indication of the
stress distribution, particularly in the areas where the beams, join
the wall.

Rosman (28) presents an elastic analysis for symmetric three
dimensional performated shafts subjected to an arbitrary torsional load.
The solution combines the solution for the bending and torsion of thin
walled bars with that for the bending of pierced shear walls (26). The
peripheral stiffening elements of the building are ignored and the beams
linking the walls are replaced by a continuous lamella. The system is
then singly indeterminate with a function representing the angle of
twist along the height of the shaft being used as the unknown.

2.4 Planar Bents

The behavior of planar bents was investigated extensively during the sixties. Many factors influence the response of planar bents. The axial loads in the various members influence the carry over and stiffness factors; these must be continually revised as the structure is loaded. When the yield condition is violated at particular locations in the structure, the overall stiffness is reduced. Both these factors result in increased displacements and a consequent increase in the overturning moments due to the vertical loads. The presence of strain hardening in a real structure, however, permits the development of a finite yielded zone and limits the magnitude of the plastic flow. The response of planar bents may be further complicated by the presence of shear walls. Because of their high stiffness and finite width the cantilever type of deformation of the walls modifies and must be compatible with the shear type of deformation of the frame elements.

2.4.1 Uncoupled Frames

An extensive literature survey on the stability of frames was presented by Le-Wu Lu (3). Particular attention was given to the methods of determining the buckling loads of partially plastic frames.

Parikh (5) applied the slope-deflection equations to obtain a second order elastic-plastic analysis procedure for frames subjected to vertical and lateral loads. Plastic hinges were assumed to form at discrete points, when the yield condition was violated. Hinges were in-

serted at the particular locations and the structure analyzed under the next increment of load. The procedure was continued until the maximum load was reached.

Davies (4) used a displacement analysis to determine the maximum load. The matrix solution was adopted from earlier work presented by Jennings and Majid (32). An incremental loading procedure was used to locate successive plastic hinges. The response of the structure (in a given increment) is linear since the axial loads are assumed to remain constant in this interval. The load increment required to raise the moment, at each elastic section, to the corresponding plastic moment value was computed at each step of the analysis. The minimum value of the load increment was then added to the previous load in order to locate the next hinge. Corresponding moment increments were added at the remaining elastic sections. If hinge unloading is detected, the analysis treats the particular section as elastic, but carrying a rotational discontinuity. Instability is defined by a change of sign in the determinant of the stiffness matrix. The determinant is recalculated as successive hinges are inserted in the structure.

A similar technique for defining collapse was adopted, in a study on planar frames, by Korn and Galambos (6). In this study it was concluded that although axial deformations may substantially alter the structure sways at working loads, at collapse the increases in deflection, due to axial deformations, are less significant. The maximum load capacity was not affected greatly by axial deformations. Curvature shorten-

ing had a negligible effect on the frame behavior.

2.4.2 Coupled Frames and Shear Walls

Khan and Sbarounis (33) used an analytical model as the basis of a first-order elastic analysis of coupled structures, which considers the interaction between frame and shear wall elements. The frames and shear walls in a structure are lumped into an equivalent frame and shear wall. The entire lateral load is applied to the wall and its deflected position calculated. The loads necessary to force the frame to assume the same deformation are calculated, and the loads on the wall are modified until the frame and shear wall are compatible, and in equilibrium.

A similar model was used by Guhamajumdar et al (8) for a second-order elastic-plastic analysis. As well as lumping member stiffnesses the plastic moment capacities are also lumped. In the case of columns the plastic moment capacities are reduced in accordance with the Moment-Thrust interaction relationships (34). The effect of vertical loads is considered by applying an equivalent lateral load to the structure (48). In applying the method, the entire structure is lumped into a single equivalent bent, consequently it is assumed that all bents translate equal amounts and no allowance is made for twisting of the floors.

Clark and MacGregor (9) used a deformation method to solve for the second-order elastic-plastic response of planar bents. The analysis includes allowances for axial shortening as well as the effect

of the axial loads on the member stiffness. The equilibrium equations are formulated on the deformed structure and are solved by an iterative procedure.

2.5 Three Dimensional Structures

In actual structures the floor diaphragms possess relatively large stiffnesses in their own planes, thus each floor has basically three degrees of freedom. Translation may occur in the two principal directions and the structure may rotate about its vertical axis. The distribution of shear to the stiffening elements is dependent on the layout of the structure, the point of load application and the interaction between the various structural elements. Resistance to translation and rotation of the structure is provided by the flexural stiffnesses of the elements and the torsional stiffness of the columns and shear walls.

It has been common practice to analyze three dimensional structures as a series of planar bents. A problem arises as to what portion of the total lateral load to assign to a particular bent. For elastic analyses recommendations were made that based this distribution on equilibrium of moments in the plane of the floor diaphragm (29,30). For buildings that exhibited reasonable symmetry the load has also been distributed on the basis of the area tributary to the bent. Alternatively, providing the layout and loading do not result in twisting of the floor diaphragm, it is possible to analyze an entire structure by enforcing equal lateral displacements on all bents.

2.5.1 Uncoupled Frames

Weaver and Nelson (35) have developed a first-order elastic analysis for three-dimensional structures, using a stiffness approach. As both axial shortening and torsional deformations are considered, the member stiffness matrices are 6 by 6 for the beams and 12 by 12 for the columns. The member stiffness matrices are transformed into a floor stiffness matrix and the resulting equilibrium equations are solved by a forward elimination process, starting at the top of the structure and working to the base, where it is assumed that column ends are fixed. This permits all the floor displacements to be obtained by back-substitution (floor by floor) and member forces are obtained by multiplying the member stiffness matrices by the corresponding displacements. For an example structure of 20 stories and a height to width ratio of 10, the neglect of axial strains in the columns resulted in considerable errors (20 percent for the floor translations).

Before an elastic-plastic analysis procedure can be developed interaction relationships must be established to represent the member response. The introduction of a third parameter, M_y, in the Moment-Thrust equations complicates considerably the relationship among the axial load, P, and the bending moments, M_x and M_y, about the principal x and y axes.

Harrison (37) investigated the biaxial bending of rectangular sections (38) and extended the approach to predict the maximum load carrying capacity of simple space frames. The predicted ultimate loads

agreed with failure loads obtained in model tests. The model frames
consisted of three rectangular columns, linked by beams, in an L shaped
plan. Bruinette (36) has also formulated a first-order elastic-plastic
analysis for space frames, first developing yield surfaces, in terms
of stress resultants.

Jonatowski and Birnstiel (39) presented a second-order
elastic-plastic analysis for space frameworks. The biaxial moment-
axial force interaction relationships developed by Santathadaporn and
Chen (21) were used in the program. The equations are formulated in
matrix displacement form. Allowance is made for the non-linear ef-
fects caused by the axial loads by using successive corrections to
account for the out of balance forces due to the joint displacements (40).
A similar iterative procedure has been used by others (8). The plastic
moment capacities of the members are revised at the start of each load
increment and are held constant for the convergence cycle. Loads are
applied only at the joints.

2.5.2 Coupled Frames and Shear Walls

Gluck (41) has extended the technique used to analyze pierced
shear walls to coupled frame-shear wall structures. The frame is re-
placed by a continuous elastic medium which is assigned lateral stiff-
nesses in the two principal directions and a torsional stiffness. In
calculating the properties of this elastic medium, points of inflection
are assumed at mid story height. The equilibrium of the system is ex-
pressed as three nonhomogeneous differential equations in terms of the

displacement functions. The displacement functions are assumed to be continuous throughout the height of the structure. The differential equations are applicable only in a region of constant member properties. Where the member properties are not uniform, equilibrium equations are written for each zone having uniform properties. The boundary conditions are satisfied at the zone junctions and the differential equations are solved for the particular form of loading applied to the structure. The contributions of both pure and warping torsion are considered in calculating the torsional stiffness of the walls. Excellent agreement was obtained between the results of this method and those obtained from a computer solution developed by Clough, King and Wilson (10).

Results of analyses presented by Winokur and Gluck (11), and Wynhoven and Adams (12) have shown that a redistribution of shears occurs among the various stiffening elements during the application of load. This redistribution is most significant when the layout and/or loading is asymmetric and in many cases cannot be ignored. Indeed, as the structural stiffness changes (as a result of yielding), the asymmetry, between the center of rigidity of the structure and the point of application of the load, may be increased. This aggravates the problem.

A method is not available to predict a first or second-order elastic-plastic response for three dimensional, coupled frame-shear wall structures.

2.6 Structural Failures and Code Requirements

In reports of structural failures of multi-story buildings reference is often made to the observed modes of collapse (42). Catastrophic failures due to torsional displacements have occurred during earthquakes (43). Exterior members are subjected to larger relative floor displacements as a result of the torsional motion. The center of rigidity and the center of mass in these cases did not coincide and mention has been made of the change in stiffness distribution as collapse progressed.

Building codes and design manuals reflect the severity of the problem. Canada (44) requires that torsional effects be included in regions where earthquake loading is considered. In California (45) the shear assumed to be resisted by external bents must be increased to account for the torsional effects caused by earthquakes.

2.7 Summary

A brief review has been presented of the work leading up to the elastic-plastic analysis of three dimensional structures. Tools are available to develop an analysis for coupled frame-shear wall structures. Many contemporary multi-story structures would fall into this classification. Structural failures have indicated that more attention must be paid during design to torsional deformations.

The complete load-displacement relationship for the structure must be predicted in order to rationally predict the ultimate strength and to obtain a knowledge of the energy absorption capacity of the

structure, and the lateral displacements at various load levels.

This dissertation presents such an analysis. Simplifying assumptions are made in order to analyze relatively large structures. The effects of these assumptions are checked and, where required, allowance can be made for the influence of the assumptions in the design process.

CHAPTER III

ANALYTICAL MODEL

3.1 Introduction

In an actual structure each stiffening element has 12 degrees of freedom (35). Thus, the number of degrees of freedom for a structure is equal to 6 times the product of the number of stiffening elements and the number of stories. In analyzing the structure each degree of freedom requires one equilibrium equation. When lateral load is applied the axial force in each member varies so that the carry over and stiffness factors are continually changing. In addition, as the response enters the inelastic range the relationships between end forces and displacements also change. It is apparent, therefore, that the number of equations and the need to continually revise the coefficients as the loading progresses, makes the application of a "rigorous" analysis to large structures difficult.

However, the analysis of the structure may be simplified greatly because of the following assumptions:

(a) Floor slabs link the stiffening elements at each floor level; the slabs behave as deep beams with extremely high stiffnesses. Consequently the floor diaphragms deform as rigid bodies with only three degrees of freedom (in their own planes).

(b) Beams linking columns and walls have negligible torsional stiffnesses relative to their bending stiffnesses.

(c) Structural arrangements are generally regular so that within each bent the joints at a particular floor level undergo similar rotations on the application of load.

By applying the above conditions to a real structure the number of degrees of freedom may be considerably reduced. Further idealizations may be made. Because of the low slenderness ratio of most stiffening elements the influence of changes of axial load on the carry over and stiffness factors is negligible. Furthermore, the total vertical load on a structure does not vary greatly during the application of lateral load, so that the increase in axial load in some of the stiffening elements is accompanied by a corresponding decrease in axial load in other elements. And finally, the behavior of members may be idealized by assuming an elastic-perfectly plastic response.

The above simplifications can be used to reduce the real structure to an analytical model, whose behavior closely follows that of the real structure. However, in the model, the number of degrees of freedom have been considerably reduced and the member forces may be expressed as linear functions of the displacements. It will now be possible to analyze large structures and study the influence of the important factors on the response.

3.2 Structure Representation

The structural arrangement is defined with respect to a system of co-ordinate axes X, Y and Z, shown in FIGURE 3.1. The displacements, u and v, are positive in the positive X and Y directions, respectively, and the rotation about the vertical or Z axis, ϕ, is positive in accordance with the left hand screw rule. An arbitrary point, O, is chosen, which forms the origin of the co-ordinate system. The structure consists of bents lying in the XZ or YZ planes.

In the analysis it is assumed that;

(a) Each floor diaphragm is infinitely stiff in its own plane but offers no resistance to forces applied perpendicular to the plane.

(b) The beams possess negligible torsional stiffnesses.

(c) The axial shortening of beams, column and wall elements, is negligible.

(d) The member response is elastic-perfectly plastic.

These assumptions effectively reduce the three dimensional structure to a series of intersecting planar bents, as shown in FIGURE 3.2. Each bent resists only in-plane loads. The columns and walls, however, provide torsional resistance as well as resisting the in-plane bending moments and axial loads.

The floor diaphragm has three degrees of freedom, defined by displacements u_o, v_o and ϕ at the reference point. The displacements of each bent may be expressed as follows:

$$u_{ji} = u_{oi} + y_j \cdot \phi_i \qquad (3.1)$$

$$v_{ji} = v_{oi} - x_j \cdot \phi_i \qquad (3.2)$$

where u and v are displacements in the X and Y directions, x and y locate bent j, and i refers to the particular floor. EQUATIONS (3.1) and (3.2) are coupled through the rotation, ϕ.

3.3 Lumping Procedure

To further simplify the analysis each bent is replaced by a simplified equivalent bent. At each floor level it is assumed that, within each bent, all beam to column joints and all beam to wall joints have equal rotations. Thus the equivalent bent has two joint rotations per floor (this is reduced to a single rotation if the bent does not contain a wall). Guhamajumdar et al (8) used this procedure to analyze symmetric structures; in fact, in this analysis the entire structure was lumped into a single equivalent bent. The original and lumped arrangements of a frame bent and a coupled frame-shear wall bent are shown in FIGURES 3.3 and 3.4 respectively.

3.3.1 Beams

For a coupled frame-shear wall bent, the beams linking the wall to the columns are lumped into a single beam, referred to as a wall beam. The beams linking one column to another are lumped into a single, equivalent beam, referred to as a frame beam. Because the ro-

tations at all beam to column joints are assumed equal, a point of inflection occurs at mid span of the frame beam. In the equivalent bent shown in FIGURE 3.4 the free end of the frame beam is placed on a pin ended roller to simulate the point of inflection.

The properties of the lumped beams are as follows;

$$L = \frac{1}{2 \times n} \cdot \sum_{m=1}^{n} L_m \tag{3.3}$$

$$L_b = \frac{1}{n_b} \cdot \sum_{m=1}^{n_b} L_{bm} \tag{3.4}$$

$$k_i = 2 \cdot \sum_{m=1}^{n} k_{mi} \tag{3.5}$$

$$k_{bi} = \sum_{m=1}^{n_b} k_{bmi} \tag{3.6}$$

where L, L_b, k_i and k_{bi} are the properties of the lumped equivalent bent, n and n_b are the number of column to column, and column to wall spans respectively, m refers to properties of members before lumping, L is the span length, k is the stiffness (I/L) and i refers to a particular floor. The factor 2 in EQUATIONS (3.3) and (3.5) is derived from the fact that only half the equivalent frame beam is represented in the lumped model. Consequently, the span length is halved and the moment of inertia is doubled as is the plastic moment capacity in EQUATION (3.7).

The plastic moment capacities of the lumped beams are,

$$M_p = 2 \cdot \sum_{m=1}^{n} M_{pm} \qquad (3.7)$$

$$M_{pb} = \sum_{m=1}^{n_b} M_{pbm} \qquad (3.8)$$

where M_p and M_{pb} are the plastic moment capacities for the frame and wall beams, respectively.

The axial force in the beams is neglected. The lumping of the plastic moment capacities is only valid if no transverse load is applied to the beams. The influence of this assumption and the manner in which the error may be reduced to a minimum, when transverse loads are present on the beams, has been considered by Nikhed (51).

For the case of lumping an uncoupled bent (FIGURE 3.3), EQUATIONS (3.4), (3.6) and (3.8) are not applicable.

3.3.2 Columns

The stiffness of the equivalent column, k_{ci}, is obtained by the following summation,

$$k_{ci} = \sum_{m=1}^{n_c} k_{cmi} \qquad (3.9)$$

where k_{cmi} is the column stiffness of an individual column in the original frame, i is the particular story and n_c is the number of individual columns in the original frame.

It is assumed that the interaction equations for wide flange sections subjected to an axial force and biaxial bending moments may

be represented by the dashed lines in FIGURE 3.5. The plastic moment capacities for bending about the x and y axes, have been divided by the plastic moment capacities in the absence of biaxial bending; the interaction between the non-dimensionalized plastic moment capacities, m_x and m_y, respectively, are plotted for various ratios of P/P_y. The curves obtained by Santathadaporn and Chen (21) are shown as solid curves in FIGURE 3.5. The differences between the two sets of curves are most noticeable at low axial load ratios. For values of P/P_y above 0.5, the approximations are fairly close to the rigorous curves, especially when bending about one axis dominates. Neglecting the influence of biaxial bending (dashed line in FIGURE 3.5), the plastic moment capacity of the column is reduced, in accordance with the following equations, for strong axis bending, (47):

$$M_{pc} = M_p \cdot 1.18 \cdot (1 - \frac{P}{P_y}) \qquad 0.15 < \frac{P}{P_y} < 1.0 \qquad (3.10)$$

$$M_{pc} = M_p \qquad 0.0 \leq \frac{P}{P_y} \leq 0.15 \qquad (3.11)$$

and

$$M_{pc} = M_p \cdot 1.19 \cdot (1 - (\frac{P}{P_y})^2) \qquad 0.4 < \frac{P}{P_y} < 1.0 \qquad (3.12)$$

$$M_{pc} = M_p \qquad 0.0 \leq \frac{P}{P_y} \leq 0.4 \qquad (3.13)$$

for weak axis bending. In EQUATIONS (3.10) to (3.13), and in FIGURE 3.5

P represents the axial force in the column, P_y is the yield load and M_p is the plastic moment capacity in the absence of axial load. The above expressions are based on the equilibrium of the fully plasticized cross section of the column, and thus denote the limits of the biaxial interaction relationship. The reduction in moment capacity due to the stability effect is insignificant provided that the slenderness ratio is below 80 and the column is in double curvature with an axial load ratio of 0.60 or less (49). For heavily loaded, slender columns a more exact analysis which includes the slenderness effects, may be required.

The plastic moment capacity, M_{pci}, for the lumped column is given by,

$$M_{pci} = \sum_{m=1}^{n_c} M_{pcmi} \qquad (3.14)$$

where M_{pcmi} is the plastic moment capacity, of the individual columns of the original frame, reduced in accordance with EQUATIONS (3.10) to (3.13) where applicable.

3.3.3 Shear Walls

The analysis of structures containing shear walls is complicated by the cross-sectional shape. Most shear walls have open cross-sections but the shape is maintained by a stiff diaphragm at each floor level. Often the shear center of the wall cross-section does not lie in the plane of the bent but in the present analysis it is assumed that

the shear center and the plane of the bent do coincide.

The total torsional resistance, M_t, of thin walled open sections may be expressed as: (47)

$$M_t = C_T\phi' - C_\omega\phi'''$$ (3.15)

where $C_T = G K_T$ and $C_\omega = EI_\omega$, and ϕ' and ϕ''' are the first and third derivatives of the rotation, ϕ, with respect to the length. G and E represent the modulus of rigidity and the modulus of elasticity respectively while K_T and I_ω denote the torsional and warping constants of the section respectively.

In the analysis it is assumed that;

(a) The angle of twist per unit length, ϕ', is constant through-out the story height of a column or wall segment.

(b) The St. Venant torsional resistance, GK_T, remains constant throughout the loading history.

(c) The contribution of the warping resistance, EI_ω, is neglected.

Since the warping resistance is neglected the torsional resistance can be expressed as a linear function of the displacements. In designing the lower stories of the walls, however, allowance must be made for the extra shear and normal stresses that will result due to the warping action.

The C_T value for the lumped model is equal to the sum of the C_T values for all of the vertical elements in the structure.

The flexural stiffness of the equivalent wall, k_{wi}, is obtained by the following summation,

$$k_{wi} = \sum_{m=1}^{n_w} k_{wmi} \qquad (3.16)$$

where k_{wmi} is the stiffness of an individual wall in the original bent, i is the particular story and n_w is the number of individual walls in the original bent. The width of the equivalent wall, L_w, is equal to the average of the widths of the individual walls.

The plastic moment capacity of individual walls is obtained by applying ultimate strength theory (50) to each wall cross-section. Allowance is made for the presence of axial load, where necessary. The plastic moment capacity, M_{pwi}, of the equivalent wall is obtained by the following summation,

$$M_{pwi} = \sum_{m=1}^{n_w} M_{pwmi} \qquad (3.17)$$

where M_{pwmi} is the ultimate moment capacity, of an individual wall in the original bent.

3.4 Loading

The lateral loads applied to the structure are specified as concentrated loads acting in the planes of the floor diaphragms. The load may be applied in either or both co-ordinate directions.

The overturning effect caused by the vertical loads, is con-

sidered by applying an equivalent shear in each story of a particular bent. This additional shear, V_{ji}, is given by,

$$V_{ji} = \frac{P_{ji} \cdot \Delta_{ji}}{h_i} \qquad (3.18)$$

where P_{ji} is the vertical load in story i of bent j, Δ_{ji} is the story sway displacement, expressed by EQUATIONS (3.1) and (3.2), and h_i represents the story height.

3.5 Summary

An analytical model has been described that considerably reduces the effort involved in the solution of large structural systems. In the model, internal resisting forces are expressed as linear functions of the structural displacements. The technique used to analyze the model will be described in CHAPTER IV.
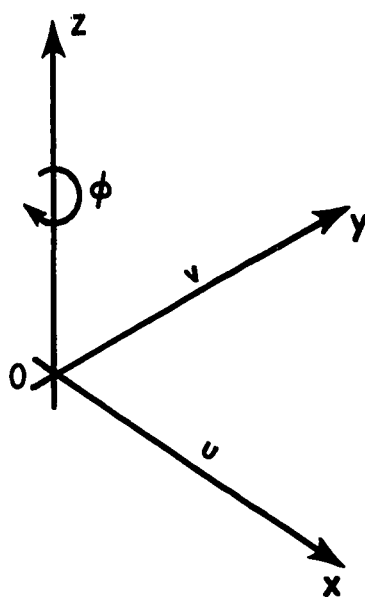
(a) CO-ORDINATE AXES
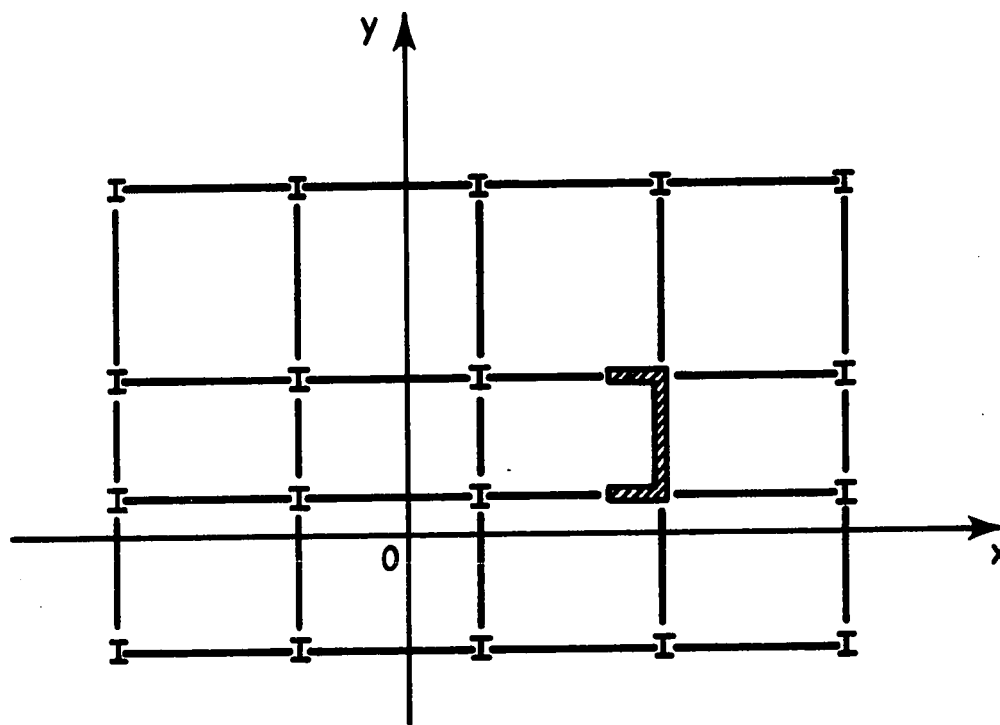
(b) STRUCTURAL ARRANGEMENT

FIGURE 3.1 ARRANGEMENT AND CO-ORDINATE SYSTEM
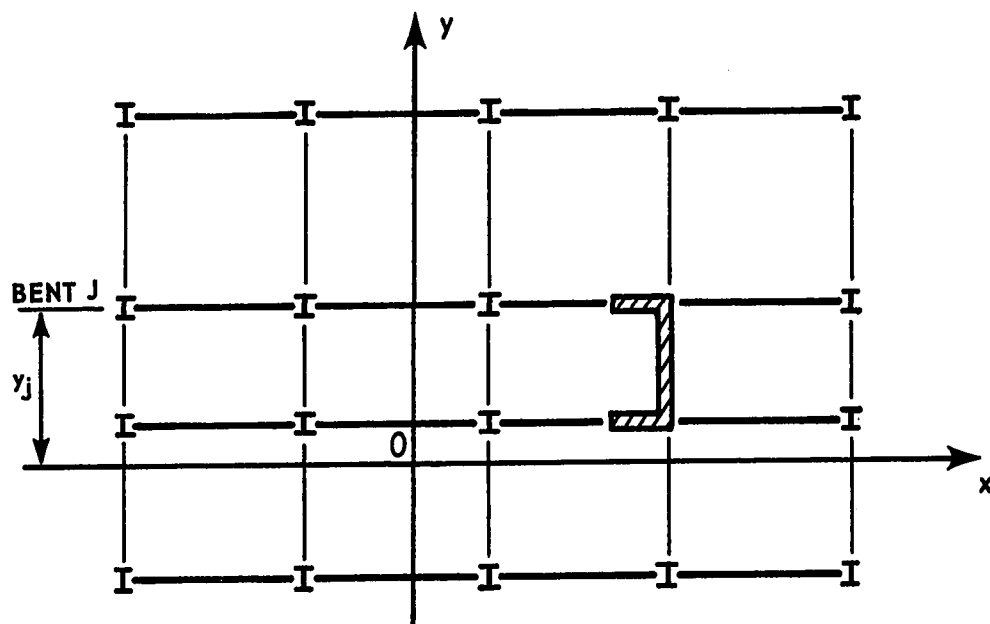
(a) X BENTS
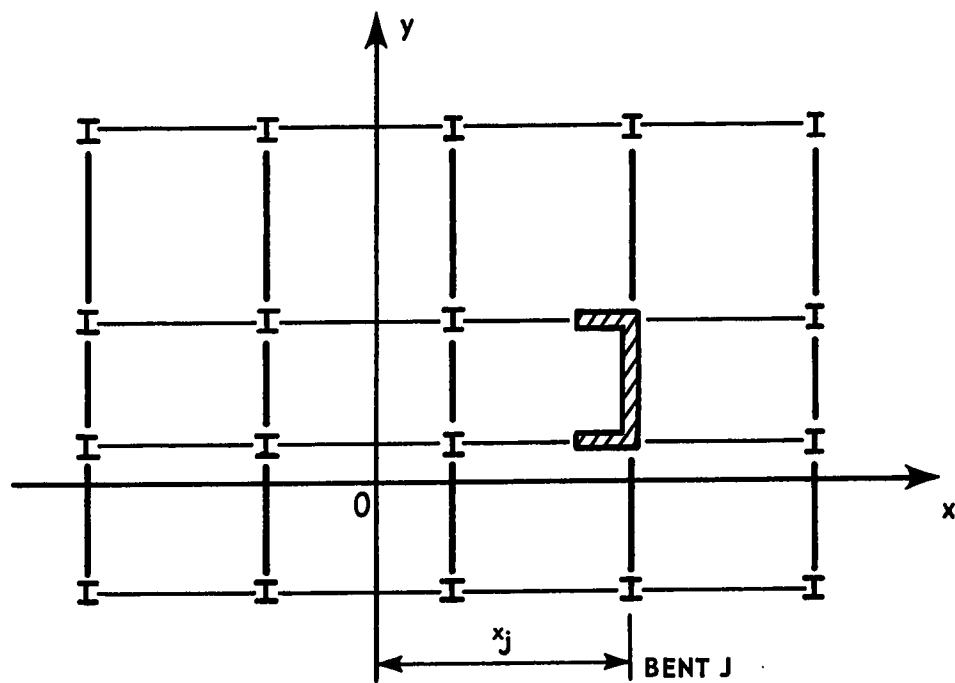
(b) Y BENTS

FIGURE 3.2 SYSTEM OF PLANAR BENTS
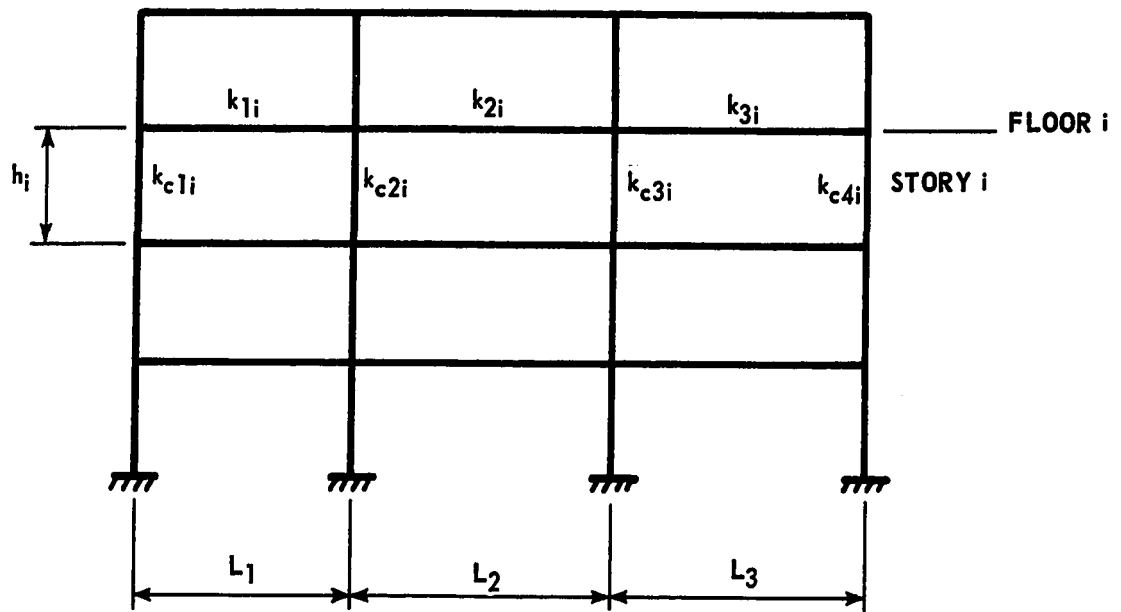
(a) PLANAR BENT
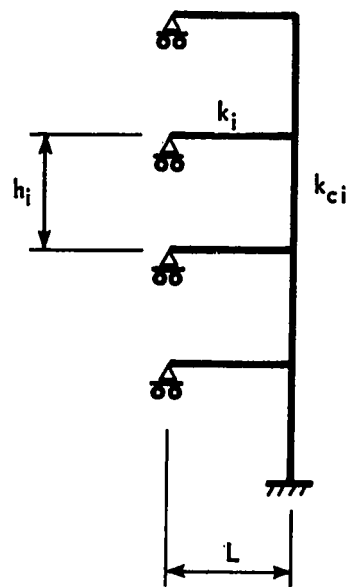
(b) EQUIVALENT BENT

FIGURE 3.3 UNCOUPLED BENT
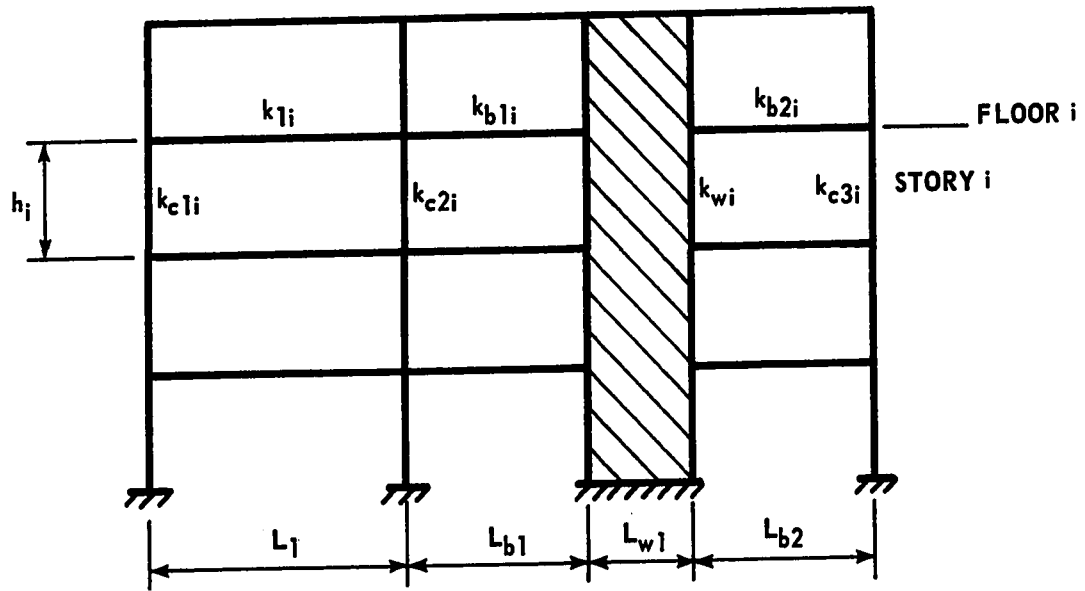
(a) PLANAR BENT
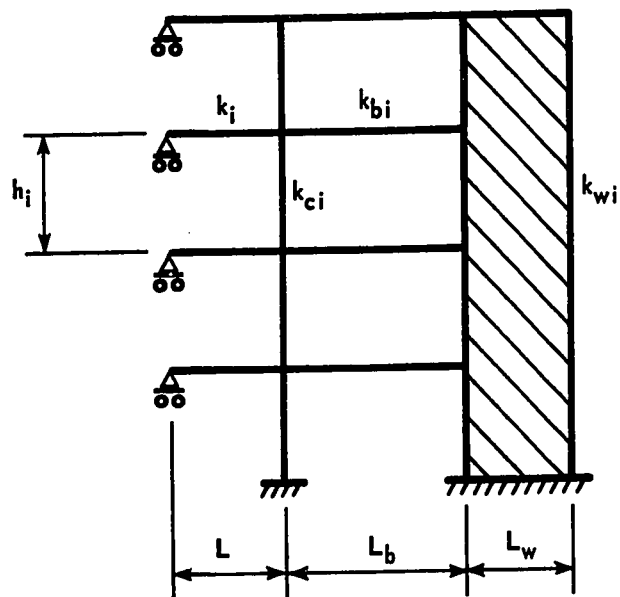
(b) EQUIVALENT BENT

FIGURE 3.4 COUPLED FRAME-SHEAR WALL BENT
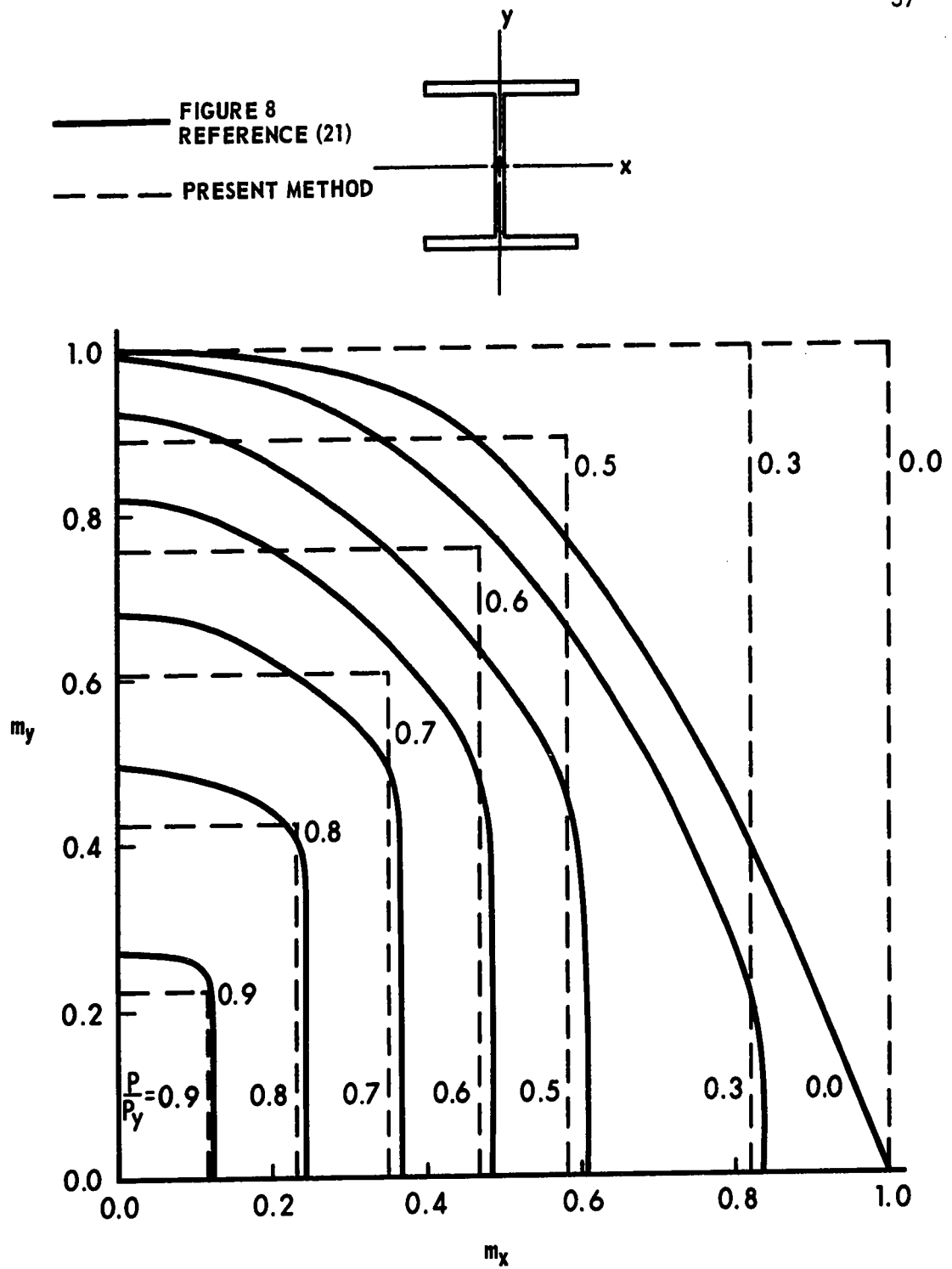
FIGURE 3.5 BIAXIAL BENDING-AXIAL LOAD INTERACTION CURVES

CHAPTER IV

METHOD OF ANALYSIS

4.1 Introduction

The analysis presented herein is based on the simplified
model described in the previous chapter. Equilibrium is formulated
on the deformed structure using the standard slope-deflection equations,
modified to account for the presence of plastic hinges as they develop.
These equations are used to express the equilibrium of the moments at
each joint and the equilibrium of the forces in the plane of each
floor diaphragm. The equilibrium equations are arranged in matrix
form and solved for the unknown displacements. The member end forces
are then obtained by back substituting the displacements in the slope
deflection equations.

The vertical loads remain constant during the analysis. The
lateral loads are incremented until the determinant of the coefficient
matrix becomes negative. At this point the incrementation procedure
is modified to trace the unloading branch of the load-displacement re-
lationship. The analysis is terminated when the displacements become
excessively large.

4.2 Slope Deflection Equations

In applying the slope-deflection equations to the individual

members in the structure, the following assumptions are made:

(a) The influence of the axial forces on the carry-over and stiffness factors is ignored.

(b) The members are prismatic.

(c) The influence of transverse beam loads on the bending moments and forces is not considered.

(d) The member response is elastic-perfectly plastic.

(e) The bending moments and rotations at the member ends are clockwise positive.

The slope-deflection equations for moments at the ends of member 1, 2, shown in FIGURE 4.1, may be written as:

$$M_{12} = C_{11} \, \theta_1 + C_{12} \, \theta_2 - (C_{11} + C_{12}) \frac{\Delta_{12}}{L} + M_{F12} \qquad (4.1a)$$

$$M_{21} = C_{21} \, \theta_1 + C_{22} \, \theta_2 - (C_{21} + C_{22}) \frac{\Delta_{12}}{L} + M_{F21} \qquad (4.1b)$$

where M_{12} and M_{21} are the moments at ends 1 and 2 respectively, θ_1 and θ_2 are member end rotations, Δ_{12} is the sway displacement between ends 1 and 2, M_{F12} and M_{F21} are the fixed end moments at ends 1 and 2 respectively. As a result of assumption (a), coefficients C_{11}, C_{12}, C_{21} and C_{22} may be defined as follows,

$$C_{11} = C_{22} = \frac{4EI}{L} \qquad (4.2a)$$

$$C_{12} = C_{21} = \frac{2EI}{L} \qquad \qquad (4.2b)$$

where E, I and L are the modulus of elasticity, moment of inertia and member length respectively.

4.2.1 Analysis in the Elastic Range

Because of assumption (c) the fixed end moment terms, M_{F12} and M_{F21}, in EQUATIONS (4.1a) and (4.1b) are equal to zero, as long as the bending moments are below the plastic capacities of the members.

For a frame beam, the form of the equations may be further simplified since the sway displacement is equal to zero and the far end of the beam is supported on a roller. The moment at the column end of the frame beam is given by,

$$M_1 = \frac{3EI}{L} \theta_1 \qquad \qquad (4.3)$$

where L is the length from column center line to the roller end.

As the wall possesses a finite width, any rotation of the beam to wall joint results in a sway displacement between the wall beam ends. The displacement is given by,

$$\Delta_{21} = -\frac{L_w}{2} \theta_2 \qquad \qquad (4.4)$$

where L_w is the wall width and θ_2 is the rotation of the beam to wall joint. The negative sign reflects the anti-clockwise sway deflection

of the wall beam which is associated with a positive joint rotation. The moments at the ends of the wall beam may be expressed in terms of the end rotations by substituting EQUATION (4.4) into EQUATIONS (4.1):

$$M_{12} = \frac{4EI}{L}\,\theta_1 + \frac{2EI}{L}\,\theta_2 + \frac{3EI}{L}\frac{L_w}{L}\,\theta_2 \qquad (4.5a)$$

$$M_{21} = \frac{2EI}{L}\,\theta_1 + \frac{4EI}{L}\,\theta_2 + \frac{3EI}{L}\frac{L_w}{L}\,\theta_2 \qquad (4.5b)$$

where L is the beam length, measured from the column center line to the wall face.

The moment equations for the columns and walls include a term resulting from the floor translations. The end moments, M_{12} and M_{21}, may be expressed by,

$$M_{12} = \frac{4EI}{h}\,\theta_1 + \frac{2EI}{h}\,\theta_2 - \frac{6EI}{h}\frac{\Delta}{h} \qquad (4.6a)$$

$$M_{21} = \frac{2EI}{h}\,\theta_1 + \frac{4EI}{h}\,\theta_2 - \frac{6EI}{h}\frac{\Delta}{h} \qquad (4.6b)$$

where
$$\Delta = u_2 - u_1 \qquad (4.7a)$$

or
$$\Delta = v_2 - v_1 \qquad (4.7b)$$

depending on the plane of the particular bent in which the columns,

and/or walls, are located, and h is the story height.

EQUATIONS (4.3) to (4.7) are applicable while the structure deforms within the elastic range. As loading continues the yield condition is violated at the ends of various members and the above equations must be correspondingly modified.

4.2.2 Frame Beam Hinging

When the moment at the end of the frame beam, computed by EQUATION (4.3), has increased to the plastic moment capacity of the section, the moment at that point remains constant for additional deformation. The frame beam no longer supplies restraint for additional rotations of the beam to column joint. The moment at the member end is given by,

$$M_1 = \pm M_p \qquad (4.8)$$

where M_p is the plastic moment capacity of the section. The sign is that of the moment at the point of plastic hinge formation.

4.2.3 Wall Beam Hinging

The moment in the wall beam may be equal to the plastic capacity at either or both ends. The equations for the three cases are as follows:

(a) Plastic hinge at end 1 only,

$$M_{12} = \pm M_p \qquad (4.9a)$$

$$M_{21} = \pm \frac{M_p}{2} + (\frac{3EI}{L} + \frac{1.5EI}{L} \frac{L_w}{L}) \theta_2 \qquad (4.9b)$$

(b) Plastic hinge at end 2 only,

$$M_{12} = \pm \frac{M_p}{2} + \frac{3EI}{L} \theta_1 + \frac{1.5EI}{L} \frac{L_w}{L} \theta_2 \qquad (4.9c)$$

$$M_{21} = \pm M_p \qquad (4.9d)$$

(c) Plastic hinges at both ends,

$$M_{12} = \pm M_p \qquad (4.9e)$$

$$M_{21} = \pm M_p \qquad (4.9f)$$

where M_p is the plastic moment capacity of the member. The sign of M_p is determined by the sign of the moment at the point of plastic hinge formation.

4.2.4 Column and Wall Hinging

As the effect of the axial load on the member stiffness is ignored, the possibility of a plastic hinge forming at a point within the height of a column or wall, is not considered. The three cases for the presence of plastic hinges are as follows:

(a) Plastic hinge at end 1 only,

$$M_{12} = \pm M_p \qquad (4.10a)$$

$$M_{21} = \pm \frac{M_p}{2} + \frac{3EI}{h} \theta_2 - \frac{3EI}{h} \frac{\Delta}{h} \qquad (4.10b)$$

(b) Plastic hinge at end 2 only,

$$M_{12} = \pm \frac{M_p}{2} + \frac{3EI}{h} \theta_1 - \frac{3EI}{h} \frac{\Delta}{h} \qquad (4.10c)$$

$$M_{21} = \pm M_p \qquad (4.10d)$$

(c) Plastic hinges at both ends,

$$M_{12} = \pm M_p \qquad (4.10e)$$

$$M_{21} = \pm M_p \qquad (4.10f)$$

4.3 Joint Equilibrium Equations

In FIGURE 4.2 a bent is shown which forms part of a three dimensional structure. The displacements are numbered by starting at the base of the structure; numbering column joint displacements before wall joint displacements; moving from the first to the last bent; then numbering the three translational displacements of the first floor followed by the joint displacements of that floor. This procedure is repeated floor by floor. The number of displacements per floor amount to N_d of which N_d-3 are joint displacements. By labelling the rotation at a particular column joint in FIGURE 4.2 as i, then, from the convention

adopted, the rotation of the wall joint is i+1, and corresponding displacements below and above this floor differ by the number of unknown displacements per floor for the entire structure, N_d.

At each joint in the structure the member end moments must be in equilibrium throughout the load-displacement response. The springs at the base of the column and wall are introduced in order to simulate the rotational restraint offered by the foundation.

4.3.1 Beam to Column Joint

Equilibrium of moments at joint i, is expressed by,

$$M_i = M_{i,i-N_d} + M_{i,i+1} + M_{i,i+N_d} + M_{i,i} \qquad (4.11)$$

where M_i is the resultant moment and the individual contribution of each member end is given by EQUATIONS (4.3) to (4.10), whichever is applicable. The equation is modified at the base of the column to allow for the base spring where,

$$M_i = M_{i,i+N_d} + k_c \cdot \theta_i \qquad (4.12)$$

and k_c represents the rotational stiffness of the spring. At the top of the structure the term $M_{i,i+N_d}$ is deleted from EQUATION (4.11) as the column does not continue above the roof line.

4.3.2 Beam to Wall Joint

Because of the finite wall width, the shear developed in the wall beam produces a moment contribution about the center of the wall, which must be included in the moment equilibrium equation. For joint i+1, in FIGURE 4.2 the resultant moment, M_{i+1}, is expressed by,

$$M_{i+1} = M_{i+1,i} + \frac{M_{i+1,i} + M_{i,i+1}}{L_b} \frac{L_w}{2} + M_{i+1,i+1-N_d}$$

$$+ M_{i+1,i+1+N_d} \tag{4.13}$$

where the second term represents the moment contribution due to the beam shear. In EQUATION (4.13) L_b and L_w are the wall beam length and wall width respectively. The equation at the base of the wall is modified to,

$$M_{i+1} = M_{i+1,i+1+N_d} + k_w \cdot \theta_{i+1} \tag{4.14}$$

where k_w represents the rotational stiffness of the spring. At the top of the structure the term $M_{i+1,i+1+N_d}$, is deleted.

4.4 Floor Equilibrium Equations

The equilibrium of those forces acting on the floor diaphragm is expressed in terms of the shears developed by the columns and walls of the story immediately above and below each floor. The resultant force exerted on the floor diaphragm by the shears in each bent must

be in equilibrium with the applied lateral loads. It is further required that the resultant torque of the forces acting on each floor diaphragm, about any point in the plane of the diaphragm, must be equal to zero. The overturning moments caused by the vertical loads (P-Δ moments) on each bent, are introduced into the equilibrium equations in the form of additional shears to be resisted in each story of every bent. The forces acting on a typical vertical member are shown in FIGURE 4.3,

$$V \cdot h = M_{12} + M_{21} - P \cdot \Delta_{12} \qquad (4.15a)$$

$$V = \frac{M_{12} + M_{21}}{h} - P \cdot \frac{\Delta_{12}}{h} \qquad (4.15b)$$

where V is the story shear available to resist lateral load. The vertical load reduces the shear available to resist lateral load by an amount given by the second term of EQUATION (4.15b).

4.4.1 Lateral Forces

The resisting force component, developed at each floor level, in each of the two principal directions is obtained by summing the forces applied to the floor diaphragm by the bents spanning in the corresponding direction. The resultant forces, F_{xi} and F_{yi}, are defined by,

$$F_{xi} = \sum_{j=1}^{N_x} (V_{j,i} - V_{j,i+1}) \qquad (4.16a)$$

$$F_{yi} = \sum_{j=N_x+1}^{N_x+N_y} (V_{j,i} - V_{j,i+1}) \tag{4.16b}$$

where $V_{j,i}$ and $V_{j,i+1}$ are the shears in stories i and i+1 of bent j, and are expressed by EQUATION (4.15b), F_{xi} and F_{yi} are the total resisting forces at floor i in the X and Y directions respectively, N_x and N_y are the total number of bents whose planes lie in the X and Y directions respectively.

In order to satisfy equilibrium, the sum of the applied lateral loads and the resisting floor forces must be equal to zero, at each floor, throughout the load-displacement response. This is expressed as:

$$F_{xi} + H_{xi} = 0 \tag{4.16c}$$

and
$$F_{yi} + H_{yi} = 0 \tag{4.16d}$$

where H_{xi} and H_{yi} are the applied lateral loads in the X and Y directions, respectively.

4.4.2 Rotational Equilibrium

For convenient reference the equilibrium of torque about a vertical axis is taken about the origin of the co-ordinate system. The torques applied to the structure are produced by the lateral loads and may be defined as,

$$T_i = H_{xi} \cdot Y_{Hi} - H_{yi} \cdot X_{Hi} \qquad (4.17a)$$

where T_i is the applied torque at floor i, Y_{Hi} and X_{Hi} are the perpendicular distances, between the origin and loads H_{xi} and H_{yi} respectively.

Resisting torques are developed firstly by the St. Venant torsion generated in the columns and walls, and secondly, by the resisting shears in each bent. The St. Venant torsion exerted on a floor diaphragm may be expressed as,

$$R_{vi} = (G\ K_T)_{i+1} \cdot \left(\frac{\phi_{i+1} - \phi_i}{h_{i+1}}\right)$$

$$- (G\ K_T)_i \cdot \left(\frac{\phi_i - \phi_{i-1}}{h_i}\right) \qquad (4.17b)$$

where R_{vi} is the St. Venant torsion exerted on floor i, $(G\ K_T)$ is the total uniform torsional stiffness of all the column and wall elements in story i, ϕ_i is the rotation, about the vertical axis, of floor i. The resisting torque developed by the shears in the bents may be expressed as,

$$R_{si} = \sum_{j=1}^{N_x} y_j \cdot (V_{j,i+1} - V_{j,i}) - \sum_{j=N_x+1}^{N_x+N_y} x_j \cdot (V_{j,i} - V_{j,i+1}) \qquad (4.17c)$$

where R_{si} is the resisting torque at floor i, x_j and y_j are the bent coordinates.

In order to satisfy equilibrium, the sum of the applied torque and the resisting torques must be equal to zero, at each floor, throughout the load-displacement response. This is expressed as,

$$T_i + R_{si} + R_{vi} = 0 \qquad (4.17d)$$

for floor i.

4.5 Matrix Formulation and Solution

The equilibrium equations may be conveniently arranged in matrix form.

$$A\delta = b \qquad (4.18)$$

where A is the square coefficient matrix whose size is equal to the total number of unknown displacements in the structure N_u, δ is a vector of unknown displacements and b is the load vector. Each row of EQUATION (4.18) corresponds to a single equilibrium equation. Because the vertical load remains constant throughout the analysis and the structure is linearly elastic, the coefficient matrix is symmetric.

The method adopted for solving EQUATION (4.18) is a modified Gauss Elimination technique. A direct solution technique was selected so that the computation time could be determined for a particular size of structure.

For large matrices the use of an iterative solution, such as Gauss Seidel, may take considerable time to converge to an acceptable result (52). The accuracy of a direct method is more often influenced by error propagation during solution and for large systems of equations this aspect must be considered before accepting the answers obtained. The commonly used Choleski's square root method (53) was not attempted for this problem since the method requires complex algebra when the determinant of the coefficient matrix becomes negative. This condition will arise on the unloading branch of the load-displacement curve as discussed in SECTION 4.6.

4.6 Loading Procedure

Two load incrementing procedures may be used in the analysis. The first consists of increasing the lateral load by a predetermined increment. With this procedure, the yield condition may be violated at several points during a particular load increment. The stiffness matrix is changed after the increment has been applied and thus the load-displacement relationship obtained is an upper bound to the "rigorous" solution. The second procedure increments the load by an amount sufficient to raise the moment at one particular point to the corresponding plastic moment value. In this manner the "rigorous" curve may be obtained in a point by point fashion. However, each cycle requires two, instead of one, analyses. The procedure may be described by considering the load-end moment curve in FIGURE 4.4. At a particular load, H_1, the structure contains N_h hinges. The load H is desired that

results in the formation of the next hinge, N_h+1. For each member end in the structure the moment at load H_1 is recorded. The load is then incremented by an amount ΔH which is predetermined. The structure is re-analyzed at load $H_2 = H_1 + \Delta H$, and the member end moments are calculated. It is then possible to determine the load increment H_1 required to bring the moment to each member end to the plastic moment capacity. This may be expressed by,

$$H' = \left(\frac{M_p - M_1}{M_2 - M_1}\right) \cdot \Delta H = R \cdot \Delta H \qquad (4.19a)$$

The total load at this stage is then:

$$H = H_1 + R \cdot \Delta H \qquad (4.19b)$$

where H is the load required to bring the moment to the plastic moment capacity, M_p, of the member. The value of R is calculated for all member ends that remain elastic. The minimum R value is chosen and this is then substituted in EQUATION (4.19b) to yield the next load value.

The determinant of the coefficient matrix, A, is calculated after each increment. The magnitude of the determinant decreases as the structure enters the inelastic range and plastic hinges form. This reflects a decrease in the structural stiffness.

Each floor of the structure has two degrees of translational

freedom and one degree of rotational freedom. When the sign of any of the three corresponding stiffness contributions becomes negative, the sign of the determinant changes also. This provides a convenient criterion for determining the maximum load carrying capacity of the structure. When the determinant changes sign the load is decremented using a procedure similar to the loading process. Exceptions to the general criterion have occurred and consideration of this problem is discussed in CHAPTER VIII. The analysis is terminated when the deformations are several times the values at the formation of the first plastic hinge. This limit is chosen so that the unloading portion of the load-displacement curve is obtained.
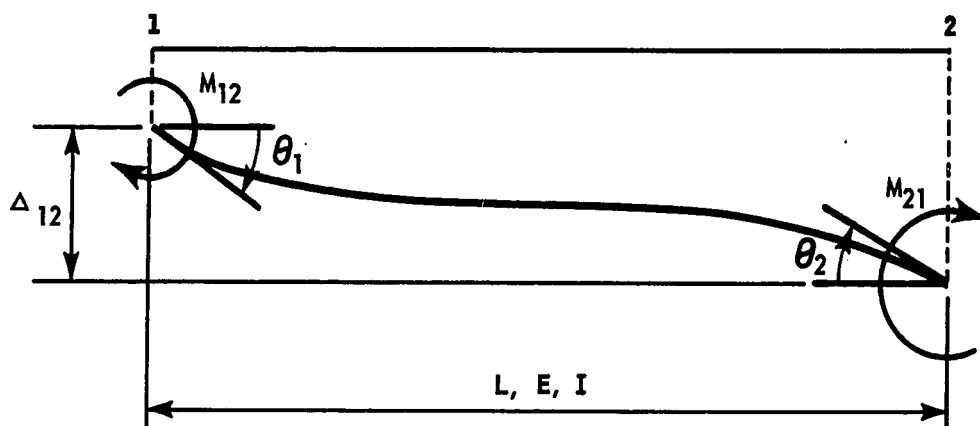
FIGURE 4.1 TYPICAL DEFORMED MEMBER

FIGURE 4.2 TYPICAL LUMPED BENT
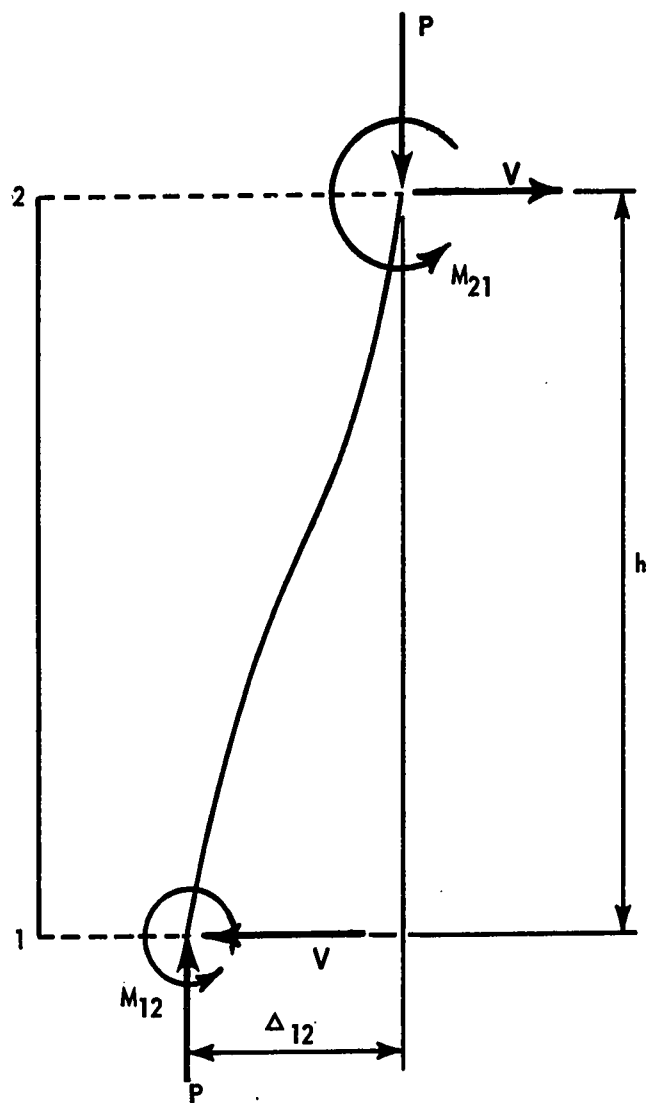
FIGURE 4.3 TYPICAL COLUMN AND WALL ELEMENT
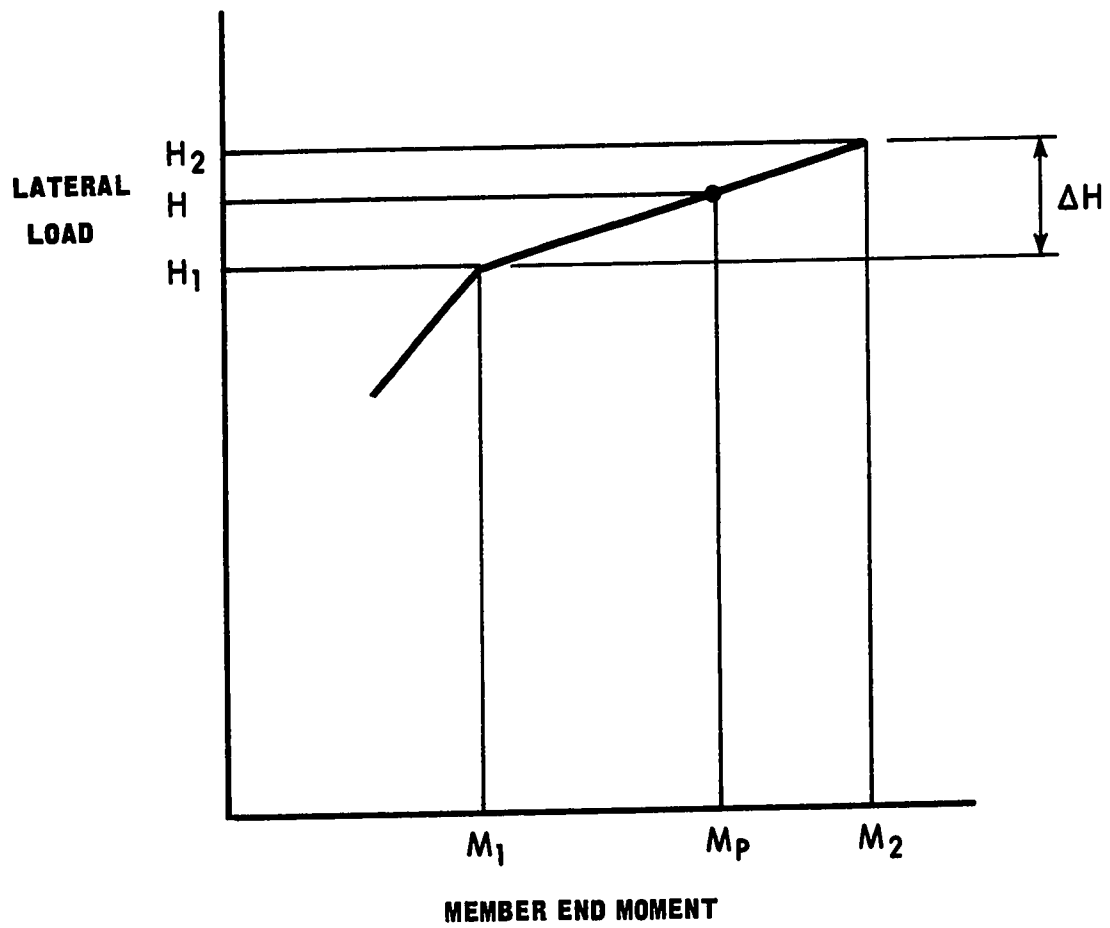
FIGURE 4.4 LOAD INCREMENT PROCEDURE

CHAPTER V

COMPUTER PROGRAM

5.1 Basic Algorithm

The method of analysis described in the previous chapter was programmed in FORTRAN IV for the IBM 360/67 system. This section will describe the basic algorithm which consists of the steps followed by the program in incrementing the load so that the structure follows the load-displacement curve from point 1 to point 2 shown in FIGURE 5.1. If at point 1, N_h hinges exist in the structure then point 2 corresponds to the load and displacement at which the member end moment at one additional location has just attained its plastic moment capacity.

The loading procedure is described in SECTION 4.6 and in the program is controlled by subroutine RECYCL. The loading procedure uses load factors instead of absolute loads, a load factor of 1.0 corresponding to the applied working load which is read in at the start of the analysis. The steps in moving from point 1 to point 2 are as follows:

1. All member end moments, corresponding to point 1 on the load-displacement curve, are recorded.

2. The coefficient matrix, A, is generated for the elastic structure, then modified so that the equilibrium equations, which are affected by the N_h plastic hinges, conform to the

slope deflection equations developed in CHAPTER IV for elastic-plastic members.

3. The load vector, b, is generated for the elastic structure and modified for the presence of plastic hinges. The lateral load factor, however, has been increased by an amount ΔH above the load factor at point 1.

4. The matrix equation, $A\delta = b$, is solved, for the displacement vector δ, using a modified Gauss Elimination algorithm which is described in SECTION 5.3.

5. The displacements, obtained in step 4, are substituted into the slope-deflection equations. The equations have been modified for those members containing one or more of the N_h hinges.

6. The ratio R, EQUATION (4.19) is calculated for all member ends: where M_1 and M_2 correspond to the moments obtained in steps 1 and 5 respectively.

7. The minimum R value is selected and substituted into EQUATION (4.19b), to obtain the load, H, corresponding to point 2 on the load-displacement curve of FIGURE 5.1. To allow for numeric errors in the program, the load factor H was increased by an additional 0.001, to ensure formation of the next hinge.

8. The equation, $A\delta = b$, is then generated again using steps 2 and 3 with a load factor, H + 0.001, obtained in step 7.

9. Steps 4 and 5 are repeated.

10. The end moments obtained are then checked against the corresponding plastic moments and a hinge inserted where the plastic moment is attained. It is possible that several hinges will form simultaneously.

11. The structure is now at point 2 on the load-displacement curve and will contain N_h + M hinges, where M is the number of hinges found in step 10. To continue along the load-displacement curve steps 1 to 11 are repeated. Before advancing to the next cycle the rotational discontinuities across all plastic hinges are calculated.

The above procedure is applicable between points a and b on the load displacement curve. Some modifications are necessary for the remainder of the curve. Before starting the analysis, all member properties, structural dimensions and loads are read into the program by subroutine READ. The required data and format is listed in APPENDIX A.2. and the nomenclature is presented in APPENDIX A.3.

The response between points 0 and a on FIGURE 5.1 is entirely elastic and point a may be located directly. The equilibrium equations are generated and solved at the working load level (load factor equal to 1.0). Ratios of member end moments to corresponding plastic moments are calculated for all member ends. The inverse of the maximum value of these ratios, corresponds to the load factor at which the first hinge will theoretically form. The load factor is set equal to this value (plus 0.001 to allow for numeric errors), and the structure is re-analyzed.

The member end moments are calculated and checked against the corresponding plastic moment capacities. Where the plastic moment is attained a hinge is inserted in the structure. The structure is now at point a on the load-displacement curve.

Before proceeding with the basic algorithm described above, subroutine RECYCL reads in the parameters that are used for control. The first of these, INCR, indicates whether the monotonically increasing loading procedure, described in SECTION 4.6, is to be used, or whether hinges are to be located individually as described above. The other parameters DISX, DISY, ISTEP, NCYCL respectively control the maximum displacements in the X and Y directions, whether the load is to be decremented when the determinant changes sign, and lastly the number of cycles at which the analysis is to be terminated.

When the structure reaches point b, on the load-displacement curve, the basic algorithm is slightly modified to allow for the decreasing load. The response on the unloading branch of the curve is stable (as for the loading branch) and plastic hinges may still be located individually. However, the following changes are required:

(a) In step 3 the lateral load factor is decreased by an amount ΔH in order to move from point 3 to point 4 on the curve.

(b) In step 7 to allow for numeric errors in the program the load factor H is reduced by an additional amount, 0.001.

Flow diagrams for most subroutines are presented in APPENDIX A.1. A description of the task performed by each subroutine is given in

APPENDIX A.2 and the nomenclature and complete program listing are presented in APPENDICES A.3 and A.4. The flow charts for simpler subroutines are not presented. These may be understood by examining the program listing in conjunction with the nomenclature.

5.2 Numbering Convention

Before the equilibrium equations are formulated, the unknown displacements are numbered. The convention adopted, illustrated in FIGURE 5.2, results in a minimum band width for the coefficient matrix, A. The rules for numbering the displacements are as follows:

1. The displacements are numbered story by story starting at the bottom of the structure.

2. The joint rotations are numbered first in each story, moving from bent to bent.

3. The bents are numbered consecutively from minimum to maximum co-ordinates, commencing with the bents in the X direction.

4. Where a bent contains both a column and wall element the column joint rotation is numbered before the wall joint rotation.

5. The joints at the base of the structure are numbered first, then the three displacements at the first floor followed by the joint rotations of that floor. This procedure is repeated floor by floor.

The program must distinguish between coupled and uncoupled

bents in order to establish the numbering convention. This is achieved by a parameter, IND, which is read in before each set of data for a particular bent.

5.3 Method of Solution

Because of the assumptions discussed in CHAPTER III the structure behaves in a linearly elastic manner during each stage of loading. Consequently, the coefficient matrix is symmetric and one-half is sufficient for solution. The half band width, above, and including the major diagonal, is generated and stored by the program. The coefficient matrix is reduced to the upper triangular form with a unit diagonal, using a modified Gauss Elimination procedure, which proceeds row by row. This algorithm was selected primarily because of its simplicity, however, it is also valid even after the determinant becomes negative. A direct method of solution was preferred to reduce the time needed to obtain an acceptable degree of accuracy.

As the slope of the load-displacement curve approaches the horizontal, the coefficient matrix, A, approaches a singular condition and solution of the system of equations normally becomes difficult, if not impossible (4,7). In the present method, however, the structural stiffness is reduced (during loading) by the formation of successive plastic hinges. Hence, the change in stiffness (for each hinge) is discrete and the possibility of the determinant of the coefficient matrix becoming zero is remote. In fact, this has not occurred for the structures analyzed to date (September 1970). The "normalized"

determinant becomes smaller as each successive hinge forms and, at the maximum load, it changes sign but always displays a finite and relatively large value.

The significance of the change in the sign of the determinant was also noted by Davies (4). Once the load was increased beyond the value at which the determinant changed sign, hinge reversal occurred in the structure and although continuation of the solution was possible mathematically the analysis was no longer valid structurally. As the determinant changes sign the lateral stiffness becomes negative and the structure can only support a reduced lateral load at increasing displacements. If an attempt is made to increase the lateral load (in the analysis) the structure can only attain an equilibrium position if the influence of the P-Δ term is decreased; this requires a decrease in displacements with an increase in lateral load; a condition that is not possible structurally. The load at which the determinant changes sign can therefore be considered as the maximum load carrying capacity of a structure. Beyond this point, increasing displacements require corresponding decreases in the lateral loads to attain equilibrium positions along the unloading branch of the load-displacement curve. Exceptions to this general rule were found during the behavior study; the cause of this, and the method used to determine the maximum load for these cases, is discussed in CHAPTER VIII.

Although the determinant has changed sign the coefficient matrix is not singular and no apparent difficulty arises in the solution of the equations.
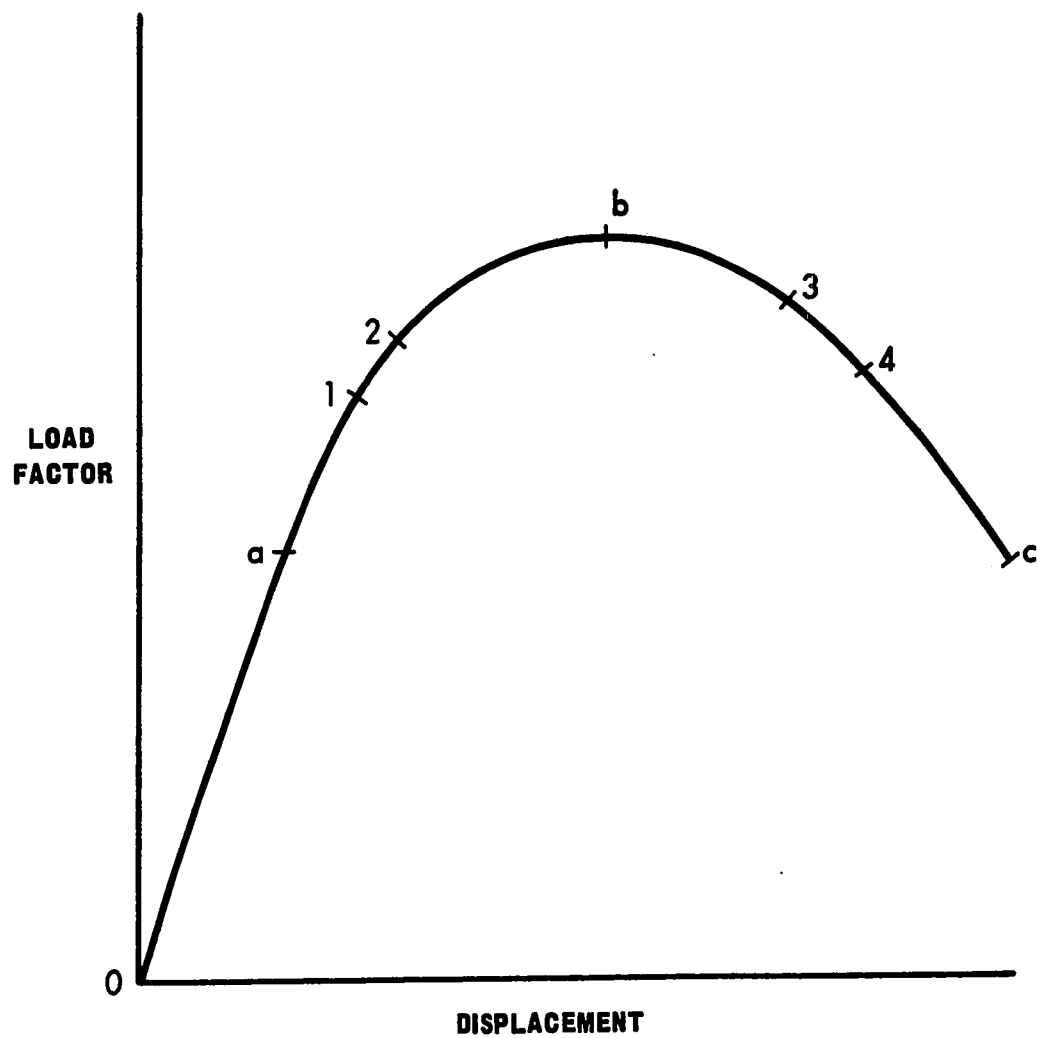
FIGURE 5.1 TYPICAL LOAD-DISPLACEMENT CURVE
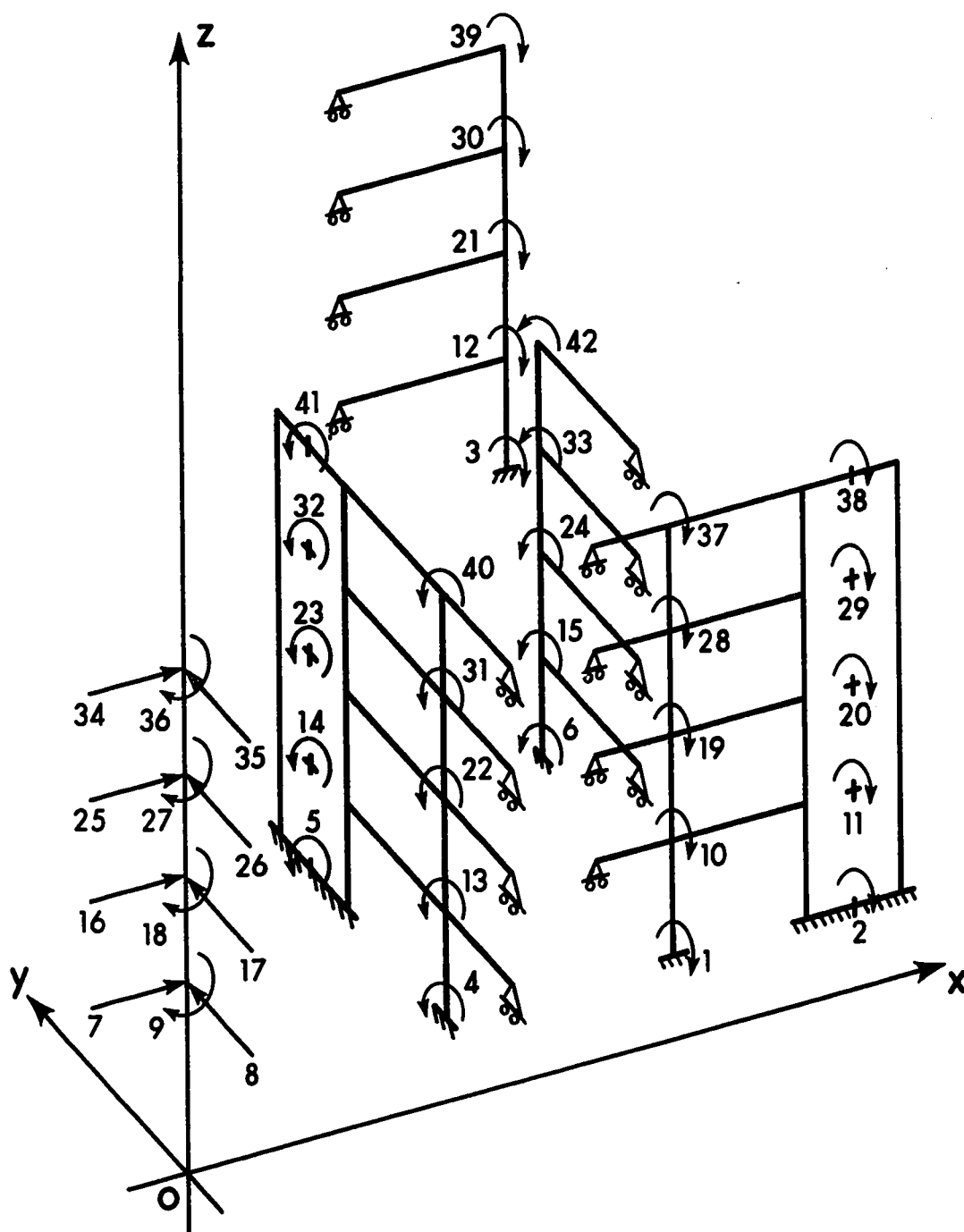
FIGURE 5.2 NUMBERING CONVENTION FOR LUMPED MODEL
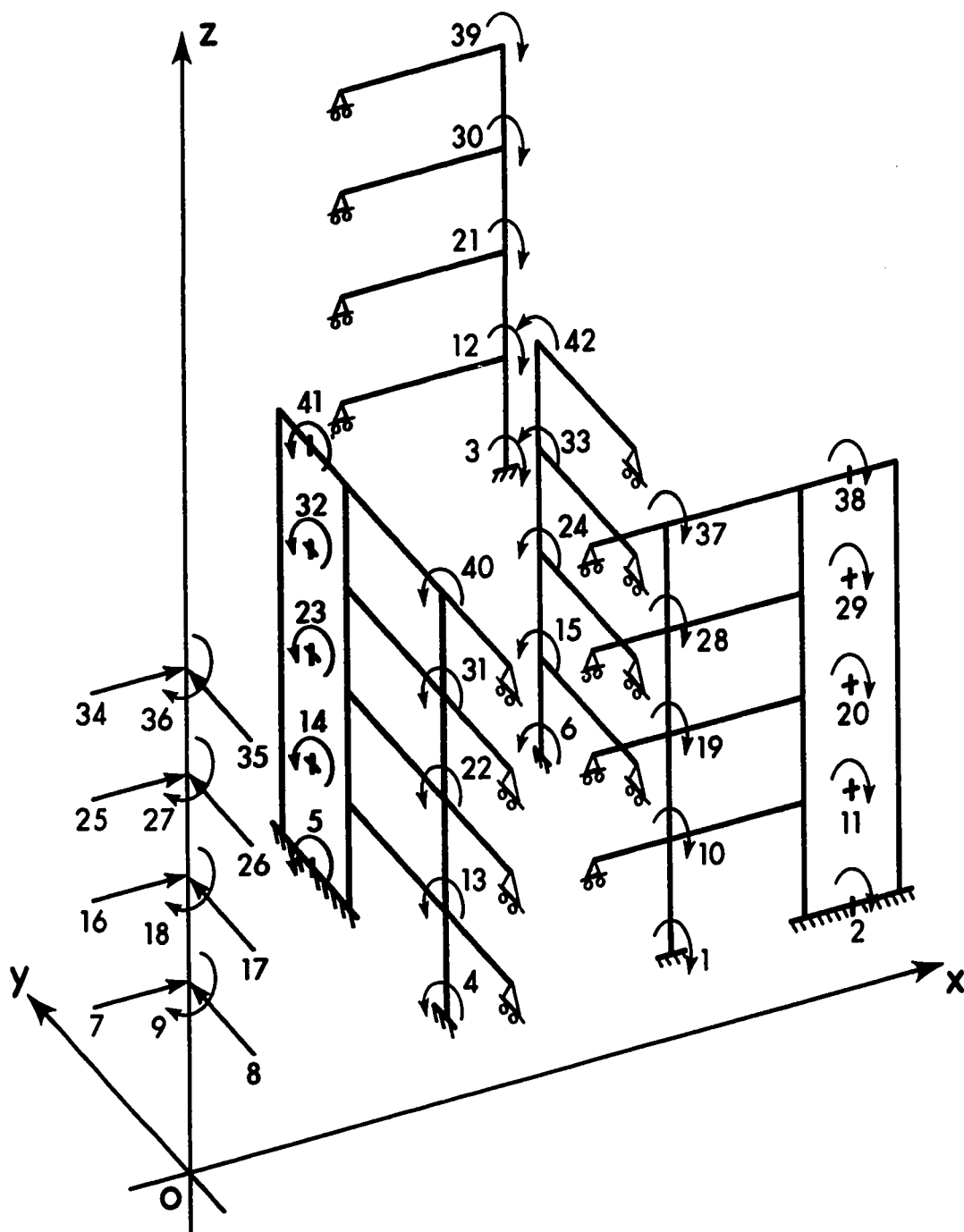
FIGURE 5.2 NUMBERING CONVENTION FOR LUMPED MODEL

CHAPTER VI

COMPARATIVE ANALYSES

6.1 Introduction

The method of analysis developed in CHAPTERS IV and V is designed to consider large multi-story structures. In its most general form the method is able to perform a second-order elastic-plastic analysis of structures which consist of planar bents spanning in two perpendicular directions. The bents may consist only of beam and column elements or may contain shear walls as well. The bents are assumed to be tied together at each floor level by diaphragms of infinite rigidity. A reference point, located on each diaphragm, is assumed to be subjected to deformation components in the two perpendicular directions and the diaphragms are free to twist about the longitudinal axis of the structure.

The methods of analysis available to date (September 1970) cannot be used to check the present method, including all of the above aspects, directly. Therefore, it is necessary to specialize the analysis and compare the influence of each aspect separately.

The validity of the first-order elastic analysis of the lumped planar bents, described in CHAPTER III, has been previously verified (12) and will not be considered. The second-order elastic-plastic response of planar bents (both uncoupled and coupled), is verified by suppressing

the three dimensional aspects of the method and analyzing two bents for which data is available in the literature. The three dimensional aspect of the method is then verified by suppressing the second-order and elastic-plastic aspects and performing first-order elastic analyses of a three dimensional space frame and a three dimensional coupled frame-shear wall structure. A comparison of the results of a three dimensional analysis, considering second-order and elastic-plastic aspects, could not be performed directly because published data is not available for structures which include rigid floor diaphragms. However, a one story space frame has been analyzed, indirectly, using the present method and the results compared with the published data for this structure.

6.2 Planar Bents

The three story planar frame, shown in FIGURE 6.1 (Frame B in reference 54) was tested at Lehigh University. The member properties used in the analysis were taken from the measured values and are presented in TABLE 6.1. For the analysis, a modulus of elasticity of 29,600 k.s.i. was adopted, and the moments of inertia, I, were adjusted so that the EI values in the analysis would correspond with the measured values. The material was A36 steel and a yield stress of 36 k.s.i. was used to calculate the reduced plastic moment capacities, M_{pc}. In the test, concentrated loads were applied to the beams as shown in FIGURE 6.1. In the analytical model, developed in CHAPTER III, transverse beam loads are considered as equivalent concentrated loads applied to

the columns and walls; the fixed end moments exerted on the joints are ignored. For large multi-bay structures the effect of this assumption is not expected to cause large discrepancies when considering the gross behavior of the structure. However, in the particular frame being considered, the beam moments have a considerable influence on the load-displacement response. Consequently, the effect of fixed end moments was temporarily included in the present method, and moments corresponding to a uniformly distributed load of 0.306 kip per lineal inch were applied at the beam ends. In FIGURE 6.2 the lateral load, H, is plotted against the first floor displacement, Δ. Ignoring the fixed end moments, the present method overestimates the ultimate load for the frame by 35 percent as shown by the dashed curve. Including the fixed end moments increases the moments in the columns and beams (on the leeward side) resulting in earlier yielding and increased story sways. These, in turn, increase the P-Δ moments, and reduce the ultimate carrying capacity of the frame.

The quantitative effect of beam load moments on the ultimate load of planar structures was studied by Nikhed (51). The use of a reduction factor was proposed, which, when applied to the plastic moment capacities of the beams would result in a conservative value for the ultimate load of the structure. This approach, however, was not used in allowing for the beam load moments in the present method (temporarily), as the former makes no allowance for earlier hinging in the columns which would occur for strong beam weak column structures, such as the

frame considered.

The present method, with fixed end moments included, closely predicted the load-displacement response for the frame as shown by the solid curve in FIGURE 6.2. The experimental curve is shown by the broken line with dots. The unloading branch obtained from the analysis (with or without the effects of fixed end moments) followed the same mechanism line (sway mechanism in the bottom story) and was only slightly steeper than the unloading branch obtained in the test. The hinge configuration obtained was in reasonable agreement with that predicted in Reference 54 and shown in FIGURE 6.1.

The twenty-four story structure shown in FIGURE 6.3, was used by Guhamajumdar et al (8) in a behavioral study of coupled frame-shear wall bents. The member properties and vertical loads are listed in TABLES 6.2 and 6.3. The modulus of elasticity was 30,000 k.s.i. for the frame members and 3,000 k.s.i. for the wall. The shear wall had a constant width of 8'-0" throughout the height of the structure, although the moment of inertia was varied so that it was 50 times the column moment of inertia, in each story. The vertical loads were maintained constant during the analysis, while the lateral loads were incremented to collapse. The results obtained by both methods are plotted in FIGURE 6.4. The lateral load, H, is plotted against the top floor displacement, Δ. The load-displacement response obtained by Guhamajumdar et al (8) is shown by the dashed curve (FIGURE 6.4), while the solid line represents the response obtained by the present method. The curves

predicted by the two methods are almost identical until a value of
H = 10.6 kips is attained. At this point a hinge forms at the base
of the wall, in both methods. The determinant in the present method
changes sign and the structure begins to unload, with increasing
displacements. The analysis by *Guhamajumdar* et al (8) does not cal-
culate the unloading branch and at a slightly higher load value failed
to converge to an equilibrium position.

6.3 Three Dimensional Structures

The twenty story structure shown in FIGURES 6.5 and 6.6 was
used by Weaver and Nelson (35) to illustrate the first-order elastic
analysis of space frames. In determining member properties for the
present analysis, the structural steel sections were considered to be
surrounded by a concrete fire proofing providing a minimum of one inch
cover, as shown in FIGURE 6.5. The modulus of elasticity for the steel
was 30,000 k.s.i. and a modular ratio of 9 was used for the concrete
fire proofing. The structure was analyzed under a lateral load of
20 p.s.f. applied to the south face. For the present method it was
necessary to lump each bent into an equivalent bent, as described in
CHAPTER III. The displacements of point A (FIGURE 6.5), in the north
direction, are plotted for each floor in FIGURE 6.7. The two trans-
lations and the rotation for the top floor of the structure (Point A)
are listed in TABLE 6.4. The results obtained by both methods are in
close agreement, with a maximum difference of less than 4 percent.

Gluck (41) used the sixteen story structure, shown in FIGURE

6.8, to illustrate a continuous method of analysis, developed for three dimensional coupled frame-shear wall structures. Member properties for each wall and frame are presented in TABLE 6.5. In both analyses the moment of inertia for the top beam was half of the value for the remaining beams. The height of each story is 3 meters, and a lateral load of 4 tons (per meter of height) is applied at the center of each floor along the widest face. The modulus of elasticity used for all members was 205 ton per cm^2. Because the internal columns have a moment of inertia equal to twice that of the external columns, and the beams are symmetrical, no error is introduced when the members are lumped within individual frames. In FIGURE 6.9, the lateral deflections and torsion angles are plotted for each floor, while in FIGURE 6.10 the story shears for Frame 1 (FIGURE 6.8) are plotted for each story. In both, FIGURES 6.9 and 6.10, the present method is represented by the dashed curve, while the results obtained by Gluck (41) are represented by the solid curve. The results obtained indicate excellent agreement between the two analyses.

The elastic-plastic response presented by Jonatowski and Birnstiel (39), for a one story space frame, shown in FIGURE 6.11, could not be checked directly by the present method since the column tops are not constrained to maintain their relative positions. However, due to the low lateral bending stiffness of the beams, little transfer of horizontal shear is expected to occur between the parallel bents. The structure could therefore be considered as two separate

planar bents, with column 4 being subjected to biaxial bending, while column 1 makes little contribution in resisting the applied loads. In calculating the M_{pc} values for column 4, the biaxial interaction curves developed by Santathadaporn and Chen (21) were used. The axial load on each column was assumed to remain constant at 107 kips. The modulus of elasticity and yield stress used were 29,000 k.s.i. and 36 k.s.i., respectively. The displacements of points 3 and 4, obtained by both methods, are plotted against the lateral load, H, in FIGURE 6.12. The present method predicts a collapse load which is 3 percent higher than that obtained by Jonatowski and Birnstiel (39).

6.4 Summary

The validity of the method of analysis was verified in this Chapter. Several structures, for which data is available in the literature, were analyzed by specializing the present method, for each particular structure, so that one aspect could be checked at a time. Close agreement was obtained in all cases. The limitations on the validity of the program, are imposed by the simplifying assumptions made in developing the analytical model. These limitations will be discussed in CHAPTER IX.

Section	Measured EI kip in^2 x 10^4	Measured M$_p$ kip in
10WF25	390	1100
5M18.9	73	400

TABLE 6.1

PROPERTIES OF BEAM AND COLUMN SECTIONS

THREE STORY PLANAR FRAME

Floor or Story	Moment of Inertia (in^4)			Plastic Moment Capacity (kip in)		
	Beam AB	Beam BC	Column	Beam AB (M_p)	Beam BC (M_p)	Column (M_{pc})
1	888	1170	14814	5404	4940	27300
2	888	1170	14814	5404	4940	27300
3	888	1170	13278	5404	4940	25400
4	888	1170	13278	5404	4940	25400
5	888	984	11452	5404	4560	21900
6	888	984	11452	5404	4560	21900
7	888	984	9716	5404	4560	18400
8	888	984	9716	5404	4560	18400
9	888	890	8306	5404	4020	15750
10	888	890	8306	5404	4020	15750
11	888	890	7098	5404	4020	13500
12	888	890	7098	5404	4020	13500
13	888	890	5850	5404	4020	11500
14	888	890	5850	5404	4020	11500
15	888	890	4850	5404	4020	10800
16	888	890	4850	5404	4020	10800
17	888	890	4130	5404	4020	10300
18	888	890	4130	5404	4020	10300
19	888	890	2970	5404	4020	6960
20	888	890	2970	5404	4020	6960
21	888	890	1620	5404	4020	5580
22	888	890	1620	5404	4020	5580
23	888	890	1100	5404	4020	5260
24	630	584	1100	3900	2960	5260

TABLE 6.2

BEAM AND COLUMN PROPERTIES TWENTY-FOUR STORY STRUCTURE

Floor or Story	Wall Properties		Loads (kips)	
	I $(\text{in}^4 \times 10^6)$	M_p $(\text{kip in} \times 10^5)$	Vertical (constant)	Horizontal (incremented)
1	7.20	3.600	12680	1.0
2	7.20	3.600	12330	1.0
3	6.47	3.235	11600	1.0
4	6.47	3.235	11000	1.0
5	5.74	2.870	10540	1.0
6	5.74	2.870	10000	1.0
7	5.01	2.505	9440	1.0
8	5.01	2.505	8930	1.0
9	4.28	2.140	8400	1.0
10	4.28	2.140	7860	1.0
11	3.55	1.775	7320	1.0
12	3.55	1.775	6790	1.0
13	2.946	1.623	6260	1.0
14	2.946	1.623	5720	1.0
15	2.227	1.473	5180	1.0
16	2.227	1.473	4650	1.0
17	2.083	1.173	4120	1.0
18	2.083	1.173	3590	1.0
19	1.485	0.873	3050	1.0
20	1.485	0.873	2520	1.0
21	0.807	0.573	1980	1.0
22	0.807	0.573	1450	1.0
23	0.548	0.274	1050	1.0
24	0.548	0.274	370	0.5

TABLE 6.3

WALL PROPERTIES AND LOADS TWENTY-FOUR STORY STRUCTURE

Method of Analysis	Displacements of Point A		
	North (in)	West (in)	Rotation (10^{-2} rad.)
Weaver and Nelson	11.88	1.22	0.57
Present	11.45	1.23	0.59

TABLE 6.4

DISPLACEMENTS OF TOP FLOOR POINT A

TWENTY STORY STRUCTURE

Wall	Moment of Inertia (m^4)	Frame	Moment of Inertia (dm^4)		
			Lateral Column	Center Column	Beam
1	5.7166	1	26.579	53.158	18.985
2	2.0834	2	26.579	53.158	18.985
3	2.0834	3	26.579	53.158	18.985
4	5.7166	4	26.579	53.158	18.985
5	1.2348	5	26.579	53.158	18.985

TABLE 6.5

MEMBER PROPERTIES SIXTEEN STORY STRUCTURE
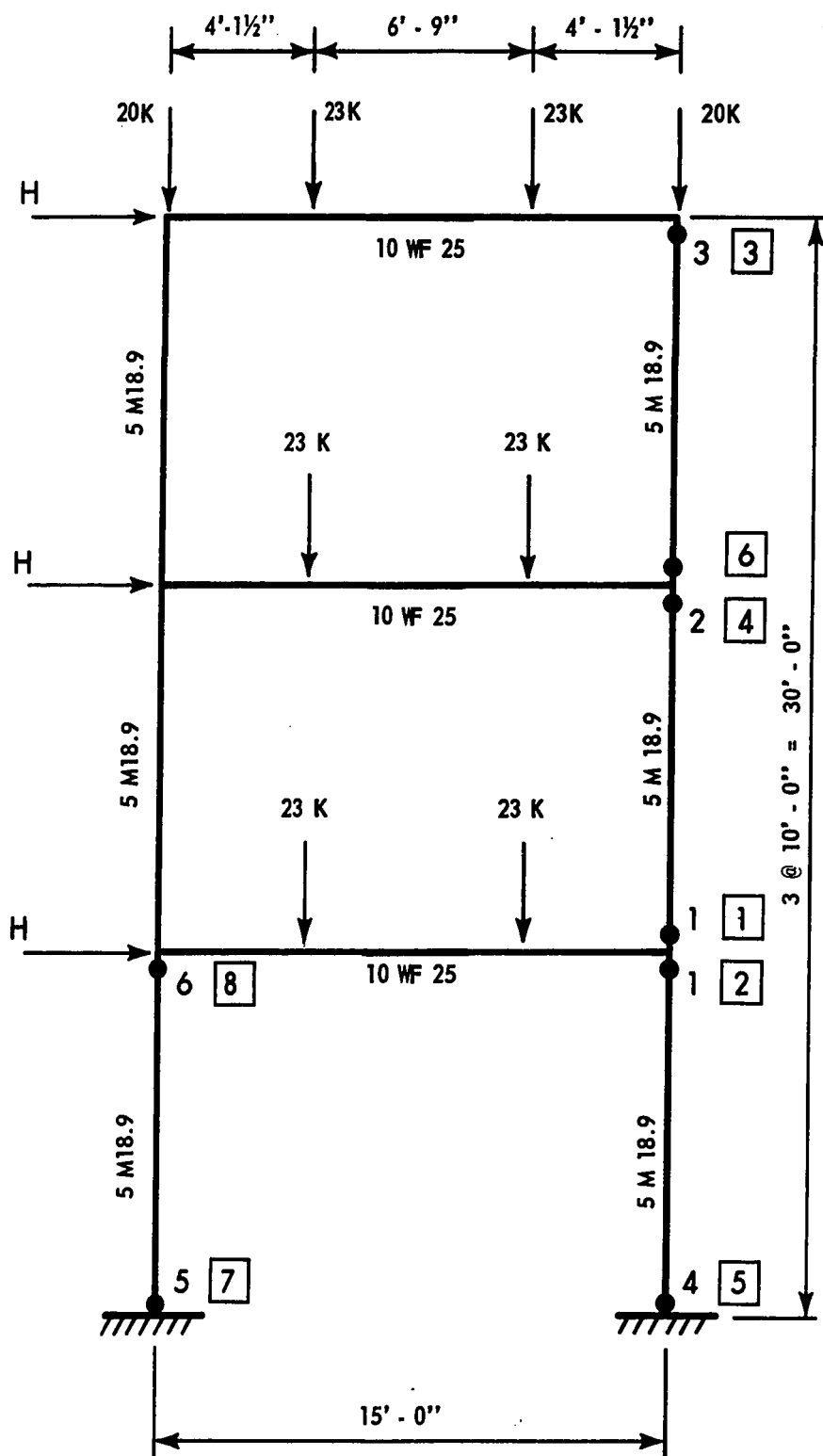
FIGURE 6.1 THREE STORY PLANAR FRAME
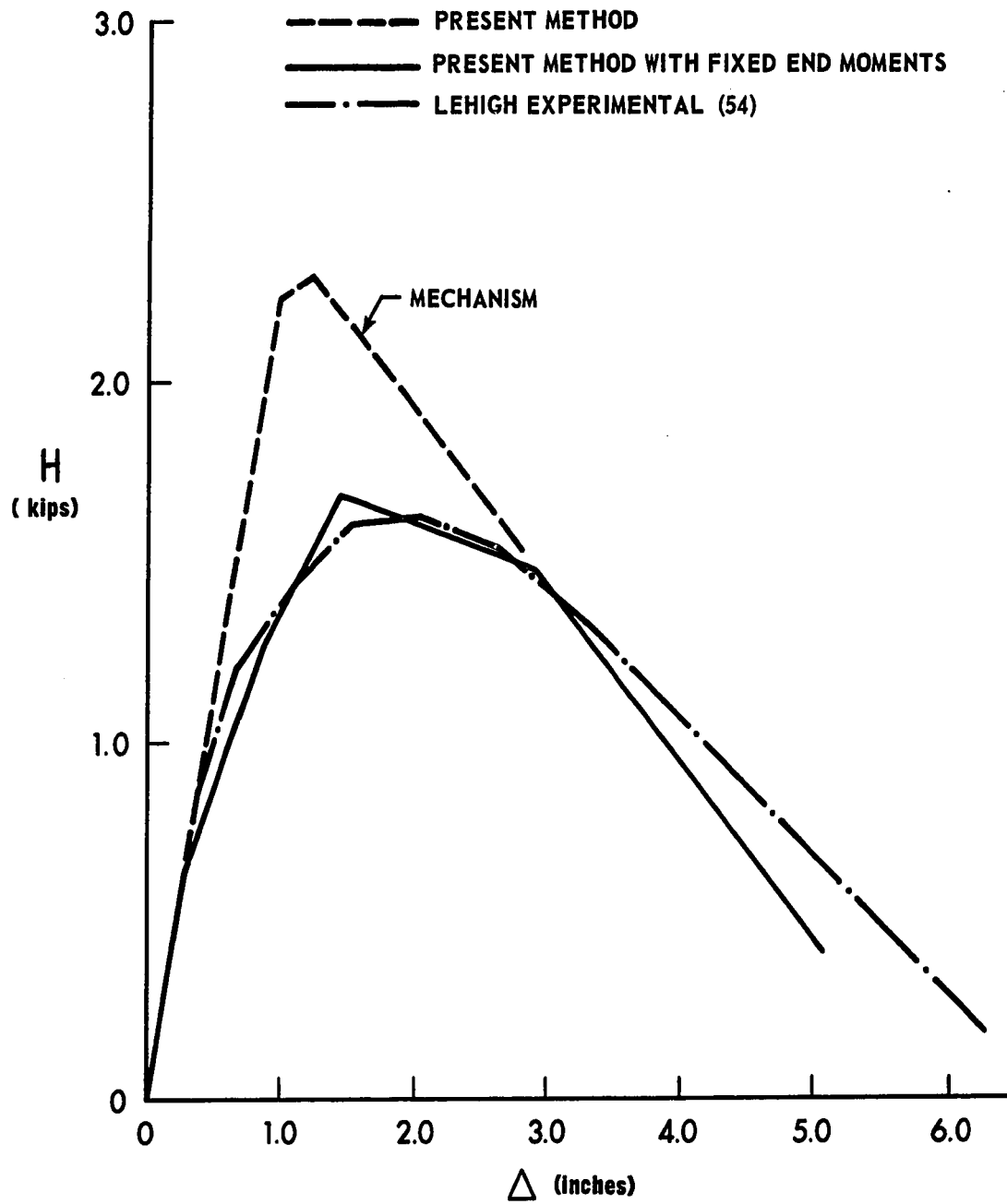
FIGURE 6.2 LOAD-DISPLACEMENT RESPONSE THREE STORY PLANAR FRAME
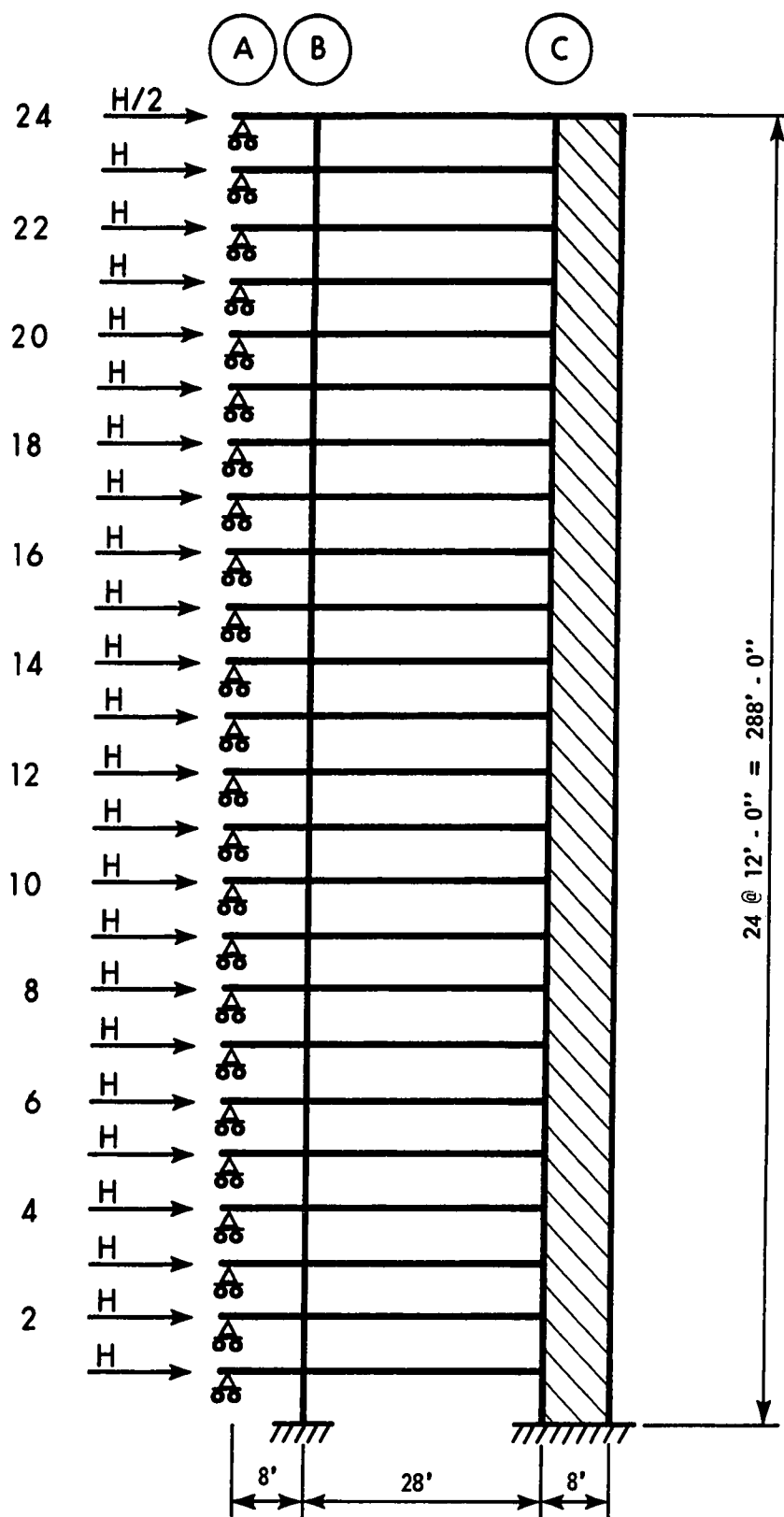
FIGURE 6.3 TWENTY-FOUR STORY PLANAR BENT

81
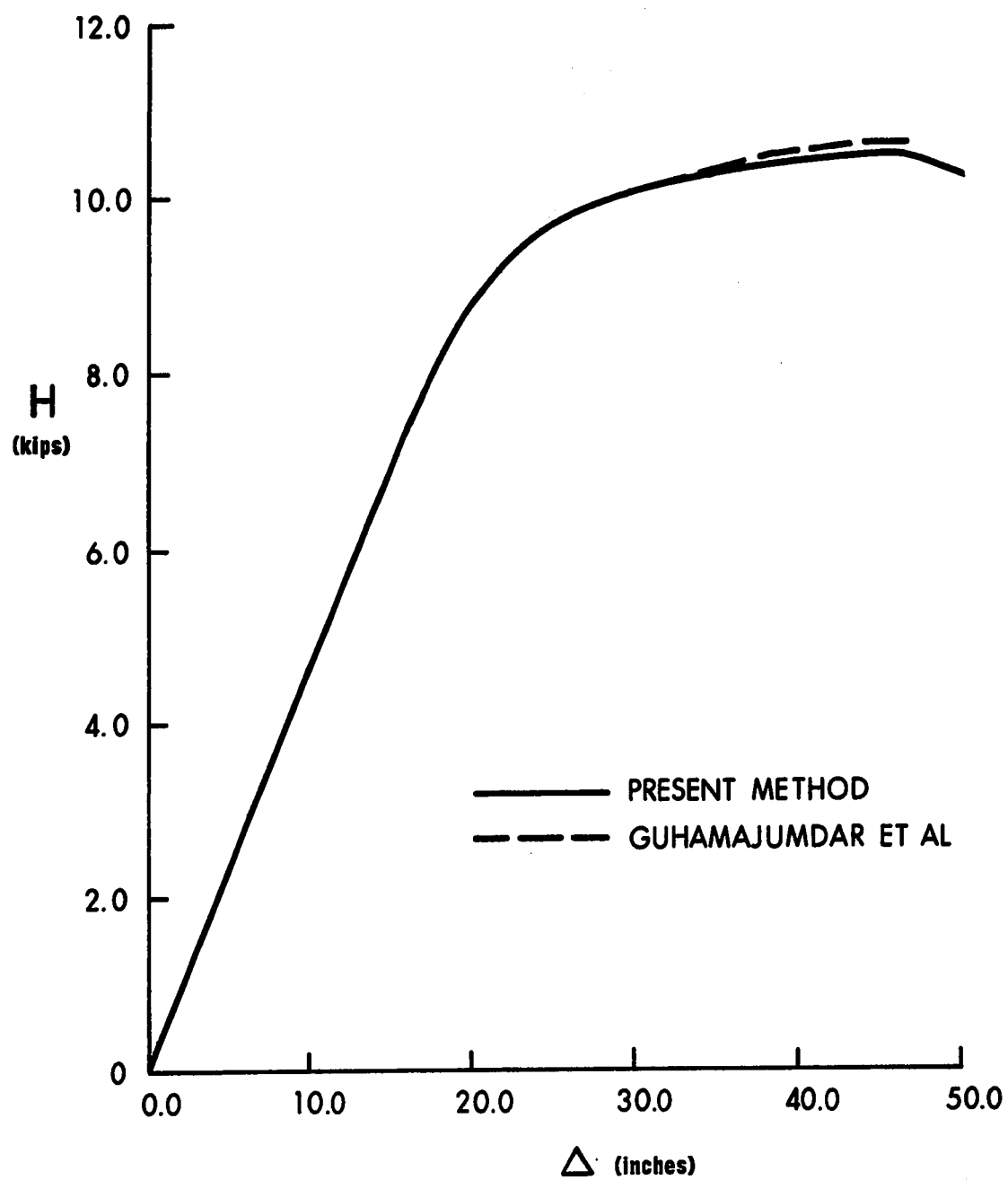
FIGURE 6.4 LOAD-DISPLACEMENT RESPONSE TWENTY-FOUR STORY STRUCTURE

COMPOSITE SECTION
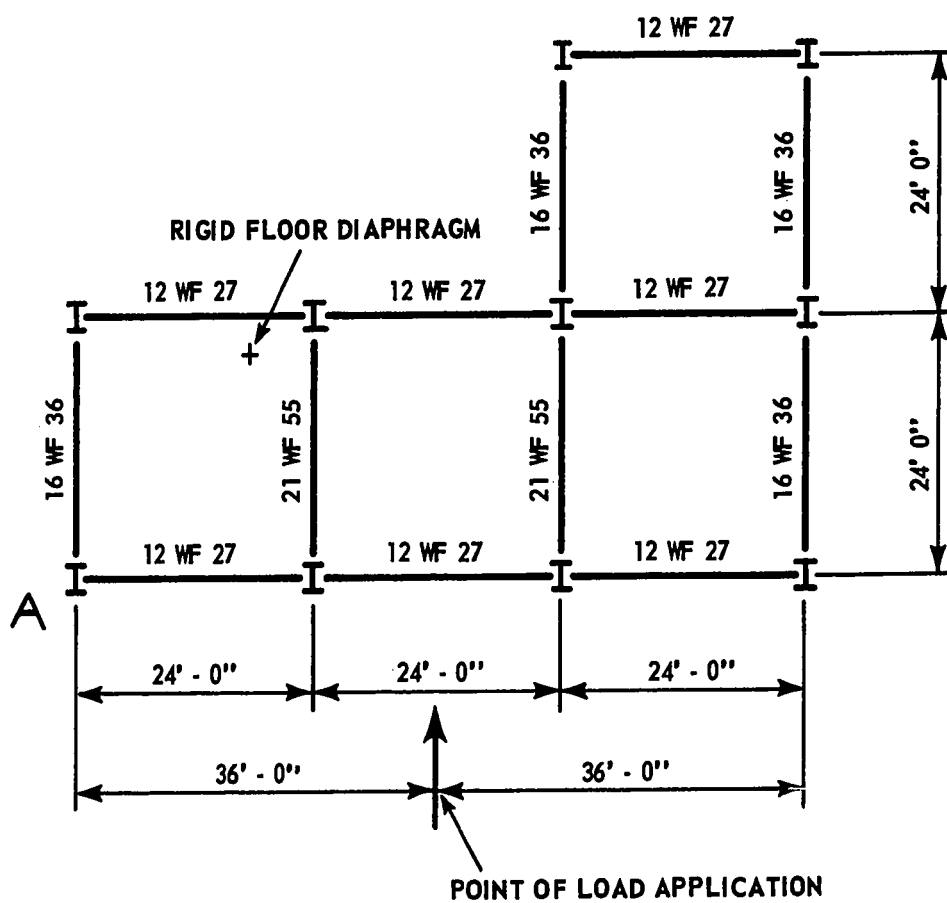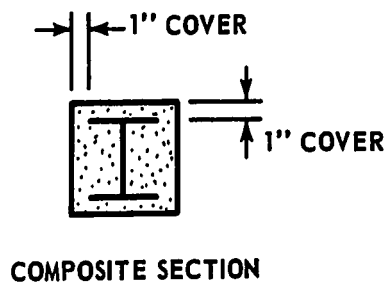
FIGURE 6.5 PLAN TWENTY STORY STRUCTURE

16 WF 36   16 WF 36   ← 8.64^k

8 WF 31

do   do   ← 17.28^k
do   do   ← 17.28^k
do   do   ← 17.28^k

10 WF 60

do   do   ← 17.28^k
do   do   ← 17.28^k
do   do   ← 17.28^k

12 WF 85

do   do   ← 17.28^k
do   do   ← 17.28^k
do   do   ← 17.28^k

12 WF 106

do   do   ← 17.28^k
do   do   ← 17.28^k
do   do   ← 17.28^k

12 WF 127

do   do   ← 17.28^k
do   do   ← 17.28^k

14 WF 142

do   do   ← 17.28^k
do   do   ← 17.28^k

14 WF 158

do   do   ← 17.28^k
do   do   ← 17.28^k

14 WF 176

do   do   ← 17.28^k

20 @ 12' - 0" = 240' - 0"

24' - 0"   24' - 0"
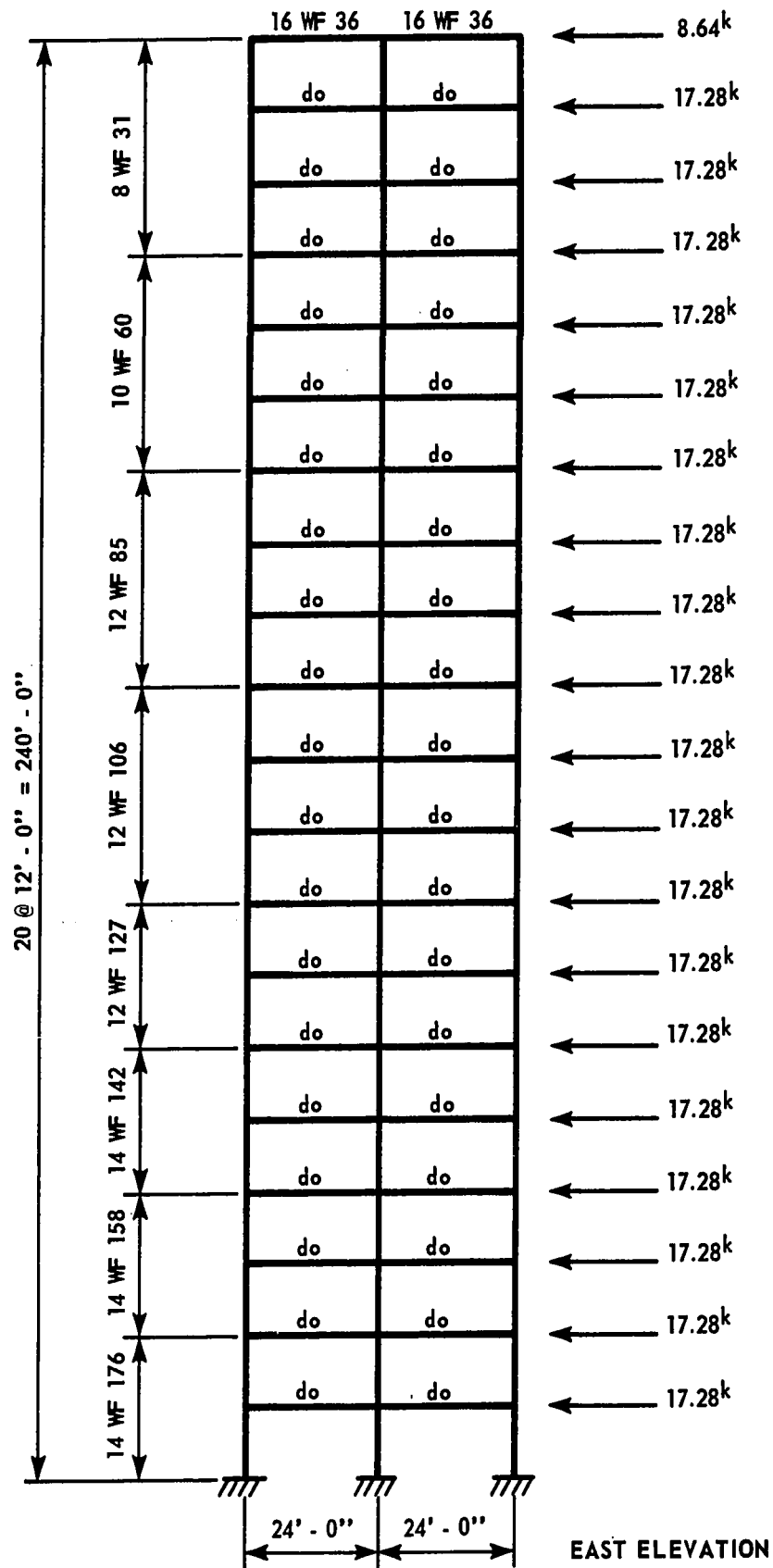
EAST ELEVATION

FIGURE 6.6 ELEVATION TWENTY STORY STRUCTURE
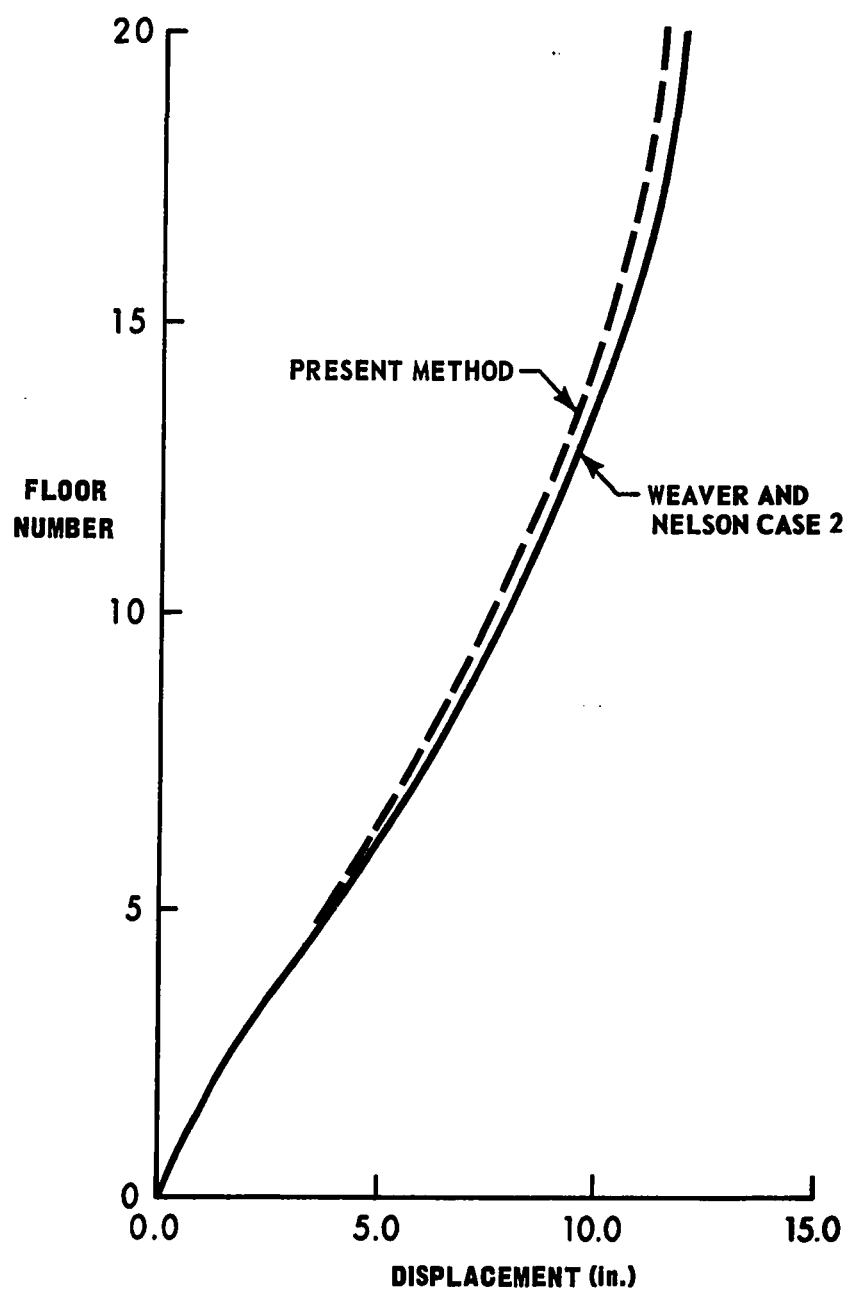
FIGURE 6.7 FLOOR DISPLACEMENTS POINT A

8 x 4.0 = 32.0

Note: all dimensions are in meters
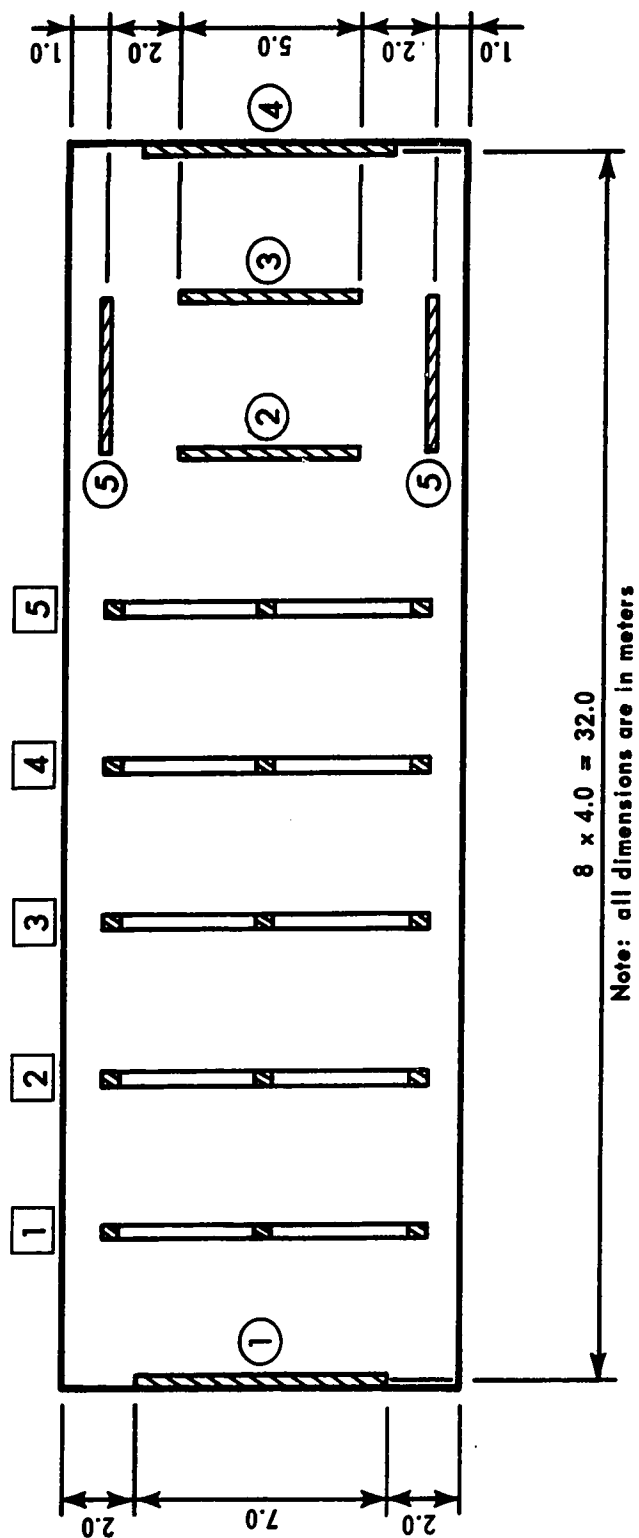
FIGURE 6.8 PLAN SIXTEEN STORY STRUCTURE
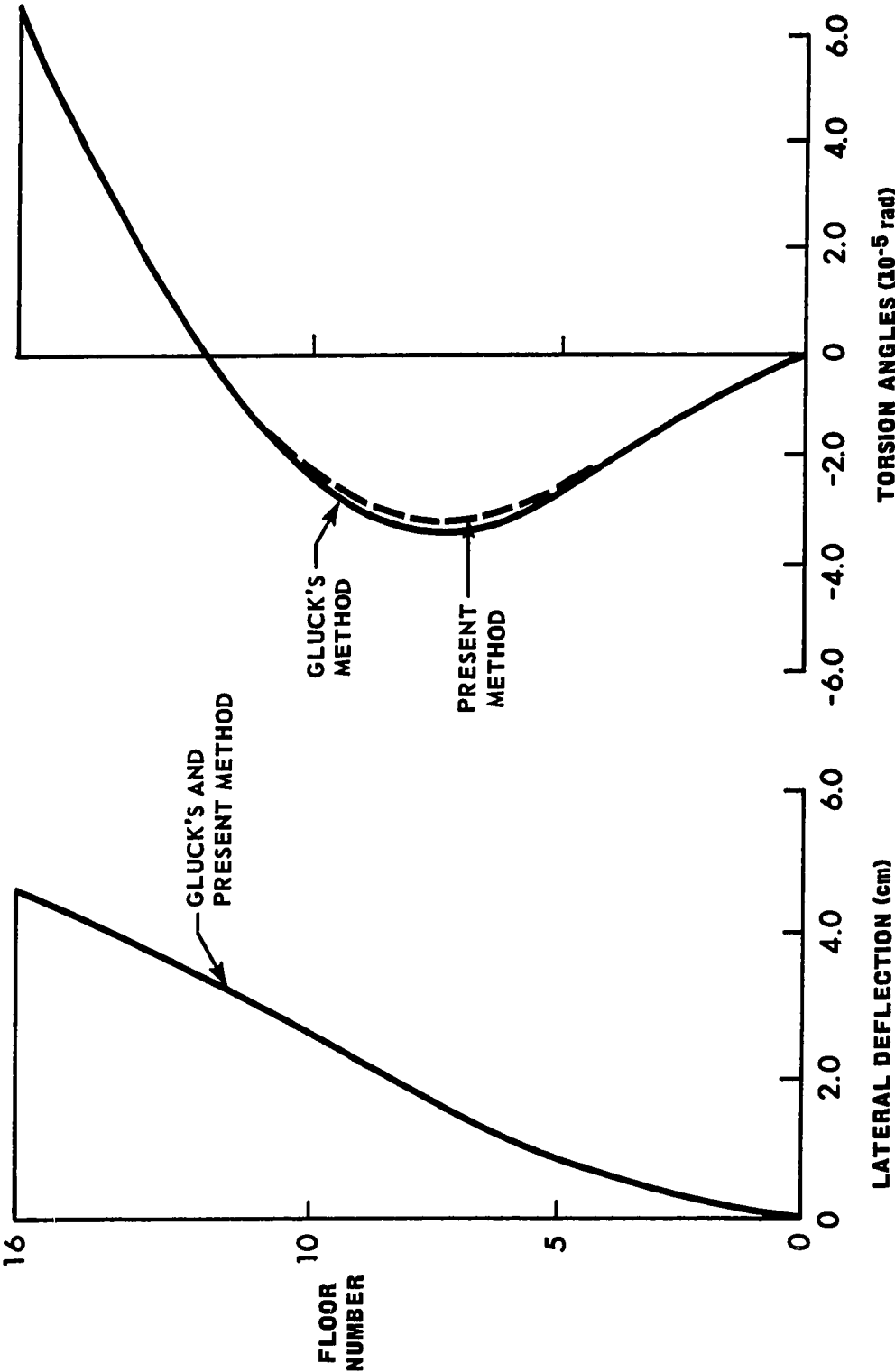
FIGURE 6.9 DISPLACEMENTS SIXTEEN STORY STRUCTURE
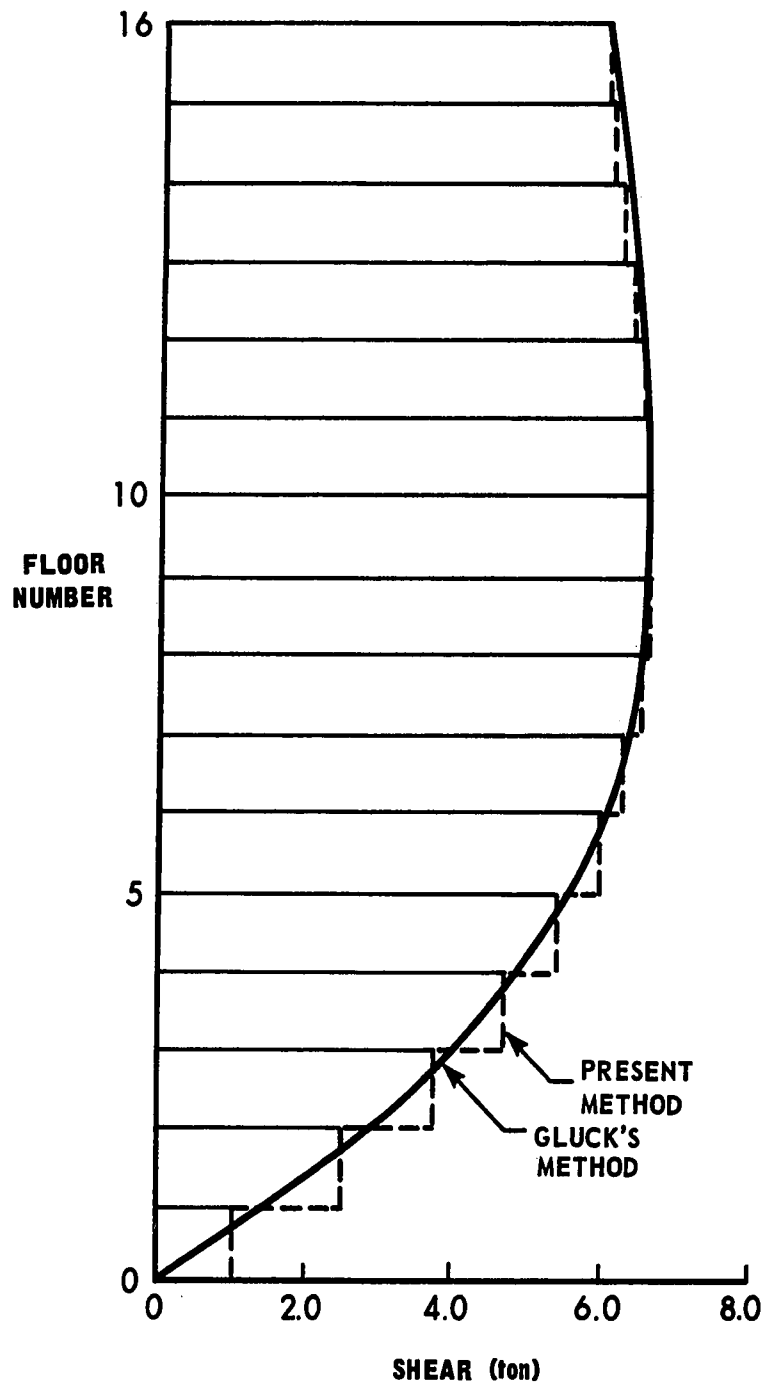
FIGURE 6.10 STORY SHEARS FRAME 1
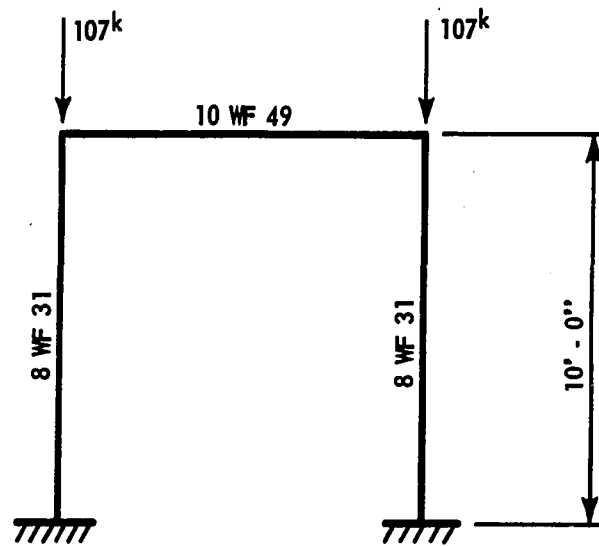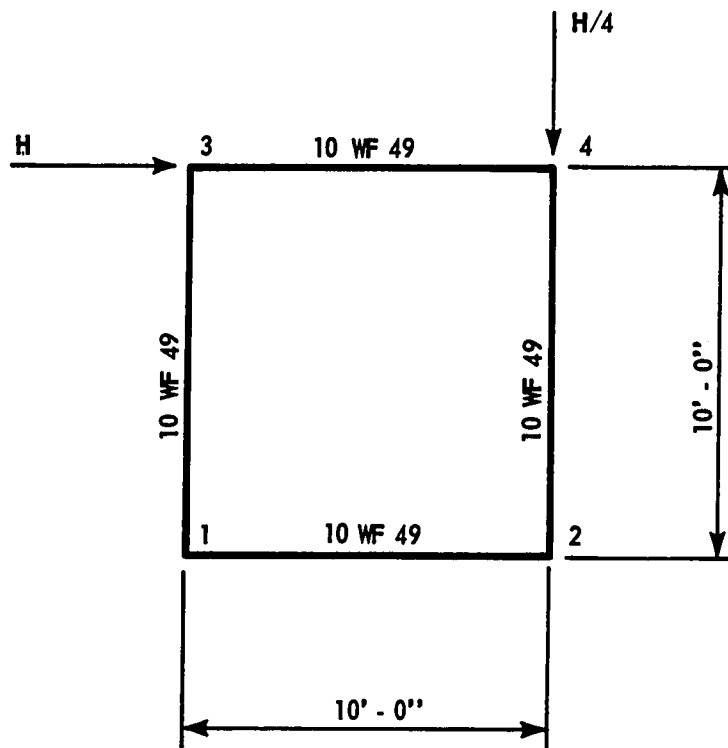
FIGURE 6.11 ONE STORY SPACE FRAME
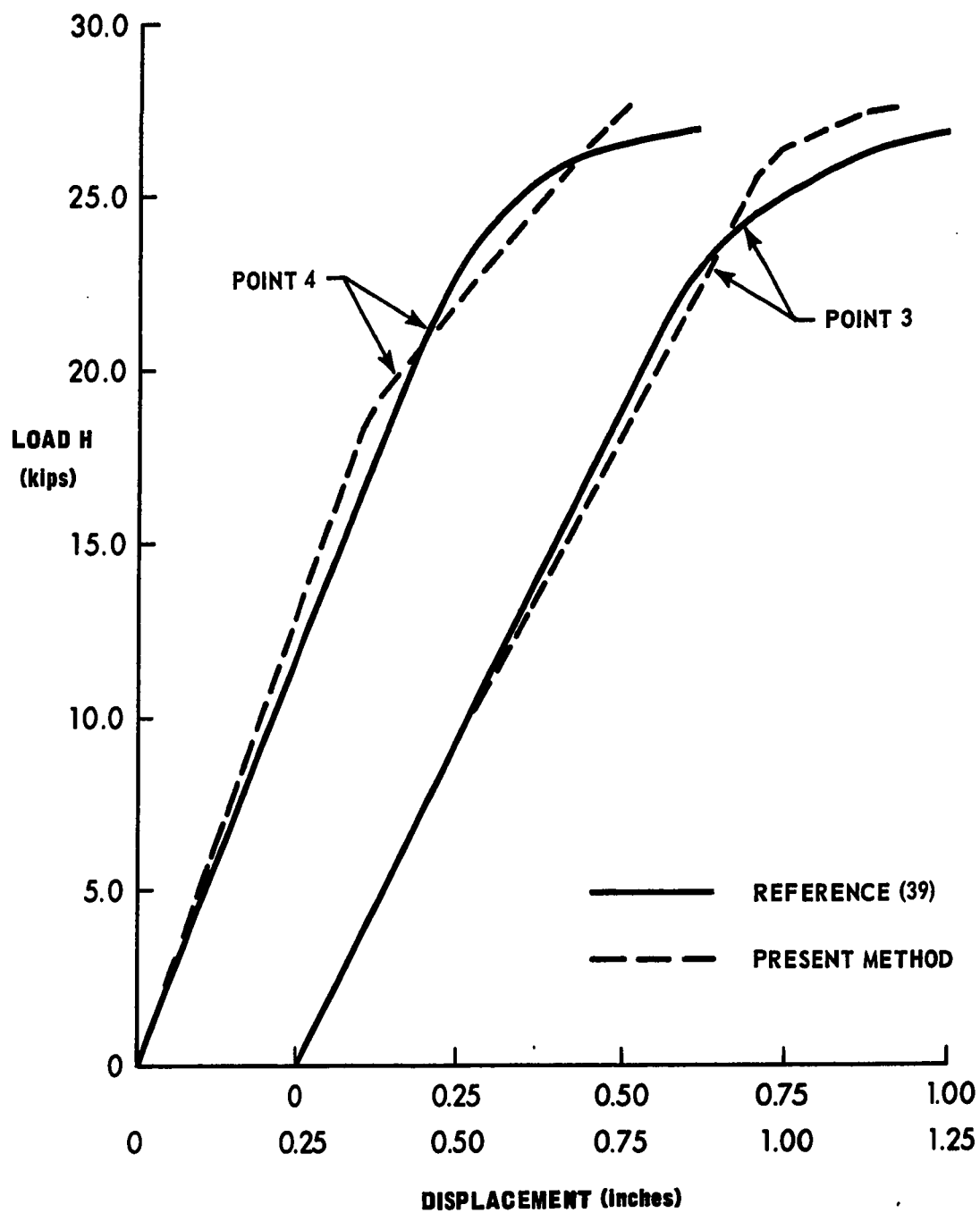
FIGURE 6.12 LOAD-DISPLACEMENT RESPONSE ONE STORY SPACE FRAME

CHAPTER VII

BEHAVIOR STUDY

7.1 Introduction

This chapter describes the structures and the program of investigation used to study the load-displacement response of three dimensional coupled frame-shear wall structures. Two basic structures were chosen as examples; the program of investigation considered:

(a) The effect of increasing asymmetry of lateral load on structures with symmetric layouts.

(b) The effect of increasing asymmetry of structural layout on structures subjected to symmetrically applied lateral loads.

(c) The influence of increasing the St. Venant torsional stiffness of structures subjected to loads causing torsion.

(d) The effect of increasing the vertical load on structures subjected to symmetrically applied lateral loads.

(e) The effect of changing the distribution of the vertical loads, so that the vertical load taken by each bent is no longer proportional to its tributary area.

(f) The influence of increasing the torsional stiffness of the structure by moving the stiffer shear wall bents toward the exterior faces of the structure.

A ten story structure and a twenty-four story structure were used to illustrate the above effects. Because of the arrangement of the ten story structure, the influence of variable (f) will not be considered for this case. The results of the study will be presented and discussed in CHAPTER VIII.

7.2 Basic Structures

The structures to be analyzed are divided into two series. The first series is denoted by the letter M, and refers to analyses performed on the ten story structure, while the letter L is used for the second series, which studies the behavior of the twenty-four story structure. Each analysis, within a series, is distinguished numerically. The basic structures are described first and variations will be described in the section discussing the influence of a particular variable.

7.2.1 Series M

This ten story structure has been used previously to illustrate the influence of torsional action in the elastic range (12). The plan and elevation of the structure are shown in FIGURE 7.1. The modulus of elasticity was 29,000 k.s.i. for the steel members and 3,160 k.s.i. for the concrete shear wall. A yield stress of 40 k.s.i. was adopted for the steel members. The vertical load on the structure was 100 p.s.f. acting on the plan areas of each level as shown in FIGURE 7.1 and the working lateral load on the long side was 16 p.s.f. resulting in the total lateral loads shown in elevation in FIGURE 7.1. The St. Venant torsional stiffness (GK_T) was 10.3 x 10^6 kip in^2 for the bottom

the factored working loads (1.30 for combined loading), presented in TABLE 6.13 of Reference 22, and reproduced in TABLE 7.8. The column live loads were reduced using the formula presented in ASA-A58.1 (55). The bents are spaced at 24'-0" which is the same spacing adopted in Reference 22. The floor beam sizes, spanning between adjacent bents, are shown in FIGURE 7.2, and are constant throughout the structure. The vertical loads are maintained constant during the analysis, while the lateral load (20 p.s.f. at working load) is incremented. The width of the structure, for calculating loads (lateral and vertical) was taken as 132 feet. This width is based on an overhang of 6 feet, on each side of the structure, and was selected so that equal vertical loads would act on each of bents 1 to 6.

For the analysis, each bent (in both perpendicular directions) is lumped into an equivalent bent, as described in CHAPTER III. The member properties for all lumped bents are presented in TABLES 7.4 to 7.7. The moment of inertia of each wall is 11.3×10^6 in^4 about the axis of symmetry, and 1.51×10^6 in^4 about a perpendicular centroidal axis, which was calculated to be 22 inches from the outside face of the wall. The St. Venant torsional stiffness (GK_T) is 230×10^6 kip in^2 for each wall. The torsional stiffness of the columns is small, in relation to that of the walls, and was neglected. Consequently, the total St. Venant torsional stiffness for the structure is 460×10^6 kip in^2. The plastic moment capacity of the wall was taken as 0.34×10^6 kip in and 0.26×10^6 kip in, about the strong and weak axes, respectively;

for the bottom six stories. For the eighteen remaining stories, the plastic moment capacities were set at one half of these values. The modulus of elasticity was 29,000 k.s.i. for the structural steel members and 3,160 k.s.i. for the reinforced concrete shear walls. The yield stress of the steel was 36 k.s.i., the specified minimum for A36 material. In lumping bents B and C, the effective wall width was set at 44 inches, twice the distance between the centroidal axis and the outside face of the wall.

7.3 Program of Investigation

The influence of each of the variables listed in SECTION 7.1 is studied by analyzing several structures. The structures used are the two basic structures described above but either the structural arrangement or the loading condition is altered where necessary to illustrate the influence of a particular parameter. The modified structures, which are used to study the load-displacement relationship, are described below.

7.3.1 Asymmetry of Lateral Load

To investigate the influence of this parameter the arrangement of the structure is symmetrical, while the point of application of the lateral load is varied. The eccentricity of lateral load is expressed as the perpendicular distance between the point of application of the lateral load and the center of the structure and will be denoted as e. For series M, the stiff shear wall bent is located at

the center of the structure ($X = 0$). The structures considered are:

(a) Series M: M1, M2, M3, M4 and M5; the eccentricity of lateral load, e, is 0, 36, 72, 144 and 360 inches, respectively, where 360 inches corresponds to one-half of the width of the structure.

(b) Series L: L1, L2, L3 and L4; the eccentricity of lateral load, e, is 0, 72, 144 and 288 inches, respectively, where 288 inches corresponds to 20 percent of the width of the structure. The ultimate load carrying capacity for a structure with a St. Venant torsional stiffness, GK_T, approaching the value for a closed section was examined by re-analyzing structure L2. The GK_T value, however, was set equal to 10 times the value for the basic structure. This revised structure was referenced as L8.

7.3.2 Asymmetry of Structural Layout

For this set of analyses, the lateral load is applied at the center of the face of the structure ($e = 0$). The structural arrangement is varied, however, as follows:

(a) Series M: The stiff shear wall bent (bent 2) is moved from the center of the structure ($X = 0$) towards the outside, by 90 inches, for each successive analysis. The structures are referenced as: M1, M6, M7, M8 and M9; where the location of the shear wall bent (defined by X in FIGURE 7.1) is 0, 90, 180, 270 and 360 inches, respectively.

(b) Series L: The coupled frame-shear wall bents (bents 3 and 4 in FIGURE 7.2) are moved, from the center to the outside of the structure, by simply exchanging locations with the uncoupled bents

(5 and 6). The structures are: L1, L5 and L6; where the locations of the shear wall bents are 3 and 4, 4 and 5, and 5 and 6, respectively.

7.3.3 St. Venant Torsional Stiffness

For this phase of the investigation, the structural arrangements are asymmetric and the lateral load is applied at the center of the face of each structure (e = 0). The St. Venant torsional stiffness, GK_T, is varied as follows:

(a) <u>Series M:</u> The shear wall bent (bent 2) is located 360 inches from the center and the structures considered are; M9, M10, M11, M12 and M13 with GK_T values of 1, 10, 20, 50 and 100 times the GK_T values of the basic structure.

(b) <u>Series L:</u> The shear wall bents (bents 3 and 4, FIGURE 7.2) are placed at locations 4 and 5. The structures are referenced as; L7, L5, L9 and L10 with GK_T values of 0, 1, 10 and 100 times the GK_T values of the basic structure.

7.3.4 Magnitude of Vertical Loads

The layout of the structures and the lateral loading are both symmetric, only the magnitude of the vertical load is varied. For comparison purposes the reduced plastic moment capacities of the columns are not changed, but remain constant at the values calculated for the basic structures. The structures considered are:

(a) <u>Series M:</u> M1, M14, M15 and M16 with vertical loads equal to 1.0, 0.0, 1.7 and 2.8 times the working load.

(b) <u>Series L:</u> L1,L11 and L12 with vertical loads equal to 1.3, 0.0 and 1.43 times the working load.

7.3.5 <u>Asymmetric Vertical Load Distribution</u>

In this group the total vertical load (and the reduced plastic moment capacities of the columns) is the same as for the basic structures, but the load applied to half of the structure (in plan) is increased, while the load on the other half is decreased. The structural layout is symmetrical, while the lateral load is applied both at, and away from, the center line towards the more heavily loaded half. The structures considered are:

(a) <u>Series M:</u> M1, M3, M17 and M18; where M1 (e = 0) and M3 (e = 72) have been previously described, and structures M17 and M18 have a vertical load of 90 p.s.f. on one half and 110 p.s.f. on the other half of the structure. This corresponds to a decrease and an increase, respectively, which represents 10 percent of the total vertical load. For structure M17 the lateral load is applied without eccentricity and for structure M18 the lateral load is applied with an eccentricity of 72 inches, from the center of the structure.

(b) <u>Series L:</u> L1, L2, L13 and L14; where L1 (e = 0) and L2 (e = 72) have been previously described, and L13 and L14 are subjected to a vertical load of 315 p.s.f. on one half and a corresponding reduction to 257 p.s.f. on the other. The changes in vertical load represent 10 percent of the vertical load on the basic structure (at a load factor of 1.30). Structure L13 has a symmetrically applied lateral load, while the lateral load on structure L14 is applied

with an eccentricity of 72 inches from the center of the structure.

7.3.6 Torsional Stiffness and Strength

This phase of the investigation studied the effect of increasing both the torsional stiffness and strength of a structure by moving the stiffer, and stronger, shear wall bents towards the exterior faces. Analyses were performed on Series L structures having the lateral loads applied with an eccentricity of 72 inches from the center of the structure. The following bent arrangements were investigated:

Series L: L2, L15, L16, L17 and L18; where L2 has been previously described. L15 and L16 have the shear wall bents placed at locations 2 and 5, and, 1 and 6, respectively. Structures L17 and L18 have the same layout as L2 and L16, respectively, but the plastic moment capacities of the shear walls have been increased by 20 percent above the corresponding values for the basic structure.

7.4 Summary

The structures to be used in a behavioral study have been described in this Chapter. The behavioral study is performed on two basic series of structures, to determine the effect on the load-displacement response of several structural parameters. The results of the study are presented and discussed in CHAPTER VIII.

Floor or Story	Beams (in^4) Bents			Columns (in^4) Bents	
	A,B	1,3,4	1,2	A,B	1-4
1	3204	1602	678	708	1446
2	3204	1602	678	708	1446
3	3204	1602	678	708	1446
4	3204	1602	678	708	1446
5	3204	1602	678	708	1446
6	3204	1602	678	150	702
7	3204	1602	678	150	702
8	3204	1602	678	150	702
9	3204	1602	678	150	702
10	3204	1602	678	150	702

TABLE 7.1

MOMENTS OF INERTIA STRUCTURE M

Floor or Story	Beams (M_p)(kip in) Bent			Columns (M_{pc})(kip in) Bent		
	A,B	1,3,4	2	A,B	1,3,4	2
1	16160	8080	4360	7000	9435	10320
2	16160	8080	4360	7000	9710	10320
3	16160	8080	4360	7000	9984	10320
4	16160	8080	4360	7000	10258	10320
5	16160	8080	4360	7000	10320	10320
6	16160	8080	4360	2230	4825	5192
7	16160	8080	4360	2230	5085	5192
8	16160	8080	4360	2230	5192	5192
9	16160	8080	4360	2230	5192	5192
10	16160	8080	4360	2230	5192	5192

TABLE 7.2

PLASTIC MOMENT CAPACITIES STRUCTURE M

Story	Vertical Loads (kips) Bents		Lateral Loads (kips)	Wall Properties	
				Moment of Inertia $(in^4 x10^6)$	Plastic Moment (kip in)
	A,B	1-4			
1	900	450	11.52	0.442	25800
2	810	405	11.52	0.442	25800
3	720	360	11.52	0.442	25800
4	630	315	11.52	0.442	25800
5	540	270	11.52	0.442	25800
6	450	225	11.52	0.442	25800
7	360	180	11.52	0.442	25800
8	270	135	11.52	0.442	25800
9	180	90	11.52	0.442	25800
10	90	45	5.76	0.442	25800

TABLE 7.3

LOADS AND WALL PROPERTIES STRUCTURE M

Floor	Bent Number				
	1,2,5,6 Frame(in^4)	3,4 Wall(in^4)	AD Frame(in^4)	B,C Wall(in^4)	BC Frame(in^4)
1	2698	1409	2900	1166	2332
2	2698	1409	2900	1166	2332
3	2698	1409	2900	1166	2332
4	2698	1409	2900	1166	2332
5	2432	1249	2900	1166	2332
6	2432	1249	2900	1166	2332
7	2432	1249	2900	1166	2332
8	2432	1249	2900	1166	2332
9	2300	1170	2900	1166	2332
10	2300	1170	2900	1166	2332
11	2300	1170	2900	1166	2332
12	2300	1170	2900	1166	2332
13	2300	1170	2900	1166	2332
14	2300	1170	2900	1166	2332
15	2300	1170	2900	1166	2332
16	2300	1170	2900	1166	2332
17	2300	1170	2900	1166	2332
18	2300	1170	2900	1166	2332
19	2300	1170	2900	1166	2332
20	2300	1170	2900	1166	2332
21	2300	1170	2900	1166	2332
22	2300	1170	2900	1166	2332
23	2300	1170	2900	1166	2332
24	1559	791	2900	1166	2332

TABLE 7.4

MOMENTS OF INERTIA BEAMS STRUCTURE L

Story	Bent Number					
	3,4 (in^4)	1,2,5,6 (in^4)	A (in^4)	B (in^4)	C (in^4)	D (in^4)
1	10413	20826	9786	6524	8680	13020
2	10413	20826	9786	6524	8680	13020
3	9366	18732	8796	5864	7944	11916
4	9366	18732	8796	5864	7944	11916
5	8438	16363	7986	5324	6524	10842
6	8438	16363	7986	5324	6524	10842
7	6854	13708	6750	4500	5864	8796
8	6854	13708	6750	4500	5864	8796
9	5768	11536	5880	3920	4908	7362
10	5768	11536	5880	3920	4908	7362
11	4948	9896	5028	3352	4292	6438
12	4948	9896	5028	3352	4292	6438
13	4189	8136	4212	2640	3532	5580
14	4189	8136	4212	2640	3532	5580
15	3378	6756	3168	2112	2980	4470
16	3378	6756	3168	2112	2980	4470
17	2859	5718	2730	1820	2272	3408
18	2859	5718	2730	1820	2272	3408
19	2117	4234	1242	828	1820	2730
20	2117	4234	1242	828	1820	2730
21	1139	2278	642	428	864	1296
22	1139	2278	642	428	864	1296
23	786	1572	265	176	428	642
24	786	1572	265	176	428	642

TABLE 7.5

MOMENTS OF INERTIA COLUMNS STRUCTURE L

Floor	Bent Number				
	1,2,5,6 Frame (kip in)	3,4 Wall (kip in)	A,D Frame (kip in)	B,C Wall (kip in)	B,C Frame (kip in)
1	15254	6885	16940	5900	11800
2	15254	6885	16940	5900	11800
3	15254	6885	16940	5900	11800
4	15254	6885	16940	5900	11800
5	14244	6380	16940	5900	11800
6	14244	6380	16940	5900	11800
7	14244	6380	16940	5900	11800
8	14244	6380	16940	5900	11800
9	13464	5990	16940	5900	11800
10	13464	5990	16940	5900	11800
11	13464	5990	16940	5900	11800
12	13464	5990	16940	5900	11800
13	13464	5990	16940	5900	11800
14	13464	5990	16940	5900	11800
15	13464	5990	16940	5900	11800
16	13464	5990	16940	5900	11800
17	13464	5990	16940	5900	11800
18	13464	5990	16940	5900	11800
19	13464	5990	16940	5900	11800
20	13464	5990	16940	5900	11800
21	13464	5990	16940	5900	11800
22	13464	5990	16940	5900	11800
23	13464	5990	16940	5900	11800
24	9786	4382	16940	5900	11800

TABLE 7.6

PLASTIC MOMENT CAPACITIES BEAMS (M_p) STRUCTURE L

Story	Bent Number					
	3,4 (kip in)	1,2,5,6 (kip in)	A (kip in)	B (kip in)	C (kip in)	D (kip in)
1	20440	40810	42540	28160	38680	58260
2	22150	44190	45420	30040	41120	61800
3	19010	37850	38460	25600	36400	54960
4	20630	41180	41340	27520	38800	58320
5	17900	33220	35880	23800	27400	51660
6	19480	36370	38700	25600	29680	55020
7	13380	26610	28620	18920	25640	38880
8	14970	29790	31500	20800	27960	42240
9	10910	21710	25080	16440	20280	30840
10	12510	24850	27960	18400	22600	34260
11	9760	19350	21540	14120	18600	28260
12	11270	22400	24180	15960	20800	31500
13	8640	15880	19120	9840	14960	25740
14	10120	18870	20760	12040	17200	28920
15	7140	14150	15060	9800	13520	20580
16	8660	17150	17520	11440	15640	23820
17	7220	14210	15000	9600	12160	18540
18	8710	17270	17160	11320	14000	21240
19	5740	11300	7770	5000	10880	16620
20	7210	14230	9540	6216	12520	19020
21	4125	8105	5688	3660	6720	10266
22	5340	10570	6810	4520	7728	11592
23	3968	7802	3558	2308	4620	6930
24	5182	10319	3558	2372	4620	6930

TABLE 7.7

PLASTIC MOMENT CAPACITIES COLUMNS (M_{pc}) STRUCTURE L

Story	Bent Number				
	1-6 (kips)	A (kips)	B (kips)	C (kips)	D (kips)
1	9936	13382	13419	16438	16376
2	9517	12816	12854	15746	15683
3	9098	12250	12290	15054	14991
4	8679	11683	11725	14362	14299
5	8259	11117	11161	13670	13606
6	7840	10550	10596	12979	12914
7	7421	9984	10031	12287	12221
8	7002	9418	9467	11595	11529
9	6583	8851	8902	10903	10837
10	6163	8285	8338	10211	10144
11	5744	7718	7773	9520	9452
12	5325	7152	7208	8828	8759
13	4906	6586	6644	8136	8067
14	4486	6019	6079	7444	7375
15	4067	5453	5515	6752	6682
16	3648	4886	4950	6061	5990
17	3229	4320	4385	5369	5297
18	2810	3754	3821	4677	4605
19	2390	3187	3256	3985	3913
20	1971	2621	2692	3293	3220
21	1552	2054	2127	2602	2528
22	1140	1536	1562	1909	1835
23	752	982	1058	1265	1205
24	294	356	433	527	450

TABLE 7.8

VERTICAL LOADS STRUCTURE L

5.76^k

11.52^k

11.52^k

11.52^k

11.52^k

11.52^k

11.52^k

11.52^k

11.52^k

11.52^k

12 WF 45

12 WF 85

10 @ 12' - 0'' = 120' - 0''

11' 8' 11'

30'

ELEVATION

18 WF 50

18 WF 50

18 WF 50

RIGID DIAPHRAGM

18 WF 50

18 WF 50

14 WF 34

18 WF 50

30'

e

30'

X

POINT OF LOAD APPLICATION

18 WF 50

18 WF 50

8' - 0'' X 0' - 6''
SHEAR WALL

18 WF 50

11' 8' 11'

A   B
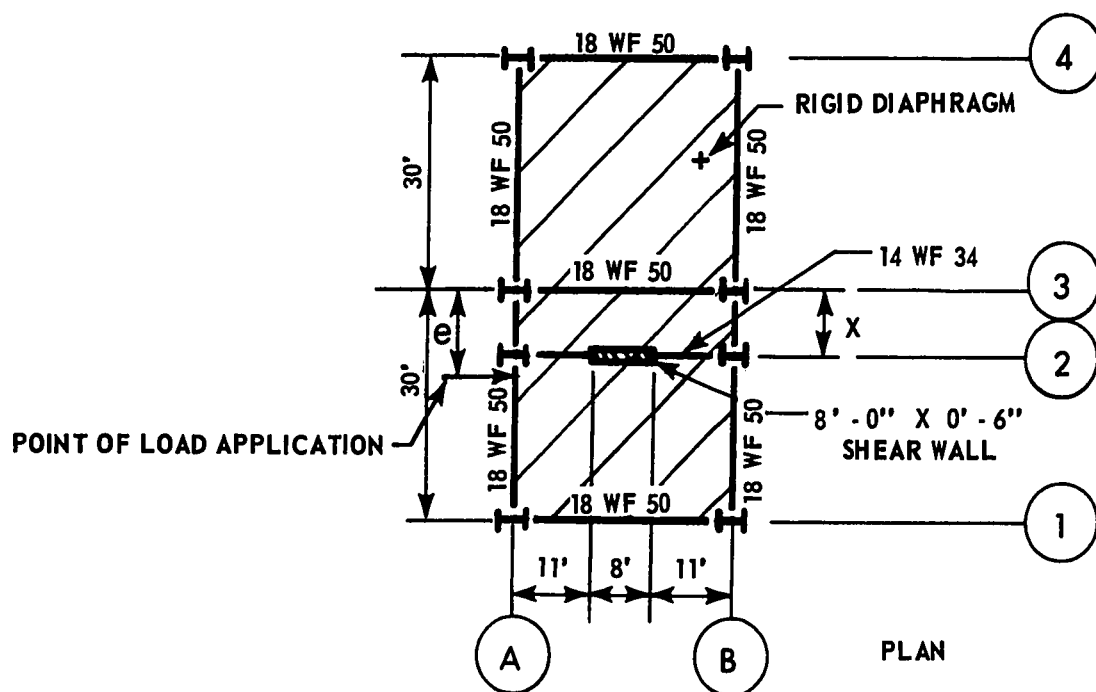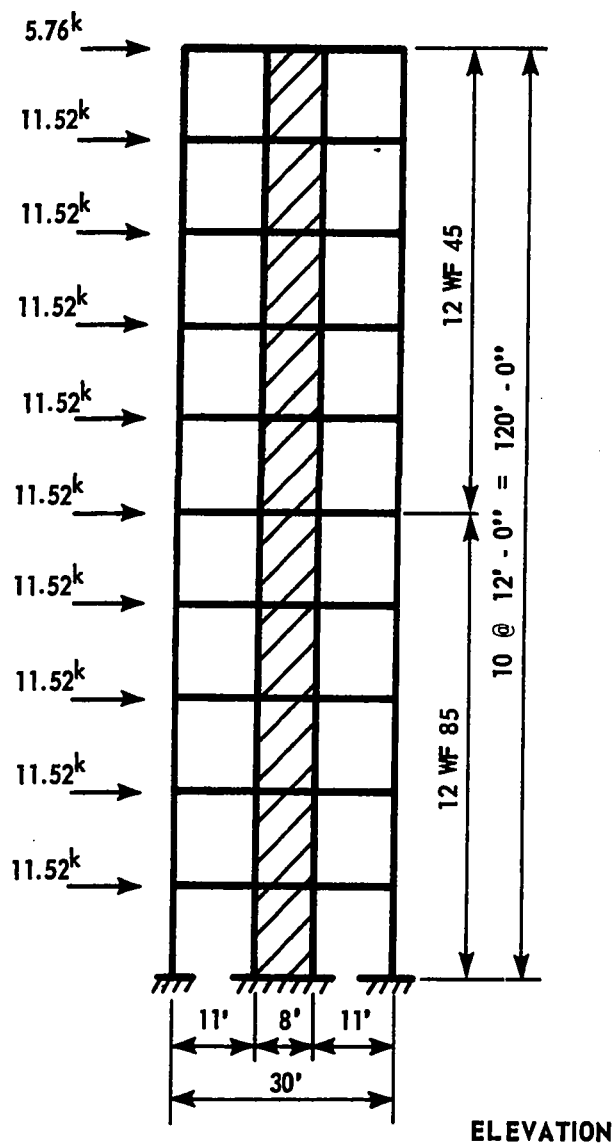
PLAN

FIGURE 7.1 TEN STORY STRUCTURE M

4

3

2

1
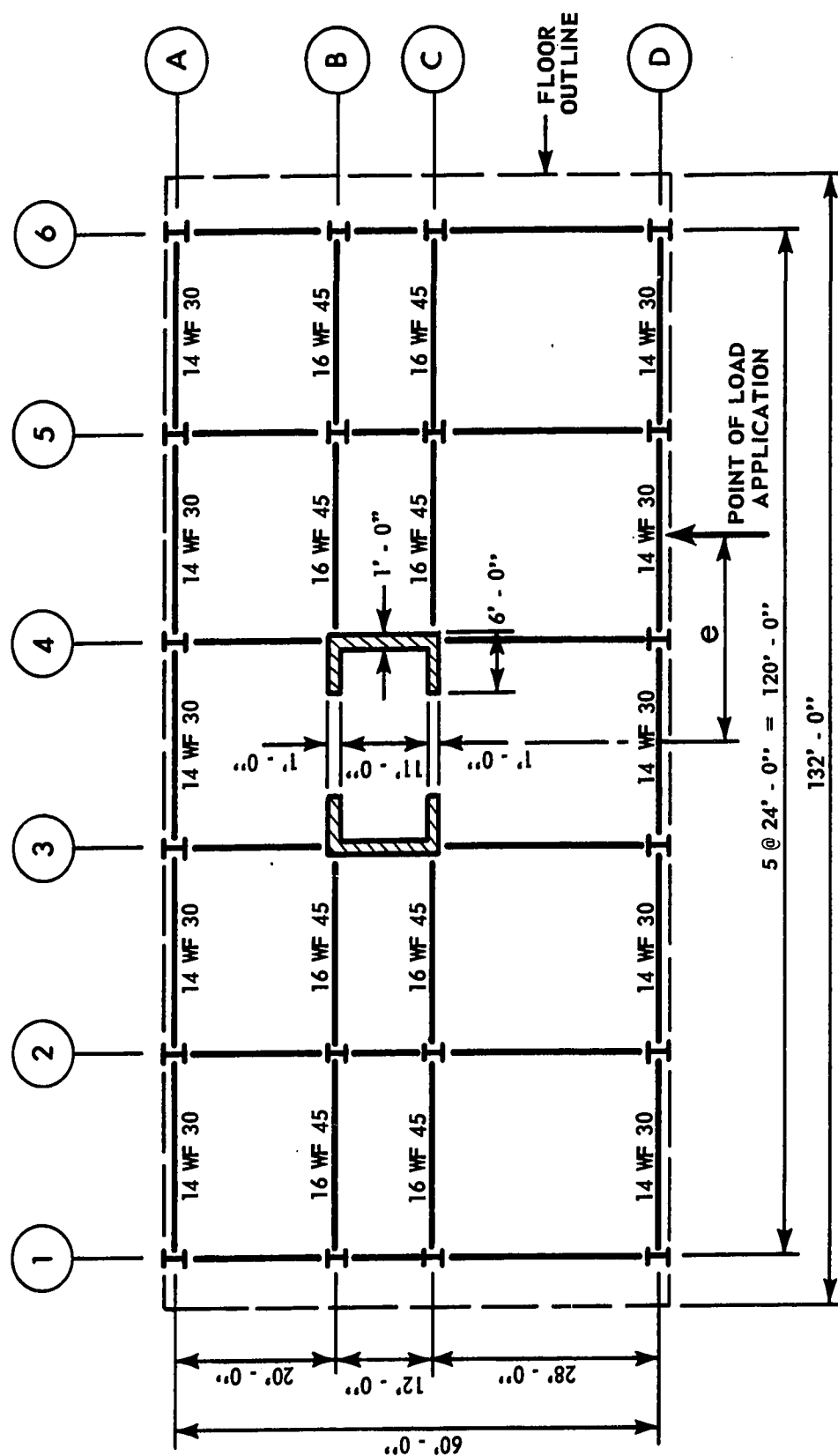
FIGURE 7.2 PLAN TWENTY-FOUR STORY STRUCTURE L

Ⓐ   Ⓑ   Ⓒ   Ⓓ

	14 B 26	12 Jr11.8	16 WF 45	

24

| 12 WF 40 | 14 WF 34 | 14 WF 40 | 12 B 16.5 | 12 WF 58 | 18 WF 55 | 12 WF 58 |

22   do   do   do

20   do   do   do

18   do   do   do

16   do   do   do

14   do   do   do

12   do   do   do

10   do   do   do

8   do   do   18 WF 60

6   do   do   do

4   do   do   20 I 65.4

2   do   do   do

0

Column labels (line A): 12 WF 40, 12 WF 58, 14 WF 78, 14 WF 111, 14 WF 127, 14 WF 150, 14 WF 176, 14 WF 202, 14 WF 228, 14 WF 264, 14 WF 287, 14 WF 314

Column labels (line B left): 14 WF 40, 12 WF 58, 14 WF 78, 14 WF 111, 14 WF 127, 14 WF 142, 14 WF 176, 14 WF 202, 14 WF 228, 14 WF 264, 14 WF 287, 14WF 314

Column labels (line C): 12 WF 58, 12 WF 79, 14 WF 111, 14 WF 136, 14 WF 158, 14 WF 184, 14 WF 219, 14 WF 246, 14 WF 287, 14 WF 314, 14 WF 370, 14 WF 398

Column labels (line D): 12 WF 58, 12 WF 79, 14 WF 111, 14 WF 136, 14 WF 158, 14 WF 193, 14 WF 219, 14 WF 246, 14 WF 287, 14 WF 342, 14 WF 370, 14 WF 398

24 @ 12' - 0" = 288' - 0"

20" - 0	12' - 0'	28' - 0"

FIGURE 7.3 ELEVATION TWENTY-FOUR STORY STRUCTURE L

CHAPTER VIII

PRESENTATION AND DISCUSSION OF RESULTS

8.1 Introduction

For the behavioral study, described in the previous chapter, a total of 36 structures were analyzed. The results obtained are presented primarily as load-displacement curves; the displacements are plotted for the center of the top floor of each structure. As a summary, the load factors and structure sways (displacement of the center of the top floor divided by the total structure height) at the formation of the first hinge and at the ultimate load carrying capacity for all of the structures are presented in TABLES 8.1 and 8.2, respectively. In order to illustrate the three dimensional aspect of the behavior, the load-floor rotation responses of the top floors are also presented where pertinent.

The data obtained for the basic structures (M1 and L1) are presented and discussed first. The influence of each of the structural parameters considered in the behavioral study is presented and discussed in the same order as in the previous chapter. The effects of the assumptions made in the analysis are discussed and methods are described that may be used to assess the influence of the major assumptions.

8.2 Basic Structures

For all structures discussed in this chapter, a load factor, λ, of 1.0 corresponds to the working lateral load, while the displacements, v, are plotted for the center of the top floor, and the floor rotations, ϕ, when plotted, also refer to the top floor of the structure.

The load-displacement response for structure M1 (FIGURE 7.1) is shown in FIGURE 8.1, while the hinge configuration is shown by the dots in FIGURE 8.3. The numbers adjacent to the dots represent the order of hinge formation. Because the loading and layout of this structure are symmetrical, no in-plane displacements occur in bents A and B and the floor rotations are zero. Bent 2 is a coupled frame-shear wall bent, which is much stiffer than the three uncoupled bents. As a result the first hinge formed at the base of the wall at a load factor of 1.34. The moments in the beams then increased rapidly with increased lateral load and considerable hinging occurred. The hinging was accompanied by a gradual decrease in the stiffness of the bent with a resulting increase in the proportion of the load carried by the remaining bents. Finally a hinge formed (λ = 3.04) at the base of the column in each of the uncoupled bents (bent 1, 3 and 4). Hinging then occurred in the frame beams of the uncoupled bents (λ = 3.67): at this stage the rotational restraint on the column vanishes (at the joint where a hinge forms), which causes a rapid decrease in lateral stiffness. The structure reached its ultimate carrying capacity at a load factor of 3.79. At this point the top floor sway was 0.011.

The unloading branch of the load-displacement curve was
flat, which may be attributed to the relatively low vertical loads
on the structure. This, in turn, produces low P-Δ moments (relative
to the primary moments) even at the large story sways. The rotational
discontinuities across the plastic hinges, calculated at various load
factors are presented in TABLE 8.3, for some of the earlier hinges
formed. Hinge reversals did not occur. At the ultimate load the total
rotational discontinuities ranged from 3 to 5 times the member end
rotations at first yield. The entire load displacement response for
this structure was developed in just under 5 minutes computing time.

The load-displacement curve obtained for structure L1
(FIGURES 7.2 and 7.3) is plotted in FIGURE 8.4. The hinge configu-
ration is shown in FIGURES 8.6 and 8.7. Because of the symmetrical
loading and structural layout no displacements occur in bents A to D
(FIGURE 7.2), and the floor rotations are zero. The first hinges form
(λ = 1.05) at the base of the shear walls in bents 3 and 4. As bents
3 and 4 are still stiffer than the uncoupled bents (bents 1,2,5 and 6),
a small increase in lateral load results in a series of hinges forming
in the beams. At a load factor of 1.37 the stiffness of bents 3 and 4
has been reduced (24 hinges in each bent) so that hinges form at floors
8 to 11 in the beams of the uncoupled bents. Beyond this point the
lateral stiffness of the structure rapidly decreases, and at a load
factor of 1.39 the normalized determinant changes sign. The structure
sways are 0.0042 and 0.0059 at load factors of 1.0 and 1.30, respectively.

The rotational discontinuities for the earlier hinges to form are presented in TABLE 8.4. No reversal is shown, and the hinge rotations at maximum load factor are 50 percent of the member end rotations at the formation of the hinge. This structure was analyzed in 15 minutes computing time.

8.3 Program of Investigation

The results obtained from the analyses of the structures described in SECTION 7.3 will now be presented and discussed. The order of presentation is the same as that adopted in describing the modifications to the basic structures, in CHAPTER VII, and the same subsection headings are used. A summary of the results obtained for all structures is presented in TABLES 8.1 and 8.2.

8.3.1 Asymmetry of Lateral Load

(a) Series M: M1, M2, M3, M4 and M5; the load-displacement curves, shown in FIGURE 8.1 are identical in the elastic range. The structural arrangements for all structures are symmetrical, and the twist caused by the asymmetry of the lateral loads results in rotation of the floor diaphragms about the center of the structure. The increase in the twisting motion is shown by the load-floor rotation curves plotted in FIGURE 8.2. The torsional stiffness (in the elastic range) is the same for each of the structures, however, the applied torque is directly proportional to the asymmetry of the load. Consequently, the floor rotations increase with the degree of asymmetry.

As the load is increased (for structures other than M1) the exterior bent, bent 1, undergoes larger displacements due to the floor rotations. This bent yields first, and as a result the center of stiffness moves from the center of the structure. This effectively increases the torque and results in increased floor rotations to maintain equilibrium. The hinge configurations, are shown in FIGURES 8.3 and 8.8 for structures M1 and M3, respectively. Hinging in bent 1 of structure M1 is initiated at $\lambda = 3.58$, while for structure M3 the first hinge forms (in bent 1), at $\lambda = 2.85$.

The load carrying capacity is reduced as the eccentricity of loading increases by the increased P-Δ moments which result from the increased floor displacements. The increased floor displacements result from the movement of the center of rotation from the center of the structure as hinging progresses. The reduction in the load carrying capacity is clearly illustrated by FIGURES 8.1 and 8.2 and the corresponding load factors are listed in TABLE 8.1.

A negative normalized determinant was observed at point 1 ($\lambda = 2.07$) on the load-displacement curve for structure M5 (FIGURE 8.1). When the load was decremented, the curve 1-3 was obtained, suggesting that the lateral stiffness was still positive at this stage. The structure was then re-analyzed by increasing the load (even though the normalized determinant was negative), until the sign of the normalized determinant became positive. The curve obtained is shown as 1-2 in FIGURES 8.1 and 8.2; where 2 is the point where the normalized deter-

minant changes sign from negative to positive. For all practical purposes this structure reaches its ultimate load carrying capacity at point 1. However, this example illustrates the fact that a negative normalized determinant does not necessarily signify attainment of the ultimate load carrying capacity. Due to the coupling of the lateral and torsional stiffnesses in the coefficient matrix, an increase in load may be obtained even with a negative determinant.

As a summary for this group of structures; the reductions in ultimate load carrying capacities are; 3, 8, 19 and 38 percent for structures L2, L3, L4 and L5, respectively. The asymmetry of load corresponds to 5, 10, 20 and 50 percent of the width of the structure, respectively.

(b) Series L: L1, L2, L3 and L4; the load-displacement curves for these structures (FIGURES 7.2 and 7.3), plotted in FIGURE 8.4, are again identical in the elastic range. The load-floor rotation curves, shown in FIGURE 8.5, exhibit behavior similar to that of the Series M structures. The notable difference is the greater reduction in ultimate load carrying capacity as the asymmetry of load is increased. This is caused by the higher axial loads that exist in the columns of Series L (P/P_y approximately 0.6 compared with 0.2 for Series M), and the corresponding increase in the severity of the P-Δ effect. The unloading branches of the load-displacement curves are also steeper.

The hinge configurations presented in FIGURES 8.6 and 8.7

for structure L1, and in FIGURES 8.9 and 8.10 for structure L4, clearly show the earlier hinging that occurs in the exterior bent (bent 6), as a result of the increased displacements caused by the floor rotations. Fewer hinges are formed in structure L4 than L1 (33 and 90, respectively) at the maximum load carrying capacity. With increasing asymmetry of load a smaller reduction in torsional stiffness (and the accompanying shift in the center of rotation) will reduce the lateral stiffness to zero, due to the increased severity of the $P-\Delta$ moments. This trend, discussed above specifically for structure L4, is also apparent, but less severe, for structures L2 and L3. The reductions in ultimate load carrying capacity, with increasing asymmetry of load, are; 17, 33 and 53 percent for structures L2, L3 and L4, respectively. The asymmetry of load corresponds to 5, 10 and 20 percent of the width of the structure, respectively. For structure L8 (equivalent to structure L2, but with the GK_T value increased by a factor of 10), the reduction in load carrying capacity was only 9 percent.

8.3.2 Asymmetry of Structural Layout

When the center of stiffness of a structure does not coincide with the point of application of lateral load an applied torque results. The behavior of these asymmetric structures will be similar to that of the symmetric structures subjected to asymmetrically applied lateral loads, however, the two effects cannot be compared directly because of the differences in the interaction between shear wall and frame elements

in the structure.

(a) Series M: M1, M6, M7, M8 and M9; the load-displacement curves for these structures (FIGURE 7.1) are presented in FIGURE 8.11. The response of the structures differ in the elastic range, as the center of rotation is offset relative to the center of the structure. After yielding occurs the severity of the P-Δ moments are increased by the increasing asymmetry of layout (due to the additional shift in the center of rotation), resulting in a reduction in ultimate load carrying capacity. The reductions in ultimate load carrying capacity are; 3, 12, 23 and 34 percent for structures M6, M7, M8 and M9, respectively. These structures correspond to eccentricities of bent 2 (from the center of the structure) of 90, 180, 270 and 360 inches, respectively. Because bent 2 carries 25 percent of the total vertical load; when its location is changed, the distribution of the vertical load is no longer symmetrical. The effect of this is to slightly modify the torsional load due to the P-Δ moments.

(b) Series L: L1, L5 and L6; the load-displacement curves for these structures (FIGURES 7.2 and 7.3) are presented in FIGURE 8.12. The change in the effective stiffnesses in the elastic and inelastic range is again apparent. The reductions in ultimate load carrying capacity are; 51 and 66 percent for structure L5 and L6 respectively. In these structures, the shear wall bent is located 1 and 2 bays, respectively, from the center of the structure.

For structures subjected to torsion, the reduction in ulti-

mate load carrying capacity is similar under increasing torsional load, regardless of whether the torsional load is due to asymmetry of load or structural arrangement. The important factor is the eccentricity between the center of stiffness (and strength) and the point of application of the lateral load.

8.3.3 St. Venant Torsional Stiffness

An increase in the St. Venant torsional stiffness, GK_T, (which is assumed to remain constant as the structure is deformed in the inelastic range) reduces the rotation of the floor diaphragms, for a particular value of the applied torque. This increased stiffness delays the yielding process and the accompanying shift in the center of rotation.

(a) Series M: M9, M10, M11, M12 and M13; the load-displacement curves for these structures (X = 360, FIGURE 7.1) are presented in FIGURE 8.13. In the elastic range the stiffness of the structure increases only slightly with a relatively large increase in GK_T. This is because in the elastic range the greatest contribution to the torsional stiffness comes from the in-plane stiffnesses of the bents. However, once the structure enters the inelastic range, the higher (and constant) GK_T values contribute significantly to the torsional stiffness of the structure, since the proportion of the torque resisted by the in-plane strength of the bents is reduced. With increasing GK_T values the reductions in ultimate load carrying capacity (relative to M1, X = 0) are 34, 29, 22, 7 and 3 percent for structures

M9, M10, M11, M12 and M13, respectively.

(b) Series L: L7, L5, L9 and L10, the load-displacement curves for these structures (shear wall bents at location 4 and 5, FIGURE 7.2), are presented in FIGURE 8.14. The lateral stiffness of the structures is increased only slightly in the elastic range, however, the significance of the increased torsional stiffness is clearly shown by the load-floor rotation curves plotted in FIGURE 8.15. The reductions in ultimate load carrying capacity (relative to structure L1) are 53, 51, 40 and 3 percent for structures L7, L5, L9 and L10, respectively. The corresponding GK_T values are 0, 1, 10 and 100 times the value for the basic structure. The small contribution of the usual St. Venant torsional stiffness to the overall torsional stiffness of the structure can be seen by comparing curves L7 ($GK_T = 0$) and L5 ($GK_T = 1$).

8.3.4 Magnitude of Vertical Load

The vertical loads on a structure reduce the plastic moment capacities of the columns resulting in earlier hinging. In addition, the P-Δ moments reduce the story shear available for resisting the applied lateral loads. In this section only the second (or stability) effect is considered; the plastic moment capacities are not changed from those of the basic structures.

(a) Series M: M1, M14, M15 and M16, the load-displacement curves for these structures, (FIGURE 7.1) are presented in FIGURE 8.16. In the absence of vertical load (M14) the maximum load approaches that

corresponding to a mechanism (λ = 4.18). As the vertical load is increased the ultimate load carrying capacity is reduced (10 percent for structure M1, and 14 and 27 percent for M15 and M16, respectively). The unloading branches of the curves become steeper as the vertical load is increased.

(b) Series L: L1, L11 and L12; the load-displacement curves for these structures (FIGURES 7.2 and 7.3), shown in FIGURE 8.17, show the same trends as for the Series M structures. With zero vertical load (L11) a mechanism load factor of 2.28 is approached. As the vertical load is increased, the sway displacements in the elastic range are increased (by 37 percent for L1) while the ultimate load carrying capacity is reduced (by 39 percent for L1 and 42 percent for L12). Structure L12 is subjected to a vertical load 10 percent above that of the basic structure (L1).

8.3.5 Asymmetric Vertical Load Distribution

(a) Series M: M1, M3, M17 and M18; the load-displacement curves for these structures (FIGURE 7.1), are plotted in FIGURE 8.18. Because of the low vertical loads the change in behavior between structures M1 and M17 is insignificant, while for structures M3 and M18 (lateral load applied with 72 inch eccentricity) the reduction in ultimate load carrying capacity, due to the eccentric application of the vertical load, is less than 2 percent.

(b) Series L: L1, L2, L13 and L14; the load-displacement and

load-floor rotation curves for these structures (FIGURES 7.2 and 7.3),

are presented in FIGURES 8.19 and 8.20, respectively. The increased

torsional load, that results from the eccentrically applied vertical

load is clearly shown by the load-floor rotation curves in FIGURE 8.20.

The reduction in ultimate load carrying capacity is 5 percent for

structure L13 with respect to that of L1. For structures L2 and L14,

the lateral load is applied with an eccentricity of 72 inches. The

reduction due to the increased effective torque is similar to a re-

duction due to increased vertical load. In both cases the effective

P-Δ moments are increased. The load carrying capacity of structure

L14 was 7 percent below that of L2.

8.3.6 Torsional Stiffness and Strength

This phase of the study investigates the increase in load

carrying capacity that results when the stiff shear wall bents are

moved towards the exterior faces of the structure.

Series L: L2, L15, L16, L17 and L18; the load-displacement

curves for these structures (FIGURES 7.2 and 7.3) are presented in

FIGURE 8.21, while the load-floor rotation curves, are plotted in

FIGURE 8.22. The increased torsional stiffness, in the elastic

range is clearly shown in FIGURE 8.22. As the structures are de-

formed inelastically, the shear walls form hinges at their bases, at

essentially the same load factors (0.90 to 0.95). This reduces the

torsional stiffness to virtually the same value for each structure.

Consequently, the increase in ultimate load carrying capacity is minimal. The load-displacement curves in FIGURE 8.21 show the effect of increasing the torsional stiffness of the structure and the strength of the shear walls. The shear wall plastic moment capacities are increased by 20 percent for structures L17 and L18. The increase in ultimate load carrying capacity is 5 percent for structure L17 (compared with L2), and 10 percent for structure L18 (compared with L16).

8.4 Warping Torsion

In the analytical model described in CHAPTER III the contribution of the warping resistance was ignored. The effect of warping, however, can be checked. The analysis calculates the floor rotations, ϕ, at each loading stage; these floor rotations may be differentiated, using a numerical procedure, to obtain the third derivative, ϕ'''. EQUATION (3.15), may be expressed as,

$$M_t = GK_T\phi' \cdot (1 - \frac{EI_\omega}{GK_T} \cdot (\frac{\phi'''}{\phi'}))$$ (8.1a)

or

$$M_t = GK_T' \cdot \phi'$$ (8.1b)

where K_T' may be considered as a modified torsional constant incorporating both the uniform and non-uniform torsion components. The term (ϕ'''/ϕ') may be calculated using a forward difference table or an interpolating polynomial. Having calculated K_T' for each story,

the structure is re-analyzed, using the revised values and the process repeated as necessary.

Using this procedure for structure L2, the torsional constant was increased for the bottom 10 stories, while for all the remaining stories (except story 17) the torsional constant was decreased, due to the negative contribution of the warping resistance. The structure was re-analyzed using the revised values of GK_T' (instead of GK_T). The change in the load-displacement response was insignificant, while the floor rotations for the revised structure were approximately 3 percent less at each floor, as shown in FIGURE 8.23. However, because the contribution of GK_T is small, relative to the overall torsional stiffness of the structure, and since the EI_ω term is relatively small for this particular channel shaped shear wall, the effect of warping torsion for this particular structure (Series L) is negligible.

8.5 Bi-axial Bending of Columns

In the analysis procedure, all columns within a bent are lumped and the resulting model is assumed to simulate the in-plane resistance of the bent. A particular column, therefore, is lumped into two (perpendicular) bents and the interaction between the two is ignored. Yet the columns (particularly the exterior columns) are subjected to bi-axial bending moments and these effects may reduce the strength of the member so that it cannot attain its computed capacity.

In order to assess the influence of bi-axial bending any

particular column may be isolated from the structure together with the beams framing into the ends of the column in both perpendicular directions. The beams are assumed to have points of inflection at midspan. The column is then subjected to the transverse displacements (in both perpendicular directions) imposed upon it during the analysis of the structure. The twisting of the column about its vertical axis is ignored. The joint rotations are unknown, these are determined from the equilibrium of moments at the joints. The equations are modified if hinges have formed in either the column or beams. In this manner it is possible to obtain the bending moments, about both perpendicular directions, for each story of the column. If the hinges formed during the checking procedure differ from those obtained in the overall analysis, the bending moments may be checked against the rigorous interaction relationship (FIGURE 3.5). If the discrepancy is significant, the M_{pc} values of the lumped bent may be revised and the structure re-analyzed.

The external column (common to bents 4 and B, FIGURE 7.1) of structure M9 was analyzed using a program based on the above method. At the ultimate load carrying capacity (λ = 2.50), the hinging in the model was almost identical to that obtained in the overall analysis. For the isolated column, however, a hinge existed at the base of the column (at λ = 2.50), while for the lumped column in the main analysis, an extra hinge had formed at the top of the second story column, as well as at the base (of bent B). This indicates, that for

this particular column, the lumping procedure is conservative.

8.6 Summary

The results obtained from the behavioral study, described in CHAPTER VII, have been presented in this chapter. The influence of several pertinent variables on the load-displacement response was illustrated and discussed. Methods were proposed to study the severity of two of the major simplifying assumptions made in developing the analytical model.

It was found that, mathematically an increase in lateral load was possible, for one particular structure, even though the determinant of the coefficient matrix had changed sign. However, for a practical structure this theoretical increase in load carrying capacity is meaningless, as the structure must be able to resist load applied simultaneously in both principal directions.

Structure	Top Floor Sway X10^{-2}		Load Factor λ		Number of Hinges at Ultimate Load
	First Hinge	Ultimate Load	First Hinge	Ultimate Load	
M1	0.18	1.11	1.34	3.79	35
M2	0.18	1.53	1.34	3.68	37
M3	0.18	1.84	1.34	3.48	39
M4	0.18	1.53	1.34	3.06	39
M5	0.17	0.92*	1.26	2.34*	49*
M6	0.21	1.67	1.40	3.66	40
M7	0.31	1.81	1.66	3.32	33
M8	0.44	1.81	1.92	2.92	31
M9	0.45	1.74	1.70	2.50	18
M10	0.45	1.87	1.70	2.71	22
M11	0.46	2.02	1.80	2.95	30
M12	0.48	2.29	1.90	3.54	38
M13	0.50	1.87	2.12	3.66	38
M14	0.18	2.62	1.37	4.18	44
M15	0.18	0.97	1.30	3.60	35
M16	0.18	0.94	1.28	3.04	28
M17	0.18	1.84	1.34	3.79	37
M18	0.18	1.69	1.33	3.43	37

*Point 2

TABLE 8.1

SWAY, LOAD AND HINGE PARAMETERS

STRUCTURE-SERIES M

Structure	Top Floor Sway X10^{-2}		Load Factor λ		Number of Hinges at Ultimate Load
	First Hinge	Ultimate Load	First Hinge	Ultimate Load	
L1	0.44	0.77	1.05	1.39	90
L2	0.38	0.54	0.90	1.15	39
L3	0.33	0.43	0.78	0.93	33
L4	0.21	0.33	0.50	0.66	33
L5	0.30	0.38	0.60	0.68	25
L6	0.26	0.35	0.40	0.47	13
L7	0.29	0.36	0.58	0.66	14
L8	0.44	0.64	1.05	1.26	81
L9	0.33	0.45	0.70	0.84	23
L10	0.39	0.77	0.88	1.35	118
L11	0.34	1.74	1.32	2.28	224
L12	0.37	0.75	1.02	1.33	144
L13	0.43	0.65	1.03	1.32	77
L14	0.37	0.49	0.88	1.07	40
L15	0.46	0.64	1.08	1.22	61
L16	0.40	0.46	0.95	1.24	61
L17	0.44	0.55	1.06	1.21	57
L18	0.44	0.67	1.06	1.36	68

TABLE 8.2

SWAY, LOAD AND HINGE PARAMETERS

STRUCTURE-SERIES L

Load Factor	Hinges in Structure M1 (10^{-3} radians)		
	Hinge at Base of Wall	Hinge in Wall Beam, Floor 1	Hinge in Wall Beam, Floor 4
Member end Rotation at Formation of Hinge	0.0	3.89	4.35
1.34	0.0		
2.21	2.05	- 0.22	- 1.05
2.46	3.20	- 2.22	- 2.73
2.84	4.75	- 4.58	- 5.04
3.03	5.50	- 5.72	- 6.14
3.55	7.34	- 8.23	- 9.70
3.57	7.42	- 8.34	- 9.90
3.67	8.20	- 9.40	- 10.59
3.69	8.42	- 9.70	- 10.79
3.74	9.79	- 11.57	- 11.75
3.76	10.90	- 13.09	- 12.42
3.78	14.02	- 17.33	- 14.87
3.77	18.80	- 23.86	- 17.52
3.59	35.83	- 47.08	- 34.11
3.58	36.12	- 47.47	- 34.38
3.41	49.38	- 65.56	- 48.18
2.41	108.48	-146.15	-130.74

TABLE 8.3

ROTATIONAL DISCONTINUITIES FOR HINGES IN STRUCTURE M1

Load Factor	Hinge in Structure L1 $(10^{-3}$ radians)		
	Hinge at Base of Wall	Hinge in Wall Beam, Floor 9	Hinge in Wall Beam, Floor 11
Member End Rotation at Formation of Hinge	0.0	6.92	6.92
1.06	0.0		
1.12	0.34		
1.14	0.46		
1.17	0.63		
1.22	0.92	-0.05	
1.23	0.97	-0.16	-0.02
1.24	1.02	-0.30	-0.14
1.26	1.14	-0.54	-0.43
1.28	1.28	-0.81	-0.71
1.29	1.35	-0.94	-0.83
1.31	1.48	-1.19	-1.08
1.32	1.53	-1.41	-1.27
1.34	1.66	-1.79	-1.62
1.37	1.84	-2.36	-2.15
1.38	1.96	-2.75	-2.51
1.39	2.10	-3.27	-3.00
1.40	2.46	-4.61	-4.24
1.38	2.59	-5.17	-4.77
1.36	2.89	-6.31	-5.84
1.35	3.00	-6.76	-6.27

TABLE 8.4

ROTATIONAL DISCONTINUITIES FOR HINGES IN STRUCTURE L1
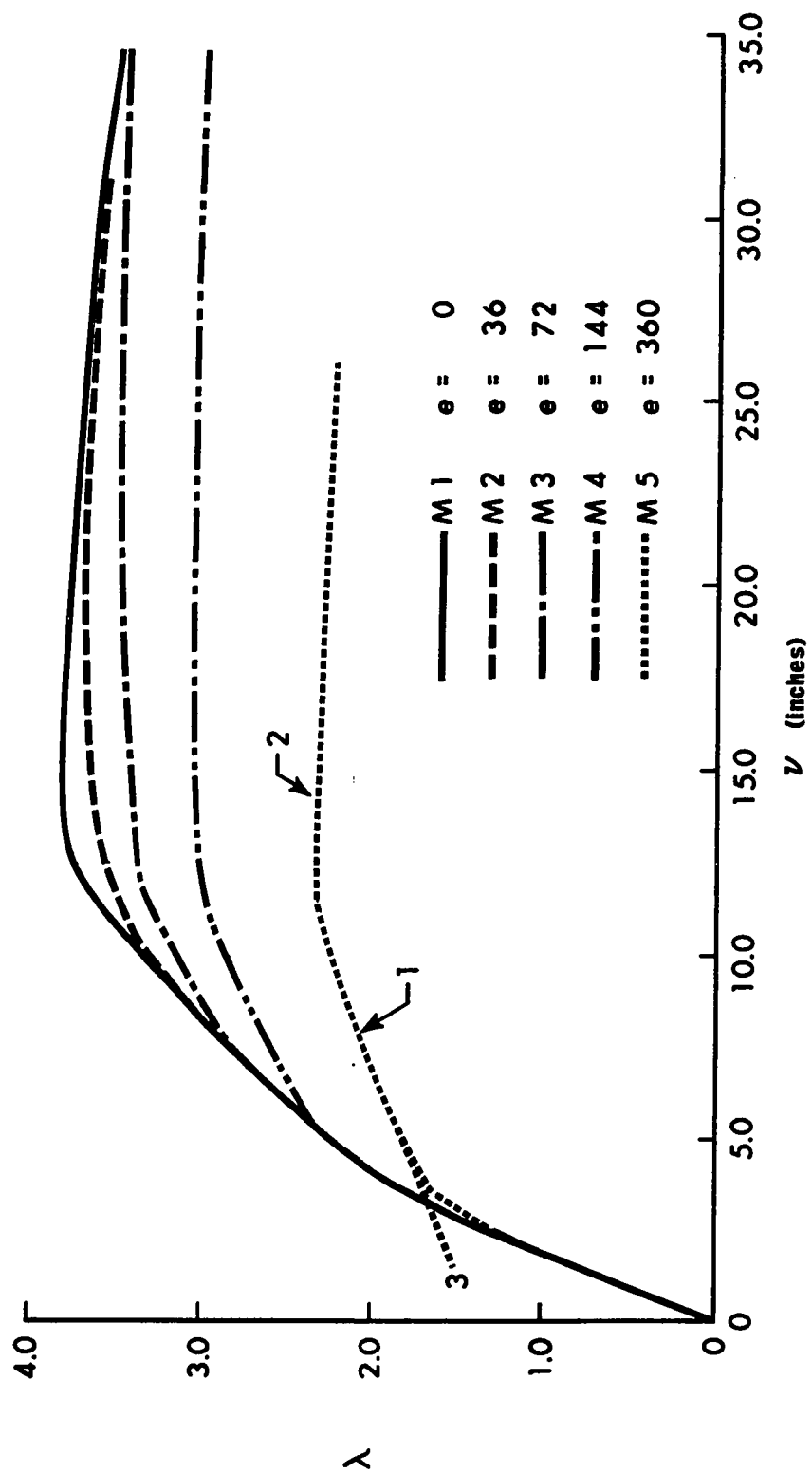
FIGURE 8.1 LOAD-DISPLACEMENT RESPONSE STRUCTURES M1-M5
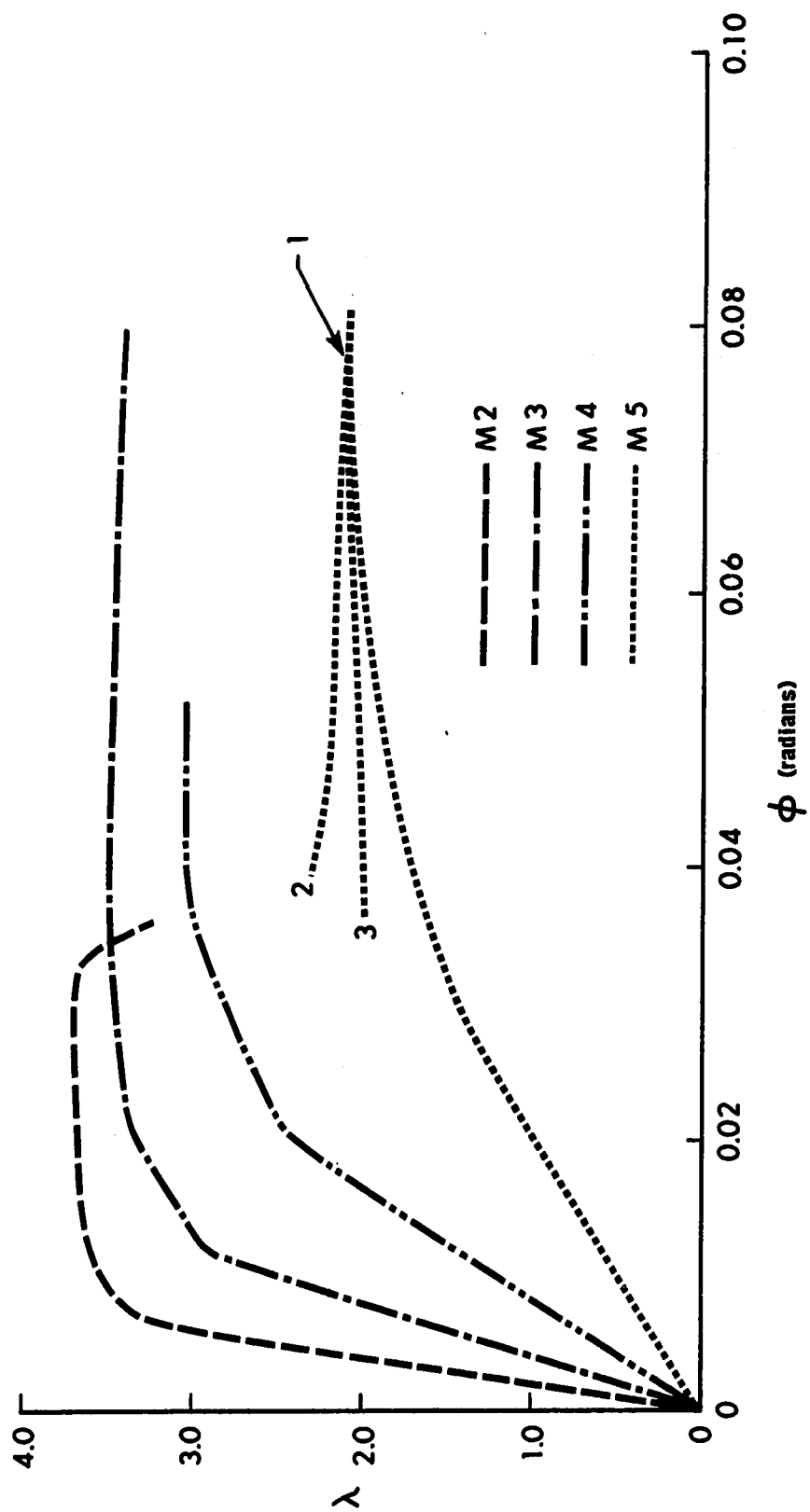
FIGURE 8.2 LOAD-FLOOR ROTATION RESPONSE STRUCTURES M2-M5
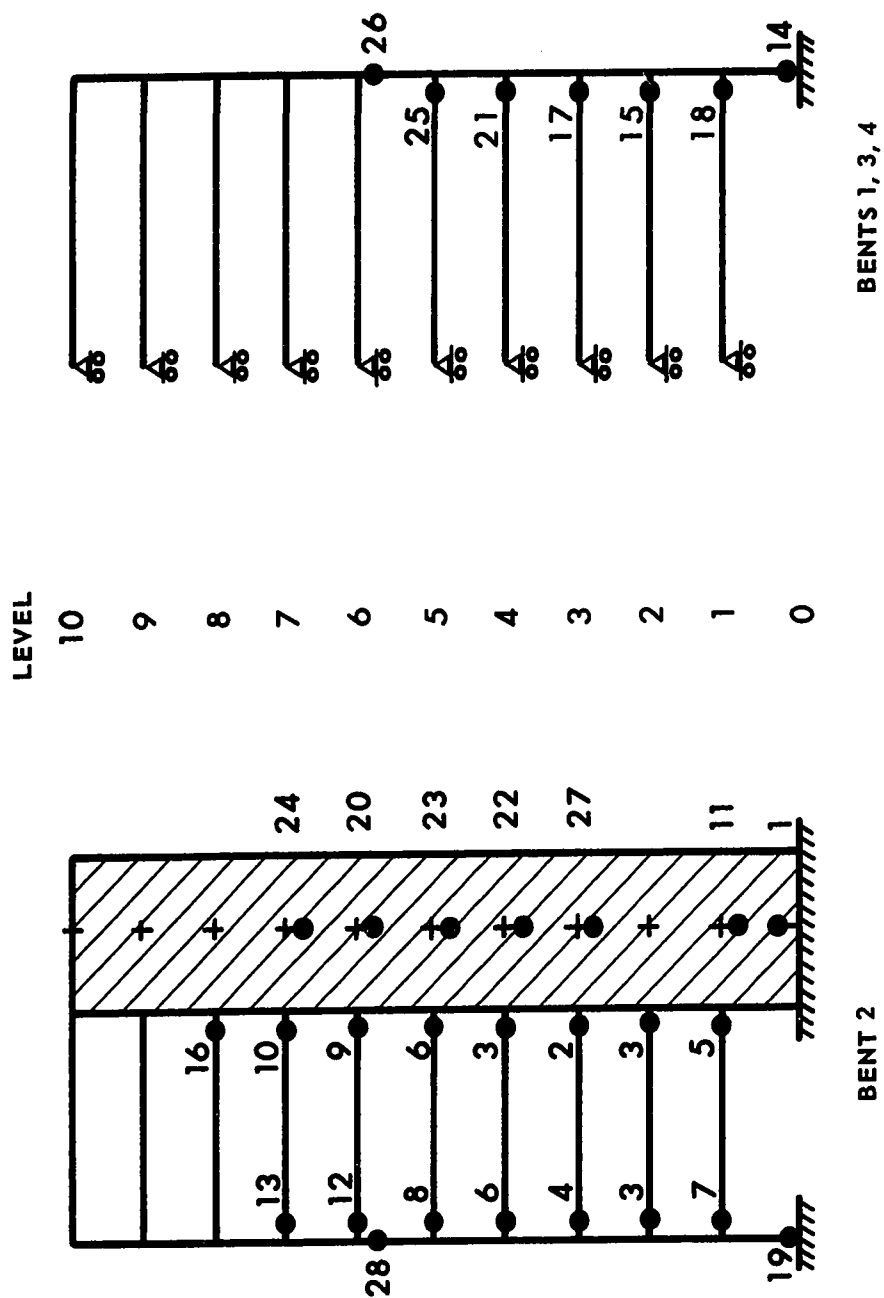
FIGURE 8.3 HINGE CONFIGURATION STRUCTURE M1
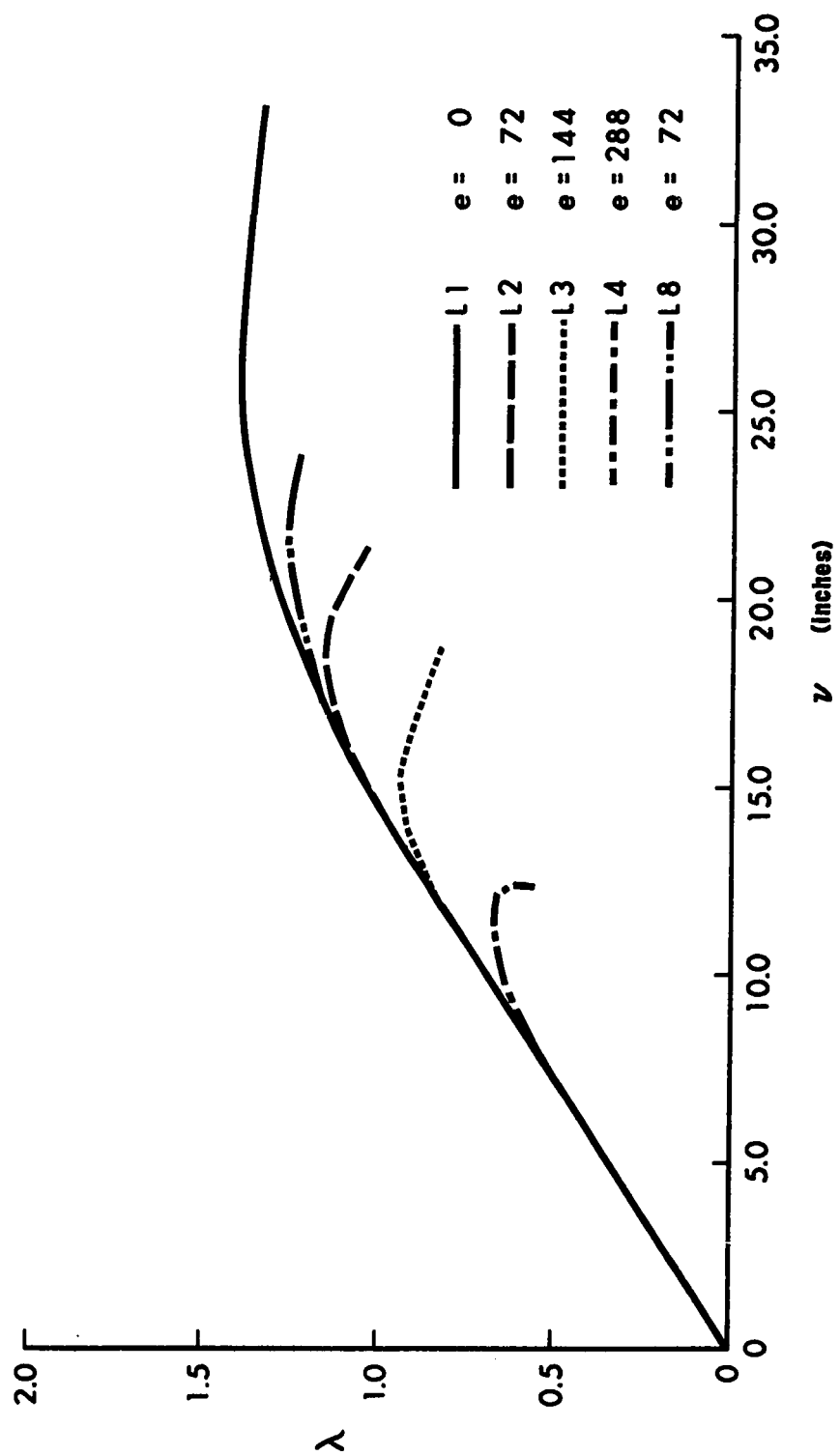
FIGURE 8.4 LOAD-DISPLACEMENT RESPONSE STRUCTURES L1–L4,L8
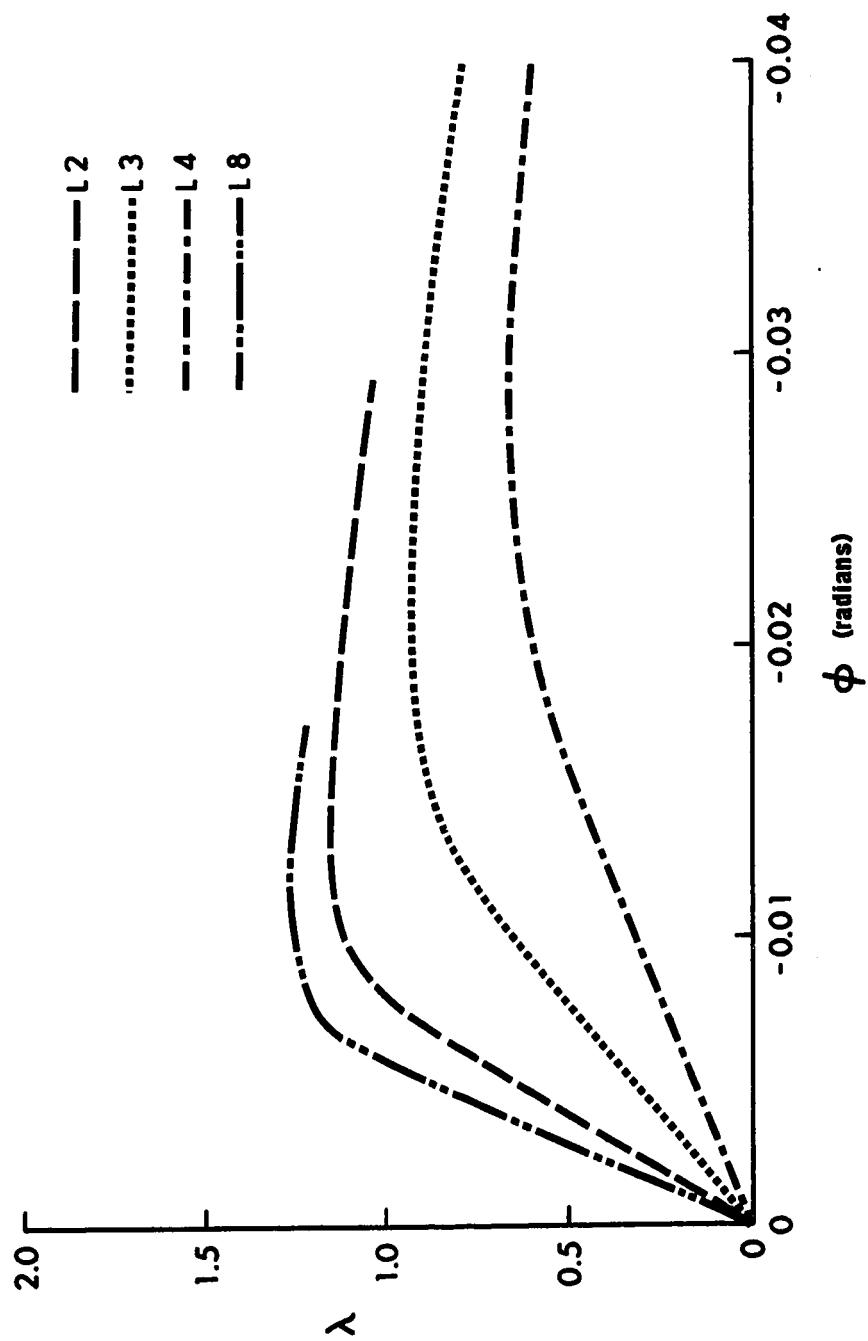
FIGURE 8.5 LOAD-FLOOR ROTATION RESPONSE STRUCTURES L2-L4,L8
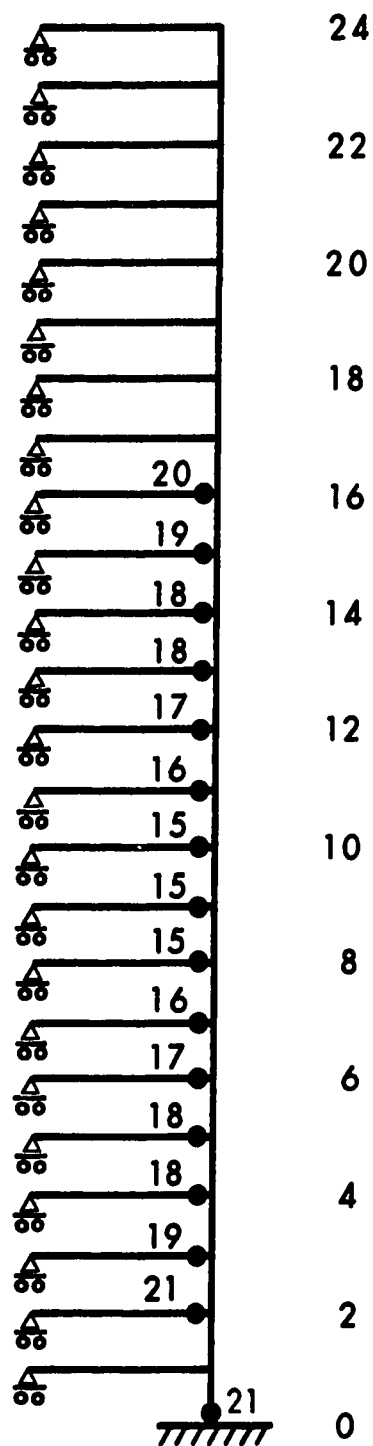
FIGURE 8.6 HINGE CONFIGURATION BENTS 1,2,5 & 6 OF STRUCTURE L1
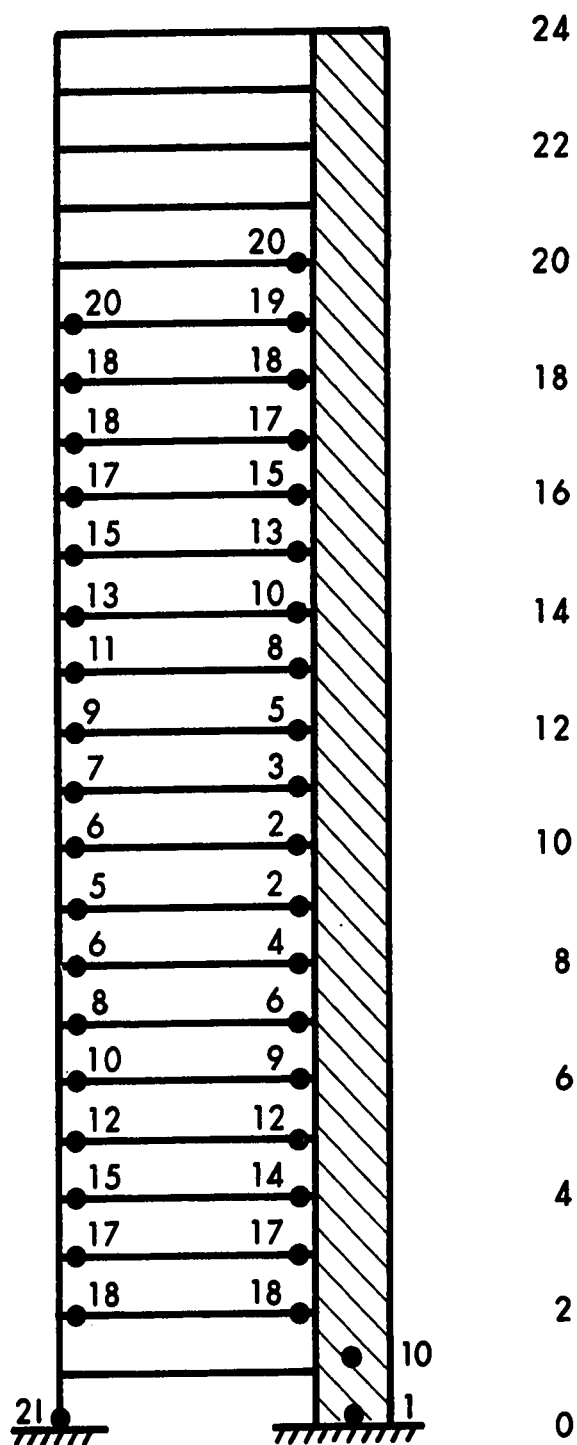
FIGURE   8.7   HINGE CONFIGURATION BENTS 3 & 4 OF STRUCTURE L1

138
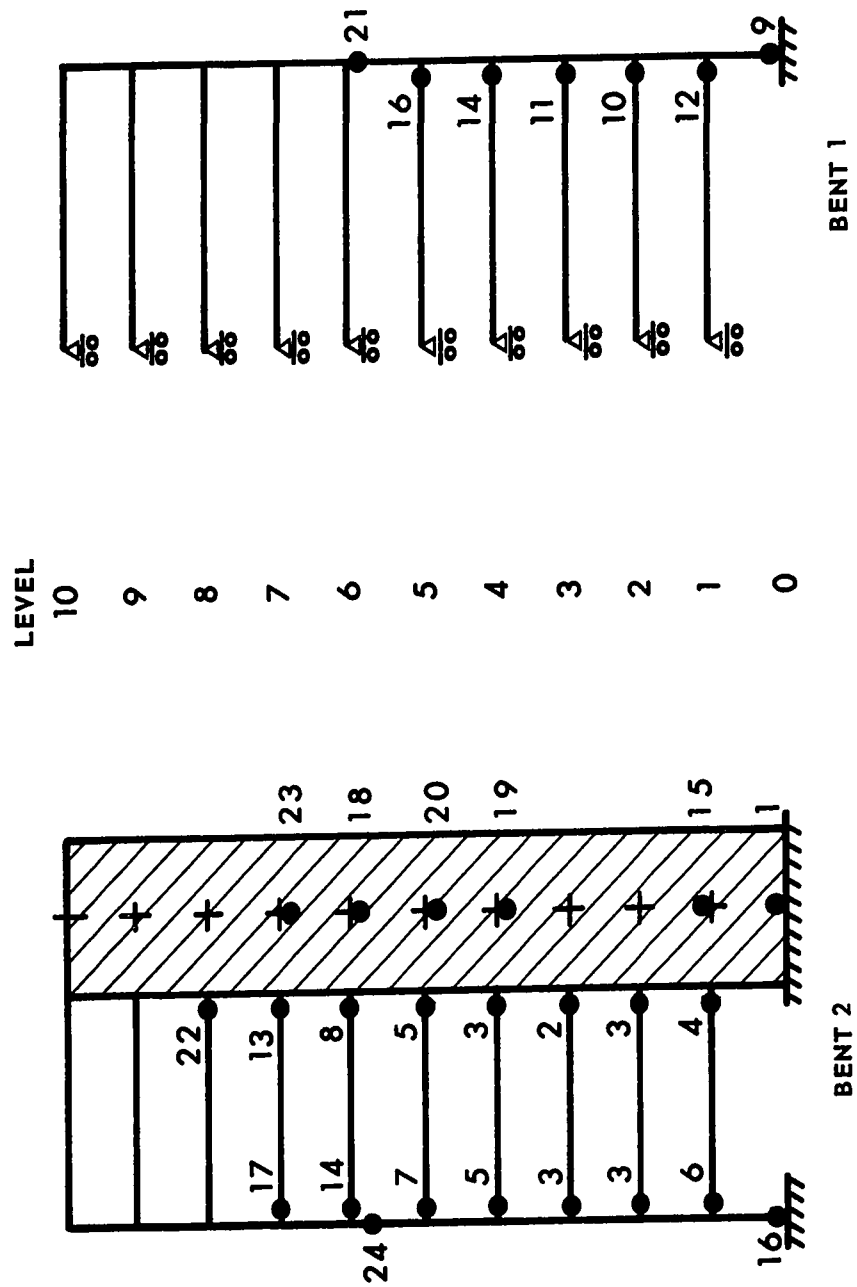

FIGURE 8.8 HINGE CONFIGURATION STRUCTURE M3
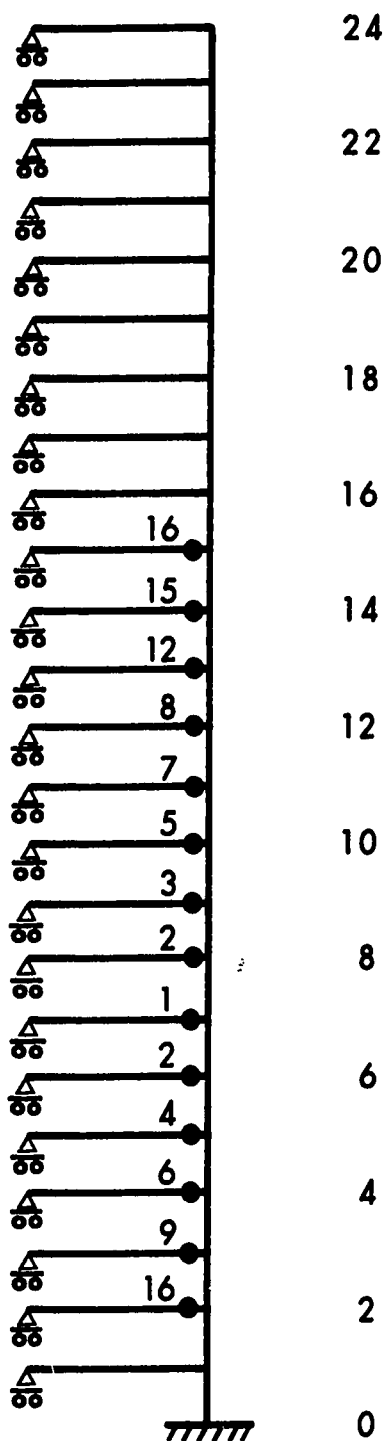
FIGURE 8.9 HINGE CONFIGURATION BENT 6 OF STRUCTURE L4
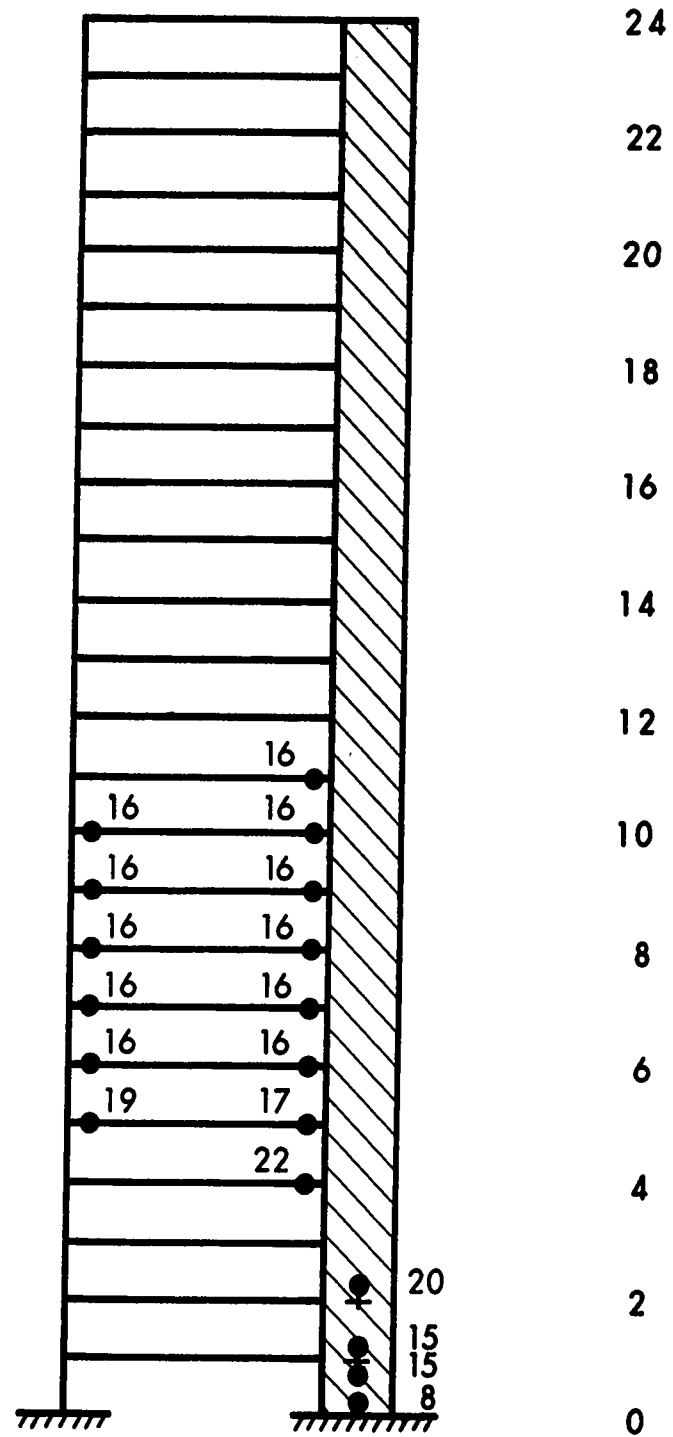
FIGURE 8.10 HINGE CONFIGURATION BENT 4 OF STRUCTURE L4
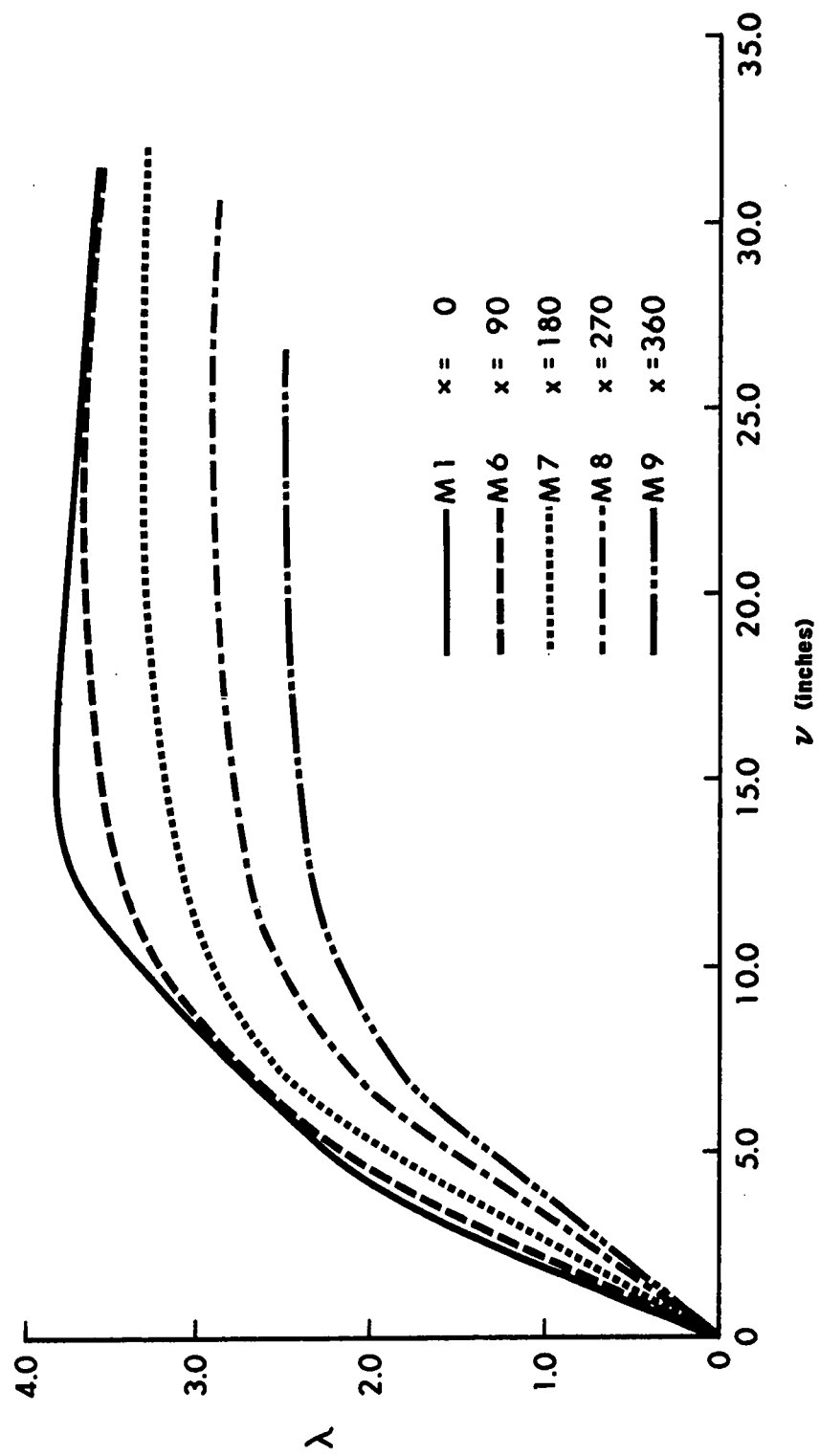
FIGURE 8.11 LOAD-DISPLACEMENT RESPONSE STRUCTURES M1,M6-M9
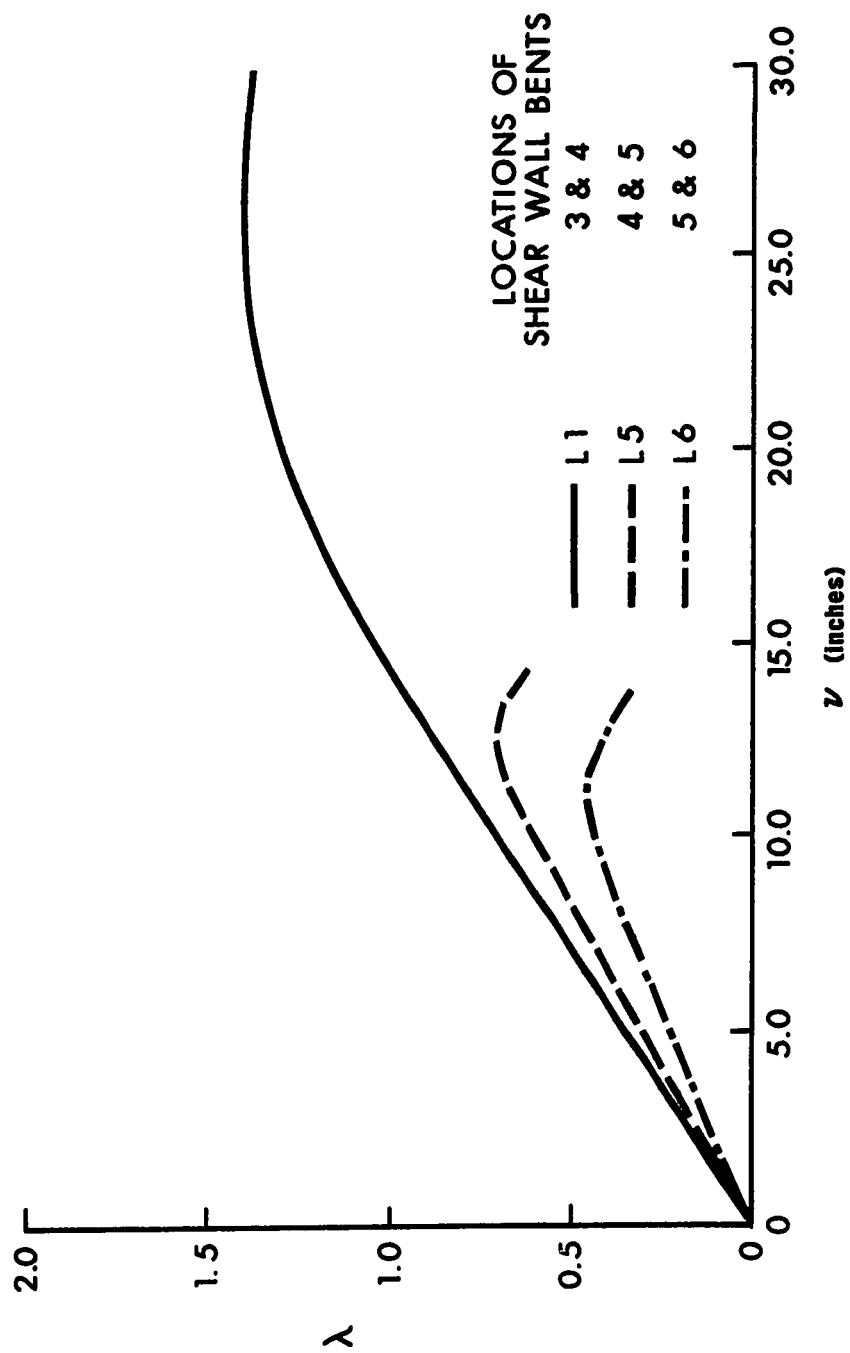
FIGURE 8.12 LOAD–DISPLACEMENT RESPONSE STRUCTURES L1,L5,L6
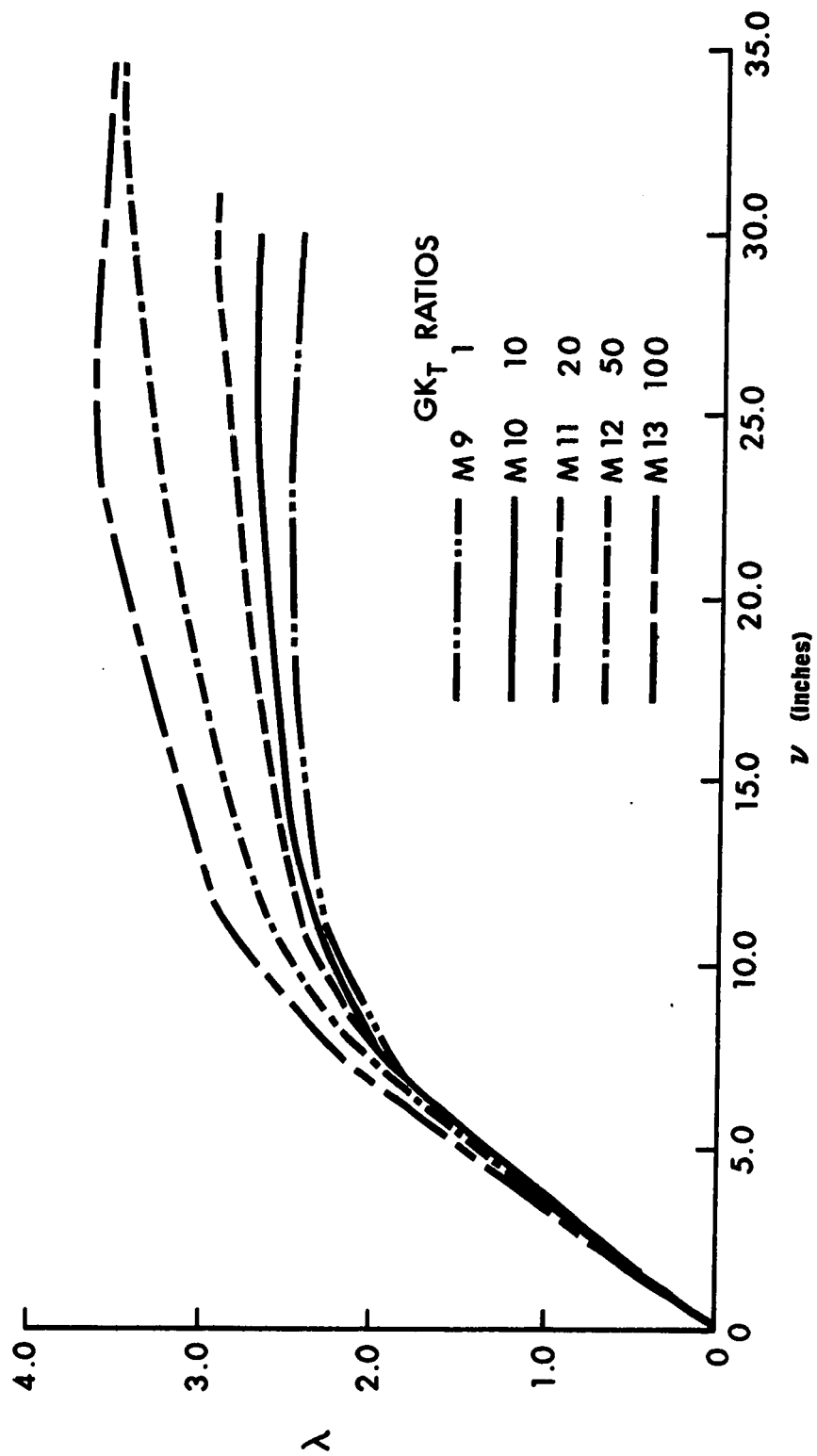
FIGURE 8.13 LOAD-DISPLACEMENT RESPONSE STRUCTURES M9-M13
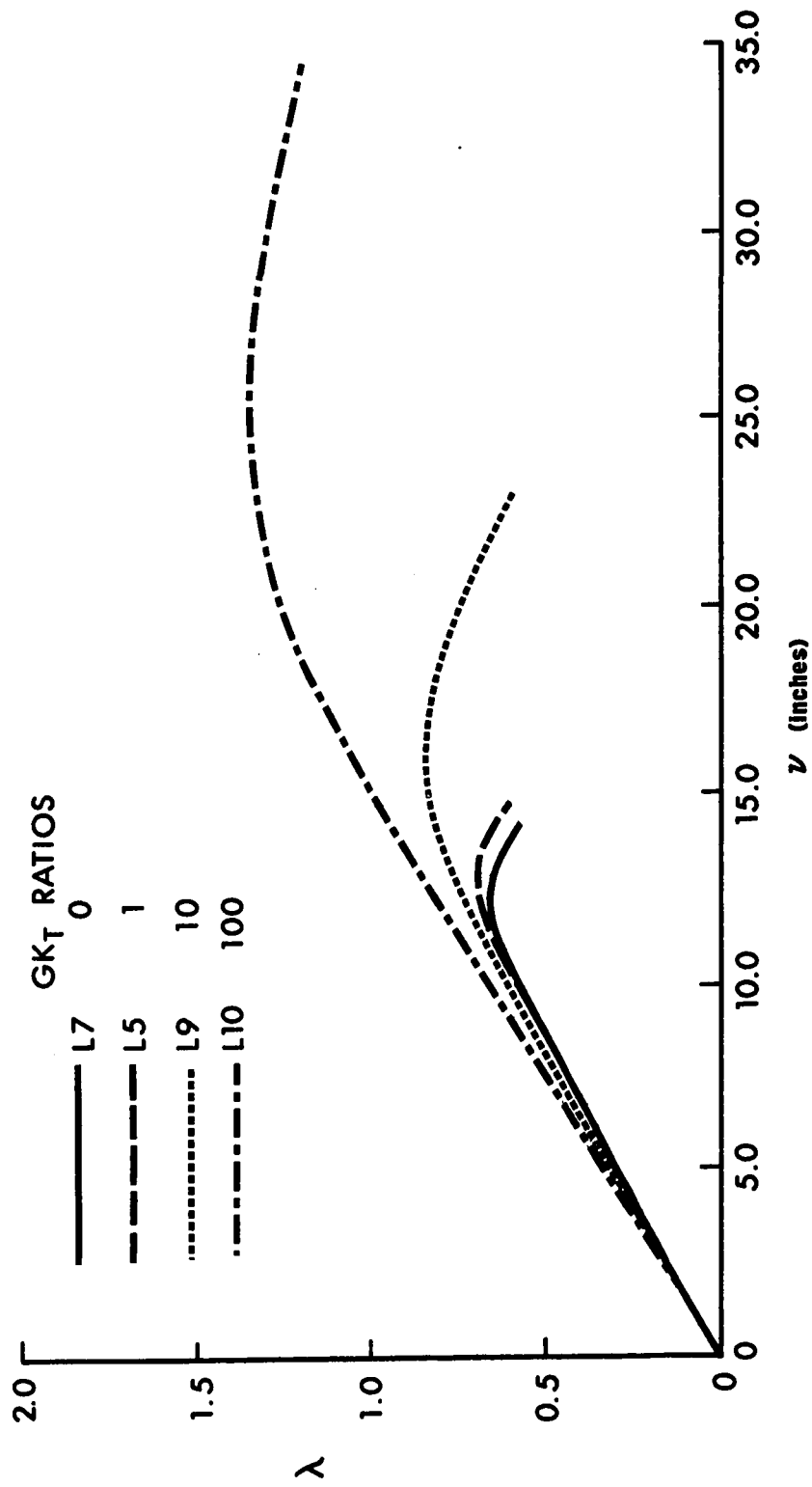
FIGURE 8.14 LOAD-DISPLACEMENT RESPONSE STRUCTURES L5,L7,L9,L10
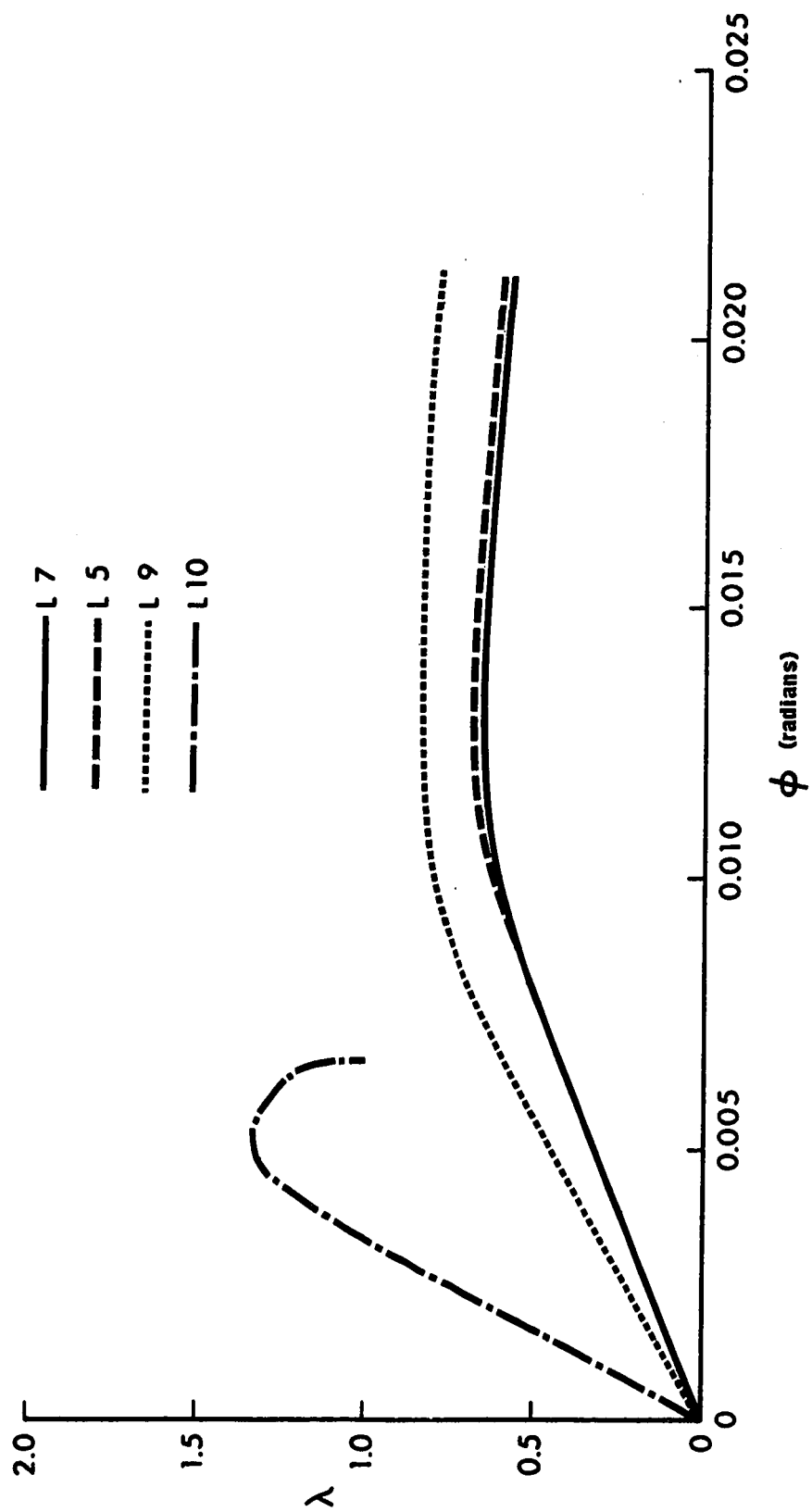
FIGURE 8.15 LOAD-FLOOR ROTATION RESPONSE STRUCTURES L5,L7,L9,L10
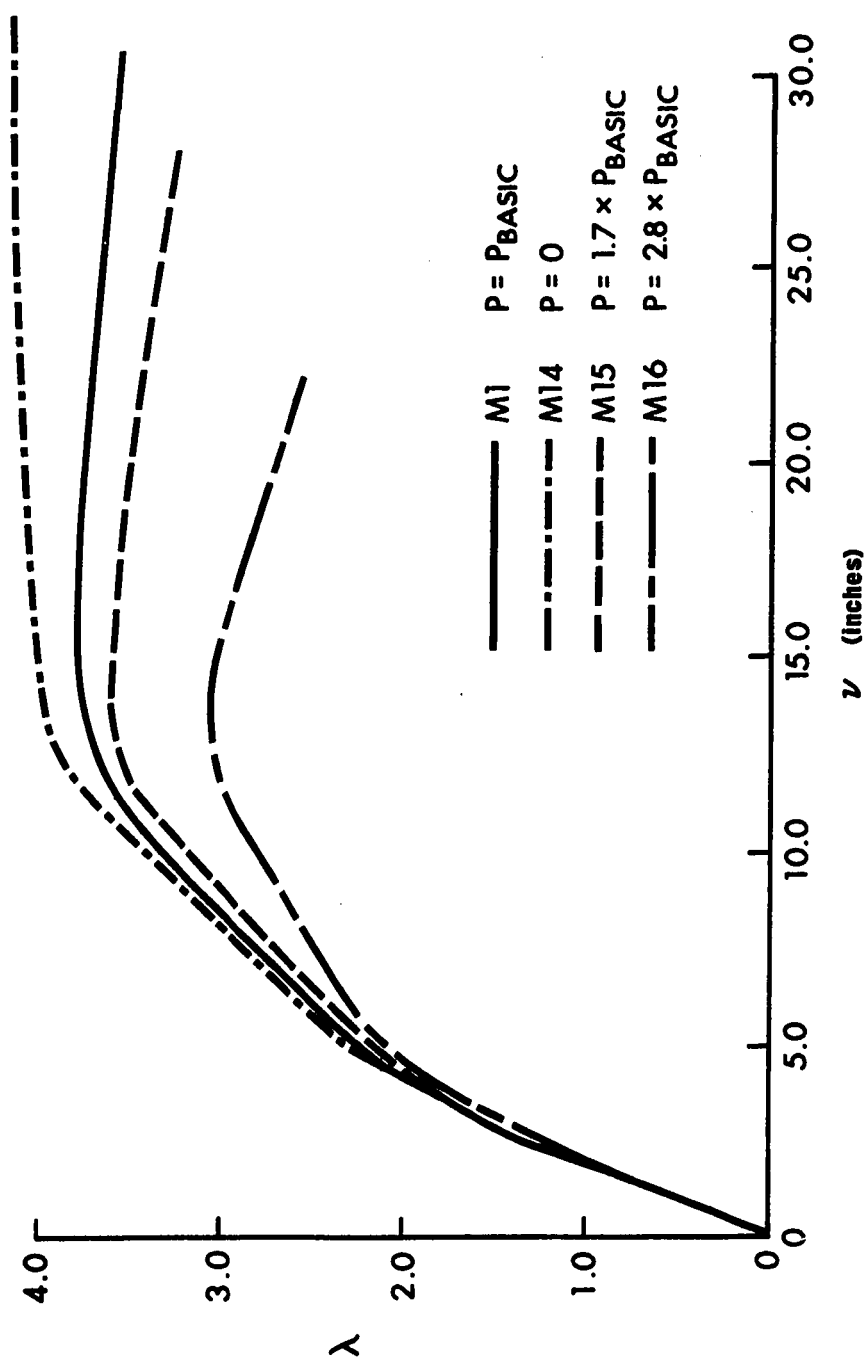
FIGURE 8.16 LOAD-DISPLACEMENT RESPONSE STRUCTURES M1,M14–M16
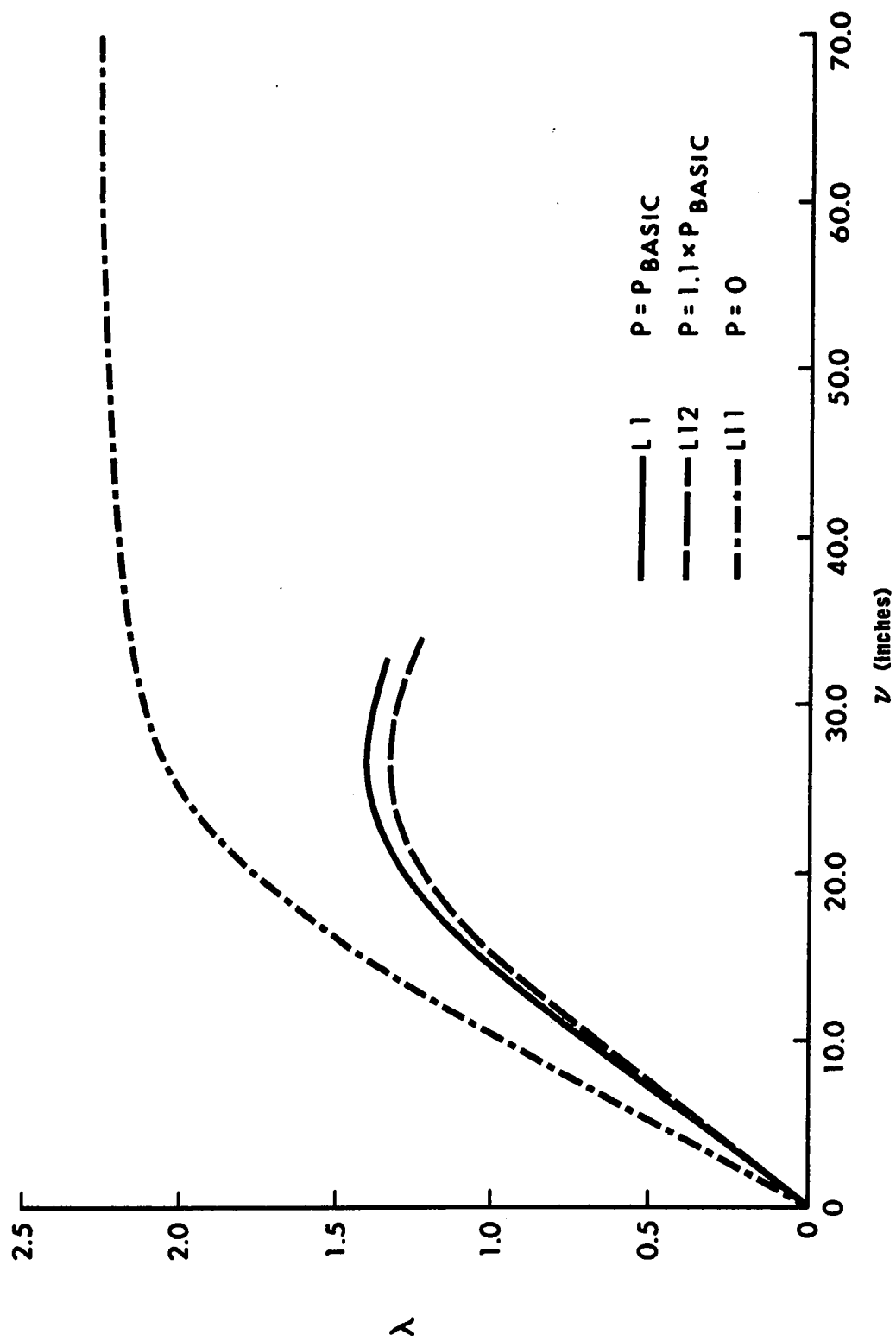
FIGURE 8.17 LOAD–DISPLACEMENT RESPONSE STRUCTURES L1,L11,L12

	ASYMMETRY OF VERTICAL LOAD	e
M 1	0	0
M17	10%	0
M 3	0	72
M18	10%	72
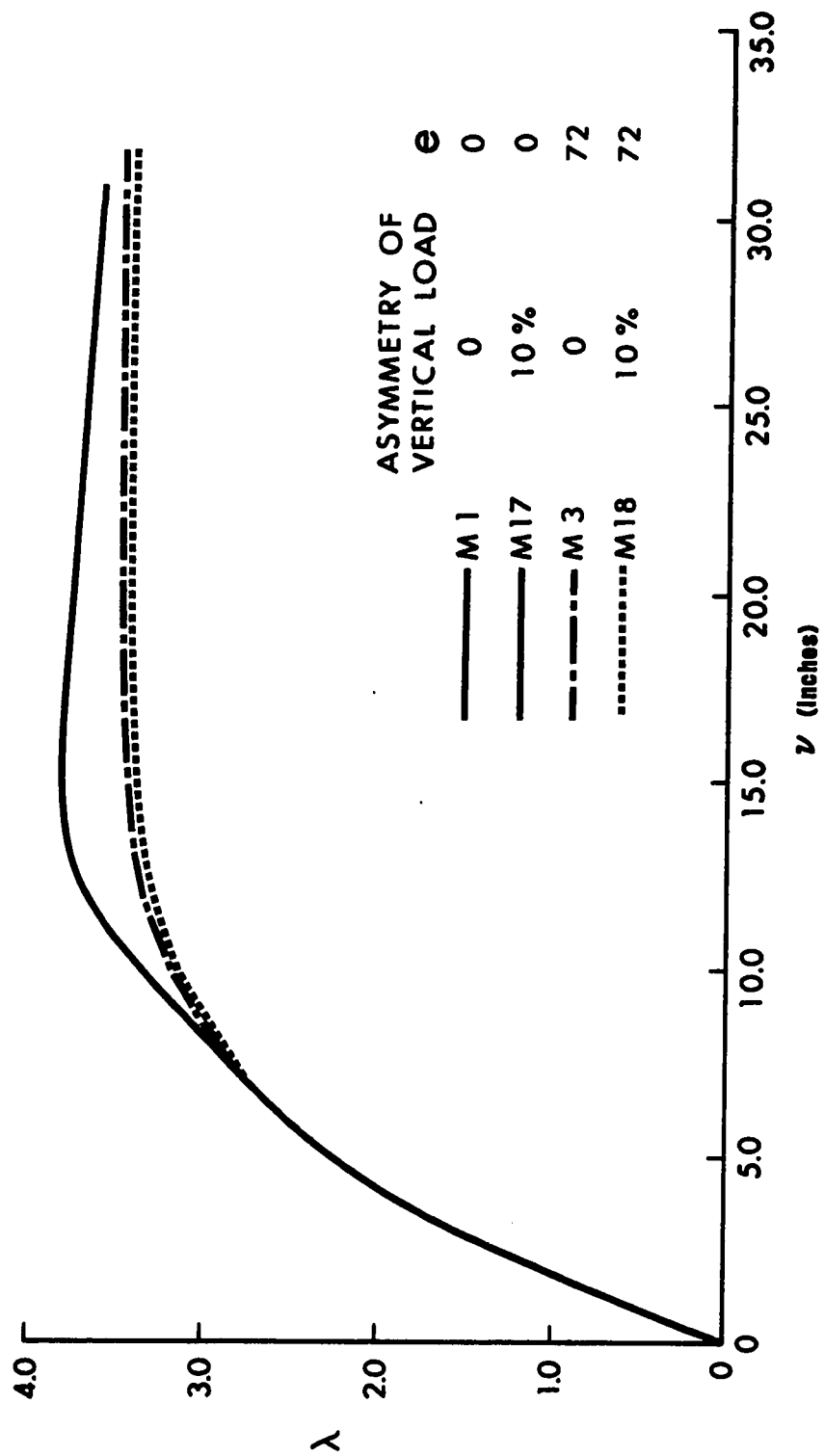
FIGURE 8.18 LOAD-DISPLACEMENT RESPONSE STRUCTURES M1,M3,M17,M18
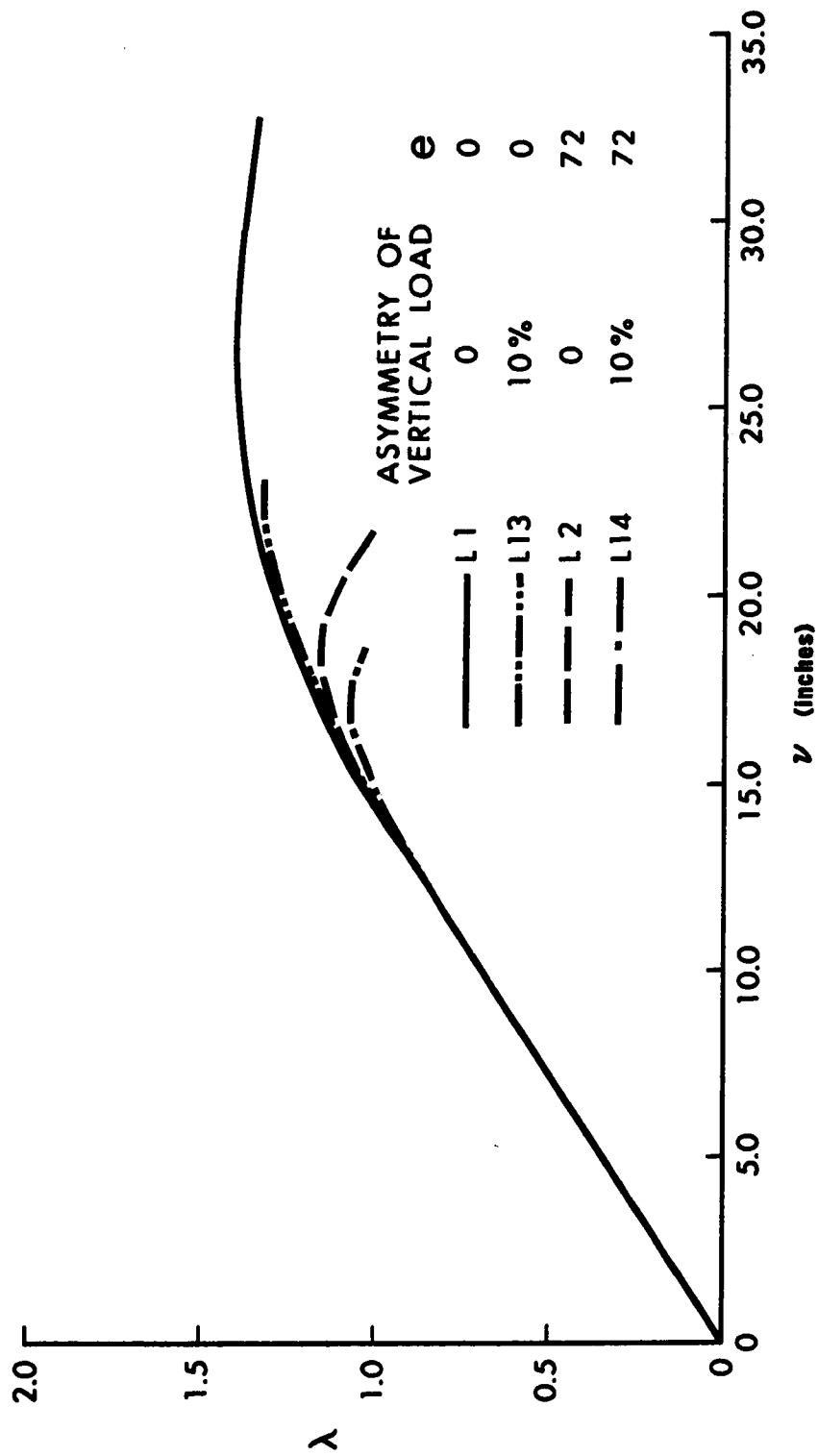
FIGURE 8.19 LOAD-DISPLACEMENT RESPONSE STRUCTURES L1,L2,L13,L14

150
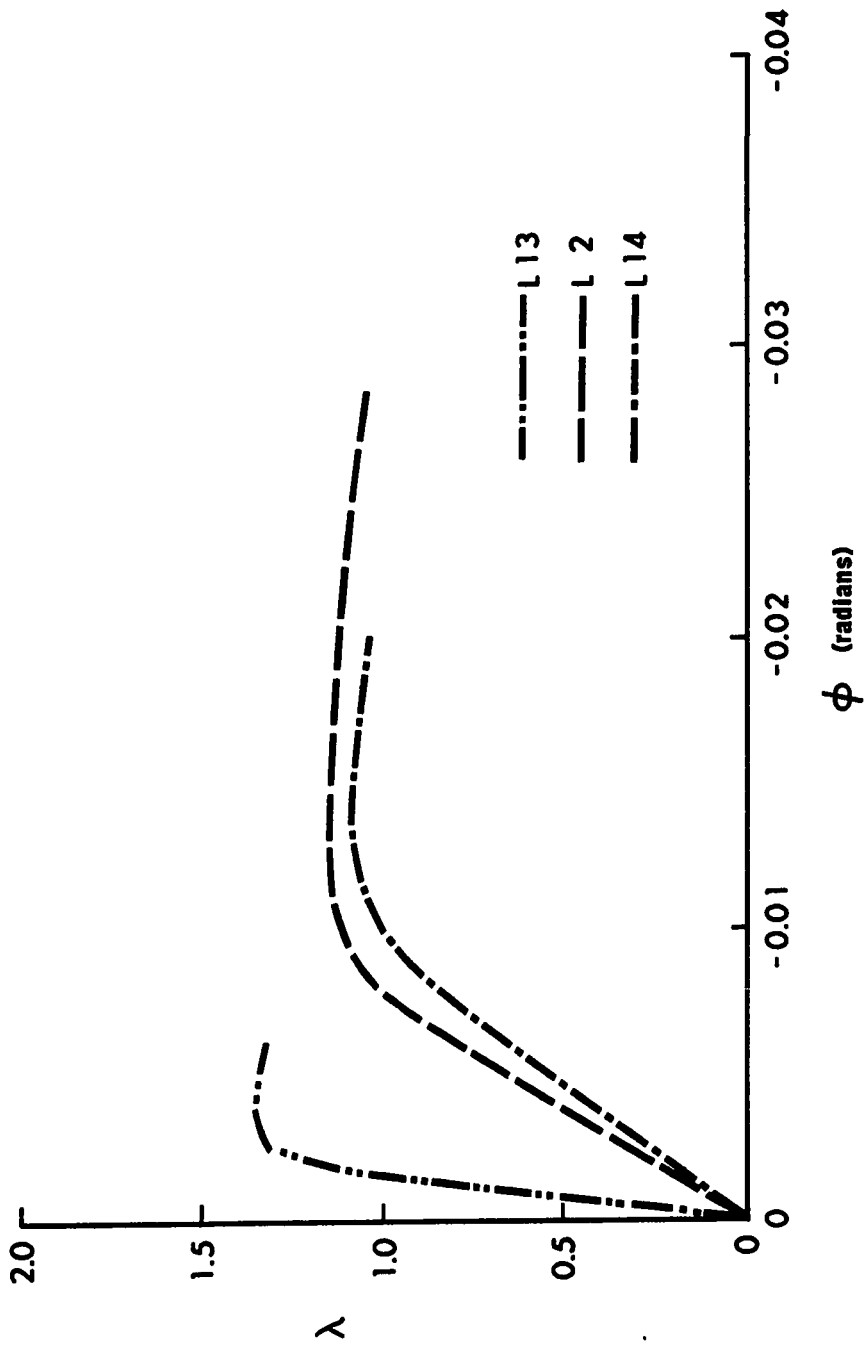
FIGURE 8.20 LOAD-FLOOR ROTATION RESPONSE STRUCTURES L2,L13,L14
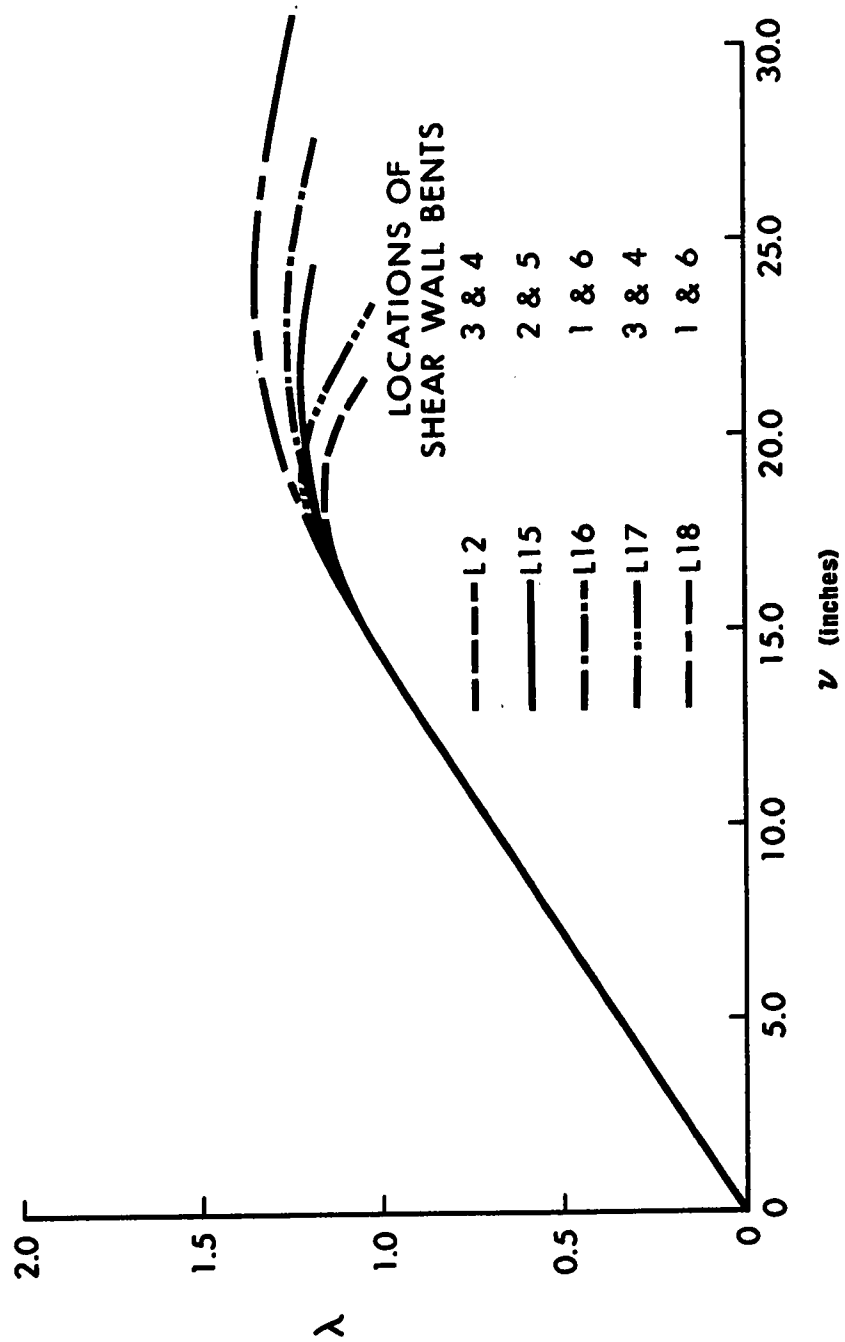
FIGURE 8.21 LOAD-DISPLACEMENT RESPONSE STRUCTURES L2,L15-L18
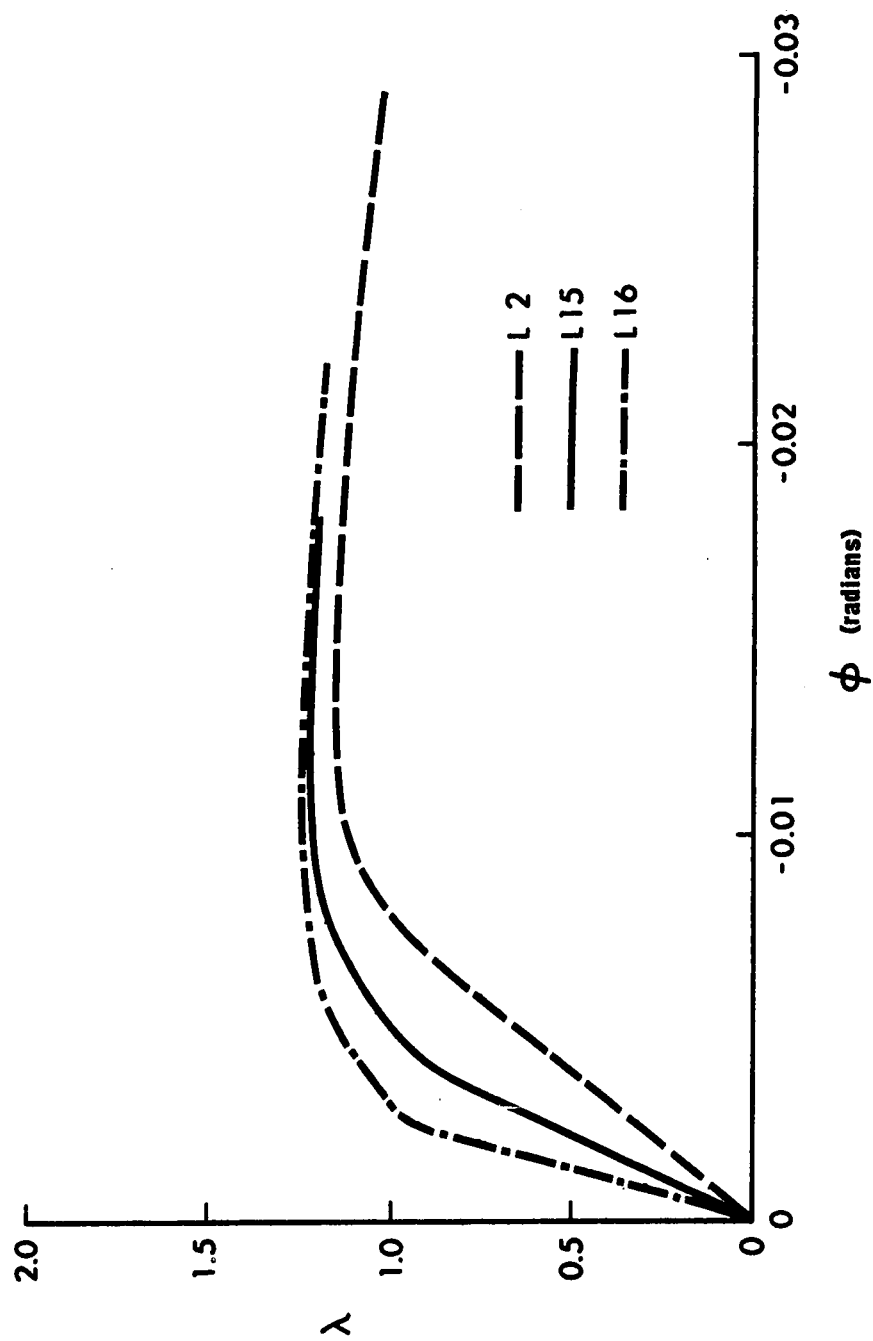
FIGURE 8.22 LOAD-FLOOR ROTATION RESPONSE STRUCTURES L2,L15,L16
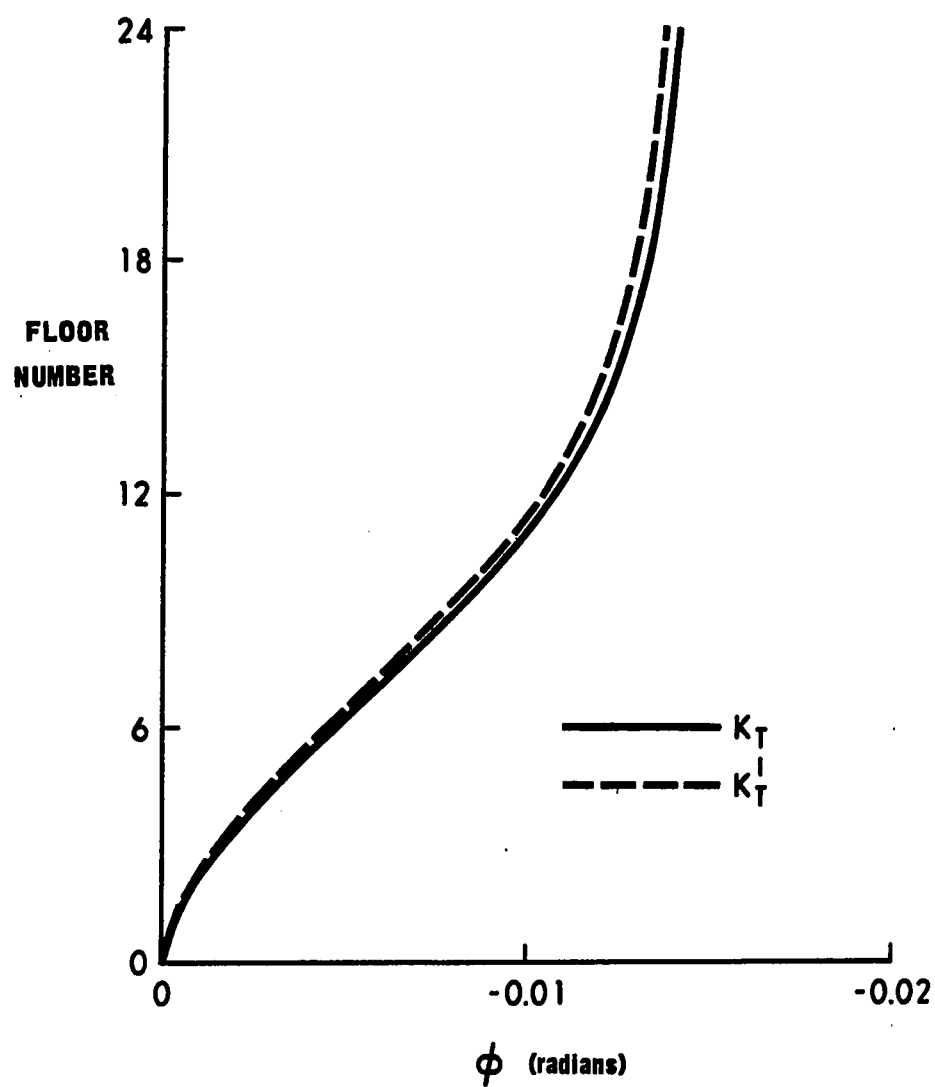
FIGURE 8.23 FLOOR ROTATIONS AT ULTIMATE LOAD STRUCTURE L2

CHAPTER IX

LIMITATIONS, CONCLUSIONS AND RECOMMENDATIONS

9.1 Limitations of Analysis

The method of analysis presented in this dissertation is able to predict the complete load-displacement response for large multi-story structures. The validity of the analysis is directly dependent on the validity of the assumptions made to simplify the method. Many of the assumptions are those common to the analysis of planar bents (6,9), and will not be discussed here. Effects such as; axial shortening, changes in axial load, changes in stiffness and carry over factors, and strain hardening of the material fall into this category and must eventually be considered. However, only the assumptions which directly affect the torsional aspects of the behavior will be discussed in this Chapter.

9.1.1 Floor Slab Stiffness

In the analysis, all column and wall elements within a bent are assumed to undergo equal lateral displacements. This implies that the floor diaphragms have infinite extensional stiffness. Since the axial forces in the beams and slabs are small the relative displacements between the column and wall elements, within a bent, will be negligible and thus the original assumption is essentially satis-

fied. For a symmetric structure the assumption of infinite floor diaphragm stiffness results in equal lateral displacements for all parallel bents. For an asymmetric structure, however, this same assumption implies that displacements of all bents will conform to a rigid body motion of the floor slab. The floor slabs form deep beams, spanning between the bents, with an effective depth generally well in excess of the bent spacing, consequently shear deformations dominate the action. If the shear stiffness of the floor diaphragm is not infinite the above motion is modified and the amount of the lateral load resisted by a particular bent will tend to be influenced more by its tributary area, and less interaction will occur between adjacent bents. Benjamin (31) has shown that a floor slab to bent stiffness ratio of approximately 2 is sufficient so that the floor slab may be considered as infinitely stiff. However, it follows that the floor slab must be designed to transmit the shear forces and bending moments that are generated between adjacent bents.

9.1.2 Lumping Procedure

The lumping of members within a bent, as described in CHAPTER III, has been studied over the complete range of behavior of the structure (51). A method has been proposed to allow for the changed hinging pattern in the floor beams due to the presence of transverse beam loads. Using this method, the adjusted lumped model conservatively predicts the ultimate load carrying capacity. The accuracy of the lumping procedure (in the elastic range) as applied to a space frame, was illustrated

by the results obtained for a twenty story example structure analyzed in SECTION 6.3. In lumping bents of a three dimensional structure, which is to be loaded into the inelastic range, problems will arise due to the different bi-axial bending moment ratios that will occur in the columns within each bent. This effect is discussed in SECTION 9.1.4.

9.1.3 Shear Deformations

Shear deformations will reduce the stiffness of the structure and through the P-Δ moments will also reduce the ultimate load carrying capacity. The magnitude of the reduction will depend on the depth to height ratios of the stiffening elements. The shear deformations may be estimated for particular members, after the structure has been analyzed, considering only bending deformations. If the shear deformations are excessive (greater than 10 percent), the structure may be re-analyzed by reducing the moments of inertia of the stiffening elements to obtain the correct total deformations. For structure L1 (CHAPTER VIII) the shear deformations exceeded 5 percent of the bending deformations only in the bottom story of the shear walls.

9.1.4 Biaxial Bending Moment-Axial Force Relationship

The biaxial bending-axial load interaction relationship, assumed in the analytical model and shown in FIGURE 3.5, may overestimate the flexural capacity of the section for lower ratios of P/P_y (less than 0.6). The critical columns will be those at the corners of the

structure, which are subjected to significant biaxial bending moments. As the torsional load increases (due to asymmetry of load and, or, structural layout), the external columns will hinge earlier than predicted. This is caused by the floor rotations, which increase the displacements perpendicular to the main direction of loading.

The influence of this action may be checked by analyzing the isolated column, using the method described in SECTION 8.5, and comparing the bending moment ratios at various stages of the load-displacement response. If the ratios fall within the range where significant differences exist between the rigorous and assumed interaction relationships, the M_{pc} values of the lumped bents are adjusted and the structure re-analyzed. For the critical columns of the structures analyzed, bending about one axis normally predominated. Thus the rectangular interaction relationships produced a close approximation of the flexural capacity.

9.2 Analysis of Computing Errors

In addition to the above simplifying assumptions, the validity of the load-displacement response may be influenced by numerical errors generated in the solution of the large system of simultaneous equations.

As a check on the accuracy of the computer program, the resisting floor forces and the resultant torque about the vertical axis, are calculated and printed at the end of each loading stage. Using single precision arithmetic (6 significant figures), the resisting floor forces for structure M1 differed from the applied loads in the

fourth significant figure (less than 1 percent). This is well within the acceptable tolerance. For structures in Series L, however, for single precision arithmetic the discrepancies between the applied loads and resisting floor forces varied from 4 to 14 percent.

An error study was performed on the equation, $A\delta = b$; the off-diagonal elements, of matrix A, may be several orders of magnitude larger than the main diagonal elements. This difference in relative magnitudes may lead to a loss of accuracy in solving the system. A convenient measure of ill conditioning is provided by the conditioning number, K, which is defined by the ratio of the extreme eigenvalues of matrix A (56).

$$K = \left|\frac{\lambda max}{\lambda min}\right| \tag{9.1}$$

The logarithm, to the base ten, of this conditioning number, is an index of the maximum number of significant digits lost in solving the system of equations (56). The conditioning number K, was calculated for series M and L structures, by making minor changes to subroutine SOLVER in the computer program (CHAPTER V). The largest eigenvalues of A and A^{-1} were calculated using the power method (52); the inverse of the maximum eigenvalue of A^{-1} corresponds to the minimum eigenvalue of A. The values obtained were:

(a) <u>Series M</u>

$$K = \frac{3.5 \cdot 10^{10}}{1.3 \cdot 10^{1}} = 2.7 \cdot 10^{9} \tag{9.2a}$$

(b) <u>Series L</u>

$$K = \frac{5.8 \cdot 10^{11}}{3.2 \cdot 10^{-1}} = 1.8 \cdot 10^{12} \qquad (9.2b)$$

The logarithms of the conditioning numbers indicate that the maximum loss of significant figures is 9 and 12, respectively. As a consequence, double precision arithmetic is required for both Series. To obtain a closer bound on the expected error for structures of Series L, the following procedure was adopted: The system $A\delta = b$ was solved for the displacement vector, δ_c (calculated): the residual, r was then calculated, where,

$$r = A\delta_c - b \qquad (9.3a)$$

this may be written as,

$$\delta_c - A^{-1}b = A^{-1}r \qquad (9.3b)$$

where $A^{-1}b$ represents the true value of the displacement vector. An estimate of the error in the displacement vector, is obtained by taking the norm of both sides (52).

$$||\delta_c - A^{-1}b|| \leq ||A^{-1}|| \cdot ||r|| \qquad (9.4)$$

where, for a symmetric matrix A,

$$\max_i |\lambda_i(A^{-1})| = ||A^{-1}|| \tag{9.5}$$

$||r||$ was $4 \cdot 10^{-7}$ and from EQUATION (9.2b) $||A^{-1}||$ is 3.2. Therefore, the error is given by,

$$||\delta_c - A^{-1}b|| \leq 3.2 \cdot 4 \cdot 10^{-7} \leq 1.28 \cdot 10^{-6} \tag{9.6}$$

EQUATION (9.6) implies that using double precision arithmetic, the results should be correct to the sixth decimal place. This was in fact so, with the resisting floor forces differing from the applied loads only in the fifth decimal place (seventh significant figure). Series L structures were re-analyzed using double precision arithmetic. The significant difference between the structures of Series M and L is the increased wall moments of inertia for Series L (11.3 x 10^6 in^4). To analyze unusually large structures, an error study should be performed as described above.

9.3 Conclusions

A method of analysis has been presented to predict the complete load-displacement response for large three dimensional coupled frame-shear wall structures. The validity of the analysis was verified by analyzing structures for which data is available in the literature. The analysis was then used to study the influence of several structural

parameters on the behavior of multi-story structures.

The structures considered in the study were of two basic types, having different structural arrangements and loading conditions. In spite of the relatively small number of structures analyzed, several trends of a general nature were evident.

The ultimate load carrying capacity of a structure is reduced when it is subjected to a torsional load. The torsional load results in twisting of the structure (about its vertical axis) as well as translation in the direction of the applied lateral load. Because of the twisting motion, the lateral displacements of the exterior bents (on one side of the structure) will be increased. This results in earlier hinging in the members of these bents, which reduces the torsional (and lateral) stiffness and causes a shift in the center of rotation of the structure. The combined effect of this action (the shift in center of rotation and correspondingly increased torsional load) produces a net increase in the sway displacements and a corresponding increase in the P-Δ moments. This increase in the P-Δ moments causes a decrease in the ultimate load carrying capacity of the structure.

For an asymmetry of lateral load corresponding to 5 percent of the width of the structure, the reduction in ultimate load carrying capacity (due to the torsional load), was 3 and 17 percent for the structures of Series M and L, respectively. The St. Venant torsional constants for the shear walls of the Series L structures were increased to the value appropriate for a closed section. Under this condition,

the reduction in ultimate load carrying capacity was 9 percent.

Many code provisions require a symmetrical structure to be designed for the torque produced by the equivalent static earthquake (lateral) load acting with an eccentricity equal to 5 percent of the building width (44,45). When the two basic structures were subjected to this minimum torsional load, the reductions in ultimate load carrying capacity obtained, (approximately 10 percent), suggest that these structures may be analyzed under symmetrically applied lateral load without the minimum eccentricity requirement.

The response of a structure under the action of a torsional load was similar regardless of whether the torsional load was caused by asymmetry of lateral or vertical load or asymmetry of structural layout. The important factors are; the distribution of stiffness and strength within the structure in relation to the point of application of the lateral loads, and the severity of the P-Δ effect.

For the particular structures considered (rectangular in plan), hinging in the bents perpendicular to the direction of the applied lateral load, occurred only after large torsional displacements. Consequently, the error in assuming a rectangular bi-axial bending moment interaction relationship, will only be significant for similar structures, whose layout is such that significant sway displacements occur perpendicular to the direction of the applied lateral load.

9.4 Recommendations

As the behavioral study was limited to two basic structural types, it is recommended that further studies be performed on different types, particularly on structures with plan layouts that differ from those of Series M and L. Additional studies should be directed at structures in which the distribution of strength does not correspond to the distribution of stiffness among the bents. Consideration should also be given to the influence of base rotations on the ultimate load carrying capacity.

In the light of the behavioral study, some general design recommendations may be made:

(a) Large degrees of asymmetry should be avoided in slender structures, as significant reductions in ultimate load carrying capacity will result.

(b) If the designer is not prepared to assess the ultimate load carrying capacity of the structure then a distribution of strength should be provided which corresponds to the distribution of stiffness.

(c) For load asymmetry not exceeding 5 percent (the minimum torsional load requirement of several design codes (44,45)), structures similar to those considered, which have symmetrical layouts and normal torsional stiffnesses, may show a reduction in ultimate load carrying capacity of approximately 10 percent.

(d) From the results of this study the hinge rotation capacity required for a structure to reach its ultimate load carrying capacity is within practical limits.

LIST OF REFERENCES

1. "Plastic Design in Steel", American Institute of Steel Construction, New York, 1959.

2. "Steel Structures for Buildings", CSA Standard S16-1965, Canadian Standards Association, Ottawa 7, Canada.

3. Lu, Le-Wu, "A Survey of Literature on the Stability of Frames", Welding Research Council, Bulletin 81, September, 1962.

4. Davies, J.M., "Collapse and Shakedown Loads of Plane Frames", Journal of the Structural Division, ASCE, Vol. 93, No. ST3, 1967.

5. Parikh, B.P., "Elastic-Plastic Analysis and Design of Unbraced Multi-Story Steel Frames", Fritz Engineering Laboratory Report No. 273.44, Lehigh University, 1966.

6. Korn, A. and Galambos, T.V., "Behavior of Elastic-Plastic Frames", Journal of the Structural Division, ASCE, Vol. 94, No. ST5, 1968.

7. Alvarez, R.J. and Birnstiel, C., "Inelastic Analysis of Multi-story Multibay Frames", Journal of the Structural Division, ASCE, Vol. 95, No. ST11, 1969.

8. Guhamajumdar, S.N., Nikhed, R.P., MacGregor, J.G. and Adams, P.F., "Approximate Analysis of Frame-Shear Wall Structures", Structural Engineering Report No. 14, Department of Civil Engineering, University of Alberta, May 1968.

9. Clark, W.J., and MacGregor, J.G., "Analysis of Reinforced Concrete Shear Wall-Frame Structures", Structural Engineering Report No. 16, Department of Civil Engineering, University of Alberta, November 1968.

10. Clough, R.W., King, I.P. and Wilson, E.L., "Structural Analysis of Multi-Story Buildings", Journal of the Structural Division, ASCE, Vol. 90, No. ST3, 1964.

11. Winokur, A. and Gluck, J., "Lateral Loads in Asymmetric Multi-story Structures", Journal of the Structural Division, ASCE, Vol. 94, No. ST3, 1968.

12. Wynhoven, J.H. and Adams, P.F., "Elastic Torsional Analysis of Multistory Structures", Structural Engineering Report No. 15, Department of Civil Engineering, University of Alberta, October 1968.

13. Beedle, L.S., Lu, Le-Wu, and Lim, L.C., "Recent Developments in Plastic Design Practice", Journal of the Structural Division, ASCE, Vol. 95, No. ST9, 1969.

14. Lay, M.G., "The Mechanics of Column Deflection Curves", Fritz Engineering Laboratory Report No. 278.12, Lehigh University, 1964.

15. Baker, J.F., Horne, M.R. and Heyman, J., "The Steel Skeleton", Vol. II, Cambridge University Press, 1956, Chapters 14 and 15.

16. Chen, W.F. and Santathadaporn, S., "Review of Column Behavior Under Biaxial Loading", Journal of the Structural Division, ASCE, Vol. 94, No. ST12, 1968.

17. Harstead, G.A., Birnstiel, C. and Leu, K.C., "Inelastic H-Columns under Biaxial Bending", Journal of the Structural Division, ASCE, Vol. 94, No. ST10, 1968.

18. Roderick, J.W., "Tests on Stanchions Bent in Single Curvature About Both Principal Axes", Report No. FE1/36, British Welding Research Association, 1953.

19. Sharma, S.S. and Gaylord, E.H., "Strength of Steel Columns with Biaxially Eccentric Load", Journal of the Structural Division, ASCE, Vol. 95, No. ST12, 1969.

20. Drucker, D.C., "The Effect of Shear on the Plastic Bending of Beams", Journal of Applied Mechanics, ASME, Vol. 78, 1956.

21. Santathadaporn, S. and Chen, W.F., "Interaction Curves for Sections Under Combined Biaxial Bending and Axial Force", Fritz Engineering Laboratory Report No. 331.3, Lehigh University, 1968.

22. "Plastic Design of Multi-Story Frames", Fritz Engineering Laboratory Report No. 273.20, Lehigh University, 1965.

23. Pfrang, E.O. and Toland, R.H., "Capacity of Wide Flange Sections Subjected to Axial Load and Biaxial Bending", University of Delaware, Newark, Delaware, 1966.

24. Beck, H., "Contribution to the Analysis of Coupled Shear Walls", Proceedings ACI., Vol. 59, 1962.

25. Rosman, R., "Approximate Analysis of Shear Walls Subject to Lateral Loads", Proceedings ACI, Vol. 61, 1964.

26. Coull, A. and Puri, R.D., "Analysis of Pierced Shear Walls", Journal of the Structural Division, ASCE, Vol. 94, No. ST8, 1968.

27. Girijavallabhan, C.V., "Analysis of Shear Walls with Openings",
    Journal of the Structural Division, ASCE, Vol. 95, No. ST10,
    1969.

28. Rosman, R., "Torsion of Perforated Concrete Shafts", Journal of
    the Structural Division, ASCE, Vol. 95, No. ST5, 1969.

29. Wilbur, J.B., "Distribution of Wind Loads to the Bents of a
    Building", Proceedings Boston Society of Civil Engineers,
    Vol. 22, 1935.

30. Blume, J.A., Newmark, N.M. and Corning, L.H., "Design of Multi-
    story Reinforced Concrete Buildings for Earthquake Motions",
    Portland Cement Association, Chicago, 1961.

31. Benjamin, J.R., "Statically Indeterminate Structures", McGraw-
    Hill, New York, 1959.

32. Jennings, A. and Majid, K., "An Elastic-Plastic Analysis by Com-
    puter for Framed Structures Loaded up to Collapse", The
    Structural Engineer, Vol. 43, No. 12, 1965.

33. Khan, F.R., and Sbarounis, J.A., "Interaction of Shear Walls with
    Frames in Concrete Structures under Lateral Loads", Journal
    of the Structural Division, ASCE, Vol. 90, No. ST3, 1964.

34. "Design Aids Booklet", Fritz Engineering Laboratory Report No.
    273.24, Lehigh University, 1965.

35. Weaver, W. and Nelson, M.F., "Three-Dimensional Analysis of Tier
    Buildings", Journal of the Structural Division, ASCE,
    Vol. 92, No. ST6, 1966.

36. Bruinette, K.E., "A General Formulation of the Elastic-Plastic Analysis of Space Frameworks", Ph.D. Thesis, University of Illinois, 1966.

37. Harrison, H.B., "The Ultimate Resistance to Horizontal Shear of a Simple Space Frame", Proceedings ICE, Vol. 39, 1968.

38. Harrison, H.B., "The Plastic Behaviour of Mild Steel Beams of Rectangular Section Bent About Both Principal Axes", The Structural Engineer, Vol. 41, No. 7, 1963.

39. Jonatowski, J.J. and Birnstiel, C., "Elasto Plastic Analysis of Space Frameworks", School of Engineering and Science, New York University, 1969.

40. Johnson, D. and Brotton, D.M., "Finite Deflection Analysis for Space Structures", Space Structures, John Wiley and Sons, New York, 1967.

41. Gluck, J., "Lateral Load Analysis of Asymmetric Multi-Story Structures", Journal of the Structural Division, ASCE, Vol. 96, No. ST2, 1970.

42. Hanson, R.D. and Degenkolb, H.J., "The Venezuela Earthquake, July 29, 1967", American Iron and Steel Institute, New York, 1968.

43. Berg, G.V. and Stratta, J.L., "Anchorage and the Alaska Earthquake of March 12, 1964", American Iron and Steel Institute, New York, 1964.

44. "National Building Code of Canada 1965", Part 4 - Design, Section 4.1, National Research Council, Ottawa, Canada, 1965.

45. "Recommended Lateral Force Requirements", Seismology Committee, Structural Engineers Association of California, San Fransicso 5, California, 1968.

46. Milner, H.R., "The Elastic Plastic Stability of Stanchions Bent About Two Axes", Ph.D. Dissertation, Imperial College, University of London, 1965.

47. Galambos, T.V., "Structural Members and Frames", Prentice Hall Inc., Englewood Cliffs, N.J., 1968.

48. Goel, S.C., "P-Δ and Axial Column Deformation in Aseismic Frames", Journal of the Structural Division, ASCE, Vol. 95, No. ST8, 1969.

49. ASCE-WRC, "Commentary on Plastic Design in Steel", ASCE Manual No. 41, 1961.

50. ACI Committee 318 - "Building Code Requirements for Reinforced Concrete (ACI 318-63)", American Concrete Institute, 1963.

51. Nikhed, R.P., "Studies of Reinforced Concrete Shear Wall-Frame Structures", Ph.D. Dissertation, University of Alberta, Edmonton, Canada, Fall 1970.

52. Ralston, A., "A First Course in Numerical Analysis", McGraw-Hill, New York, 1965.

53. Weaver, W., "Computer Programs for Structural Analysis", Van Nostrand Company, Princeton, N.J., 1967.

54. Yarimci, E., "Incremental Inelastic Analysis of Framed Structures and Some Experimental Verifications", Fritz Engineering Laboratory Report No. 273.45, Lehigh University, 1966.

55. American Standards Association, "American Standard Building Code Requirements for Minimum Design Loads in Buildings and Other Structures", ASA, A58.1, 1955.

56. Rosanoff, R.A. and Ginsburg, T.A., "Matrix Error Analysis for Engineers", Matrix Methods in Structural Mechanics, Proceedings of Conference held at Wright-Patterson Air Force Base, Ohio, 1965.

APPENDIX A

COMPUTER PROGRAM

A.1 Flow Diagrams for Computer Program
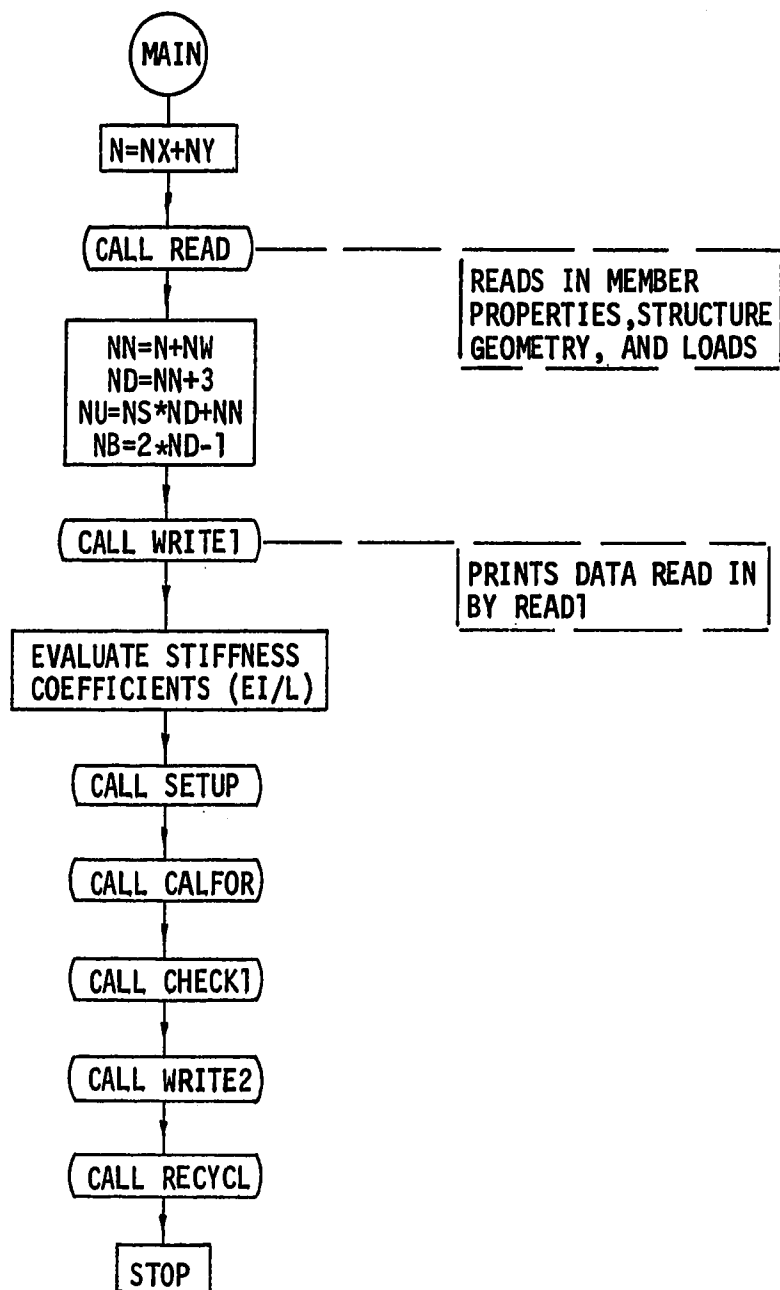
FIGURE A.1 FLOW DIAGRAM MAIN PROGRAM

SETUP

A(I,J)=0.0
B(I)=0.0
I=1,NU
J=1,NB

J=1

EVALUATE COEFFICIENTS
FOR MOMENT EQUATION
AT BASE OF STIFFENING
ELEMENT J

J=J+1

? J>N

NO

YES

J=1

EVALUATE COEFFICIENTS
FOR MOMENT EQUATION
AT FLOOR K=1,NS FOR
COLUMN ELEMENT J

IND(J)=0 ?

YES

J=J+1

J>N ?

NO

YES

NO

EVALUATE COEFFICIENTS
FOR MOMENT EQUATION
AT FLOOR K=1,INS FOR
WALL ELEMENT J

J=J+1

? J>N

NO

YES

1
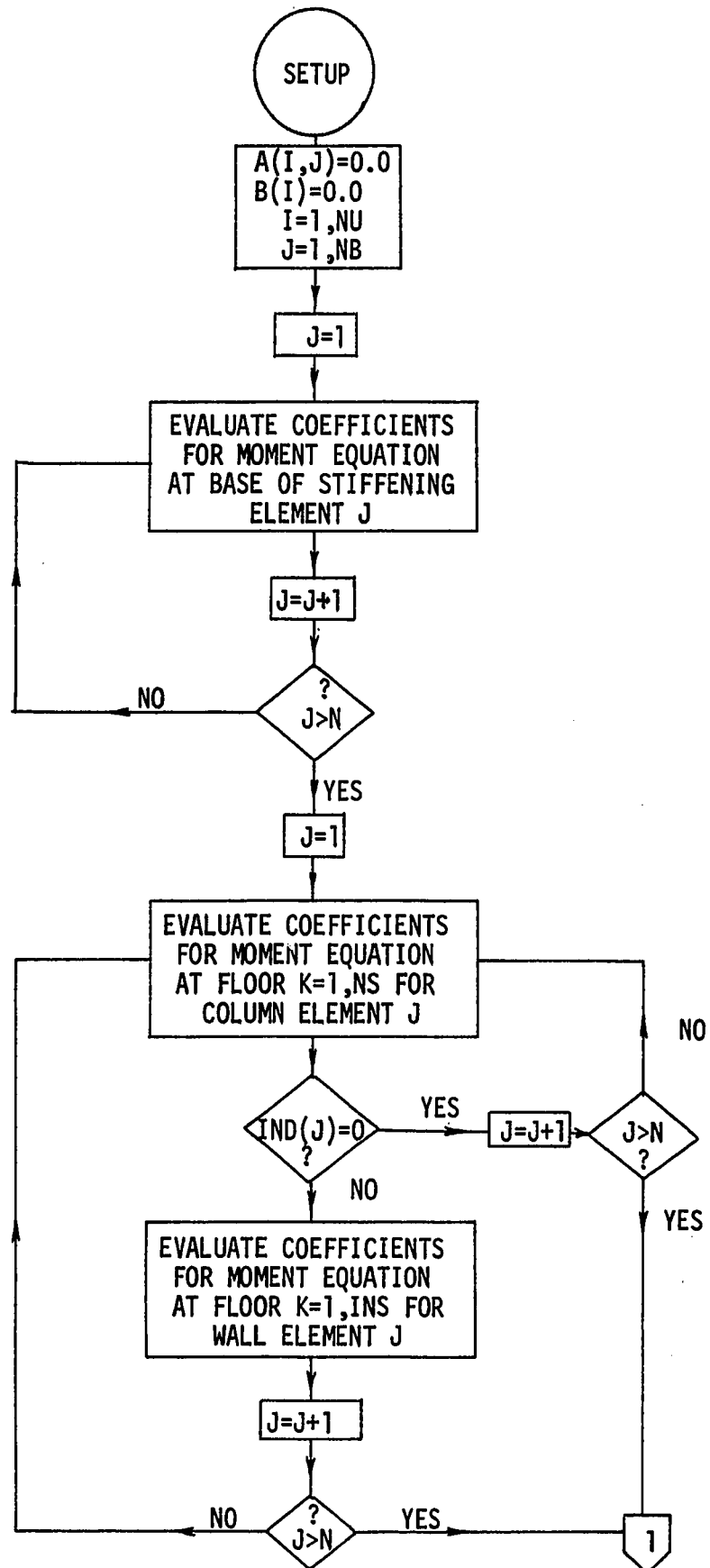
FIGURE A.2 FLOW DIAGRAM SUBROUTINE SETUP
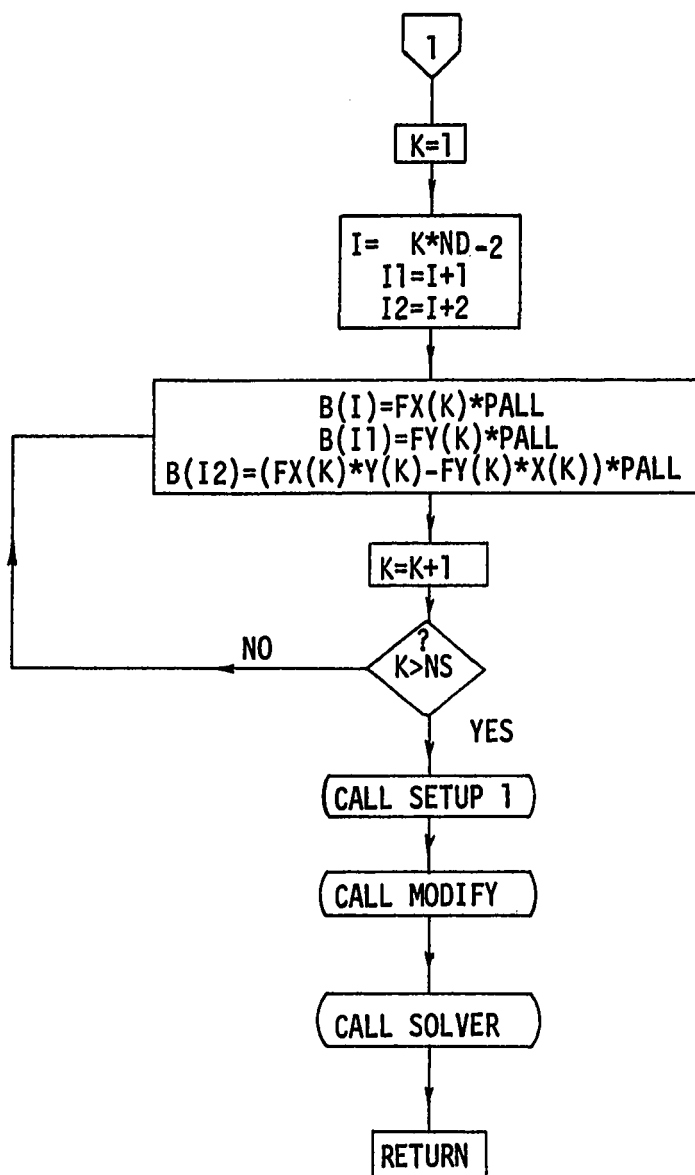
FIGURE A.2   FLOW DIAGRAM SUBROUTINE SETUP (continued)

FIGURE A.3   FLOW DIAGRAM SUBROUTINE SETUP 1

```
        ┌───┐
        │ 2 │
        └─┬─┘
          │
┌───────────────────────┐
│ EVALUATE COEFFICIENTS │
│     A(I,J),J=1,NB     │
└───────────┬───────────┘
            │
┌───────────────────────┐
│ EVALUATE COEFFICIENTS │
│     A(I1,J),J=1,NB    │
└───────────┬───────────┘
            │
┌───────────────────────┐
│ EVALUATE COEFFICIENTS │
│     A(I2,J),J=1,NB    │
└───────────┬───────────┘
            │
      ┌───────────┐
      │  RETURN   │
      └───────────┘
```
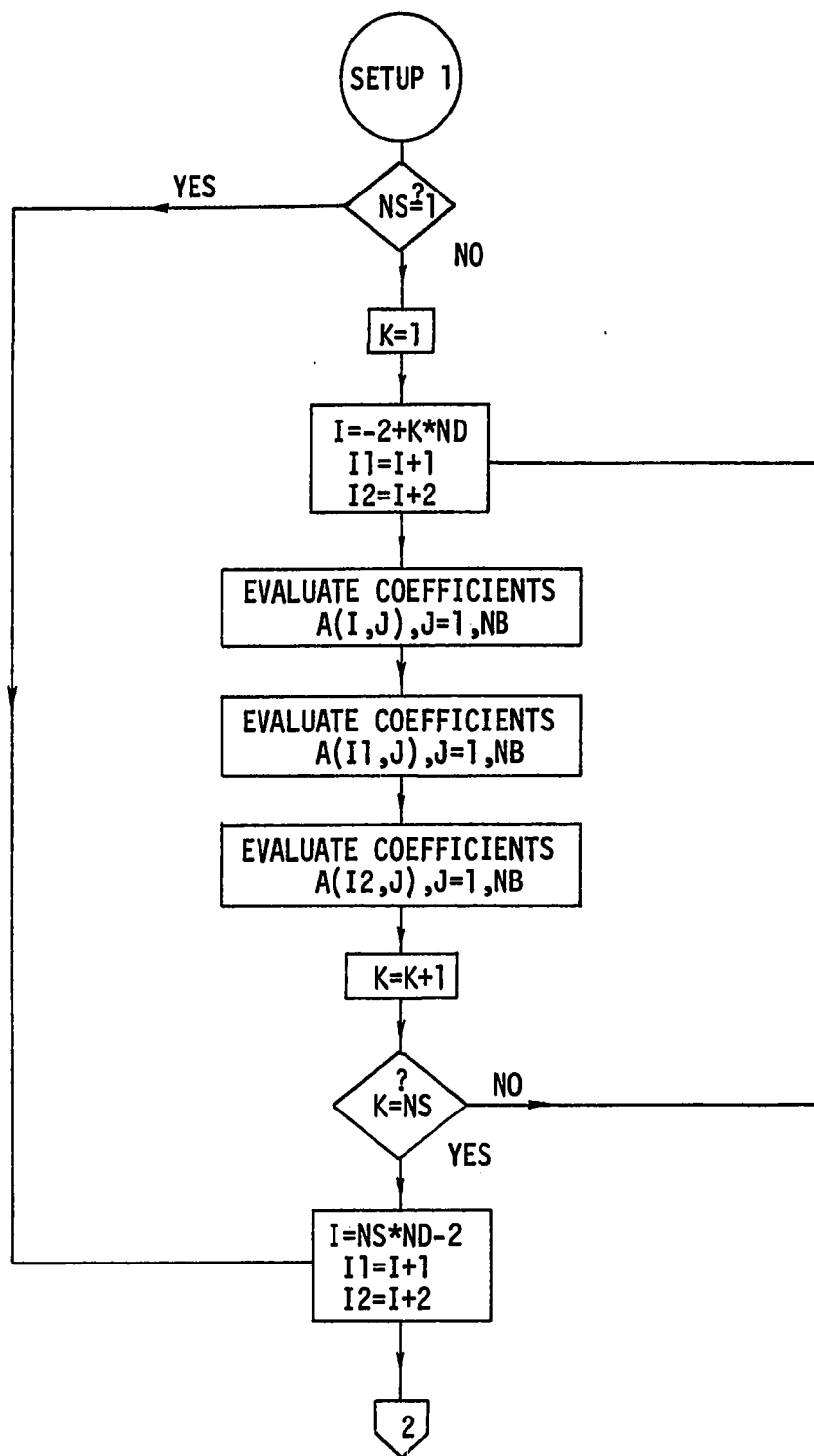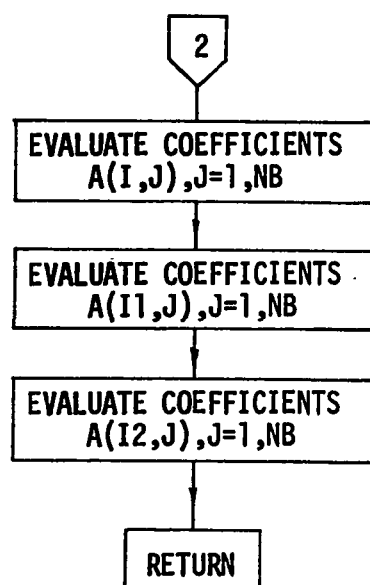
FIGURE A.3   FLOW DIAGRAM SUBROUTINE SETUP 1 (continued)
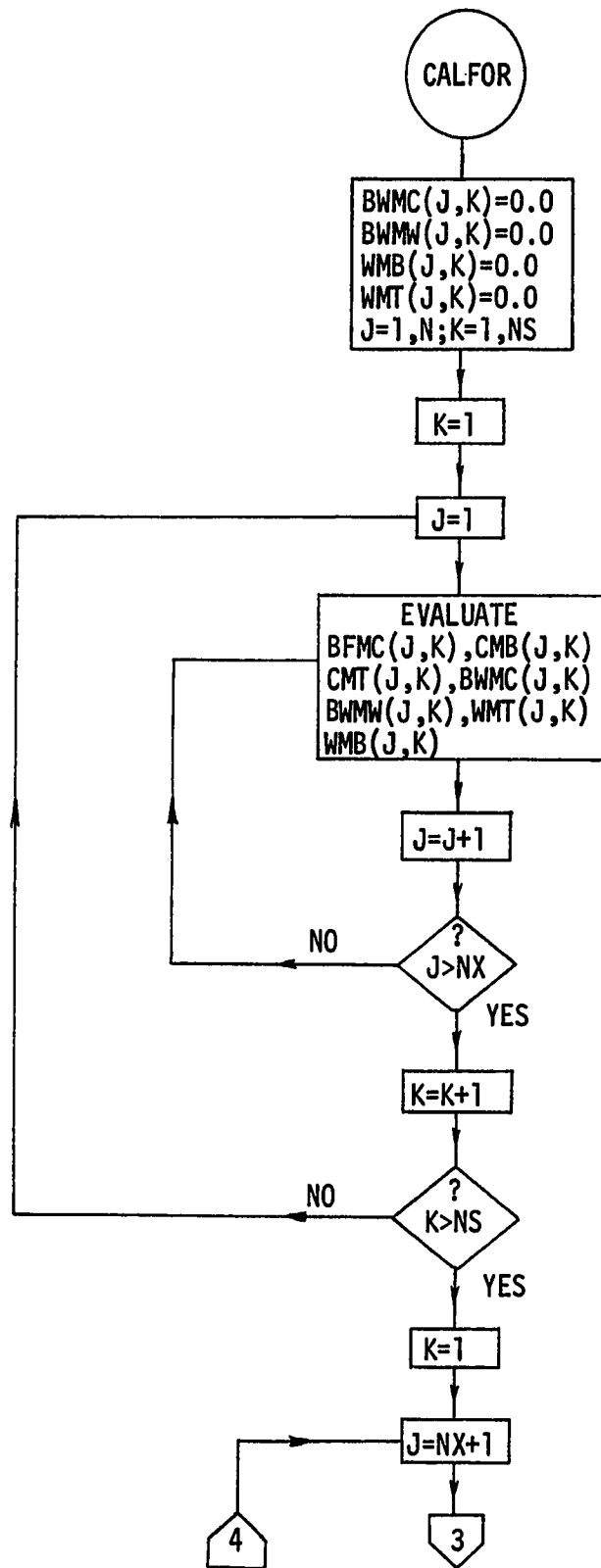
FIGURE A.4   FLOW DIAGRAM SUBROUTINE CALFOR
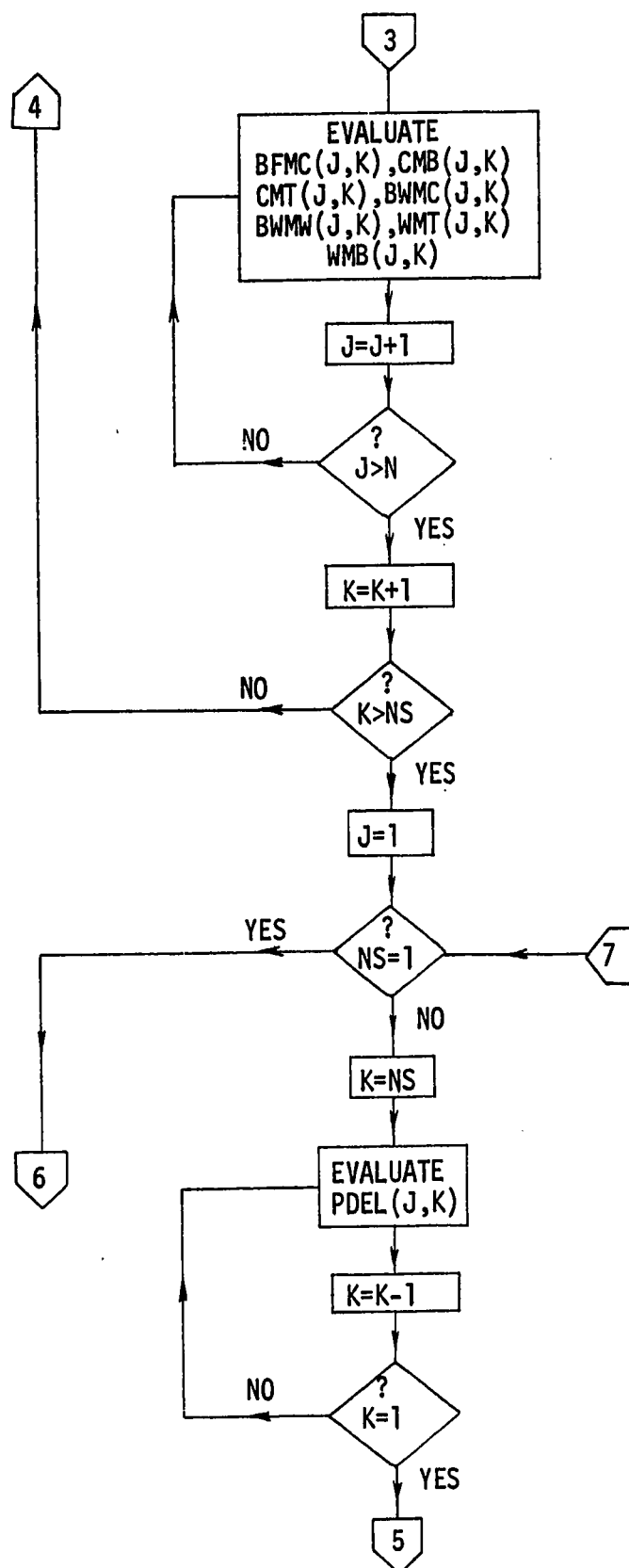
FIGURE A.4 FLOW DIAGRAM SUBROUTINE CALFOR (continued)
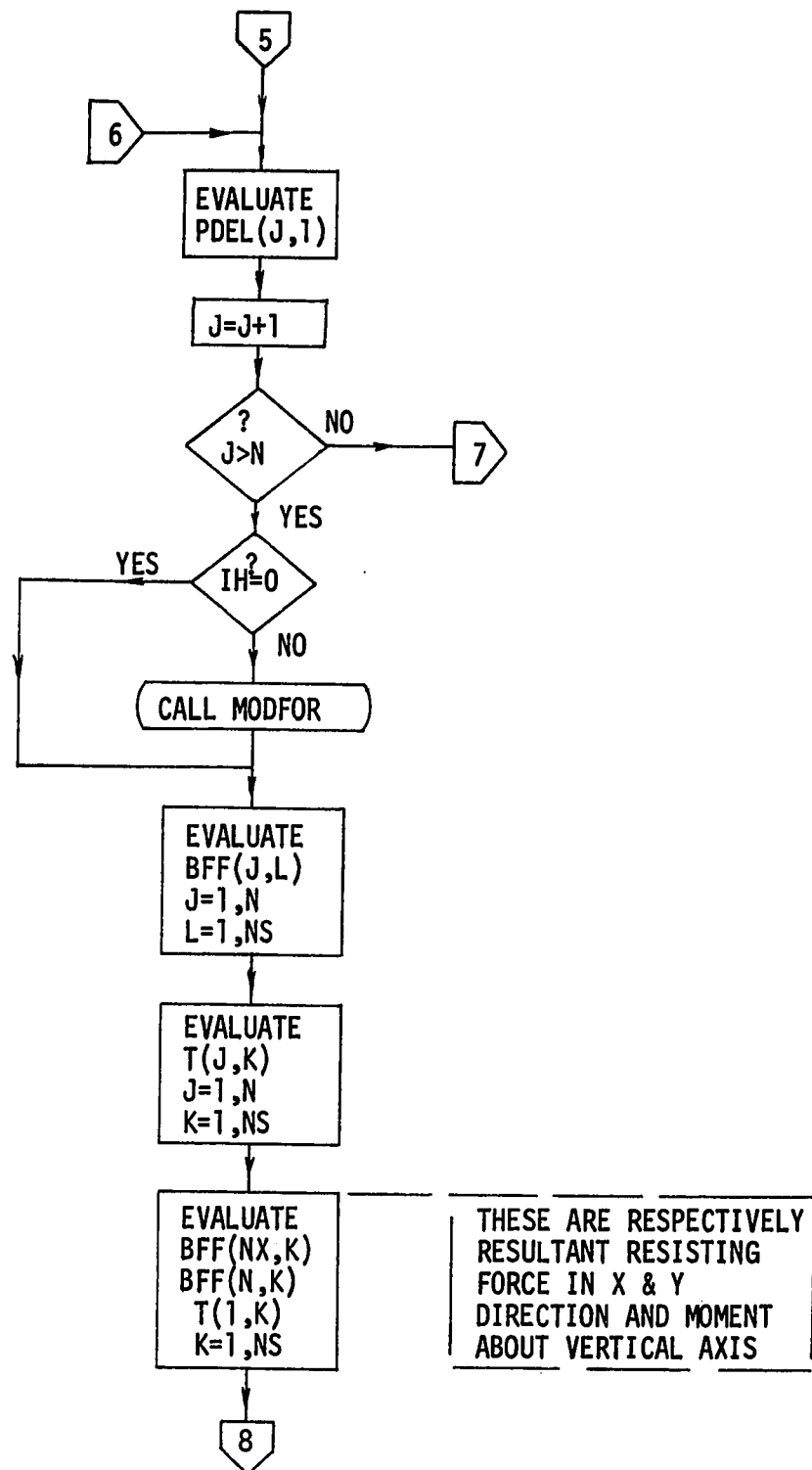
FIGURE A.4 FLOW DIAGRAM SUBROUTINE CALFOR (continued)
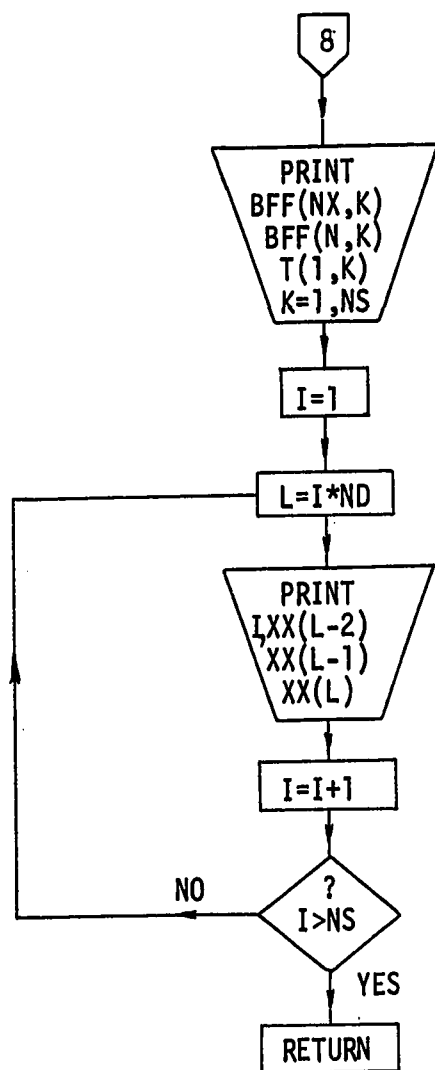
FIGURE A.4 FLOW DIAGRAM SUBROUTINE CALFOR (continued)
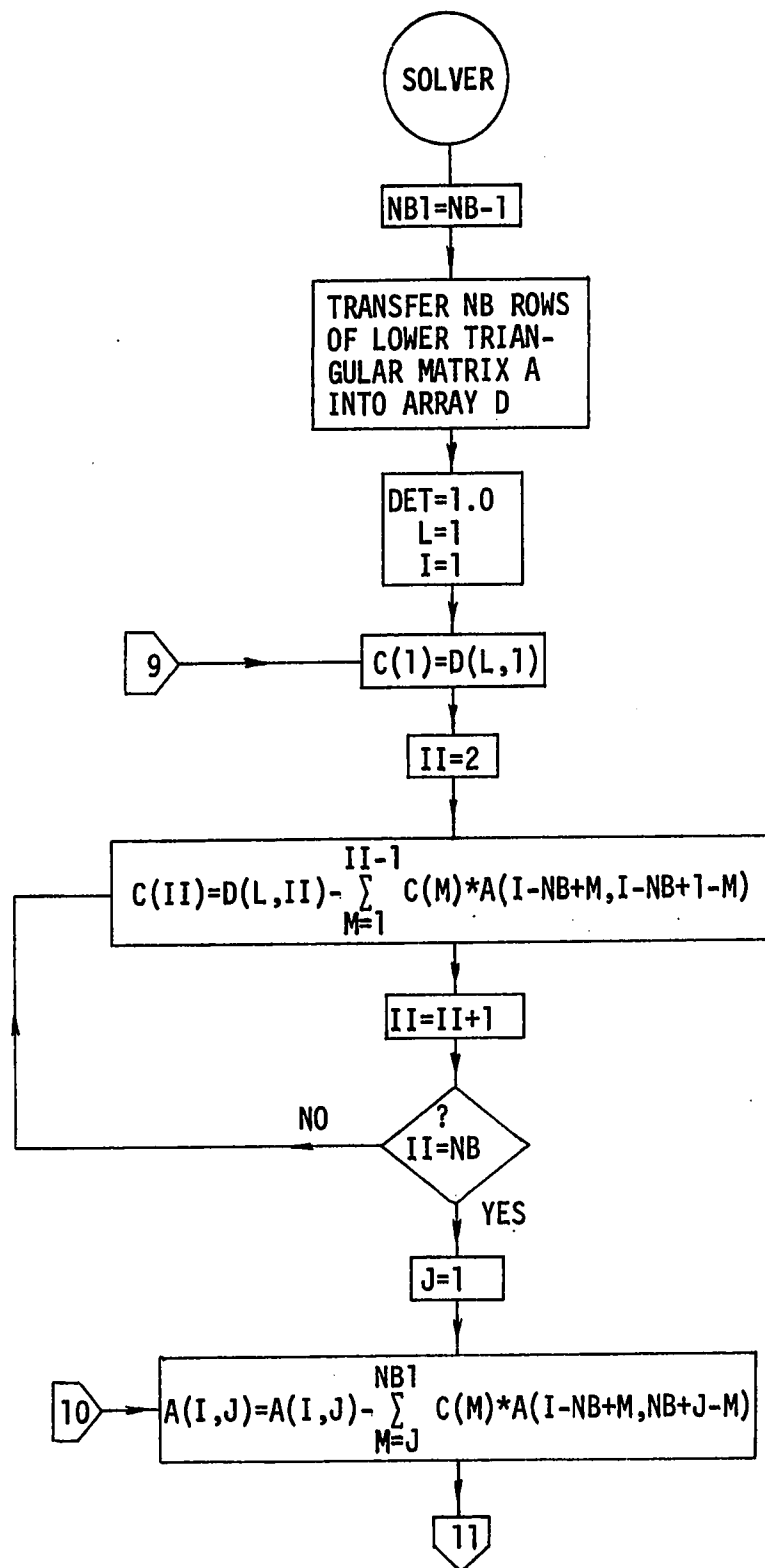
FIGURE A.5 FLOW DIAGRAM SUBROUTINE SOLVER
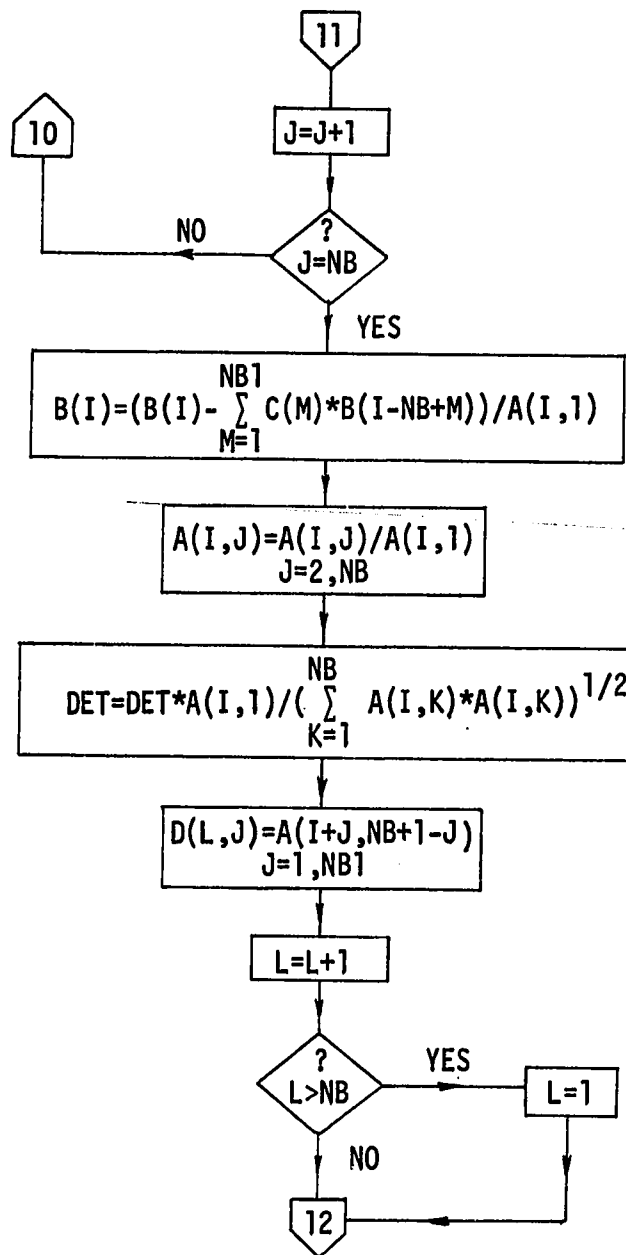
FIGURE A.5   FLOW DIAGRAM SUBROUTINE SOLVER (continued)
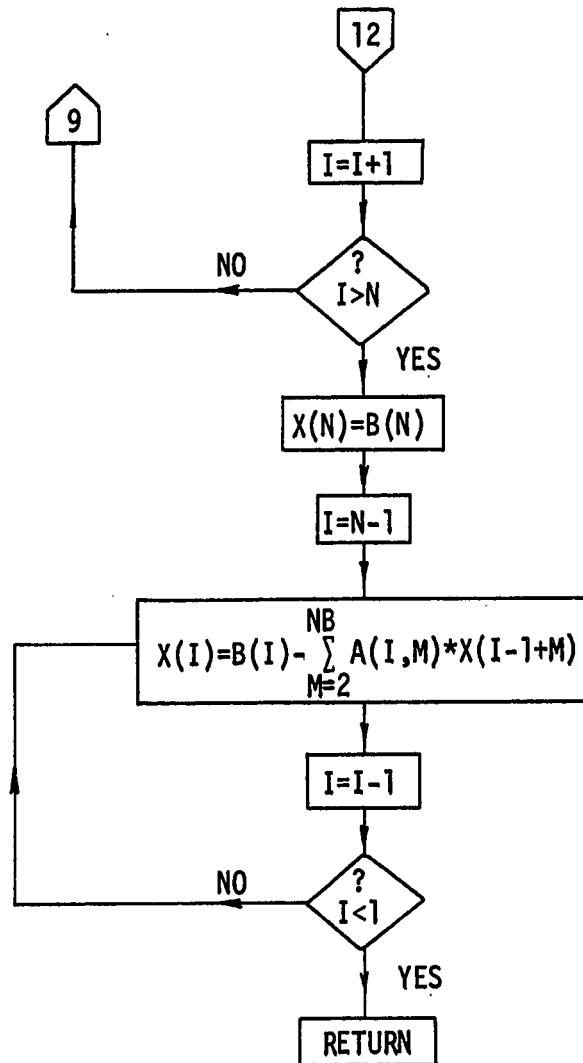
FIGURE A.5 FLOW DIAGRAM SUBROUTINE SOLVER (continued)
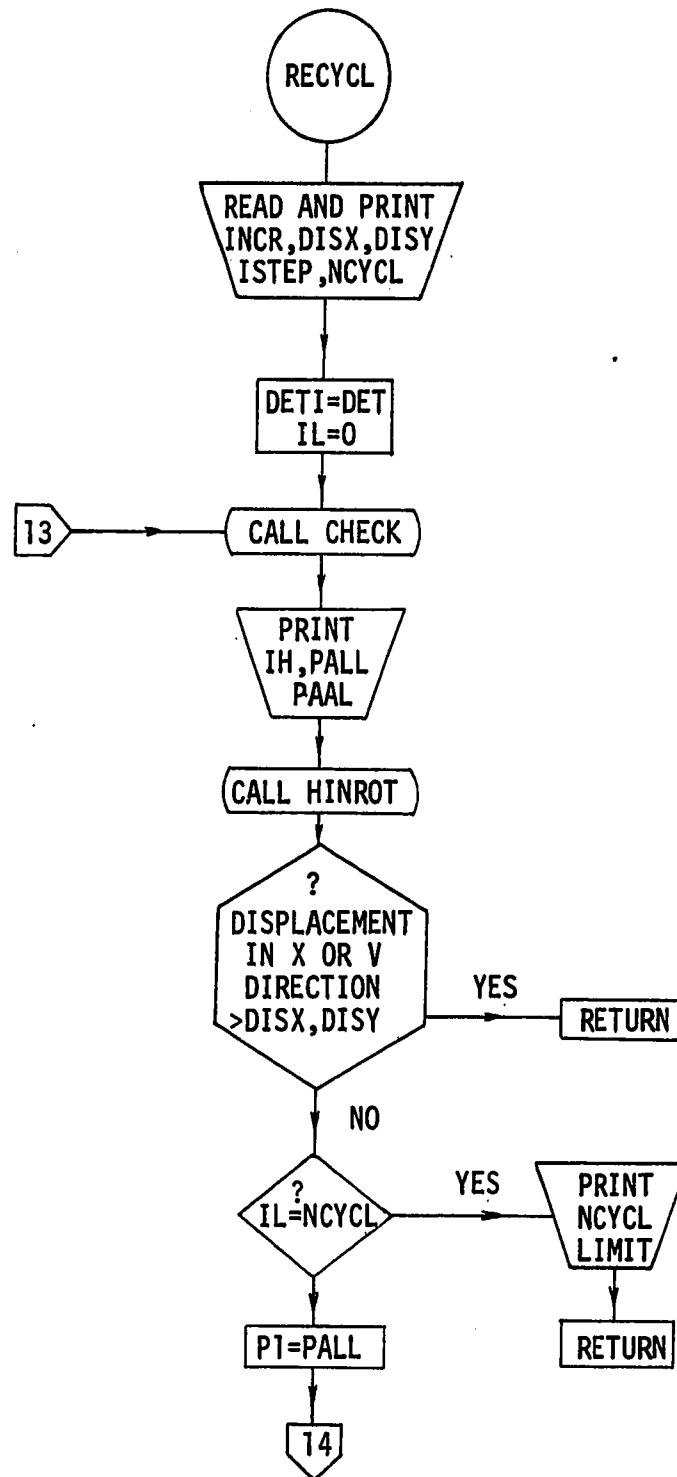
FIGURE A.6   FLOW DIAGRAM SUBROUTINE RECYCL
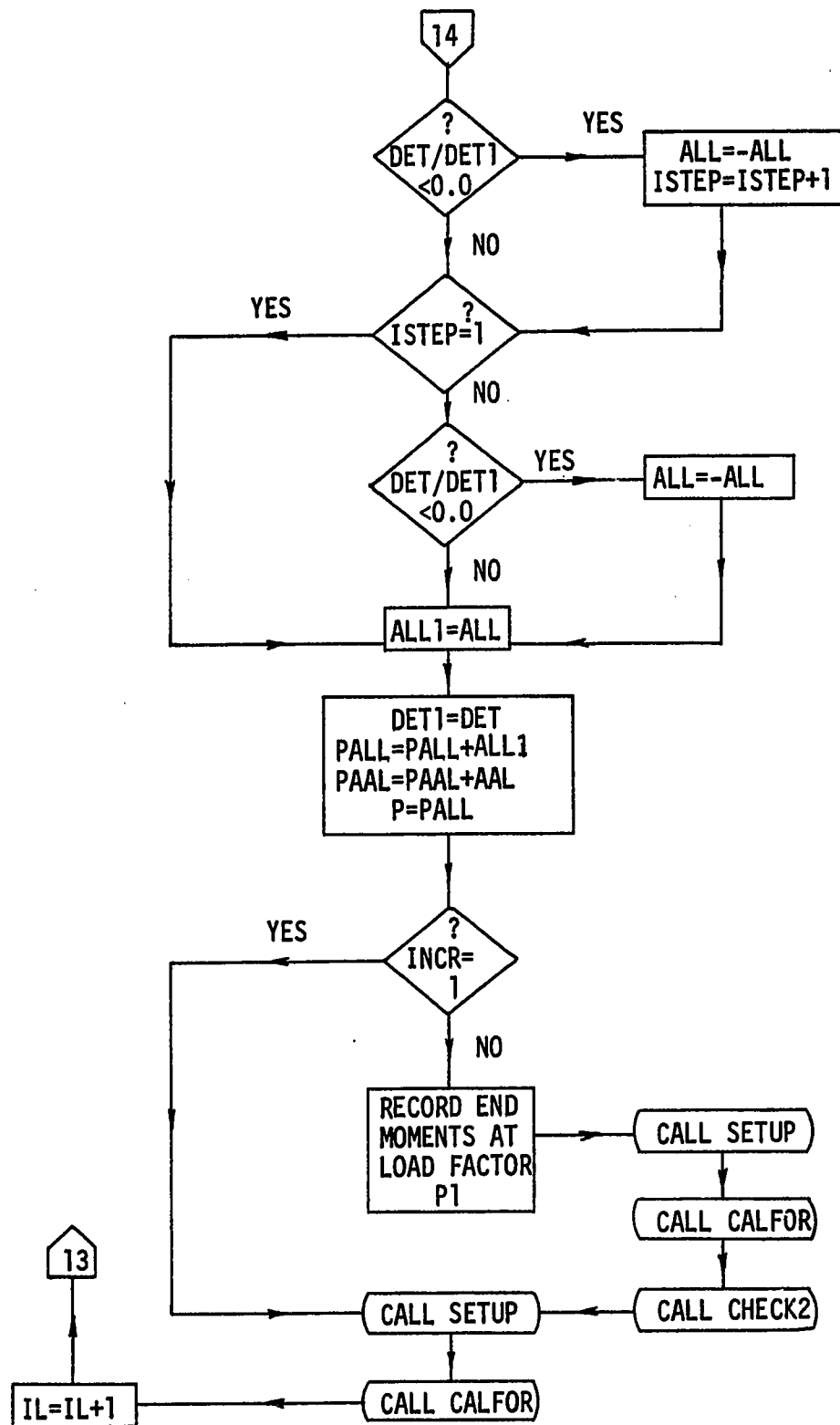
FIGURE A.6   FLOW DIAGRAM SUBROUTINE RECYCL (continued)

A.2 Subroutine Listing and Data Cards

1. MAIN   - Calls subroutines to read and print data, initializes analysis then hands control to RECYCL subroutine, which performs load incrementation procedure.

2. READ   - Reads member properties, structure geometry and loading.

3. WRITE1   - prints data read in by READ.

4. SETUP   - Calculates and stores the coefficients for the moment equilibrium equations of the elastic structure.

5. SETUP1   - Calculates and stores the coefficients for the floor force equilibrium equations of the elastic structure.

6. MODIFY   - Modifies the coefficients of the equilibrium equations where plastic hinges have formed in the beams and columns.

7. MODFY1   - Modifies the coefficients of the equilibrium equations where plastic hinges have formed in the walls.

8. SOLVER   - Modified Gauss Elimination algorithm. Solves the equilibrium equations, stored as a banded upper triangular array.

9. CALFOR   - Computes member end forces for displacements assuming the structure to be elastic.

10. MODFOR   - Modifies member end forces where the presence of plastic hinges change the equations used in CALFOR.

11. CHECK   - Checks member end moments against corresponding plastic moment values. Where the yield condition is attained a plastic hinge is inserted in the structure and noted.

12. CHECK1   - Calculates the load factor that will result in the formation of the first hinge. This requires computation of the moment to plastic moment ratio for each member end; then selecting the maximum.

13. CHECK2   - Selects successive load factors, which will result in the formation of one additional hinge during each cycle.

14. RECYCL   - Controls the load incrementation procedure and is the main subroutine in developing the load-response curve for the structure. Controls to select the type of load incrementation, number of cycles, maximum displacement before termination, and when unloading is to commence, are read in by this subroutine.

15. WRITE2   - Prints all the member end moments when called.

16. HINROT   - Calculates the rotational discontinuities that exist across the plastic hinges after each load change.

       Data is transmitted to the program by means of punched cards. The information on, and format of, each card and the order in which they must be read is as follows:

1. NS,NX,NY,E,EW,YS,ALL,AAL; Format (3I5,5F8.2)

2. H;Format (10F8.2)

3. IND,ESC,ESW; Format (I10,2E11.4)

4. BF,BW,W,CI,WI,BFI,BWI,CM,WM,BFM,BWM; Format (3F5.1,F8.1,E12.5,
   2F8.1,F6.0,E11.4,2F6.0)

5. PC; Format (10F8.3)

6. GKT; Format (6E12.5)

7. FX; Format (10F8.3)

8. FY; Format (10F8.3)

9. YFX; Format (10F8.3)

10. XFY; Format (10F8.3)

11. Y; Format (10F8.3)

12. X; Format (10F8.3)

13. INCR,DISX,DISY,ISTEP,NCYCL; Format (I10,2F10.2,2I10)

For each bent there will be one card number 3, and NS times
card number 4, corresponding to the number of stories. The bents will
be placed in numeric order starting with the bent in the X direction
having the minimum co-ordinate and finishing with the bent in the Y
direction having the maximum co-ordinate, see FIGURE 3.2. All bents
will be read in before card number 5.

A.3 Nomenclature for Fortran IV Program

In the following nomenclature, subscript I refers to a parti-
cular floor or story and subscript J refers to a particular bent.

E,EW   - Modulus of elasticity of frame and wall respectively
            (ksi).

YS   - Yield stress of frame members (ksi).

PALL,PAAL — Load factors; lateral and vertical load.

ALL,AAL — Preset load factor increments; lateral and vertical load.

DET — Determinant of coefficient matrix.

UT,VT — Displacement of top floor in X and Y directions respectively (in).

P — Load factor.

X(J),Y(J) — Bent co-ordinates (in).

ESC(J),ESW(J) — Stiffness of rotational springs at base of column and wall respectively (kip in radian^{-1}).

H(I) — Story height (in).

GKT(I) — St. Venant torsional stiffness (kip in^2).

FX(I),FY(I) — Applied lateral load; X and Y directions (kip).

YFX(I),XFY(I) — Co-ordinates of lateral loads (in).

RIH(K) — Rotation of member end at formation of plastic hinge, (radian).

PMH(K) — Moment at formation of plastic hinge (kip in).

BF(J,I) — Frame beam span (in).

BW(J,I) — Wall beam span (in).

W(J,I) — Wall width (in).

CI(J,I) — Column moment of inertia (in^4).

WI(J,I) — Wall moment of inertia (in^4).

BFI(J,I) — Frame beam moment of inertia (in^4).

BWI(J,I) — Wall beam moment of inertia (in^4).

CM(J,I)	- Plastic moment of column (kip in).
WM(J,I)	- Plastic moment of wall (kip in).
BFM(J,I)	- Plastic moment of frame beam (kip in).
BWM(J,I)	- Plastic moment of wall beam (kip in).
PC(J,I)	- Vertical load on bents (kip).
A	- Coefficient matrix.
B	- Load vector.
XX	- Displacement vector.
PDEL(J,I)	- Story shear caused by P-delta moments (kip).
BFMC(J,I)	- Frame beam moment at column end (kip in).
BWMC(J,I)	- Wall beam moment at column end (kip in).
BWMW(J,I)	- Wall beam moment at wall end (kip in).
CMT(J,I)	- Moment at top of column (kip in).
CMB(J,I)	- Moment at bottom of column (kip in).
WMB(J,I)	- Moment at bottom of wall (kip in).
WMT(J,I)	- Moment at top of wall (kip in).
BFF(J,I)	- Resisting floor force exerted by bent (kip).
BFC(J,I)	- Frame beam moment at plastic hinge formation.
BWC(J,I)	- Wall beam moment at plastic hinge formation.
BWW(J,I)	- Wall beam moment at plastic hinge formation.
CT(J,I)	- Column moment at plastic hinge formation.
CB(J,I)	- Column moment at plastic hinge formation.
WB(J,I)	- Wall moment at plastic hinge formation.
WT(J,I)	- Wall moment at plastic hinge formation.

NS	- Number of stories.
NX,NY	- Number of bents, X and Y directions.
NX1	- NX+1, number of first bent in the Y direction.
NS1	- NS-1, number of stories minus one.
N	- NX+NY, total number of bents.
NW	- Number of wall elements per story.
NN	- N+NW, number of joint rotations per floor.
ND	- NN+3, number of displacements per floor.
NU	- ND·NS+NN, number of displacements for complete structure.
NB	- ND·2-1, band width of coefficient matrix.
IH	- Total number of plastic hinges formed.
IND(J)	- Indicates whether a particular bent contains a wall; 1 - yes, 0 - no.
IK(J)	- Indicates number ordering of column and wall elements.
IHF(K)	- Floor on which hinge, K, is located.
PINC(K)	- Load factor at which hinge, K, formed.
IHB(K)	- Bent in which hinge, K, is located.
IHL(K)	- Location of hinge K; 1-bottom of column, 3-top of column, 4-frame beam, 5-bottom of wall, 7-top of wall, 8-wall beam at wall end, 9-wall beam at column end.
C,D	- Temporary storage arrays in subroutine SOLVER.

BFMC1(J,I)

BWMC1(J,I)

BWMW1(J,I)   - Temporary storage arrays in subroutines RECYCL and

CMT1(J,I)   CHECK2, used in the incremental loading procedure

CMB1(J,I)   to locate plastic hinges individually.

WMB1(J,I)

WMT1(J,I)

INCR   - Indicates type of loading procedure to be used;

                    0-locate hinges individually, 1-increment load by

                    preset amount (ALL).

DISX,DISY   - Maximum displacement in X and Y direction at which

                    analysis is to be terminated. Expressed as ratio

                    of displacements at formation of first hinge.

ISTEP   - Indicates whether loading is to be decremented at

                    change in sign of determinant. 0-reduce load at

                    first change in sign, -1 - do not reduce load until

                    second change in sign.

NCYCL   - Number of cycles in loading procedure before analysis

                    is to be terminated.

A.4 Listing of the Program

```
      COMMON E,EW,YS,PALL,PAAL,DET,DET1,UT,UT1,VT,VT1,P,P1,X(12),Y(12),H
     1(30),ESC(12),ESW(12),GKT(30),FX(30),FY(30),YFX(30),XFY(30),RIH(300
     2),PMH(300),PINC(300),BF(12,30),BW(12,30),W(12,30),BWC(12,30),ALL
     3,CI(12,30),WI(12,30),BFI(12,30),BWI(12,30),CM(12,30),WM(12,30),BFM
     4(12,30),BWM(12,30),PC(12,30),WB(12,30),A(422,33),B(422),XX(422),WT
     5(12,30),PDEL(12,30),BFMC(12,30),BWMC(12,30),BWMW(12,30),CMT(12,30)
     6,CMB(12,30),WMT(12,30),WMB(12,30),BFF(12,30),CB(12,30),CT(12,30),B
     7FC(12,30),BWW(12,30),AAL,NS,NX,NY,NX1,NS1,N,ND,NN,NU,NB,IH,IND(12)
     8,IK(12),IHF(300),IHB(300),IHL(300)
      CALL READ
      NS1=NS-1
      NX1=NX+1
      PALL=1.0
      PAAL=1.0
      IH=0
      NW=0
      DO 10 I=1,N
      NW=NW+IND(I)
   10 CONTINUE
      NN=N+NW
      ND=NN+3
      NU=NS*ND+NN
      NB=2*ND-1
      IK(1)=1+IND(1)
      DO 11 I=2,N
      IK(I)=IK(I-1)+IND(I)+1
   11 CONTINUE
      CALL WRITE1
      DO 1 J=1,NS
      GKT(J)=GKT(J)/H(J)
    1 CONTINUE
      DO 20 I=1,N
      DO 21 J=1,NS
      CI(I,J)=E*CI(I,J)/H(J)
      WI(I,J)=EW*WI(I,J)/H(J)
      BFI(I,J)=E*BFI(I,J)/BF(I,J)
      BWI(I,J)=E*BWI(I,J)/BW(I,J)
      CB(I,J)=0.0
      CT(I,J)=0.0
      BFC(I,J)=0.0
      WB(I,J)=0.0
      WT(I,J)=0.0
      BWW(I,J)=0.0
      BWC(I,J)=0.0
   21 CONTINUE
   20 CONTINUE
      CALL SETUP
      CALL CALFOR
      CALL CHECK1
      CALL WRITE2
      UT1=UT
```

```
      VT1=VT
      WRITE(6,22)
      CALL RECYCL
   22 FORMAT(1H0//,T5,'HINGE LOCATION LEGEND :'//T5,'1= BOTTOM OF COLUMN
     1 , 3= TOP OF COLUMN , 4= FRAME BEAM , 5= BOTTOM OF WALL  '/T5,'7=
     2TOP OF WALL , 8= WALL BEAM AT WALL END , 9= WALL BEAM AT COLUMN ')
      WRITE(6,23)
   23 FORMAT(1H0//,T5,'HINGE NUMBER',T20,'BENT NUMBER',T35,'FLOOR NUMBER
     1',T50,'LOCATION',T65,'LOAD FACTOR')
      DO 24 I=1,IH
      WRITE(6,25)I,IHB(I),IHF(I),IHL(I),PINC(I)
   25 FORMAT(1H0/,T9,I3,T25,I2,T39,I2,T53,I1,T68,F5.3)
   24 CONTINUE
      STOP
      END



      SUBROUTINE    READ
      COMMON E,EW,YS,PALL,PAAL,DET,DET1,UT,UT1,VT,VT1,P,P1,X(12),Y(12),H
     1(30),ESC(12),ESW(12),GKT(30),FX(30),FY(30),YFX(30),XFY(30),RIH(300
     2),PMH(300),PINC(300),BF(12,30),BW(12,30),W(12,30),BWC(12,30),ALL
     3,CI(12,30),WI(12,30),BFI(12,30),BWI(12,30),CM(12,30),WM(12,30),BFM
     4(12,30),BWM(12,30),PC(12,30),WB(12,30),A(422,33),B(422),XX(422),WT
     5(12,30),PDEL(12,30),BFMC(12,30),BWMC(12,30),BWMW(12,30),CMT(12,30)
     6,CMB(12,30),WMT(12,30),WMB(12,30),BFF(12,30),CB(12,30),CT(12,30),B
     7FC(12,30),BWW(12,30),AAL,NS,NX,NY,NX1,NS1,N,ND,NN,NU,NB,IH,IND(12)
     8,IK(12),IHF(300),IHB(300),IHL(300)
      READ(5,1)NS,NX,NY,E,EW,YS,ALL,AAL
    1 FORMAT(3I5,5F8.2)
      READ(5,3)(H(I),I=1,NS)
    3 FORMAT(10F8.2)
      N=NX+NY
      DO 4 I=1,N
      READ(5,9)IND(I),ESC(I),ESW(I)
    9 FORMAT(I10,2E11.4)
      DO 5 J=1,NS
      READ(5,6)(BF(I,J),BW(I,J),W(I,J),CI(I,J),WI(I,J),BFI(I,J),BWI(I,J)
     1,CM(I,J),WM(I,J),BFM(I,J),BWM(I,J))
    6 FORMAT(3F5.1,F8.1,E12.5,2F8.1,F6.0,E11.4,2F6.0)
    5 CONTINUE
      READ(5,8)(PC(I,J),J=1,NS)
    4 CONTINUE
      READ(5,7)(GKT(I),I=1,NS)
    7 FORMAT(6E12.5)
      READ(5,8)(FX(I),I=1,NS)
      READ(5,8)(FY(I),I=1,NS)
      READ(5,8)(YFX(I),I=1,NS)
      READ(5,8)(XFY(I),I=1,NS)
      READ(5,8)(Y(I),I=1,NX)
      READ(5,8)(X(I),I=1,NY)
    8 FORMAT(10F8.3)
      RETURN
      END
```

```
      SUBROUTINE   WRITE1
      COMMON E,EW,YS,PALL,PAAL,DET,DET1,UT,UT1,VT,VT1,P,P1,X(12),Y(12),H
     1(30),ESC(12),ESW(12),GKT(30),FX(30),FY(30),YFX(30),XFY(30),RIH(300
     2),PMH(300),PINC(300),BF(12,30),BW(12,30),W(12,30),BWC(12,30),ALL
     3,CI(12,30),WI(12,30),BFI(12,30),BWI(12,30),CM(12,30),WM(12,30),BFM
     4(12,30),BWM(12,30),PC(12,30),WB(12,30),A(422,33),B(422),XX(422),WT
     5(12,30),PDEL(12,30),BFMC(12,30),BWMC(12,30),BWMW(12,30),CMT(12,30)
     6,CMB(12,30),WMT(12,30),WMB(12,30),BFF(12,30),CB(12,30),CT(12,30),B
     7FC(12,30),BWW(12,30),AAL,NS,NX,NY,NX1,NS1,N,ND,NN,NU,NB,IH,IND(12)
     8,IK(12),IHF(300),IHB(300),IHL(300)
      WRITE(6,1)
    1 FORMAT(1H1,T50,'* * * * * *', /T50,'INPUT   DATA', /T50,'* * * * *
     1*')
      WRITE(6,2)NS,NX,NY
    2 FORMAT(1H0//,T15,'NUMBER OF STORIES = ',I2,6X,'NUMBER OF X BENTS =
     1 ',I2,6X,'NUMBER OF Y BENTS = ',I2)
      WRITE(6,3)
    3 FORMAT(1H0//,T30,'UNITS ARE KIP ,INCH ,AND KIP PER SQUARE INCH.')
      WRITE(6,4)E,EW,YS
    4 FORMAT(1H0//,T15,'MODULUS OF ELASTICITY IS ',F8.1,' FOR FRAME MEMB
     1ERS AND ',F8.1,' FOR THE WALLS',', YEILD STRESS FOR COLUMNS IS ',
     2F8.2//)
      WRITE(6,35)ALL,AAL
   35 FORMAT(1H0/,T15,'LATERAL LOAD INCREMENT IS ',F6.3,' AXIAL LOAD IN
     1CREMENT IS ',F6.3//)
      WRITE(6,5)
    5 FORMAT(1H0//,T5,'FLOOR NUMBER',T23,'STORY HEIGHT',T40,'TORSIONAL C
     1OEFFICIENT',T72,'APPLIED LOAD(KIP)',T101,'POINT OF APPLICATION(IN)
     2' /,T27,'IN',T42,'GKT (KIP-IN.SQ)',T68,'X DIRECTION',T83,'Y DIRECT
     3ION',T100,' LOAD FX ',T115,' LOAD FY ')
      DO 6 I=1,NS
      WRITE(6,7)I,H(I),GKT(I),FX(I),FY(I),YFX(I),XFY(I)
    7 FORMAT(1H0,T9,I2,T23,F8.2,T43,E12.5,T68,F8.3,T83,F8.3,T101,F8.3,T1
     116,F8.3)
    6 CONTINUE
      WRITE(6,16)
   16 FORMAT(1H1,T5,'AXIAL LOADS ON X BENTS'//)
      WRITE(6,17)(I,I=1,NX)
   17 FORMAT(1H0,T5,'STORY',T12,10(2X,'BENT ',I2,2X))
      DO 19 I=1,NS
      WRITE(6,20)(I,(PC(J,I),J=1,NX))
   19 CONTINUE
   20 FORMAT(1H0,T7,I2,T12,10(2X,F8.1,1X))
      WRITE(6,21)
   21 FORMAT(1H1,T5,'AXIAL LOADS ON Y BENTS'//)
      WRITE(6,17)(I,I=1,NY)
      DO 24 I=1,NS
      WRITE(6,20)(I,(PC(J,I),J=NX1,N))
   24 CONTINUE
      DO 8 I=1,N
      IF(I.GT.NX)GO TO 9
      WRITE(6,10)I,Y(I),ESC(I),ESW(I)
   10 FORMAT(1H1,2X,'BENT X NUMBER',I5,2X,'MEMBER PROPERTIES'///3X,'DIST
     1ANCE FROM REFERENCE POINT = ',F8.2///3X,'SPRING CONSTANTS; COLUMN
     2= ',E11.4,' WALL = ',E11.4///)
```

```
      GO TO 11
 9 L=I-NX
   WRITE(6,12)L,X(L),ESC(I),ESW(I)
12 FORMAT(1H1,2X,'BENT Y NUMBER',I5,2X,'MEMBER PROPERTIES'///2X,'DIST
  1ANCE FROM REFERENCE POINT = ',F8.2///3X,'SPRING CONSTANTS; COLUMN
  2= ',E11.4,'  WALL = ',E11.4///)
11 CONTINUE
   WRITE(6,14)
14 FORMAT(1H0/,T2,'STORY',T10,'BEAM-SPAN(IN)',T25,'WALL-WIDTH',T49,'M
  1OMENTS OF INERTIA(IN4)',T89,'PLASTIC MOMENT CAPACITIES(KIP-IN)'//
  2T2,'NUMBER',T11,'FRAME',T18,'WALL',T28,'(IN)',T40,'COLUMN',T51,'WA
  3LL',T60,'FRAME-BEAM',T73,'WALL-BEAM',T84,'COLUMN(MPC)',T98,'WALL',
  4T106,'FRAME-BEAM',T119,'WALL-BEAM')
   DO 13 J=1,NS
   WRITE(6,15)J,BF(I,J),BW(I,J),W(I,J),CI(I,J),WI(I,J),BFI(I,J),BWI(I
  1,J),CM(I,J),WM(I,J),BFM(I,J),BWM(I,J)
15 FORMAT(1H0 ,T4,I2,T10,F5.1,T18,F5.1,T26,F5.1,T38,F8.0,T47,E12.5,T6
  12,F8.0,T74,F8.0,T86,F7.0,T94,E11.4,T109,F7.0,T120,F7.0)
13 CONTINUE
 8 CONTINUE
   WRITE(6,25)
25 FORMAT(1H0/////,T50,'* * * * *',/T50,'OUTPUT DATA',/T50,'* * * *
  1 * *')
   RETURN
   END


   SUBROUTINE   SETUP
   COMMON E,EW,YS,PALL,PAAL,DET,DET1,UT,UT1,VT,VT1,P,P1,X(12),Y(12),H
  1(30),ESC(12),ESW(12),GKT(30),FX(30),FY(30),YFX(30),XFY(30),RIH(300
  2),PMH(300),PINC(300),BF(12,30),BW(12,30),W(12,30),BWC(12,30),ALL
  3,CI(12,30),WI(12,30),BFI(12,30),BWI(12,30),CM(12,30),WM(12,30),BFM
  4(12,30),BWM(12,30),PC(12,30),WB(12,30),A(422,33),B(422),XX(422),WT
  5(12,30),PDEL(12,30),BFMC(12,30),BWMC(12,30),BWMW(12,30),CMT(12,30)
  6,CMB(12,30),WMT(12,30),WMB(12,30),BFF(12,30),CB(12,30),CT(12,30),B
  7FC(12,30),BWW(12,30),AAL,NS,NX,NY,NX1,NS1,N,ND,NN,NU,NB,IH,IND(12)
  8,IK(12),IHF(300),IHB(300),IHL(300)
   DO 4 I=1,NU
   DO 5 J=1,NB
   A(I,J)=0.0
 5 CONTINUE
   B(I)=0.0
 4 CONTINUE
   DO 7 J=1,N
   I=IK(J)-IND(J)
   C1=CI(J,1)
   C2=6.0*C1/H(1)
   L=2+NN-I
   L1=L+1
   L2=L+2
   A(I,1)=4.0*C1+ESC(J)
   A(I,1+ND)=2.0*C1
   IF(J.GT.NX)GO TO 8
   A(I,L)=-C2
   A(I,L2)=-C2*Y(J)
   GO TO 9
 8 A(I,L2)=C2*X(J-NX)
   A(I,L1)=-C2
```

```
 9 IF(IND(J).EQ.0)GO TO 50
   I=I+1
   W1=WI(J,1)
   W2=6.0*W1/H(1)
   L=2+NN-I
   L1=L+1
   L2=L+2
   A(I,1)=4.0*W1+ESW(J)
   A(I,1+ND)=2.0*W1
   IF(J.GT.NX)GO TO 12
   A(I,L)=-W2
   A(I,L2)=-W2*Y(J)
   GO TO 50
12 A(I,L2)=W2*X(J-NX)
   A(I,L1)=-W2
50 CONTINUE
 7 CONTINUE
   DO 13 J=1,N
   I=IK(J)-IND(J)
   L1=NN+2-I
   L2=L1+1
   L3=L1+2
   DO 14 K=1,NS
   I=I+ND
   C1=CI(J,K)
   B1=BWI(J,K)
   B2=3.0*B1*W(J,K)/BW(J,K)
   IF(K.LT.NS)GO TO 20
   A(I,1)=4.0*C1+3.0*BFI(J,K)+4.0*B1
   A(I,2)=2.0*B1+B2
   GO TO 51
20 C2=CI(J,K+1)
   C3=6.0*C2/H(K+1)
   A(I,1)=4.0*C1+4.0*C2+3.0*BFI(J,K)+4.0*B1
   A(I,2)=2.0*B1+B2
   A(I,1+ND)=2.0*C2
   IF(J.GT.NX)GO TO 15
   A(I,L1)=-C3
   A(I,L3)=-C3*Y(J)
   GO TO 51
15 A(I,L3)=C3*X(J-NX)
   A(I,L2)=-C3
51 CONTINUE
14 CONTINUE
   IF(IND(J).EQ.0)GO TO 52
17 I=IK(J)
   L1=NN+2-I
   L2=L1+1
   L3=L1+2
   DO 18 K=1,NS
   I=I+ND
   W1=WI(J,K)
   B1=BWI(J,K)
   B2=3.0*B1*W(J,K)*W(J,K)/(BW(J,K)*BW(J,K))
   IF(K.LT.NS)GO TO 21
   A(I,1)=4.0*W1+B2+6.0*B1*W(J,K)/BW(J,K)+4.0*B1
   GO TO 53
21 W2=WI(J,K+1)
```

```
      W3=6.0*W2/H(K+1)
      A(I,1)=4.0*W1+4.0*W2+B2+6.0*B1*W(J,K)/BW(J,K)+4.0*B1
      A(I,1+ND)=2.0*W2
      IF(J.GT.NX)GO TO 19
      A(I,L1)=-W3
      A(I,L3)=-W3*Y(J)
      GO TO 53
   19 A(I,L3)=W3*X(J-NX)
      A(I,L2)=-W3
   53 CONTINUE
   18 CONTINUE
   52 CONTINUE
   13 CONTINUE
      DO 22 K=1,NS
      I=-2
      I=I+K*ND
      I1=I+1
      I2=I+2
      B(I)= FX(K)*PALL
      B(I1)= FY(K)*PALL
      B(I2)=(-FY(K)*XFY(K)+FX(K)*YFX(K))*PALL
   22 CONTINUE
      CALL SETUP1
   23 CONTINUE
      CALL MODIFY
      CALL SOLVER(A,B,XX,NU,NB,DET)
      UT=XX(NS*ND-2)
      VT=XX(NS*ND-1)
   24 CONTINUE
      WRITE(6,103)(XX(I),I=1,NU)
  103 FORMAT(1H0,(T5,'DISPLACEMENTS ARE ',8(E12.5,1X)))
      RETURN
      END




      SUBROUTINE    SETUP1
      COMMON E,EW,YS,PALL,PAAL,DET,DET1,UT,UT1,VT,VT1,P,P1,X(12),Y(12),H
     1(30),ESC(12),ESW(12),GKT(30),FX(30),FY(30),YFX(30),XFY(30),RIH(300
     2),PMH(300),PINC(300),BF(12,30),BW(12,30),W(12,30),BWC(12,30),ALL
     3,CI(12,30),WI(12,30),BFI(12,30),BWI(12,30),CM(12,30),WM(12,30),BFM
     4(12,30),BWM(12,30),PC(12,30),WB(12,30),A(422,33),B(422),XX(422),WT
     5(12,30),PDEL(12,30),BFMC(12,30),BWMC(12,30),BWMW(12,30),CMT(12,30)
     6,CMB(12,30),WMT(12,30),WMB(12,30),BFF(12,30),CB(12,30),CT(12,30),B
     7FC(12,30),BWW(12,30),AAL,NS,NX,NY,NX1,NS1,N,ND,NN,NU,NB,IH,IND(12)
     8,IK(12),IHF(300),IHB(300),IHL(300)
      IF(NS1.EQ.0)GO TO 70
      DO 23 K=1,NS1
      H1=H(K)
      H2=H(K+1)
      H3=H1*H1
      H4=H2*H2
      I=-2
      I=I+K*ND
      I1=I+1
      I2=I+2
      SU1=0.0
      SU2=0.0
```

```
      SU3=0.0
      SU4=0.0
      DO 24 J=1,NX
      SU1=SU1+(12.0/H3)*(CI(J,K)+WI(J,K))+(12.0/H4)*(CI(J,K+1)+WI(J,K+1)
     1)-PAAL*PC(J,K)/H1-PAAL*PC(J,K+1)/H2
      SU2=SU2+Y(J)*(+12.0*(CI(J,K)+WI(J,K))/H3+12.0*(CI(J,K+1)+WI(J,K+1)
     1)/H4-PAAL*PC(J,K)/H1-PAAL*PC(J,K+1)/H2)
      SU3=SU3-(12.0/H4)*(CI(J,K+1)+WI(J,K+1))+PAAL*PC(J,K+1)/H2
      SU4=SU4-Y(J)*(12.0*(CI(J,K+1)+WI(J,K+1))/H4-PAAL*PC(J,K+1)/H2)
   24 CONTINUE
      A(I,1)=SU1
      A(I,3)=SU2
      A(I,1+ND)= SU3
      A(I,3+ND)= SU4
      DO 25 J=1,NX
      JJ=IK(J)-IND(J)
      A(I,3+JJ)=-6.0*(CI(J,K)/H1-CI(J,K+1)/H2)
      A(I,3+JJ+ND)=+6.0*CI(J,K+1)/H2
      IF(IND(J).EQ.0)GO TO 55
      A(I,4+JJ)=-6.0*(WI(J,K)/H1-WI(J,K+1)/H2)
      A(I,4+JJ+ND)=+6.0*WI(J,K+1)/H2
   55 CONTINUE
   25 CONTINUE
      SU1=0.0
      SU2=0.0
      SU3=0.0
      SU4=0.0
      DO 26 J=NX1,N
      L=J-NX
      SU1=SU1+(12.0/H3)*(CI(J,K)+WI(J,K))+(12.0/H4)*(CI(J,K+1)+WI(J,K+1)
     1)-PAAL*PC(J,K)/H1-PAAL*PC(J,K+1)/H2
      SU2=SU2-X(L)*(12.0*(CI(J,K)+WI(J,K))/H3+12.0*(CI(J,K+1)+WI(J,K+1))
     1/H4-PAAL*PC(J,K)/H1-PAAL*PC(J,K+1)/H2)
      SU3=SU3-(12.0/H4)*(CI(J,K+1)+WI(J,K+1))+PAAL*PC(J,K+1)/H2
      SU4=SU4+X(L)*(+12.0*(CI(J,K+1)+WI(J,K+1))/H4-PAAL*PC(J,K+1)/H2)
   26 CONTINUE
      A(I1,1)=SU1
      A(I1,2)=SU2
      A(I1,1+ND)= SU3
      A(I1,2+ND)= SU4
      DO 27 J=NX1,N
      JJ=IK(J)-IND(J)
      A(I1,2+JJ)=-6.0*(CI(J,K)/H1-CI(J,K+1)/H2)
      A(I1,2+JJ+ND)=+6.0*CI(J,K+1)/H2
      IF(IND(J).EQ.0)GO TO 57
      A(I1,3+JJ)=-6.0*(WI(J,K)/H1-WI(J,K+1)/H2)
      A(I1,3+JJ+ND)=+6.0*WI(J,K+1)/H2
   57 CONTINUE
   27 CONTINUE
      SU1=0.0
      SU2=0.0
      SU5=0.0
      DO 28 J=1,NX
      SU1=SU1+(Y(J)*Y(J))*((+12.0/H3)*(CI(J,K)+WI(J,K))+(12.0/H4)*(CI(J,
     1K+1)+WI(J,K+1))-PAAL*PC(J,K)/H1-PAAL*PC(J,K+1)/H2)
      SU2=SU2-(Y(J)*Y(J))*((12.0/H4)*(CI(J,K+1)+WI(J,K+1))-PAAL*PC(J,K+1
     1)/H2)
      SU5=SU5-12.0*Y(J)*(CI(J,K+1)+WI(J,K+1))/H4+Y(J)*PAAL*PC(J,K+1)/H2
```

```
   28 CONTINUE
      SU3=0.0
      SU4=0.0
      SU6=0.0
      DO 29 J=NX1,N
      L=J-NX
      SU3=SU3+(X(L)*X(L))*((+12.0/H3)*(CI(J,K)+WI(J,K))+(12.0/H4)*(CI(J,
     1K+1)+WI(J,K+1))-PAAL*PC(J,K)/H1-PAAL*PC(J,K+1)/H2)
      SU4=SU4-(X(L)*X(L))*((12.0/H4)*(CI(J,K+1)+WI(J,K+1))-PAAL*PC(J,K+1
     1)/H2)
      SU6=SU6+12.0*X(L)*(CI(J,K+1)+WI(J,K+1))/H4-X(L)*PC(J,K+1)*PAAL/H2
   29 CONTINUE
      A(I2,1)=SU1+SU3+GKT(K)+GKT(K+1)
      A(I2,1+ND)= SU2+SU4-GKT(K+1)
      A(I2,ND-1)=SU5
      A(I2,ND)=SU6
      DO 30 J=1,NX
      JJ=IK(J)-IND(J)
      A(I2,1+JJ)=-6.0*Y(J)*(CI(J,K)/H1-CI(J,K+1)/H2)
      A(I2,1+JJ+ND)=+6.0*CI(J,K+1)*Y(J)/H2
      IF(IND(J).EQ.0)GO TO 58
      A(I2,2+JJ)=-6.0*Y(J)*(WI(J,K)/H1-WI(J,K+1)/H2)
      A(I2,2+JJ+ND)=+6.0*WI(J,K+1)*Y(J)/H2
   58 CONTINUE
   30 CONTINUE
      DO 31 J=NX1,N
      L=J-NX
      JJ=IK(J)-IND(J)
      A(I2,1+JJ)=6.0*X(L)*(CI(J,K)/H1-CI(J,K+1)/H2)
      A(I2,1+JJ+ND)=-6.0*CI(J,K+1)*X(L)/H2
      IF(IND(J).EQ.0)GO TO 59
      A(I2,2+JJ)=6.0*X(L)*(WI(J,K)/H1-WI(J,K+1)/H2)
      A(I2,2+JJ+ND)=-6.0*WI(J,K+1)*X(L)/H2
   59 CONTINUE
   31 CONTINUE
   23 CONTINUE
   70 I=NS*ND-2
      H1=H(NS)
      H2=H1*H1
      I1=I+1
      I2=I+2
      SU1=0.0
      SU2=0.0
      DO 32 J=1,NX
      SU1=SU1+(12./H2)*(CI(J,NS)+WI(J,NS))-PC(J,NS)*PAAL/H1
      SU2=SU2+((12./H2)*(CI(J,NS)+WI(J,NS))-PC(J,NS)*PAAL/H1)*Y(J)
   32 CONTINUE
      A(I,1)=SU1
      A(I,3)=SU2
      DO 33 J=1,NX
      JJ=IK(J)-IND(J)
      A(I,3+JJ)=-6.0*CI(J,NS)/H1
      IF(IND(J).EQ.0)GO TO 60
      A(I,4+JJ)=-6.0*WI(J,NS)/H1
   60 CONTINUE
   33 CONTINUE
      SU1=0.0
      SU2=0.0
```

```
      DO 39 J=NX1,N
      L=J-NX
      SU1=SU1+(12./H2)*(CI(J,NS)+WI(J,NS))-PC(J,NS)*PAAL/H1
      SU2=SU2-((12./H2)*(CI(J,NS)+WI(J,NS))-PC(J,NS)*PAAL/H1)*X(L)
   39 CONTINUE
      A(I1,1)=SU1
      A(I1,2)=SU2
      DO 34 J=NX1,N
      JJ=IK(J)-IND(J)
      A(I1,2+JJ)=-6.0*CI(J,NS)/H1
      IF(IND(J).EQ.0)GO TO 61
      A(I1,3+JJ)=-6.0*WI(J,NS)/H1
   61 CONTINUE
   34 CONTINUE
      SU1=0.0
      DO 35 J=1,NX
      SU1=SU1+Y(J)*Y(J)*((12.0/H2)*(CI(J,NS)+WI(J,NS))-PC(J,NS)*PAAL/H1)
   35 CONTINUE
      SU2=0.0
      DO 36 J=NX1,N
      L=J-NX
      SU2=SU2+X(L)*X(L)*((12.0/H2)*(CI(J,NS)+WI(J,NS))-PC(J,NS)*PAAL/H1)
   36 CONTINUE
      A(I2,1)=SU1+SU2+GKT(NS)
      DO 37 J=1,NX
      JJ=IK(J)-IND(J)
      A(I2,1+JJ)=-6.0*CI(J,NS)*Y(J)/H1
      IF(IND(J).EQ.0)GO TO 62
      A(I2,2+JJ)=-6.0*WI(J,NS)*Y(J)/H1
   62 CONTINUE
   37 CONTINUE
      DO 38 J=NX1,N
      L=J-NX
      JJ=IK(J)-IND(J)
      A(I2,1+JJ)=+6.0*CI(J,NS)*X(L)/H1
      IF(IND(J).EQ.0)GO TO 63
      A(I2,2+JJ)=+6.0*WI(J,NS)*X(L)/H1
   63 CONTINUE
   38 CONTINUE
      RETURN
      END

      SUBROUTINE   SOLVER(A,B,X,N,NB,DET)
      DIMENSION A(422,33),B(422),X(422),C(33),D(33,32)
      NB1=NB-1
      DO 2 I=2,NB
      D(1,I-1)=A(I,NB+2-I)
      DO 2 J=1,NB1
      D(I,J)=0.0
      I1=I-NB+J
      IF(I1.LT.1)GO TO 50
      D(I,J)=A(I1,NB+1-J)
   50 CONTINUE
    2 CONTINUE
      DET=1.0
      L=1
      DO 14 I=1,N
      C(1)=D(L,1)
```

```
      I1=I-NB
      DO 4 II=2,NB1
      SUM=0.0
      J=II-1
      IF(NB1.LT.2)GO TO 30
      DO 5 JJ=1,J
      IF(I1+JJ.LT.1)GO TO 5
      SUM=SUM-C(JJ)*A(I1+JJ,II+1-JJ)
    5 CONTINUE
      C(II)=D(L,II)+SUM
    4 CONTINUE
   30 IM=NB
      IF(I.GT.N-NB)IM=N-I+1
      CO 6 J=1,IM
      SUM=0.0
      DO 7 JJ=J,NB1
      IF(J.GT.NB1)GO TO 31
      IF(I1+JJ.LT.1)GO TO 8
      SUM=SUM-C(JJ)*A(I1+JJ,NB+J-JJ)
    8 CONTINUE
    7 CONTINUE
   31 A(I,J)=A(I,J)+SUM
      IF(J.GT.NB1)GO TO 32
    6 CONTINUE
   32 SUM=0.0
      DO 9 JJ=1,NB1
      IF((I1+JJ).LT.1)GO TO 26
      SUM=SUM-C(JJ)*B(I1+JJ)
   26 CONTINUE
    9 CONTINUE
      B(I)=(B(I)+SUM)/A(I,1)
      DO 10 J=2,NB
      A(I,J)=A(I,J)/A(I,1)
   10 CONTINUE
      AL=0.0
      DO 61 K=1,NB
      AL=AL+A(I,K)*A(I,K)
   61 CONTINUE
      DET=DET*A(I,1)/SQRT(AL)
   25 CONTINUE
      A(I,1)=1.0
      IF(I.GT.N-NB)GO TO 12
      DO 11 J=1,NB1
      D(L,J)=A(I+J,NB+1-J)
   11 CONTINUE
   12 L=L+1
      IF(L.GT.NB)L=1
   14 CONTINUE
C
C     BACK SUBSTITUTION TO SOLVE FOR UNKNOWN X
C
      X(N)=B(N)
      II=N-1
      DO 20 I=1,II
      N1=N-I
      SUM=0.0
      DO 21 J=2,NB
      IF((N1-1+J).GT.N)GO TO 27
```

```
      SUM=SUM-A(N1,J)*X(N1-1+J)
 27 CONTINUE
 21 CONTINUE
      X(N1)=B(N1)+SUM
 20 CONTINUE
      WRITE(6,28)DET
 28 FORMAT(1H0,T5,'NORMALISED DETERMINANT = ',E11.4//)
      RETURN
      END

      SUBROUTINE   CALFOR
      COMMON E,EW,YS,PALL,PAAL,DET,DET1,UT,UT1,VT,VT1,P,P1,X(12),Y(12),H
     1(30),ESC(12),ESW(12),GKT(30),FX(30),FY(30),YFX(30),XFY(30),RIH(300
     2),PMH(300),PINC(300),BF(12,30),BW(12,30),W(12,30),BWC(12,30),ALL
     3,CI(12,30),WI(12,30),BFI(12,30),BWI(12,30),CM(12,30),WM(12,30),BFM
     4(12,30),BWM(12,30),PC(12,30),WB(12,30),A(422,33),B(422),XX(422),WT
     5(12,30),PDEL(12,30),BFMC(12,30),BWMC(12,30),BWMW(12,30),CMT(12,30)
     6,CMB(12,30),WMT(12,30),WMB(12,30),BFF(12,30),CB(12,30),CT(12,30),B
     7FC(12,30),BWW(12,30),AAL,NS,NX,NY,NX1,NS1,N,ND,NN,NU,NB,IH,IND(12)
     8,IK(12),IHF(300),IHB(300),IHL(300)
      DIMENSION T(12,30)
      DO 50 J=1,N
      DO 51 K=1,NS
      BWMC(J,K)=0.0
      BWMW(J,K)=0.0
      WMB(J,K)=0.0
      WMT(J,K)=0.0
 51 CONTINUE
 50 CONTINUE
      DO 1 K=1,NS
      H1=H(K)
      DO 2 J=1,NX
      J1=IK(J)-IND(J)+(K-1)*ND
      J2=(K-2)*ND+NN+1
      X1=XX(J1)
      X2=XX(J1+1)
      X3=XX(J1+ND)
      X4=XX(J1+1+ND)
      IF(K.EQ.1)GO TO 80
      X5=XX(J2)
      X6=XX(J2+2)
 80 X7=XX(J2+ND)
      X8=XX(J2+2+ND)
      BFMC(J,K)=3.0*BFI(J,K)*X3
      IF(K.EQ.1)GO TO 3
      CMB(J,K)=CI(J,K)*(4.0*X1+2.0*X3+(6.0/H1)*(X5-X7+Y(J)*(X6-X8)))
      CMT(J,K)=CI(J,K)*(2.0*X1+4.0*X3+(6.0/H1)*(X5-X7+Y(J)*(X6-X8)))
      GO TO 4
  3 CMB(J,K)=CI(J,K)*(4.0*X1+2.0*X3-(6.0/H1)*(X7+Y(J)*X8))
      CMT(J,K)=CI(J,K)*(2.0*X1+4.0*X3-(6.0/H1)*(X7+Y(J)*X8))
  4 IF(IND(J).EQ.0)GO TO 6
      BWMC(J,K)=BWI(J,K)*(4.0*X3+(2.0+3.0*W(J,K)/BW(J,K))*X4)
      BWMW(J,K)=BWI(J,K)*(2.0*X3+(4.0+3.0*W(J,K)/BW(J,K))*X4)
      IF(K.EQ.1)GO TO 5
      WMT(J,K)=WI(J,K)*(2.0*X2+4.0*X4+(6.0/H1)*(X5-X7+Y(J)*(X6-X8)))
      WMB(J,K)=WI(J,K)*(4.0*X2+2.0*X4+(6.0/H1)*(X5-X7+Y(J)*(X6-X8)))
      GO TO 6
  5 WMT(J,K)=WI(J,K)*(2.0*X2+4.0*X4-(6.0/H1)*(X7+Y(J)*X8))
```

```
      WMB(J,K)=WI(J,K)*(4.0*X2+2.0*X4-(6.0/H1)*(X7+Y(J)*X8))
    6 CONTINUE
    2 CONTINUE
    1 CONTINUE
      DO 7 K=1,NS
      H1=H(K)
      DO 8 J=NX1,N
      L=J-NX
      J1=IK(J)-IND(J)+(K-1)*ND
      J2=(K-2)*ND+NN+2
      X1=XX(J1)
      X2=XX(J1+1)
      X3=XX(J1+ND)
      X4=XX(J1+1+ND)
      IF(K.EQ.1)GO TO 81
      X5=XX(J2)
      X6=XX(J2+1)
   81 X7=XX(J2+ND)
      X8=XX(J2+1+ND)
      BFMC(J,K)=3.0*BFI(J,K)*X3
      IF(K.EQ.1)GO TO 9
      CMB(J,K)=CI(J,K)*(4.0*X1+2.0*X3+(6.0/H1)*(X5-X7-X(L)*(X6-X8)))
      CMT(J,K)=CI(J,K)*(2.0*X1+4.0*X3+(6.0/H1)*(X5-X7-X(L)*(X6-X8)))
      GO TO 10
    9 CMB(J,K)=CI(J,K)*(4.0*X1+2.0*X3-(6.0/H1)*(X7-X(L)*X8))
      CMT(J,K)=CI(J,K)*(2.0*X1+4.0*X3-(6.0/H1)*(X7-X(L)*X8))
   10 IF(IND(J).EQ.0)GO TO 12
      BWMC(J,K)=BWI(J,K)*(4.0*X3+(2.0+3.0*W(J,K)/BW(J,K))*X4)
      BWMW(J,K)=BWI(J,K)*(2.0*X3+(4.0+3.0*W(J,K)/BW(J,K))*X4)
      IF(K.EQ.1)GO TO 11
      WMT(J,K)=WI(J,K)*(2.0*X2+4.0*X4+(6.0/H1)*(X5-X7-X(L)*(X6-X8)))
      WMB(J,K)=WI(J,K)*(4.0*X2+2.0*X4+(6.0/H1)*(X5-X7-X(L)*(X6-X8)))
      GO TO 12
   11 WMT(J,K)=WI(J,K)*(2.0*X2+4.0*X4-(6.0/H1)*(X7-X(L)*X8))
      WMB(J,K)=WI(J,K)*(4.0*X2+2.0*X4-(6.0/H1)*(X7-X(L)*X8))
   12 CONTINUE
    8 CONTINUE
    7 CONTINUE
      DO 21 J=1,N
      L=J-NX
      IF(NS1.EQ.C)GO TO 70
      DO 22 I=1,NS1
      K=NS-I+1
      J2=(K-2)*ND+NN+1
      IF(J.GT.NX)GO TO 23
      PDEL(J,K)=PC(J,K)*(XX(J2+ND)-XX(J2)+Y(J)*(XX(J2+2+ND)-XX(J2+2)))*
     1PAAL
      GO TO 24
   23 J3=J2+1
      PDEL(J,K)=PC(J,K)*(XX(J3+ND)-XX(J3)-X(L)*(XX(J2+2+ND)-XX(J2+2)))*
     1PAAL
   24 CONTINUE
   22 CONTINUE
   70 IF(J.GT.NX)GO TO 25
      PDEL(J,1)=PC(J,1)*(XX(NN+1)+Y(J)*XX(NN+3))*PAAL
      GO TO 26
   25 PDEL(J,1)=PC(J,1)*(XX(NN+2)-X(L)*XX(NN+3))*PAAL
   26 CONTINUE
```

```
 21 CONTINUE
    IF(IH.EQ.0)GO TO 30
    CALL MODFOR
 30 CONTINUE
    DO 13 J=1,N
    BFF(J,NS)=(CMB(J,NS)+CMT(J,NS)+WMB(J,NS)+WMT(J,NS)+PDEL(J,NS))/H(N
   1S)
    IF(NS.EQ.1)GO TO 72
    DO 14 K=2,NS
    L=NS+1-K
    BFF(J,L)=(CMB(J,L)+CMT(J,L)+WMT(J,L)+WMB(J,L)+PDEL(J,L))/H(L)-(CMB
   1(J,L+1)+CMT(J,L+1)+WMB(J,L+1)+WMT(J,L+1)+PDEL(J,L+1))/H(L+1)
 14 CONTINUE
 72 CONTINUE
 13 CONTINUE
    DO 40 K=1,NS
    DO 41 J=1,NX
    T(J,K)=BFF(J,K)*Y(J)
 41 CONTINUE
    DO 42 J=1,NY
    L=J+NX
    T(L,K)=-BFF(L,K)*X(J)
 42 CONTINUE
    SUM=0.0
    DO 43 J=1,N
    SUM=SUM+T(J,K)
 43 CONTINUE
    T(1,K)=SUM+(FX(K)*YFX(K)-FY(K)*XFY(K))*PALL
 40 CONTINUE
    IF(NS1.EQ.0)GO TO 71
    IF(NS1.EQ.1)GO TO 73
    T(1,NS)=T(1,NS)-GKT(NS)*(XX(NS*ND)-XX((NS-1)*ND))
    DO 44 K=2,NS1
    L1=K*ND
    L2=L1-ND
    L3=L1+ND
    T(1,K)=T(1,K)-GKT(K)*(XX(L1)-XX(L2))+GKT(K+1)*(XX(L3)-XX(L1))
 44 CONTINUE
 73 T(1,1)=T(1,1)-GKT(1)*XX(ND)+GKT(2)*(XX(ND+ND)-XX(ND))
 71 CONTINUE
    DO 15 K=1,NS
    SUM=0.0
    DO 16 J=1,NX
    SUM=SUM+BFF(J,K)
 16 CONTINUE
    BFF(NX,K)=SUM
 15 CONTINUE
    DO 17 K=1,NS
    SUM=0.0
    DO 18 J=NX1,N
    SUM=SUM+BFF(J,K)
 18 CONTINUE
    BFF(N,K)=SUM
 17 CONTINUE
    WRITE(6,19)(BFF(NX,K),K=1,NS)
 19 FORMAT(1H0,T5,'RESISTING FORCE X= ',10F10.5)
    WRITE(6,20)(BFF(N,K),K=1,NS)
 20 FORMAT(1H0,T5,'RESISTING FORCE Y= ',10F10.5)
    WRITE(6,45)(T(1,K),K=1,NS)
```

```
   45 FORMAT(1H0,T5,'RESULTANT MOMENT = ',10E10.3)
      WRITE(6,27)
   27 FORMAT(1H1,T5,'FLOOR NUMBER',T22,'DISPLACEMENT X',T39,'DISPLACEMEN
     1T Y',T58,'FLOOR ROTATION'/)
      DO 28 I=1,NS
      L=I*ND
      WRITE(6,29)I,XX(L-2),XX(L-1),XX(L)
   28 CONTINUE
   29 FORMAT(1H0,T11,I2,T23,E11.4,T40,E11.4,T61,E11.4)
      RETURN
      END

      SUBROUTINE   MODFOR
      COMMON E,EW,YS,PALL,PAAL,DET,DET1,UT,UT1,VT,VT1,P,P1,X(12),Y(12),H
     1(30),ESC(12),ESW(12),GKT(30),FX(30),FY(30),YFX(30),XFY(30),RIH(300
     2),PMH(300),PINC(300),BF(12,30),BW(12,30),W(12,30),BWC(12,30),ALL
     3,CI(12,30),WI(12,30),BFI(12,30),BWI(12,30),CM(12,30),WM(12,30),BFM
     4(12,30),BWM(12,30),PC(12,30),WB(12,30),A(422,33),B(422),XX(422),WT
     5(12,30),PDEL(12,30),BFMC(12,30),BWMC(12,30),BWMW(12,30),CMT(12,30)
     6,CMB(12,30),WMT(12,30),WMB(12,30),BFF(12,30),CB(12,30),CT(12,30),B
     7FC(12,30),BWW(12,30),AAL,NS,NX,NY,NX1,NS1,N,ND,NN,NU,NB,IH,IND(12)
     8,IK(12),IHF(300),IHB(300),IHL(300)
      DO 31 I=1,IH
      J1=IHF(I)
      J2=IHB(I)
      J3=IHL(I)
      I1=IK(J2)-IND(J2)+(J1-1)*ND
      I2=(J1-2)*ND+NN+1
      I3=I2+1
      H1=H(J1)
      X1=XX(I1+ND)
      X2=XX(I2+ND)
      X3=XX(I3+ND)
      X4=XX(I1+1+ND)
      X5=XX(I2+2+ND)
      C1=3.0*CI(J2,J1)
      W1=3.0*WI(J2,J1)
      IF(J3.EQ.1)GO TO 33
      IF(J3.EQ.3)GO TO 34
      IF(J3.EQ.4)GO TO 35
      IF(J3.EQ.5)GO TO 36
      IF(J3.EQ.7)GO TO 37
      IF(J3.EQ.8)GO TO 38
      IF(J3.EQ.9)GO TO 39
      GO TO 32
   33 PM=CB(J2,J1)
      CMB(J2,J1)=PM
      IF(CT(J2,J1).NE.0.0)GO TO 32
      IF(J2.GT.NX)GO TO 40
      IF(J1.EQ.1)GO TO 41
      CMT(J2,J1)=0.50*PM+C1*(X1+(XX(I2)-X2+Y(J2)*(XX(I2+2)-X5))/H1)
      GO TO 32
   41 CMT(J2,J1)=0.50*PM+C1*(X1-(X2+Y(J2)*X5)/H1)
      GO TO 32
   40 IF(J1.EQ.1)GO TO 42
      CMT(J2,J1)=0.50*PM+C1*(X1+(XX(I3)-X3-X(J2-NX)*(XX(I2+2)-X5))/H1)
      GO TO 32
   42 CMT(J2,J1)=0.50*PM+C1*(X1-(X3-X(J2-NX)*X5)/H1)
```

```
        GO TO 32
34 PM=CT(J2,J1)
   CMT(J2,J1)=PM
   IF(CB(J2,J1).NE.0.0)GO TO 32
    IF(J2.GT.NX)GO TO 43
   IF(J1.EQ.1)GO TO 44
   CMB(J2,J1)=0.50*PM+C1*(XX(I1)+(XX(I2)-X2+Y(J2)*(XX(I2+2)-X5))/H1)
   GO TO 32
44 CMB(J2,J1)=0.50+C1*(XX(I1)-(X2+Y(J2)*X5)/H1)
   GO TO 32
43 IF(J1.EQ.1)GO TO 45
   CMB(J2,J1)=.5*PM+C1*(XX(I1)+(XX(I3)-X3+X(J2-NX)*(X5-XX(I3+1)))/H1)
   GO TO 32
45 CMB(J2,J1)=0.50*PM+C1*(XX(I1)+(-X3+X(J2-NX)*X5)/H1)
   GO TO 32
35 PM=BFC(J2,J1)
   BFMC(J2,J1)=PM
   GO TO 32
36 PM=WB(J2,J1)
   WMB(J2,J1)=PM
   IF(WT(J2,J1).NE.0.0)GO TO 32
   IF(J2.GT.NX)GO TO 46
   IF(J1.EQ.1)GO TO 47
   WMT(J2,J1)=.50*PM+W1*(X4+(XX(I2)-X2+Y(J2)*(XX(I2+2)-X5))/H1)
   GO TO 32
47 WMT(J2,J1)=0.50*PM+W1*(X4-(X2+Y(J2)*X5)/H1)
   GO TO 32
46 IF(J1.EQ.1)GO TO 48
   WMT(J2,J1)=0.50*PM+W1*(X4+(XX(I3)-X3-X(J2-NX)*(XX(I3+1)-X5))/H1)
   GO TO 32
48 WMT(J2,J1)=0.50*PM+W1*(X4+(-X3+X(J2-NX)*X5)/H1)
   GO TO 32
37 PM=hT(J2,J1)
   WMT(J2,J1)=PM
   IF(WB(J2,J1).NE.0.0)GO TO 32
   IF(J2.GT.NX)GO TO 49
   IF(J1.EQ.1)GO TO 50
   WMB(J2,J1)=.50*PM+W1*(XX(I1+1)+(XX(I2)-X2+Y(J2)*(XX(I2+2)-X5))/H1)
   GO TO 32
50 WMB(J2,J1)=0.50*PM+W1*(XX(I1+1)-(X2+Y(J2)*X5)/H1)
   GO TO 32
49 IF(J1.EQ.1)GO TO 51
   WMB(J2,J1)=0.50*PM+W1*(XX(I1+1)+(XX(I3)-X3-X(J2-NX)*(XX(I3+1)-X5))
  1/H1)
   GO TO 32
51 WMB(J2,J1)=0.50*PM+W1*(XX(I1+1)-(X3-X(J2-NX)*X5)/H1)
   GO TO 32
38 PM=BWW(J2,J1)
   BWMW(J2,J1)=PM
   IF(BWC(J2,J1).NE.0.0)GO TO 32
   BWMC(J2,J1)=.5*PM+BWI(J2,J1)*(3.0*X1+1.5*W(J2,J1)*X4/BW(J2,J1))
   GO TO 32
39 PM=BWC(J2,J1)
   BWMC(J2,J1)=PM
   IF(BWW(J2,J1).NE.0.0)GO TO 32
   BWMW(J2,J1)=0.50*PM+BWI(J2,J1)*X4*(3.0+1.5*W(J2,J1)/BW(J2,J1))
32 CONTINUE
```

```
   31 CONTINUE
      RETURN
      END


      SUBROUTINE    WRITE2
      COMMON E,EW,YS,PALL,PAAL,DET,DET1,UT,UT1,VT,VT1,P,P1,X(12),Y(12),H
     1(30),ESC(12),ESW(12),GKT(3C),FX(30),FY(30),YFX(30),XFY(30),RIH(300
     2),PMH(300),PINC(300),BF(12,30),BW(12,30),W(12,30),BWC(12,30),ALL
     3,CI(12,30),WI(12,30),BFI(12,30),BWI(12,30),CM(12,30),WM(12,30),BFM
     4(12,30),BWM(12,30),PC(12,30),WB(12,30),A(422,33),B(422),XX(422),WT
     5(12,30),PDEL(12,30),BFMC(12,30),BWMC(12,30),BWMW(12,30),CMT(12,30)
     6,CMB(12,30),WMT(12,30),WMB(12,30),BFF(12,30),CB(12,30),CT(12,30),B
     7FC(12,30),BWW(12,30),AAL,NS,NX,NY,NX1,NS1,N,ND,NN,NU,NB,IH,IND(12)
     8,IK(12),IHF(300),IHB(300),IHL(300)
      DO 1 I=1,NX
      WRITE(6,2)I
    2 FORMAT(1H0/,2X,'BENT X NUMBER',T23,I2//)
      WRITE(6,3)
    3 FORMAT(1H0,T2,'STORY NUMBER',T27,'WALL MOMENTS',T57,'COLUMN MOMENT
     1S',T88,'WALL-BEAM MOMENTS',T117,'FRAME-BEAM'//T22,'BOTTOM',T39,'TO
     2P',T54,'BOTTOM',T71,'TOP',T84,'COLUMN-END',T101,'WALL-END',T118,'M
     3OMENT')
      DO 4 J=1,NS
      WRITE(6,5)J,WMB(I,J),WMT(I,J),CMB(I,J),CMT(I,J),BWMC(I,J),BWMW(I,J
     1),BFMC(I,J)
    5 FORMAT(1H0,T7,I2,T20,E11.4,T35,E11.4,T52,E11.4,T67,E11.4,T84,E11.4
     1,T99,E11.4,T116,E11.4)
    4 CONTINUE
    1 CONTINUE
      DO 6 I=NX1,N
      L=I-NX
      WRITE(6,7)L
    7 FORMAT(1H0/,2X,'BENT Y NUMBER',T23,I2//)
      WRITE(6,3)
      DO 8 J=1,NS
      WRITE(6,5)J,WMB(I,J),WMT(I,J),CMB(I,J),CMT(I,J),BWMC(I,J),BWMW(I,J
     1),BFMC(I,J)
    8 CONTINUE
    6 CONTINUE
      RETURN
      END


      SUBROUTINE    RECYCL
      COMMON E,EW,YS,PALL,PAAL,DET,DET1,UT,UT1,VT,VT1,P,P1,X(12),Y(12),H
     1(30),ESC(12),ESW(12),GKT(30),FX(30),FY(30),YFX(30),XFY(30),RIH(300
     2),PMH(300),PINC(300),BF(12,30),BW(12,30),W(12,30),BWC(12,30),ALL
     3,CI(12,30),WI(12,30),BFI(12,30),BWI(12,30),CM(12,30),WM(12,30),BFM
     4(12,30),BWM(12,30),PC(12,30),WB(12,30),A(422,33),B(422),XX(422),WT
     5(12,30),PDEL(12,30),BFMC(12,30),BWMC(12,30),BWMW(12,30),CMT(12,30)
     6,CMB(12,30),WMT(12,30),WMB(12,30),BFF(12,30),CB(12,30),CT(12,30),B
     7FC(12,30),BWW(12,30),AAL,NS,NX,NY,NX1,NS1,N,ND,NN,NU,NB,IH,IND(12)
     8,IK(12),IHF(300),IHB(300),IHL(300)
      DIMENSION BFMC1(11,24),BWMC1(11,24),BWMW1(11,24),CMT1(11,24),CMB1(
     111,24),WMT1(11,24),WMB1(11,24)
      READ(5,11)INCR,DISX,DISY,ISTEP,NCYCL
   11 FORMAT(I10,2F10.2,2I10)
      WRITE(6,13)INCR,ISTEP,NCYCL
```

```
 13 FORMAT(1H0//,T5,'*** INCR = ',I2,' ***    0= HINGE BY HINGE, 1= INC
   1REMENT BY ALL'//T5,'*** ISTEP = ',I2,' ***   -1= MISS FIRST NEGATIV
   2E NORMALIZED DETERMINANT, 0= REDUCE LOAD WHEN DETERMINANT IS NEGAT
   3IVE'//T5,'*** NCYCL = ',I3,' ***')
    WRITE(6,14)DISX,DISY
 14 FORMAT(1H0//,T5,'LIMIT ON U =',F9.1,' LIMIT ON V =',F9.1)
    DET1=DET
    IL=0
  1 CALL CHECK
    WRITE(6,2)IH,PALL,PAAL
  2 FORMAT(1H0///,T5,'TOTAL HINGES FORMED = ',I3,T33,'LOAD FACTOR = ',
   1F6.3,T60,'AXIAL LOAD FACTOR = ',F6.3)
    CALL HINROT
    WRITE(6,17)IL
 17 FORMAT(1H0//,T5,'*** END OF OUTPUT DATA FOR CYCLE ',I4,' ***'//)
    IF(UT/UT1.GT.DISX.OR.VT/VT1.GT.DISY)GO TO 7
    IF(IL.EQ.NCYCL)GO TO 15
    P1=PALL
    IF(DET/DET1.LT.0.0)ALL=-ALL
    IF(DET/DET1.LT.0.0)ISTEP=ISTEP+1
    IF(ISTEP.EQ.1)GO TO 10
    IF(DET/DET1.LT.0.0)ALL=-ALL
 10 ALL1=ALL
    DET1=DET
    PALL=PALL+ALL1
    PAAL=PAAL+AAL
    P=PALL
    IF(INCR.EQ.1)GO TO 12
    DO 3 I=1,N
    DO 4 J=1,NS
     CMB1(I,J)=CMB(I,J)
    CMT1(I,J)=CMT(I,J)
     IF(BFI(I,1).EQ.0.0)GO TO 5
    BFMC1(I,J)=BFMC(I,J)
  5 IF(IND(I).EQ.0)GO TO 6
     WMT1(I,J)=WMT(I,J)
    WMB1(I,J)=WMB(I,J)
     BWMC1(I,J)=BWMC(I,J)
    BWMW1(I,J)=BWMW(I,J)
  6 CONTINUE
  4 CONTINUE
  3 CONTINUE
    CALL SETUP
    CALL CALFOR
    CALL CHECK2(ISTEP,BFMC1,BWMC1,BWMW1,CMT1,CMB1,WMT1,WMB1)
 12 CALL SETUP
    CALL CALFOR
    IL=IL+1
    GO TO 1
 15 WRITE(6,16)
 16 FORMAT(1H0//,T5,'*** ANALYSIS TERMINATED BY LIMIT ON CYCLES ***')
  7 RETURN
    END

    SUBROUTINE   CHECK
    COMMON E,EW,YS,PALL,PAAL,DET,DET1,UT,UT1,VT,VT1,P,P1,X(12),Y(12),H
   1(30),ESC(12),ESW(12),GKT(3C),FX(30),FY(30),YFX(30),XFY(30),RIH(300
   2),PMH(300),PINC(300),BF(12,30),BW(12,30),W(12,30),BWC(12,30),ALL
   3,CI(12,30),WI(12,30),BFI(12,30),BWI(12,30),CM(12,30),WM(12,30),BFM
```

```
      4(12,30),BWM(12,30),PC(12,30),WB(12,30),A(422,33),B(422),XX(422),WT
      5(12,30),PDEL(12,30),BFMC(12,30),BWMC(12,30),BWMW(12,30),CMT(12,30)
      6,CMB(12,30),WMT(12,30),WMB(12,30),BFF(12,30),CB(12,30),CT(12,30),B
      7FC(12,30),BWW(12,30),AAL,NS,NX,NY,NX1,NS1,N,ND,NN,NU,NB,IH,IND(12)
      8,IK(12),IHF(300),IHB(300),IHL(300)
        DO 1 J=1,NS
        DO 2 I=1,N
        J1=IK(I)-IND(I)+(J-1)*ND
        J2=J1+ND
        J3=J1+1
        J4=J2+1
        IF( ABS(CMB(I,J)).GE.CM(I,J))GO TO 3
     4 IF( ABS(CMT(I,J)).GE.CM(I,J))GO TO 5
        IF(BFM(I,J).EQ.0.0)GO TO 8
     6 IF( ABS(BFMC(I,J)).GE.BFM(I,J))GO TO 7
     8 IF(IND(I).EQ.0)GO TO 9
        IF( ABS(WMB(I,J)).GE.WM(I,J))GO TO 10
    11 IF( ABS(WMT(I,J)).GE.WM(I,J))GO TO 12
    13 IF( ABS(BWMW(I,J)).GE.BWM(I,J))GO TO 14
    15 IF( ABS(BWMC(I,J)).GE.BWM(I,J))GO TO 16
        GO TO 9
     3 IF(CB(I,J).NE.0.0)GO TO 4
        IH=IH+1
        IHF(IH)=J
        IHB(IH)=I
        IHL(IH)=1
        RIH(IH)=XX(J1)
        PINC(IH)=PALL
        CB(I,J)=CM(I,J)*CMB(I,J)/ ABS(CMB(I,J))
        WRITE(6,17)IH,I,J,IHL(IH),RIH(IH)
        GO TO 4
     5 IF(CT(I,J).NE.0.0)GO TO 6
        IH=IH+1
        IHF(IH)=J
        IHB(IH)=I
        IHL(IH)=3
        RIH(IH)=XX(J2)
        PINC(IH)=PALL
        CT(I,J)=CM(I,J)*CMT(I,J)/ ABS(CMT(I,J))
        WRITE(6,17)IH,I,J,IHL(IH),RIH(IH)
        GO TO 6
     7 IF(BFC(I,J).NE.0.0)GO TO 8
        IH=IH+1
        IHF(IH)=J
        IHB(IH)=I
        IHL(IH)=4
        RIH(IH)=XX(J2)
        PINC(IH)=PALL
        BFC(I,J)=BFM(I,J)*BFMC(I,J)/ ABS(BFMC(I,J))
        WRITE(6,18)IH,I,J,IHL(IH),RIH(IH)
        GO TO 8
    10 IF(WB(I,J).NE.0.0)GO TO 11
        IH=IH+1
        IHF(IH)=J
        IHB(IH)=I
        IHL(IH)=5
        RIH(IH)=XX(J3)
        PINC(IH)=PALL
```

```
      WB(I,J)=WM(I,J)*WMB(I,J)/ ABS(WMB(I,J))
      WRITE(6,17)IH,I,J,IHL(IH),RIH(IH)
      GO TO 11
   12 IF(WT(I,J).NE.0.0)GO TO 13
      IH=IH+1
      IHF(IH)=J
      IHB(IH)=I
      IHL(IH)=7
      RIH(IH)=XX(J4)
      PINC(IH)=PALL
      WT(I,J)=WM(I,J)*WMT(I,J)/ ABS(WMT(I,J))
      WRITE(6,17)IH,I,J,IHL(IH),RIH(IH)
      GO TO 13
   14 IF(BWW(I,J).NE.0.0)GO TO 15
      IH=IH+1
      IHF(IH)=J
      IHB(IH)=I
      IHL(IH)=8
      RIH(IH)=XX(J4)
      PINC(IH)=PALL
      BWW(I,J)=BWM(I,J)*BWMW(I,J)/ ABS(BWMW(I,J))
      WRITE(6,18)IH,I,J,IHL(IH),RIH(IH)
      GO TO 15
   16 IF(BWC(I,J).NE.0.0)GO TO 9
      IH=IH+1
      IHF(IH)=J
      IHB(IH)=I
      IHL(IH)=9
      RIH(IH)=XX(J2)
      PINC(IH)=PALL
      BWC(I,J)=BWM(I,J)*BWMC(I,J)/ ABS(BWMC(I,J))
      WRITE(6,18)IH,I,J,IHL(IH),RIH(IH)
    9 CONTINUE
    2 CONTINUE
    1 CONTINUE
   17 FORMAT(1H0,T5,'HINGE NUMBER ',I3,' FOUND IN BENT ',I3,' IN STORY '
     1,I3,' AT LOCATION ',I3,', ROTATION OF MEMBER END = ',E12.5)
   18 FORMAT(1H0,T5,'HINGE NUMBER ',I3,' FOUND IN BENT ',I3,' AT FLOOR '
     1,I3,' AT LOCATION ',I3,', ROTATION OF MEMBER END = ',E12.5)
      RETURN
      END


      SUBROUTINE   CHECK1
      COMMON E,EW,YS,PALL,PAAL,DET,DET1,UT,UT1,VT,VT1,P,P1,X(12),Y(12),H
     1(30),ESC(12),ESW(12),GKT(30),FX(30),FY(30),YFX(30),XFY(30),RIH(300
     2),PMH(300),PINC(300),BF(12,30),BW(12,30),W(12,30),BWC(12,30),ALL
     3,CI(12,30),WI(12,30),BFI(12,30),BWI(12,30),CM(12,30),WM(12,30),BFM
     4(12,30),BWM(12,30),PC(12,30),WB(12,30),A(422,33),B(422),XX(422),WT
     5(12,30),PDEL(12,30),BFMC(12,30),BWMC(12,30),BWMW(12,30),CMT(12,30)
     6,CMB(12,30),WMT(12,30),WMB(12,30),BFF(12,30),CB(12,30),CT(12,30),B
     7FC(12,30),BWW(12,30),AAL,NS,NX,NY,NX1,NS1,N,ND,NN,NU,NB,IH,IND(12)
     8,IK(12),IHF(300),IHB(300),IHL(300)
      DO 1 I=1,N
      DO 2 J=1,NS
      CMB(I,J)= ABS(CMB(I,J)/CM(I,J))
      CMT(I,J)= ABS(CMT(I,J)/CM(I,J))
      IF(BFMC(I,J).EQ.0.0)GO TO 3
      BFMC(I,J)= ABS(BFMC(I,J)/BFM(I,J))
```

```
  3 IF(IND(I).EQ.0)GO TO 4
    WMB(I,J)= ABS(WMB(I,J)/WM(I,J))
    WMT(I,J)= ABS(WMT(I,J)/WM(I,J))
    BWMC(I,J)= ABS(BWMC(I,J)/BWM(I,J))
    BWMW(I,J)= ABS(BWMW(I,J)/BWM(I,J))
  4 CONTINUE
  2 CONTINUE
  1 CONTINUE
    R=0.0
    INS=NS1
    IF(NS1.EQ.0)INS=1
    DO 5 I=1,N
    DO 6 J=1,INS
    IF(NS.GT.1)GO TO 10
    CMB(I,J+1)=0.0
    CMT(I,J+1)=0.0
    BFMC(I,J+1)=0.0
    WMB(I,J+1)=0.0
    WMT(I,J+1)=0.0
    BWMC(I,J+1)=0.0
    BWMW(I,J+1)=0.0
 10 X1=AMAX1(CMB(I,J),CMB(I,J+1))
    X2=AMAX1(CMT(I,J),CMT(I,J+1))
    X3=AMAX1(BFMC(I,J),BFMC(I,J+1))
    IF(IND(I).EQ.0)GO TO 7
    X4=AMAX1(WMB(I,J),WMB(I,J+1))
    X5=AMAX1(WMT(I,J),WMT(I,J+1))
    X6=AMAX1(BWMC(I,J),BWMC(I,J+1))
    X7=AMAX1(BWMW(I,J),BWMW(I,J+1))
    R=AMAX1(R,X1,X2,X3,X4,X5,X6,X7)
    GO TO 8
  7 R=AMAX1(R,X1,X2,X3)
  8 CONTINUE
  6 CONTINUE
  5 CONTINUE
    PALL=1.0/R
    PALL=PALL+0.0001
    CALL SETUP
    CALL CALFOR
    RETURN
    END

    SUBROUTINE   CHECK2(ISTEP,BFMC1,BWMC1,BWMW1,CMT1,CMB1,WMT1,WMB1)
    COMMON E,EW,YS,PALL,PAAL,DET,DET1,UT,UT1,VT,VT1,P,P1,X(12),Y(12),H
   1(30),ESC(12),ESW(12),GKT(30),FX(30),FY(30),YFX(30),XFY(30),RIH(300
   2),PMH(300),PINC(300),BF(12,30),BW(12,30),W(12,30),BWC(12,30),ALL
   3,CI(12,30),WI(12,30),BFI(12,30),BWI(12,30),CM(12,30),WM(12,30),BFM
   4(12,30),BWM(12,30),PC(12,30),WB(12,30),A(422,33),B(422),XX(422),WT
   5(12,30),PDEL(12,30),BFMC(12,30),BWMC(12,30),BWMW(12,30),CMT(12,30)
   6,CMB(12,30),WMT(12,30),WMB(12,30),BFF(12,30),CB(12,30),CT(12,30),B
   7FC(12,30),BWW(12,30),AAL,NS,NX,NY,NX1,NS1,N,ND,NN,NU,NB,IH,IND(12)
   8,IK(12),IHF(300),IHB(300),IHL(300)
    DIMENSION BFMC1(11,24),BWMC1(11,24),BWMW1(11,24),CMT1(11,24),CMB1(
   111,24),WMT1(11,24),WMB1(11,24)
    DO 1 I=1,N
    DO 2 J=1,NS
    DEN=CMB(I,J)-CMB1(I,J)
    IF(CB(I,J).NE.0.0)GO TO 15
```

```
      CMB1(I,J)= ABS((CM(I,J)- ABS(CMB1(I,J)))/DEN)
      GO TO 10
   15 CMB1(I,J)=100.0
   10 DEN=CMT(I,J)-CMT1(I,J)
      IF(CT(I,J).NE.0.0)GO TO 16
      CMT1(I,J)= ABS((CM(I,J)- ABS(CMT1(I,J)))/DEN)
      GO TO 11
   16 CMT1(I,J)=100.0
   11 DEN=BFMC(I,J)-BFMC1(I,J)
      IF(BFC(I,J).NE.0.0)GO TO 17
      IF(BFMC1(I,J).EQ.0.0)GO TO 3
      BFMC1(I,J)= ABS((BFM(I,J)- ABS(BFMC1(I,J)))/DEN)
      GO TO 3
   17 BFMC1(I,J)=100.0
    3 IF(IND(I).EQ.0)GO TO 4
      DEN=WMB(I,J)-WMB1(I,J)
      IF(WB(I,J).NE.0.0)GO TO 18
      WMB1(I,J)= ABS((WM(I,J)- ABS(WMB1(I,J)))/DEN)
      GO TO 12
   18 WMB1(I,J)=100.0
   12 DEN=WMT(I,J)-WMT1(I,J)
      IF(WT(I,J).NE.0.0)GO TO 19
      WMT1(I,J)= ABS((WM(I,J)- ABS(WMT1(I,J)))/DEN)
      GO TO 13
   19 WMT1(I,J)=100.0
   13 DEN=BWMC(I,J)-BWMC1(I,J)
      IF(BWC(I,J).NE.0.0)GO TO 20
      BWMC1(I,J)= ABS((BWM(I,J)- ABS(BWMC1(I,J)))/DEN)
      GO TO 14
   20 BWMC1(I,J)=100.0
   14 DEN=BWMW(I,J)-BWMW1(I,J)
      IF(BWW(I,J).NE.0.0)GO TO 21
      BWMW1(I,J)= ABS((BWM(I,J)- ABS(BWMW1(I,J)))/DEN)
      GO TO 4
   21 BWMW1(I,J)=100.0
    4 CONTINUE
    2 CONTINUE
    1 CONTINUE
      R=100.0
      INS=NS1
      IF(NS1.EQ.0)INS=1
      DO 5 I=1,N
      DO 6 J=1,INS
      IF(NS.NE.1)GO TO 40
      CMB1(I,J+1)=100.
      CMT1(I,J+1)=100.
      BFMC1(I,J+1)=100.
      WMB1(I,J+1)=100.
      WMT1(I,J+1)=100.
      BWMC1(I,J+1)=100.
      BWMW1(I,J+1)=100.
   40 X1=AMIN1(CMB1(I,J),CMB1(I,J+1))
      X2=AMIN1(CMT1(I,J),CMT1(I,J+1))
      IF(BFI(I,J).EQ.0.0)GO TO 9
      X3=AMIN1(BFMC1(I,J),BFMC1(I,J+1))
      GO TO 30
    9 X3=100.0
   30 IF(IND(I).EQ.0)GO TO 7
```

```
      X4=AMIN1(WMB1(I,J),WMB1(I,J+1))
      X5=AMIN1(WMT1(I,J),WMT1(I,J+1))
      X6=AMIN1(BWMC1(I,J),BWMC1(I,J+1))
      X7=AMIN1(BWMW1(I,J),BWMW1(I,J+1))
      R=AMIN1(R,X1,X2,X3,X4,X5,X6,X7)
      GO TO 8
    7 R=AMIN1(R,X1,X2,X3)
    8 CONTINUE
    6 CONTINUE
    5 CONTINUE
      PALL=P1+R*(P-P1)
      PALL=PALL+0.0001
      IF(ISTEP.EQ.1)PALL=PALL-0.0002
      RETURN
      END

      SUBROUTINE   HINROT
      COMMON E,EW,YS,PALL,PAAL,DET,DET1,UT,UT1,VT,VT1,P,P1,X(12),Y(12),H
     1(30),ESC(12),ESW(12),GKT(30),FX(30),FY(30),YFX(30),XFY(30),RIH(300
     2),PMH(300),PINC(300),BF(12,30),BW(12,30),W(12,30),BWC(12,30),ALL
     3,CI(12,30),WI(12,30),BFI(12,30),BWI(12,30),CM(12,30),WM(12,30),BFM
     4(12,30),BWM(12,30),PC(12,30),WB(12,30),A(422,33),B(422),XX(422),WT
     5(12,30),PDEL(12,30),BFMC(12,30),BWMC(12,30),BWMW(12,30),CMT(12,30)
     6,CMB(12,30),WMT(12,30),WMB(12,30),BFF(12,30),CB(12,30),CT(12,30),B
     7FC(12,30),BWW(12,30),AAL,NS,NX,NY,NX1,NS1,N,ND,NN,NU,NB,IH,IND(12)
     8,IK(12),IHF(300),IHB(300),IHL(300)
      DIMENSION RIH1(300),RIH2(300)
      IF(IH.EQ.0)RETURN
      DO 1 I=1,IH
      J1=IHF(I)
      J2=IHB(I)
      J3=IHL(I)
      I1=IK(J2)-IND(J2)+(J1-1)*ND
      I2=(J1-2)*ND+NN+1
      I3=I2+1
      H1=H(J1)
      H2=3.0/H1
      X1=XX(I1+ND)
      X2=XX(I2+ND)
      X3=XX(I3+ND)
      X4=XX(I2+2+ND)
      X5=XX(I1+1+ND)
      IF(J3.EQ.1)GO TO 2
      IF(J3.EQ.3)GO TO 3
      IF(J3.EQ.4)GO TO 4
      IF(J3.EQ.5)GO TO 5
      IF(J3.EQ.7)GO TO 6
      IF(J3.EQ.8)GO TO 7
      IF(J3.EQ.9)GO TO 8
      GO TO 9
    2 C1=CB(J2,J1)/(2.0*CI(J2,J1))
      IF(CT(J2,J1).NE.0.0)GO TO 10
      IF(J2.GT.NX)GO TO 11
      IF(J1.EQ.1)GO TO 12
      RIH1(I)= .50*(C1-X1+H2*(X2-XX(I2)+Y(J2)*(X4-XX(I2+2))))-XX(I1)
      GO TO 9
   12 RIH1(I)= .50*(C1-X1+H2*(X2+Y(J2)*X4))-XX(I1)
      GO TO 9
   11 IF(J1.EQ.1)GO TO 13
```

```
      RIH1(I)= .50*(C1-X1+H2*(X3-XX(I3)-X(J2-NX)*(X4-XX(I2+2))))-XX(I1)
      GO TO 9
   13 RIH1(I)= .50*(C1-X1+H2*(X3-X(J2-NX)*X4))-XX(I1)
      GO TO 9
   10 IF(J1.EQ.1)GO TO 40
      SW=(X2-XX(I2)+Y(J2)*(X4-XX(I2+2)))/H1
      IF(J2.GT.NX)SW=(X3-XX(I3)-X(J2-NX)*(X4-XX(I2+2)))/H1
      GO TO 44
   40 SW=(X2+Y(J2)*X4)/H1
      IF(J2.GT.NX)SW=(X3-X(J2-NX)*X4)/H1
   44 IF(CB(J2,J1)*CT(J2,J1).GT.0.0)GO TO 14
      RIH1(I)= C1+SW-XX(I1)
      GO TO 9
   14 RIH1(I)= C1/3.0+SW-XX(I1)
      GO TO 9
    3 C1=CT(J2,J1)/(2.0*CI(J2,J1))
      IF(CB(J2,J1).NE.0.0)GO TO 15
      IF(J2.GT.NX)GO TO 16
      IF(J1.EQ.1)GO TO 17
      RIH1(I)= .50*(C1-XX(I1)+H2*(X2-XX(I2)+Y(J2)*(X4-XX(I2+2))))-X1
      GO TO 9
   17 RIH1(I)= .50*(C1-XX(I1)+H2*(X2+Y(J2)*X4))-X1
      GO TO 9
   16 IF(J1.EQ.1)GO TO 18
      RIH1(I)= .50*(C1-XX(I1)+H2*(X3-XX(I3)-X(J2-NX)*(X4-XX(I2+2))))-X1
      GO TO 9
   18 RIH1(I)= .50*(C1-XX(I1)+H2*(X3-X(J2-NX)*X4))-X1
      GO TO 9
   15 IF(J1.EQ.1)GO TO 41
      SW=(X2-XX(I2)+Y(J2)*(X4-XX(I2+2)))/H1
      IF(J2.GT.NX)SW=(X3-XX(I3)-X(J2-NX)*(X4-XX(I2+2)))/H1
      GO TO 45
   41 SW=(X2+Y(J2)*X4)/H1
      IF(J2.GT.NX)SW=(X3-X(J2-NX)*X4)/H1
   45 IF(CB(J2,J1)*CT(J2,J1).GT.0.0)GO TO 19
      RIH1(I)= C1+SW-X1
      GO TO 9
   19 RIH1(I)= C1/3.0+SW-X1
      GO TO 9
    4 RIH1(I)= BFC(J2,J1)/(3.0*BFI(J2,J1))-X1
      GO TO 9
    5 W1=WB(J2,J1)/(2.0*WI(J2,J1))
      IF(WT(J2,J1).NE.0.0)GO TO 20
      IF(J2.GT.NX)GO TO 21
      IF(J1.EQ.1)GO TO 22
      RIH1(I)= .50*(W1-X5+H2*(X2-XX(I2)+Y(J2)*(X4-XX(I2+2))))-XX(I1+1)
      GO TO 9
   22 RIH1(I)= .50*(W1-X5+H2*(X2+Y(J2)*X4))-XX(I1+1)
      GO TO 9
   21 IF(J1.EQ.1)GO TO 23
      RIH1(I)=.50*(W1-X5+H2*(X3-XX(I3)-X(J2-NX)*(X4-XX(I2+2))))-XX(I1+1)
      GO TO 9
   23 RIH1(I)= .50*(W1-X5+H2*(X3-X(J2-NX)*X4))-XX(I1+1)
      GO TO 9
   20 IF(J1.EQ.1)GO TO 42
      SW=(X2-XX(I2)+Y(J2)*(X4-XX(I2+2)))/H1
      IF(J2.GT.NX)SW=(X3-XX(I3)-X(J2-NX)*(X4-XX(I2+2)))/H1
      GO TO 46
```

```
42 SW=(X2+Y(J2)*X4)/H1
   IF(J2.GT.NX)SW=(X3-X(J2-NX)*X4)/H1
46 IF(WB(J2,J1)*WT(J2,J1).GT.0.0)GO TO 24
   RIH1(I)= W1+SW-XX(I1+1)
   GO TO 9
24 RIH1(I)= W1/3.0+SW-XX(I1+1)
   GO TO 9
 6 W1=WT(J2,J1)/(2.0*WI(J2,J1))
   IF(WB(J2,J1).NE.0.0)GO TO 25
   IF(J2.GT.NX)GO TO 26
   IF(J1.EQ.1)GO TO 27
   RIH1(I)= .50*(W1-XX(I1+1)+H2*(X2-XX(I2)+Y(J2)*(X4-XX(I2+2))))-X5
   GO TO 9
27 RIH1(I)= .50*(W1-XX(I1+1)*H2*(X2+Y(J2)*X4))-X5
   GO TO 9
26 IF(J1.EQ.1)GO TO 28
   RIH1(I)= .5*(W1-XX(I1+1)*H2*(X3-XX(I3)-X(J2-NX)*(X4-XX(I2+2))))-X5
   GO TO 9
28 RIH1(I)= .50*(W1-XX(I1+1)*H2*(X3-X(J2-NX)*X4))-X5
   GO TO 9
25 IF(J1.EQ.1)GO TO 43
   SW=(X2-XX(I2)+Y(J2)*(X4-XX(I2+2)))/H1
   IF(J2.GT.NX)SW=(X3-XX(I3)-X(J2-NX)*(X4-XX(I2+2)))/H1
   GO TO 47
43 SW=(X2+Y(J2)*X4)/H1
   IF(J2.GT.NX)SW=(X3-X(J2-NX)*X4)/H1
47 IF(WB(J2,J1)*WT(J2,J1).GT.0.0)GO TO 29
   RIH1(I)= W1+SW-X5
   GO TO 9
29 RIH1(I)= W1/3.0+SW-X5
   GO TO 9
 7 IF(BWC(J2,J1).NE.0.0)GO TO 30
   RIH1(I)= .5*(BWW(J2,J1)/(2.*BWI(J2,J1))-X1-(1.5*W(J2,J1)/BW(J2,J1
  1)*X5)-X5
   GO TO 9
30 SW=-W(J2,J1)*X5/(2.0*BW(J2,J1))
   IF(BWC(J2,J1)*BWW(J2,J1).GT.0.0)GO TO 31
   RIH1(I)= BWW(J2,J1)/(2.0*BWI(J2,J1))+SW-X5
   GO TO 9
31 RIH1(I)= BWW(J2,J1)/(6.0*BWI(J2,J1))+SW-X5
   GO TO 9
 8 IF(BWW(J2,J1).NE.0.0)GO TO 32
   RIH1(I)= .50*(BWC(J2,J1)/(2.0*BWI(J2,J1))-X5*(1.0+1.5*W(J2,J1)/BW(
  1J2,J1)))-X1
   GO TO 9
32 SW=-W(J2,J1)*X5/(2.0*BW(J2,J1))
   IF(BWC(J2,J1)*BWW(J2,J1).GT.0.0)GO TO 33
   RIH1(I)= BWC(J2,J1)/(2.0*BWI(J2,J1))+SW-X1
   GO TO 9
33 RIH1(I)= BWC(J2,J1)/(6.0*BWI(J2,J1))+SW-X1
 9 CONTINUE
   RIH2(I)=RIH1(I)/RIH(I)
 1 CONTINUE
   WRITE(6,35)PALL
35 FORMAT(1H0//,T5,'ROTATION OF HINGES AND ROTATION RATIOS AT LOAD FA
  1CTOR ',F6.3,' ARE AS FOLLOWS'//T5,'HINGE',T15,'HINGE ROTATION',T35
  2,'RATIO PLASTIC/YIELD')
   DO 36 I=1,IH
```

```
      WRITE(6,37)I,RIH1(I),RIH2(I)
   36 CONTINUE
   37 FORMAT(1H0,T5,I3,T15,E12.5,T38,E12.5)
      RETURN
      END

      SUBROUTINE   MODIFY
      COMMON E,EW,YS,PALL,PAAL,DET,DET1,UT,UT1,VT,VT1,P,P1,X(12),Y(12),H
     1(30),ESC(12),ESW(12),GKT(30),FX(30),FY(30),YFX(30),XFY(30),RIH(300
     2),PMH(300),PINC(300),BF(12,30),BW(12,30),W(12,30),BWC(12,30),ALL
     3,CI(12,30),WI(12,30),BFI(12,30),BWI(12,30),CM(12,30),WM(12,30),BFM
     4(12,30),BWM(12,30),PC(12,30),WB(12,30),A(422,33),B(422),XX(422),WT
     5(12,30),PDEL(12,30),BFMC(12,30),BWMC(12,30),BWMW(12,30),CMT(12,30)
     6,CMB(12,30),WMT(12,30),WMB(12,30),BFF(12,30),CB(12,30),CT(12,30),B
     7FC(12,30),BWW(12,30),AAL,NS,NX,NY,NX1,NS1,N,ND,NN,NU,NB,IH,IND(12)
     8,IK(12),IHF(300),IHB(300),IHL(300)
      IF(IH.EQ.0)RETURN
      DO 1 I=1,NS
      DO 2 J=1,N
      I1=IK(J)-IND(J)
      I2=(I-1)*ND-2
      I3=I2+2+I1
      IF(CB(J,I).NE.0.0.OR.CT(J,I).NE.0.0)GO TO 22
    3 IF(BFC(J,I).NE.0.0)GO TO 4
    5 IF(IND(J).EQ.0)GO TO 16
    6 IF(WB(J,I).NE.0.0.OR.WT(J,I).NE.0.0)GO TO 7
    8 IF(BWW(J,I).NE.0.0.OR.BWC(J,I).NE.0.0)GO TO 9
      GO TO 16
   22 C=CI(J,I)
      C1=C/H(I)
      C2=C1/H(I)
      IF(CB(J,I).NE.0.0.AND.CT(J,I).NE.0.0)GO TO 10
      IF(CT(J,I).NE.0.0)GO TO 11
      S11=-4.0
      S12=-2.0
      S13=+6.0
      S14=-6.0
      S15=+1.0
      S16=0.0
      S21=-2.0
      S22=-1.0
      S23=+3.0
      S24=-3.0
      S25=+0.50
      S26=0.0
      GO TO 12
   11 S11=-1.0
      S12=-2.0
      S13=+3.0
      S14=-3.0
      S15=0.0
      S16=0.50
      S21=-2.0
      S22=-4.0
      S23=+6.0
      S24=-6.0
      S25=0.0
      S26=1.0
```

```
      GO TO 12
   10 S11=-4.0
      S12=-2.0
      S13=+6.0
      S14=-6.0
      S15=+1.0
      S16=0.0
      S21=-2.0
      S22=-4.0
      S23=+6.0
      S24=-6.0
      S25=0.0
      S26=1.0
   12 S1=S11+S21
      S2=S12+S22
      S3=S13+S23
      S4=S14+S24
      S5=S15+S25
      S6=S16+S26
      IF(J.GT.NX)GO TO 13
      IF(I.EQ.1)GO TO 14
      L=I1+3
      A(I2,1)=A(I2,1)+S4*C2
      A(I2,3)=A(I2,3)+S4*C2*Y(J)
      A(I2,L)=A(I2,L)+S1*C1
      A(I2,1+ND)=A(I2,1+ND)+S3*C2
      A(I2,3+ND)=A(I2,3+ND)+S3*C2*Y(J)
      A(I2,L+ND)=A(I2,L+ND)+S2*C1
      B(I2)=B(I2)-( S5*CB(J,I)+ S6*CT(J,I))/H(I)
      L=I2+2
      L1=I1+1
      A(L,1)=A(L,1)+S4*C2*Y(J)*Y(J)
      A(L,L1)=A(L,L1)+S1*C1*Y(J)
      A(L,ND-1)=A(L,ND-1)+S3*C2*Y(J)
      A(L,ND+1)=A(L,ND+1)+S3*C2*Y(J)*Y(J)
      A(L,L1+ND)=A(L,L1+ND)+S2*C1*Y(J)
      B(L)=B(L)-( S5*CB(J,I)+ S6*CT(J,I))*Y(J)/H(I)
   14 L=NN-I1+2
      A(I3,1)=A(I3,1)+S11*C
      A(I3,L)=A(I3,L)+S13*C1
      A(I3,L+2)=A(I3,L+2)+S13*C1*Y(J)
      A(I3,1+ND)=A(I3,1+ND)+S12*C
      B(I3)=B(I3)-S15*CB(J,I)-S16*CT(J,I)
      L=I2+ND
      L1=L+2
      A(L,1)=A(L,1)-S3*C2
      A(L,3)=A(L,3)-S3*C2*Y(J)
      A(L,I1+3)=A(L,I1+3)-S2*C1
      B(L)=B(L)+( S5*CB(J,I)+ S6*CT(J,I))/H(I)
      A(L1,1)=A(L1,1)-S3*C2*Y(J)*Y(J)
      A(L1,I1+1)=A(L1,I1+1)-S2*C1*Y(J)
      B(L1)=B(L1)+( S5*CB(J,I)+ S6*CT(J,I))*Y(J)/H(I)
      L=I3+ND
      A(L,1)=A(L,1)+S22*C
      B(L)=B(L)-S25*CB(J,I)-S26*CT(J,I)
      GO TO 17
   13 M=J-NX
      IF(I.EQ.1)GO TO 15
```

```
      L=I2+1
      L1=I1+2
      A(L,1)=A(L,1)+S4*C2
      A(L,2)=A(L,2)-S4*C2*X(M)
      A(L,L1)=A(L,L1)+S1*C1
      A(L,1+ND)=A(L,1+ND)+S3*C2
      A(L,2+ND)=A(L,2+ND)-S3*C2*X(M)
      A(L,L1+ND)=A(L,L1+ND)+S2*C1
      B(L)=B(L)-( S5*CB(J,I)+ S6*CT(J,I))/H(I)
      L=I2+2
      L1=I1+1
      A(L,1)=A(L,1)+S4*C2*X(M)*X(M)
      A(L,L1)=A(L,L1)-S1*C1*X(M)
      A(L,ND)=A(L,ND)-S3*C2*X(M)
      A(L,ND+1)=A(L,ND+1)+S3*C2*X(M)*X(M)
      A(L,L1+ND)=A(L,L1+ND)-S2*C1*X(M)
      B(L)=B(L)+( S5*CB(J,I)+ S6*CT(J,I))*X(M)/H(I)
   15 L=NN-I1+3
      A(I3,1)=A(I3,1)+S11*C
      A(I3,L)=A(I3,L)+S13*C1
      A(I3,L+1)=A(I3,L+1)-S13*C1*X(M)
      A(I3,1+ND)=A(I3,1+ND)+S12*C
      B(I3)=B(I3)-S15*CB(J,I)-S16*CT(J,I)
      L=I2+1+ND
      A(L,1)=A(L,1)-S3*C2
      A(L,2)=A(L,2)+S3*C2*X(M)
      A(L,I1+2)=A(L,I1+2)-S2*C1
      B(L)=B(L)+( S5*CB(J,I)+ S6*CT(J,I))/H(I)
      L=I2+2+ND
      A(L,1)=A(L,1)-S3*C2*X(M)*X(M)
      A(L,I1+1)=A(L,I1+1)+S2*C1*X(M)
      B(L)=B(L)-( S5*CB(J,I)+ S6*CT(J,I))*X(M)/H(I)
      L=I3+ND
      A(L,1)=A(L,1)+S22*C
      B(L)=B(L)-S25*CB(J,I)-S26*CT(J,I)
      GO TO 17
    4 L=I*ND+I1
      A(L,1)=A(L,1)-3.0*BFI(J,I)
      B(L)=B(L)-BFC(J,I)
      GO TO 18
    7 CALL MODFY1(I1,I2,I3,J,I)
      GO TO 8
   18 GO TO 5
   17 GO TO 3
    9 L=I*ND+I1
      C=BWI(J,I)
      C1=C*W(J,I)/BW(J,I)
      C2=C1*W(J,I)/BW(J,I)
      IF(BWW(J,I).NE.0.0.AND.BWC(J,I).NE.0.0)GO TO 30
      IF(BWW(J,I).NE.0.0)GO TO 31
      S11=-4.0*C
      S12=-2.0*C-3.0*C1
      S13=+BWC(J,I)
      S22=-1.0*C-3.0*C1-2.25*C2
      S23=+BWC(J,I)*(0.50+0.25*W(J,I)/BW(J,I))
```

```
      S4=0.0
      S5=0.0
      GO TO 32
   31 S11=-1.0*C
      S12=-2.0*C-1.50*C1
      S13=+0.50*BWW(J,I)
      S22=-4.0*C-4.50*C1-2.25*C2
      S23=+BWW(J,I)*(1.0+0.75*W(J,I)/BW(J,I))
      S4=0.0
      S5=0.0
      GO TO 32
   30 S11=-4.0*C
      S12=-2.0*C-3.0*C1
      S13=+BWC(J,I)
      S22=-4.0*C-6.0*C1-3.0*C2
      S23=+BWW(J,I)*(1.+0.5*W(J,I)/BW(J,I))+BWC(J,I)*0.50*W(J,I)/BW(J,I)
      S4=0.0
      S5=0.0
   32 CONTINUE
      A(L,1)=A(L,1)+S11
      A(L,2)=A(L,2)+S12
      B(L)=B(L)-S13+S4
      A(L+1,1)=A(L+1,1)+S22
      B(L+1)=B(L+1)-S23+S5
   16 CONTINUE
    2 CONTINUE
    1 CONTINUE
      RETURN
      END

      SUBROUTINE    MODFY1(I1,I2,I3,J,I)
      COMMON E,EW,YS,PALL,PAAL,DET,DET1,UT,UT1,VT,VT1,P,P1,X(12),Y(12),H
     1(30),ESC(12),ESW(12),GKT(30),FX(30),FY(30),YFX(30),XFY(30),RIH(300
     2),PMH(300),PINC(300),BF(12,30),BW(12,30),W(12,30),BWC(12,30),ALL
     3,CI(12,30),WI(12,30),BFI(12,30),BWI(12,30),CM(12,30),WM(12,30),BFM
     4(12,30),BWM(12,30),PC(12,30),WB(12,30),A(422,33),B(422),XX(422),WT
     5(12,30),PDEL(12,30),BFMC(12,30),BWMC(12,30),BWMW(12,30),CMT(12,30)
     6,CMB(12,30),WMT(12,30),WMB(12,30),BFF(12,30),CB(12,30),CT(12,30),B
     7FC(12,30),BWW(12,30),AAL,NS,NX,NY,NX1,NS1,N,ND,NN,NU,NB,IH,IND(12)
     8,IK(12),IHF(300),IHB(300),IHL(300)
      I3=I3+1
      IF(WB(J,I).NE.0.0.AND.WT(J,I).NE.0.0)GO TO 1
      IF(WT(J,I).NE.0.0)GO TO 2
      S11=-4.0
      S12=-2.0
      S13=+6.0
      S14=-6.0
      S15=+1.0
      S16=0.0
      S21=-2.0
      S22=-1.0
      S23=+3.0
      S24=-3.0
      S25=+0.5
      S26=0.0
      GO TO 3
    2 S11=-1.0
      S12=-2.0
```

```
      S13=+3.0
      S14=-3.0
      S15=0.0
      S16=+0.5
      S21=-2.0
      S22=-4.0
      S23=+6.0
      S24=-6.0
      S25=0.0
      S26=+1.0
      GO TO 3
    1 S11=-4.0
      S12=-2.0
      S13=+6.0
      S14=-6.0
      S15=+1.0
      S16=0.0
      S21=-2.0
      S22=-4.0
      S23=+6.0
      S24=-6.0
      S25=0.0
      S26=+1.0
    3 CONTINUE
      S1=S11+S21
      S2=S12+S22
      S3=S13+S23
      S4=S14+S24
      S5=S15+S25
      S6=S16+S26
      WO=WI(J,I)
      W1=WO/H(I)
      W2=W1/H(I)
      IF(J.GT.NX)GO TO 10
      IF(I.EQ.1)GO TO 11
      L=I1+4
      A(I2,1)=A(I2,1)+S4*W2
      A(I2,3)=A(I2,3)+S4*W2*Y(J)
      A(I2,L)=A(I2,L)+S1*W1
      A(I2,1+ND)=A(I2,1+ND)+S3*W2
      A(I2,3+ND)=A(I2,3+ND)+S3*W2*Y(J)
      A(I2,L+ND)=A(I2,L+ND)+S2*W1
      B(I2)=B(I2)-(S5*WB(J,I)+S6*WT(J,I))/H(I)
      L=I2+2
      L1=I1+2
      A(L,1)=A(L,1)+S4*W2*Y(J)*Y(J)
      A(L,L1)=A(L,L1)+S1*W1*Y(J)
      A(L,ND-1)=A(L,ND-1)+S3*W2*Y(J)
      A(L,ND+1)=A(L,ND+1)+S3*W2*Y(J)*Y(J)
      A(L,L1+ND)=A(L,L1+ND)+S2*W1*Y(J)
      B(L)=B(L)-(S5*WB(J,I)+S6*WT(J,I))*Y(J)/H(I)
   11 L=NN-I1+1
      A(I3,1)=A(I3,1)+S11*WO
      A(I3,L)=A(I3,L)+S13*W1
      A(I3,L+2)=A(I3,L+2)+S13*W1*Y(J)
      A(I3,1+ND)=A(I3,1+ND)+S12*WO
      B(I3)=B(I3)-S15*WB(J,I)-S16*WT(J,I)
      L=I2+ND
```

```
      L1=L+2
      A(L,1)=A(L,1)-S3*W2
      A(L,3)=A(L,3)-S3*W2*Y(J)
      A(L,I1+4)=A(L,I1+4)-S2*W1
      B(L)=B(L)+(S5*WB(J,I)+S6*WT(J,I))/H(I)
      A(L1,1)=A(L1,1)-S3*W2*Y(J)*Y(J)
      A(L1,I1+2)=A(L1,I1+2)-S2*W1*Y(J)
      B(L1)=B(L1)+(S5*WB(J,I)+S6*WT(J,I))*Y(J)/H(I)
      L=I3+ND
      A(L,1)=A(L,1)+S22*W0
      B(L)=B(L)-S25*WB(J,I)-S26*WT(J,I)
      GO TO 12
   10 M=J-NX
      IF(I.EQ.1)GO TO 13
      L=I2+1
      L1=I1+3
      A(L,1)=A(L,1)+S4*W2
      A(L,2)=A(L,2)-S4*W2*X(M)
      A(L,L1)=A(L,L1)+S1*W1
      A(L,1+ND)=A(L,1+ND)+S3*W2
      A(L,2+ND)=A(L,2+ND)-S3*W2*X(M)
      A(L,L1+ND)=A(L,L1+ND)+S2*W1
      B(L)=B(L)-(S5*WB(J,I)+S6*WT(J,I))/H(I)
      L=I2+2
      L1=I1+2
      A(L,1)=A(L,1)+S4*W2*X(M)*X(M)
      A(L,L1)=A(L,L1)-S1*W1*X(M)
      A(L,ND)=A(L,ND)-S3*W2*X(M)
      A(L,ND+1)=A(L,ND+1)+S3*W2*X(M)*X(M)
       A(L,L1+ND)=A(L,L1+ND)-S2*W1*X(M)
      B(L)=B(L)+(S5*WB(J,I)+S6*WT(J,I))*X(M)/H(I)
   13 L=NN-I1+2
      A(I3,1)=A(I3,1)+S11*W0
      A(I3,L)=A(I3,L)+S13*W1
      A(I3,L+1)=A(I3,L+1)-S13*W1*X(M)
      A(I3,1+ND)=A(I3,1+ND)+S12*W0
      B(I3)=B(I3)-S15*WB(J,I)-S16*WT(J,I)
      L=I2+ND+1
      A(L,1)=A(L,1)-S3*W2
      A(L,2)=A(L,2)+S3*W2*X(M)
      A(L,I1+3)=A(L,I1+3)-S2*W1
      B(L)=B(L)+(S5*WB(J,I)+S6*WT(J,I))/H(I)
      L=I2+2+ND
      A(L,1)=A(L,1)-S3*W2*X(M)*X(M)
      A(L,I1+2)=A(L,I1+2)+S2*W1*X(M)
      B(L)=B(L)-(S5*WB(J,I)+S6*WT(J,I))*X(M)/H(I)
      L=I3+ND
      A(L,1)=A(L,1)+S22*W0
      B(L)=B(L)-S25*WB(J,I)-S26*WT(J,I)
   12 RETURN
      END
```